Bergvesenet
Postboks 3021, 7002 Trondheim

Rapportarkivet

Bergvesenet rapport nr	Intern Journal nr	Internt arkiv nr	Rapport lokalisering	Gradering
BV 1979			Trondheim	
Kommer fra ..arkiv	**Ekstern rapport nr**	**Oversendt fra**	**Fortrolig pga**	**Fortrolig fra dato:**

Tittel

Time domain EM survey in the Løkken region in 1985

Forfatter	Dato	Bedrift
Lakanen, Ensio	22.03 1986	Outokumpu Oy Orkla Industrier A/S

Kommune	Fylke	Bergdistrikt	1: 50 000 kartblad	1: 250 000 kartblad
Meldal	Sør-Trøndelag	Trondheimske	15213	

Fagområde	Dokument type	Forekomster
Geofysikk		Løkken
Råstofftype	**Emneord**	
Malm/metall		

Sammendrag

6.1979

TIME DOMAIN EM SURVEY IN THE LØKKEN REGION IN 1985

Summary

Data acquisition by EM37 equipment was successfully completed in the late summer 1985. In the environments of Løkken mine an area of about 26 km^2, 15 km from west to east, was surveyed equaling 46 kilometers or 429 occupied stations measured. Power lines and civilization bothered somewhat, but one line could be successfully shut off for the measuring. Data processing and interpretation were straightforward using available programs. Only faint indications were probably obtained from the Løkken orebody, but no anomalies of possible new massive-like large good conductors were observed. "Vasskis" horizons are found almost everywhere, and in many places there exists another parallel but inconsistent zone of same anomaly character. The used method is not very accurate to outcropping twin conductors, and the results must be correlated by for instance Genie-measurements surveyed later here.

Introduction

Transient or time domain EM (TDEM) method has been noticed suitable for fast deep reconnaissance sounding and profiling in prospecting of massive sulfide orebodies, which are good conductors. The depth penetration of the method depends on the resistivity of the ground, the size of the energizing loop and the current intensity flowing in the loop. In quite resistive ground (> 1000 ohmmeters) and with a reasonably large loop and portable power source, the depth range to detect middle sized orebodies is down to 500 m. The method is geometry dependent, which means that profitably situated bodies, i.e. as large projection as possible is parallel to the loop and below it, produce multifold anomaly intensities compared to perpendicular position. So the system is sensitive to horizontal bodies below the loop, and vertical ones outside the loop. Therefore quite resistive halfspace below the loop produces anomaly level that limits the detectability of a deep target. Also a suitably situated conductive host rock layer or dike with

8

a large parallel projection causes a marked anomaly threshold. It is self-evident that power grid lines can also have harmful effects to this kind of sensitive system. A more thorough treatment of the method and some cases are included in appendix 1.

The details of the survey sites and layouts have been described in appendix 2. Covered 15 km long (E-W direction) region have been divided to ten subareas, each of which have their own appendix no.s from 3 to 12 starting from west. There are a layout map scaled 1:5000 and the results plotted as profiles, all the 20 channels drawn logarithmically and also linearly, if useful, Z and X (one Y) components, the latter below. Thin plate models interpreted are included for each Z-component anomaly. Depth inversion or DIT-plots have been processed and plotted, too.

Three areas measured in a grid, Høydal, Urvatnet and Åmot have been drawn as contoured maps, every fifth channel both Z and X components.

Data processing and interpretations have been carried out by HP9845 micro having 512 kb of memory and programs made by Outokumpu Oy, Exploration. This started already during the survey. Evaluation of the data is, however, mainly qualitative. In a fixed loop mode TDEM is good at locating conductive bodies, but does not give accurate estimates for their geometric or physical parameters. 15 transient decay curves and their time constants have been shown in appendix 13/1. To find out the true detectability in different situations four profiles have been specially modeled with a thin plate approximation and results shown in appendices 13/2-5.

Survey results

Not a single distinct anomaly of deep-seated origin was found.

8 Two profiles in Björnli (app. 8) pass over the Løkken orebody, which lies at a depth of about 400 - 500 m, but the ore has been mostly excavated already. This was the only place, where there were some free space left and even here it was too many power lines and too close housing.

So the results are full of surface disturbances, only a small indication of possible bedrock conductor can be found in profile 250 W in channels 19 - 20. DIT-plot does not support its different nature, but it is possible to make a thin plate model that fits the data and is situated at the right place (app.13/ 2). But it is too small indication to be pinpointed in a virgin soil.

In Moen the profile 0 pass over the untouched Løkken orebody lying at a depth of 700 - 800 m. DIT-plot (app. 5/3) here shows, how nicely the results can indicate a large gently dipping conductive horizon, probably "vasskis". The depth at point 400 N, just above the Løkken orebody, can be measured to be 800 - 900 m. This and also the next point 600 N show a minor increase in conductivity-thickness product, and in linear plot (app. 5/4) a small anomalous lump can be noticed. This again can be nicely modeled with a thin plate analogous to Løkken orebody (app. 13/3). It seems quite reasonable to assume that there is something extra conductivity besides the "vasskis". But it could be regarded just to be a change of conductivity or thickness of the "vasskis" horizon. Anyway this is what we must be looking after in this region. DIT-plot indicates that "vasskis" can be remarkably homogeneous and this gives more hope that it is possible to find and discriminate an analogous orebody even close to vasskis and quite deep, if it only existed.

Surface-bound "vasskis" anomalies seem to be present almost everywhere. The strongest anomaly is found in Damlia (app. 6/2), where it has been drilled to be surely "vasskis". It can be thought to be the same horizon as in Moen, though in Moen it does not come to surface, as it was proven by Genie.

"Empty" areas are Blokkum and Mogset, and almost empty profiles are in Högåsen Y 33.5, Urvatnet Y 43.0 and Åmot Y 42.0.

A northerly dip can be determined almost everywhere, and mostly gentle. Quite vertical dip exists in Urvatnet, however.

8

Anomaly twins are common in Högåsen, Høydal, Urvatnet and Åmot. They can be caused by two parallel conductive horizons at the surface, and this was proven in most cases by Genie measurement. Very often Genie gave two or three parallel anomalies and EM37 one or two, but two times in Høydal Genie had only one and EM37 two clear anomalies, profiles Y 37.5 and 38.0. See also horizontal projection maps (app.s 2/3 and 2/4). When modeling it was found surprisingly difficult to locate these parallel conductors accurately, because they screen each others, the one in the transmitter loop side being in a better position. In the resistive environment the anomaly shape does not change much, may one or both conductors be "blind" bodies even to 100 - 200 m down.

In Høydal it is interesting to notice that the anomaly, closer to transmitter loop can be connected to Høydal orebody. This conductive horizon is more variable from one profile to another. Its depth, conductivity and thickness may vary a lot. This has an analogy with Moen profile, too. So this double anomaly must be looked at very carefully. Wherever this more northern parallel conductive horizon is not verified to be caused by "vasskis", it should be checked. Though really good massive type does not exist in surveyed profiles.

Transient decay curves (app. 13/1) and calculated time constants confirm strongly that the best conductivity-thickness product is met in Moen and Damlia (note that Moen has a different time scale and the eighteenth channel is 0, because it could not be measured at that last profile of the whole survey). Time constant is about 5 ms in Moen and increasing close to 5 also in Damlia. In Björnli the two last channels rise the time constant to about 2.3 ms. The best anomaly in Høydal in profile Y 37.0 gives about 1.4 ms. Others are too small to earn special observing. Decay curves of peak to peak values did not change time constants or any parameter of some interest.

Högåsen profile Y 32.50 (app. 13/4) and Høydal
8 Y 37.50 (app. 13/5) were modeled putting an extra imagined thin plate at variable depth and with an extinction angle dip, 45° N and finally 5° N. The model corresponds a good

conductor of less than five million tons. It is noticed that from the depth of 200 m when in extinction angle the response is strong enough to become observed in spite of the "vasskis" and overburden anomalies. The difference is still visible when the model is at 300 m, but it is doubtful to be recognized anymore. With a probable dip of 45° N the response is well discernible when at 500 m and with a most advantageous dip of 5° N the anomaly is readable even at 800 m and the body is only 200 m long in the direction of dip (800 m long in the strike direction). The same remarks apply to Høydal situation (app. 13/5).

Conclusions and recommendations

This large survey succeeded well. Measurements were completed as scheduled, data processing and interpretation occured straightforwardly. Test profiles over the Løkken orebody were not, however, quite successful, but that was expected, because either the civilization masked when shallow enough, or it was too deep. The probable indications were found after all.

The results are not as desired. Any new interesting large massive orebody was not observed, and it can be convinced that till the depth of 200 - 300 m in the surveyed area there does not exist any economic copper ore, and probably this is true even to 500 m.

The known "vasskis" horizons are present almost everywhere, dipping north, but they are not so good conductors as massive sulfide ore. In many places there is a more inconsistent parallel horizon of approximately same conductivity. In analogy to Løkken and Høydal this might be ore potential horizon, and should be carefully looked at in that respect. But only less conductive or smaller orebodies are to be found close to surface in the surveyed area.

This method is not very accurate for locating outcropping conductive bodies, so the results of Genie when available should be used for that purpose, and it is not a wonder that TDEM interpretations given do not always correlate exactly.

8

In similar areas this kind of geophysics are highly recommended as before. If the depth range is to be increased AMT or multifrequency high-power dipole-dipole system like Maxiprobe should be applied.

Ensio Lakanen

Distributed to: Gudmund Grammeltvedt, Løkken Gruber AS & Co.
UKP OKME

Abbreviations

TDEM	=	time domain electromagnetic method
	=	transient electromagnetic method
EM 37	=	Geonics Ltd.'s transient electromagnetic equipment
HI	=	High frequency = 25 Hz pulse frequency
MD	=	Medium frequency = 6.25 Hz pulse frequency
Z	=	Z- or vertical component of electromagnetic field (time derivative)
X	=	X horizontal " "
Y	=	Y " " "

(X is the direction of survey line, Y is perpendicular to it, note that X and Y are used as coordinate axes as well)

nV/Am^2	=	unit of the time derivative of the electromagnetic field normalized by the transmitter loop current (nanovolts per Ampermeter squared)
TR = Tx	=	transmitter
ch.	=	channel
DIT	=	depth inversion techniques = apparent resistivity versus depth inversion
Ra	=	apparent resistivity
mean	=	mean of apparent resistivity at one station
± dec.	=	one order of magnitude more or less than mean
Rx	=	receiver

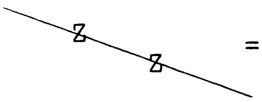

= electric power line

APPENDICES

1/1	Introduction to TDEM
1/2	A successful application of the transient method
1/3	Geonics Ltd., Technical Note TN-12
2/1	TDEM survey in Løkken, overall survey layout 1:50000
2/2	Description of survey details
2/3	Horizontal projection map of interpreted conductive zones in Moen-Damlia-Högåsen
2/4	Horizontal projection map of interpreted conductive zones in Høydal
3/1	Area Svinsås, survey layout 1:5000
3/2	" 1, profile 600 W with interpreted plate model
3/3	" 2, profile 150 W with interpreted plate model
3/4	" 1-2, profiles 600 W and 150 W, DIT-plots 1:10000
4/1	Area Blokkum, survey layout 1:5000
4/2	" , profile Y 30.30
4/3	" , " " " , DIT-plot 1:10000
5/1	Area Moen, survey layout 1:5000
5/2	" , profile 0 with interpreted plate model
5/3	" , " ", DIT-plot 1:10000
5/4	" , " ", reduced linear plot
6/1	Area Damlia, survey layout 1:5000
6/2	" , profile Y 31.75 with interpreted plate model
6/3	" , " " " , DIT-plot 1:10000
7/1	Area Högåsen, survey layout 1:5000
7/2	" , profile Y 32.50 with interpreted plate models
7/3	" , profile Y 33.00
7/4	" , profile Y 33.50
7/5	" , profile Y 33.50, Y-component
7/6	" , profiles 32.50 - 33.50, DIT-plots 1:10000
8/1	Area Björnli, survey layout 1:5000
8/2	" , profile 250 W
8/3	" , profile 0
8/4	" , profiles 250 W and 0, DIT-plots 1:10000
9/1	Area Mogset, survey layout 1:5000
9/2	" , profile Y 33.35
9/3	" , " " " , DIT-plot 1:10000

10/1 Area Høydal, survey layout 1:5000
10/2 " 1, profile Y 36.75 with interpreted plate model
10/3 " , profile Y 37.00 with interpreted plate model
10/4 " 2, profile Y 37.25 with interpreted plate model
10/5 " , profile Y 37.50 with interpreted plate models
10/6 " 3, profile Y 37.75 with interpreted plate models
10/7 " , profile Y 38.00 with interpreted plate models
10/8 " 4, profile Y 38.25 with interpreted plate models
10/9 " , profile Y 38.50 with interpreted plate models
10/10 " , profile Y 38.75 with interpreted plate models
10/11 " 1, profiles Y 36.75 and 37.00, DIT-plots 1:10000
10/12 " 2, profiles Y 37.25 and 37.50, DIT-plots 1:10000
10/13 " 3, profiles Y 37.75 and 38.00, DIT-plots 1:10000
10/14 " 4, profiles Y 38.25 - 38.75, DIT-plots 1:10000
10/15 " , contoured map 1:5000, channel 5, Z comp.
10/16 " , " " " ", X "
10/17 " , " " " 10, Z "
10/18 " , " " " 10, X "
10/19 " , " " " 15, Z "
10/20 " , " " " 15, X "
11/1 Area Urvatnet, survey layout 1:5000
11/2 " 1, profile Y 40.00 with interpreted plate model
11/3 " 2, profile Y 40.50 with interpreted plate model
11/4 " 3, profile Y 41.00 with interpreted plate model
11/5 " 4, profile Y 41.55 with interpreted plate model
11/6 " 5, profile Y 42.00 with interpreted plate model
11/7 " 6, profile Y 42.50 with interpreted plate model
11/8 " 7, profile Y 43.00 with interpreted plate model
8 11/9 " 1-2, profiles Y 40.00 and 40.50, DIT-plots 1:10000
11/10 " 3-4, profiles Y 41.00 and 41.55 DIT-plots 1:10000

11/11	Area Urvatnet 5-6, profiles Y 42.00 and Y 42.50, DIT-plots 1:10000
11/12	" 7, profile Y 43.00 DIT-plot 1:10000
11/13	" , contoured map 1:5000, channel no. 5,Z
11/14	" , " " " " ",X
11/15	" , " " " " 10,Z
11/16	" , " " " " 10,X
11/17	" , " " " " 15,Z
11/18	" , " " " " 15,X
12/1	Area Åmot, survey layout 1:5000
12/2	" 2, profile Y 41.00 with interpreted plate model
12/3	" , profile Y.41.50 with interpreted plate models
12/4	" 1, profile Y 42.00
12/5	" 1-2, profiles Y 41.000, 41.50 and 42.00, DIT-plots 1:10000
12/6	" , contoured map 1:5000, channel no. 5,Z
12/7	" , contoured map 1:5000, " ,X
12/8	" , " " " 10,Z
12/9	" , " " " 10,X
13/1	Transients and time constants of 15 different stations
13/2	Special modeling results of area Björnli, profile 250 W
13/3	" " " " Moen " 0
13/4	" " " " Högåsen " Y 32.50
13/ 5	" " " " Høydal " Y 37.50

INTRODUCTION TO TDEM

By the time domain electromagnetic (TDEM) or transient EM methods it is understood a system, where transmitter energy excites the ground, is cut off and the measurements are done a certain time after the primary has disappeared. The first of the kind was a galvanic method called Eltran (Blau, 1933). The inductive technique was first investigated by Kraev (1937), Tikhonov (1946) and Sheinman (1947). The method developed in the 50s has been widely used for mapping structures in petroleum prospecting and is known as "transient sounding" (Vanyan, 1960). The earliest disclosure to determine the parameters of massive sulfide orebodies was by Wait (1951). The first equipment, Newmont EMP, was developed in 1956 consisting of a large transmitter loop and roving receiver. The current source was composed of ninety 12 V automobile batteries. This system was successfully tested in Cyprus in 1964 (Dolan, 1970). A small-scale, low-power, reconnaissance version and a drill hole version were field tested in South Africa in 1970 (Nabighian 1984).

In 1958 Barringer developed the first airborne TDEM system, INPUT (Barringer, 1962). The Russians paid their attention to a one-loop modification in which generation and reception of the field are accomplished with the aid of one and the same loop. The research resulted in development of a light portable equipment, MPPO-1, commercially manufactured since 1966 (Velikin and Bulgakov, 1967). In 1970s many new TDEM systems were developed: Crone PEM in 1972 initially as a small scale battery operated loop-loop system, UTEM using a triangular pulse became operational in 1972, Newmont Exploration Ltd. tested the first fully digital version of EMP (Mark 5) in 1975, Australian CSIRO designed a microprocessor-controlled unit in 1977 and Geonics EM37 was introduced in 1980.

The first equipment purchased to Finland by Suomen Malmi Oy was Crone PEM, in 1976; perhaps because it reminded so much the popular slingram system. Need to make deeper prospecting brought

Sirotem in 1978, again bought by Suomen Malmi Oy and field tested by Outokumpu Oy Exploration. A drill hole probe for Sirotem was soon also included. The University of Oulu bought the Russian MPP3 system in 1980 and Outokumpu Oy Exploration Geonics EM37 in 1984.

First the proponents of TDEM technique expected to detect EM reflections from boundaries between layers in analogy with the seismic method, until Yost (1952) proved that the transient signals do not allow sufficient resolution to identify individual reflections. The Russians went on developing this sounding principle, but the western world turned more to use profiling for locating sulfide orebodies. At the same time in 1960s the Russians developed a joined sounding and profiling system (MPPO) capable to work in the both applications. This has been probably the most used EM method in the Soviet Union, and it has replaced even slingram for locating shallow conductors. In the reconnaissance work the loop size is increased to 800 x 800 m and more detailed investigation may need only 5 x 5 m loop. A crew of five men and sequential measurement of different time ranges or channels does not make it very cost-effective in the search for shallow targets. Its advantage is that it does not produce "false" anomalies of alluvium, fracture zones or rough topography.

In the western world TDEM became popular because from the results it was easier qualitatively to discriminate conductive overburden effect and the response of a more local conductive orebody underneath. This is especially needed in Australia. Instrument technology progressed profitably to TDEM making it more cost-effective to gather data of larger EM frequency range. In Finland the method has been used mainly to survey deeper targets than slingram, which is still the "first" method to map shallow conductors. A reasonable depth range of the portable TDEM system is from 100 to 500 m.

Now more effective (and heavier) equipments are developed to map geological structures 2 - 3 km deep for petroleum prospecting (Keller et al., 1984). But the method's resolution is still poor and it seems propable that in pace with progressing instrument technology frequency domain EM systems with better resolution proved by Maxiprobe (Sinha, 1979) will override TDEM in few years.

The principle of TDEM measurement is shown in Figures 1 - 3. A dc current pulse is fed into a transmitter loop (Tx) lasting some tens or hundreds of milliseconds. Then it is cut off as quickly as possible, which is normally less than 0.5 ms and depending on the loop size. This is because no electronics can stand an instantaneous cut-off. The measurement is undertaken by the same or another loop or a smaller coil, called roving coil (receiver, Rx). The timing of measurement is selected to cover a range from as close to cut-off as reasonable to 100 - 200 ms after it. The best instruments start from about 50 μs, but some primary is still on. Time range is divided to 20 - 30 gates, called channels, their width is logarithmically increasing when getting farther from the cut-off.

INPUT and UTEM systems are using different kind of transmitter pulse, half sine and triangular, respectively. The last one is technically difficult to form, and the primary is not off at all so that the system is not a "pure" TDEM. But it has the advantage that instead of measuring time derivative of inductive field it measures the field itself. Other transmitter pulses are also possible, a train of random length pulses is one of the most interesting, but difficult to handle (Duncan et al., 1980).

In theory the successive channels are composed of information on different frequencies, and it can be transformed to frequency domain (FD), if it were ideal data. But very small noise can cause a large variation when inversing to FD so that in practice it does not work. From FD to TD the transformation works better! The main problem of TDEM system is that so wide EM spectrum must be observed at the same time, and all the filters of the noise components shorten the total range. The power grid frequency and its harmonics must be filtered, however. In more progressed instruments filtering is helped selecting a transmitted pulse repetition rate so that the power grid frequency is a paired harmonics. Now that the measurement is done summing up sequentially + and - pulses, the response of the power grid is hopefully cancelled out. The sferics is difficult to filter, but integration or summing up of many pulses decreases random noise. This means, however, longer measuring times, normally 1 - 2 minutes, but this is still reasonable, when all the channels are observed at the same time.

When the ground is energized by a loop a magnetic field (Figure 4) charges the conductors, which are like resistance-inductance circuits (Figure 5). After cut-off it takes some time before these natural circuits are discharged again. In a conductor eddy currents are circling around gradually weakening and wandering from the surface inward (Figure 6). The current causes an inductive field postulated by Lentz's law and it is picked up by the receiver loop or coil as a transient voltage with some time constant. Quite lately it was discovered that the primary field after cut-off starts diffusing out- and downward (Nabighian, 1979). To illustrate the happening he called them "smoke rings" (Figure 7). The velocity of the movement depends on the conductivity of the ground being the velocity of light in free space and some km/s in a good conductor. This phenomenon has some harmful consequences: The primary is not totally off during the measurement. It energizes the ground from different directions during its passage. It may move with different velocities to different directions causing nonsymmetrical effects (McCracken, 1981). Quite inconvenient galvanic effects - current gathering and channelling - have been observed (McNeill et al., 1984). This further poors down the resolution of TDEM. One advantage is that the wandering primary can excite quite far away targets, and especially this is useful in deep drill hole measurements. The passage of the primary can be observed in a drill hole and used as an extra parameter (Dyck and West, 1984). TDEM has some analogy with IP when surface charges in a conductor are developed like capacitors. So it is a little bit more sensitive to disseminations than FD systems, but on the other hand so high frequencies as VLF cannot be observed, because of the difficulty to measure close enough to cut-off.

Interpretation of TDEM is not an easy task and the exact way is too cumbersome. During the 1960s the transient response of simple bodies (spheres, cylinders and plates) both in free space and in a conducting host rock environment was studied either analytically (Nabighian, 1970) or through analog modeling. The Russian geophysicists carried out extensive research to understand the general asymptotic behavior of transient fields (Velikin and Bulgakov, 1967). The work on modeling complicated 2 and 3D structures started in the 1970s and is still continuing. In spite of rapid progress of computer technology the analytic modeling of 2D bodies by finite difference method requires 8 hours on a VAX-780 (Barnett, 1984). One improvement is achieved when so called eigencurrent approximation by Annan (1974) is approved for plate model. Dyck (1981) made a program utilizing this, and the calculation takes then 4 minutes. Still more practical solution was found out by Nabighian starting to use equivalent current filament approximation (Barnett, 1984). This is quite suitable for targets not outcropping or intersected by a drill hole being measured. When the transmitter loop is large, the homogeneous half-space generates a distinct anomaly response even in a resistive ground (1000 ohmm) so that it must be regarded in the interpretation process of earlier channels.

1D modeling is easier to do and quite applicable even to more complicated structures as a first approximation, provided the interpreter understands, how 2 and 3D effects manifest themselves. Even 1D analytic solution is so time-consuming that approximative schemes have been created. Spies (1980) published 2-layer model curves, and Lakanen (1986) derived a nomogram to determine apparent resistivity versus inversed depth (DIT) suitable also for multilayer case. This scheme is accurate for a system, where resistivity can be calculated. For the present it is easy to do in the area, where the primary field's moment is vertical, i.e. inside the transmitter loop (early channels) or the outward moving "smoke ring" (later channels), but the work is going on to get rid of this restriction. Pseudosection is a display related to DIT, but where the depth has not been inversed, instead the channel number is used as a vertical scale, and apparent resistivity is contoured.

Some asymptote approximations of the transient curve are common estimates. Lamontagne (1975) suggests that with a fixed large loop mode decay curve should be constructed using peak to peak values. Time constant of the even part of the transient in milliseconds is related to conductivity, size and geometry of the target (Kaufman, 1978; Velikin and Bulgakov, 1967). From small-scale model curves interpretation nomograms have been derived for certain bodies (sphere, thin plate, etc.) and their parameters (depth, radius, etc.). Just recently mathematical modeling has been developed to the point, where the same kind of interpretation criteria can be found out; for instance Gallagher et al. (1985) have calculated curves of a thin plate model for EM37 system as a function of conductance, depth, depth extent, dip and strike length. Some useful nomograms are published. SanFilipo et al. (1985) have calculated response of a 3D prism body and the effect of a conductive half-space and compared the results to 2D situation.

Examples

One thoroughly treated TDEM-case, Kiuruvesi, Kalliokylä, is presented in appendix 1/2. Geonics Ltd made three short EM37 surveys in Sweden, Norway and Finland, the last one was Hannukainen in Kolari (appendix 1/3). Kalliokylä and Hannukainen were similar types, a good large conductor dipping gently. Anomalies in both cases were strong and clear and conductors were easily followed to the depth of at least 500 m. In Hannukainen there were also measured with Maxiprobe system. A comparison shows that there is much more details in the results of Maxiprobe, but EM37 does locate the good conductor well.

One more example is shown here to demonstrate, what kind of an anomaly can be expected with EM37 coming from a large enough conductor at the depth of 400 m. The drilling found black schist just as interpreted, and the conductor is not known to come closer to the surface, Figures 8 - 11. The case is going to be presented in IMM Meeting in Kuopio, 1 - 5 September in 1986 by Rekola.

Some ambiquities of large fixed loop TDEM have been published by Spies and Parker (1984) showing examples, where conductivity variation of overburden causes similar anomalies as bedrock conductors. One separate shallow conductor can be located accurately and the dip determined, but the second parallel nearby conductor behind is difficult to locate precisely with known interpretation means. A large fixed loop system is strongly focusing energy. The moment is strongest in the loop and directed downward. A conductor, whose surface is intersected in the most perpendicular angle by the moment, is energized best, and therefore the system is very geometry sensitive. The most flat lying conductors just below the transmitter loop produce the strongest anomalies (just as overburden). Vertical conductors are best indicated, when situated outside the loop, but they do not get so much energy. And there is an extinction angle, when the energy flows parallel to the conductor and does not induce it, unless it is so long that some part of it is intersected by the moment (Gallagher et al., 1985).

REFERENCES

Annan, A.P., 1974, The equivalent source method for electromagnetic scattering analysis and its geophysical application: Ph. D. thesis, Memorial Univ. of Newfoundland.

Barnett, C.T., 1984, Simple inversion of time-domain electromagnetic data: Geophysics, v. 49, p. 925 - 933.

Barringer, A.R., 1962, A new approach to exploration - the INPUT airborne electrical pulse prospecting system: Mining Congress Journal, v. 48, p. 49 - 52.

Blau, L.W., 1933, U.S. Patent No. 1,911,137.

Dolan, W.M., 1970, Geophysical detection of deeply buried sulfide bodies in weathered regions: Geol. Soc. of Canada Econ. Geol. Rep. 26, p. 336 - 344.

Duncan, P.M., Hwang, A., Edwards, R.N., Bailey, R.C., and Garland, G.D., 1980, The development and applications of a wide band electromagnetic sounding system using a pseudo-noise source: Geophysics, v. 45, p. 1276 - 1296.

Dyck, A.V., 1981, Method for quantitative interpretation of wideband drill hole EM surveys in mineral exploration: Res. in Applied Geophys. No. 23, Geophysics Lab., Univ. of Toronto.

Dyck, A.V., and West, G.F., 1984, The role of simple computer models in interpretations of wide-band drill-hole electromagnetic surveys in mineral exploration: Geophysics, v. 49, p. 957 980.

Gallagher, P.R., Ward, S.H., and Hohmann, G.W., 1985, A model study of a thin plate in free space for the EM37 transient electromagnetic system: Geophysics, v. 50, p. 1002 - 1019.

Kaufman, A.A., 1978, Frequency and transient responses of electromagnetic fields created by currents in confined conductors: Geophysics, v. 43, p. 1002 - 1010.

Keller, G.V., Pritchard, J.I., Jacobson, J.J., and Harthill, N., 1984, Megasource time-domain electromagnetic sounding methods: Geophysics, v. 49, p. 993 - 1009.

Kraev, A.P., 1937, Transient process in a homogeneous submerged medium: Sci. Rep. Leningrad State Univ., No. 14, Soc. Physical Sciences, Issue 3, v. III.

Lakanen, M.E., 1986, A successful application of the transient method, in Electromagnetic methods: S.E. Hjelt and A.F. Fokin, Eds., Report of investigation, Geological Survey of Finland.

Lamontagne, Y., 1975, Applications of wideband time-domain electromagnetic measurements in mineral exploration: Ph. D. thesis, Univ. of Toronto.

McCracken, K.G., 1981, Current gathering effects in EM: Geophysics, v. 46, p. 433 (abstr. only).

McNeill, J.D., Bosnar, M. and Levy, G.M., 1983, Large loop transient EM surveys in a resistive environment - three case-histories: Geonics Ltd., Technical report.

McNeill, J.D., Edwards, R.N., and Levy G.M., 1984, Approximate calculations of the transient electromagnetic response from buried conductors in a conductive half-space: Geophysics, v. 49, p. 918 - 924.

Nabighian, M.N., 1970, Quasi-static transient response of a conducting sphere in a dipolar field: Geophysics, v. 35, p. 303 - 309.

Nabighian, M.N., 1979, Quasi-static transient response of a conducting half-space - An approximate representation: Geophysics, v. 44, p. 1700 - 1705.

Nabighian, M.N., 1984, Time-domain electromagnetic methods of exploration - Foreword and introduction: Geophysics, v. 49, p. 849 - 853.

SanFilipo, W.A., Eaton, P.A., and Hohmann, G.W., 1985, The effect of a conductive half-space on the transient electromagnetic response of a three-dimensional body: Geophysics, v. 50, p. 1144 - 1162.

Sheinman, S.M., 1947, Concerning transient electromagnetic fields in the earth: Prikladnaia Geofiz., no. 3.

Spies, B.R., 1980, TEM in Australian conditions: Ph. D. thesis, Macquarie University.

Spies, B.R., and Parker, P.D., 1984, Limitations of large-loop transient electromagnetic surveys in conductive terrains: Geophysics, v. 49, p. 902 - 912.

Tikhonov, A.N., 1946, On the transient electric current in a homogeneous conducting half-space: Izvestia Akad. Nauk, SSSR, Seria Geograf i Geofiz., v. 10, no. 3.

Vanyan, L.L., 1960, Elementary theory for transient electromagnetic fields: Prikladnaia Geofizika, no. 25.

Velikin, A.B., and Bulgakov, Yu. I., 1967, Transient method of electrical prospecting (one-loop version): Presented at International Seminar on Geophysical Methods of Prospecting for Ore Minerals, Moscow.

Wait, J.R., 1951, Transient EM propagation in a conducting medium: Geophysics, v. 16, p. 213 - 221.

Yost, W.J., 1952, The interpretation of electromagnetic reflection data in geophysical exploration, Part I, General theory: Geophysics, v. 17, p. 89 - 108.

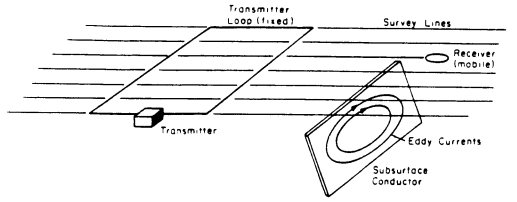

FIGURE 1. Survey configuration.

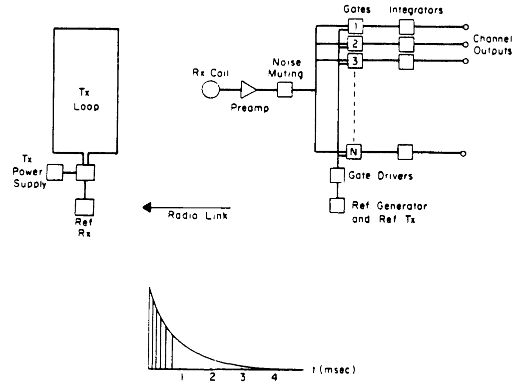

FIGURE 3. Block diagram and typical transient (showing initial gates).

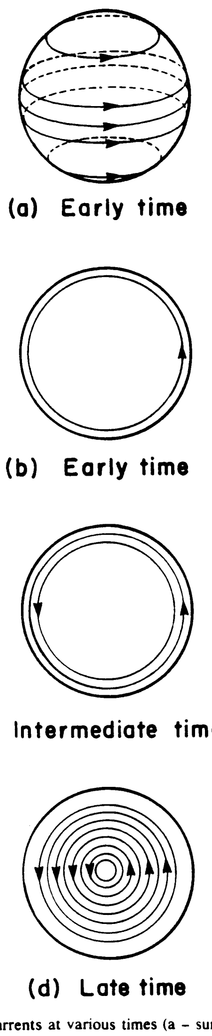

FIGURE 6. Sphere currents at various times (a – surface currents; b–d – equatorial/plane currents).

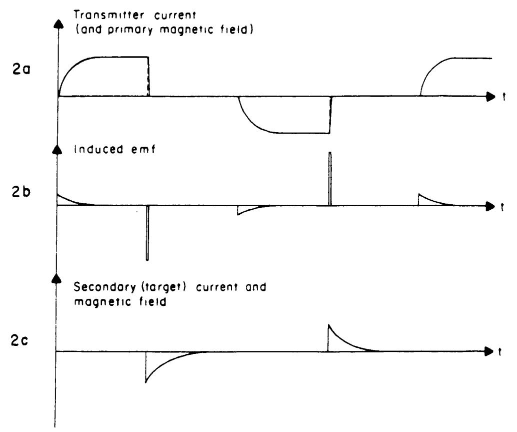

FIGURE 2. System waveforms.

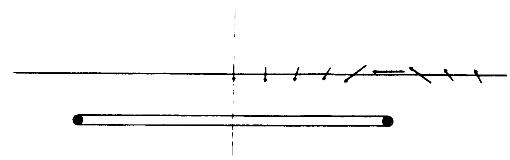
FIGURE 4. Magnetic field above current ring.

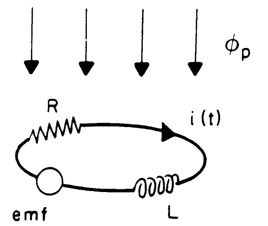

FIGURE 5. Wire loop target.

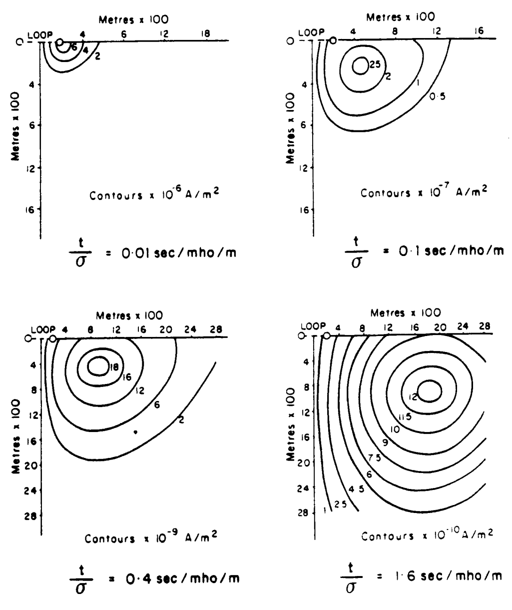

FIGURE 7. Computed contours of current density passing through loop centre (loop has dimensions 400 × 800 m (5)).

422112 SORSANSALO Y=182.3

432 EM37 MD/Z TR loop 500*500m

1:10000 centre Y=182.3/X=89.5

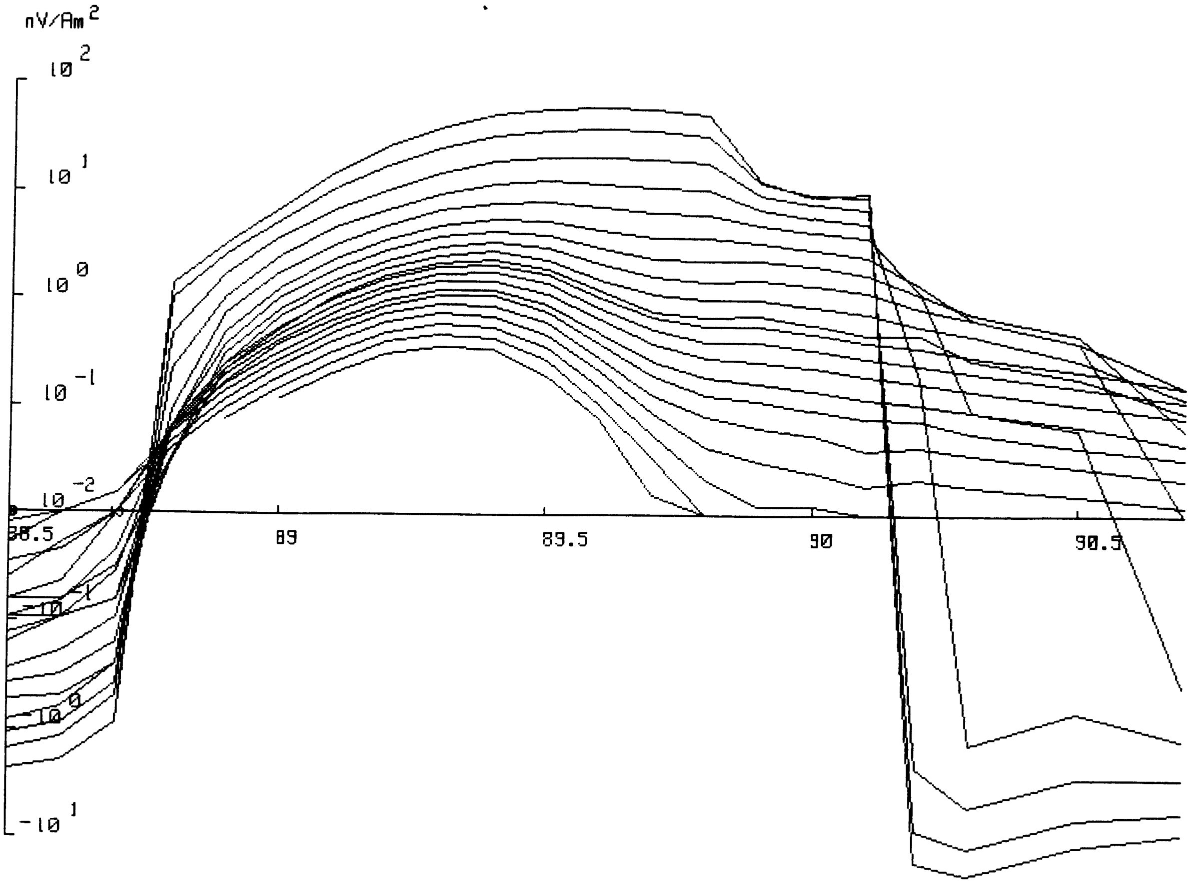

422112 SORSANSALO Y=182.3

432 EM37 MD/X TR loop 500*500m

1:10000 centre Y=182.3/X=89.5

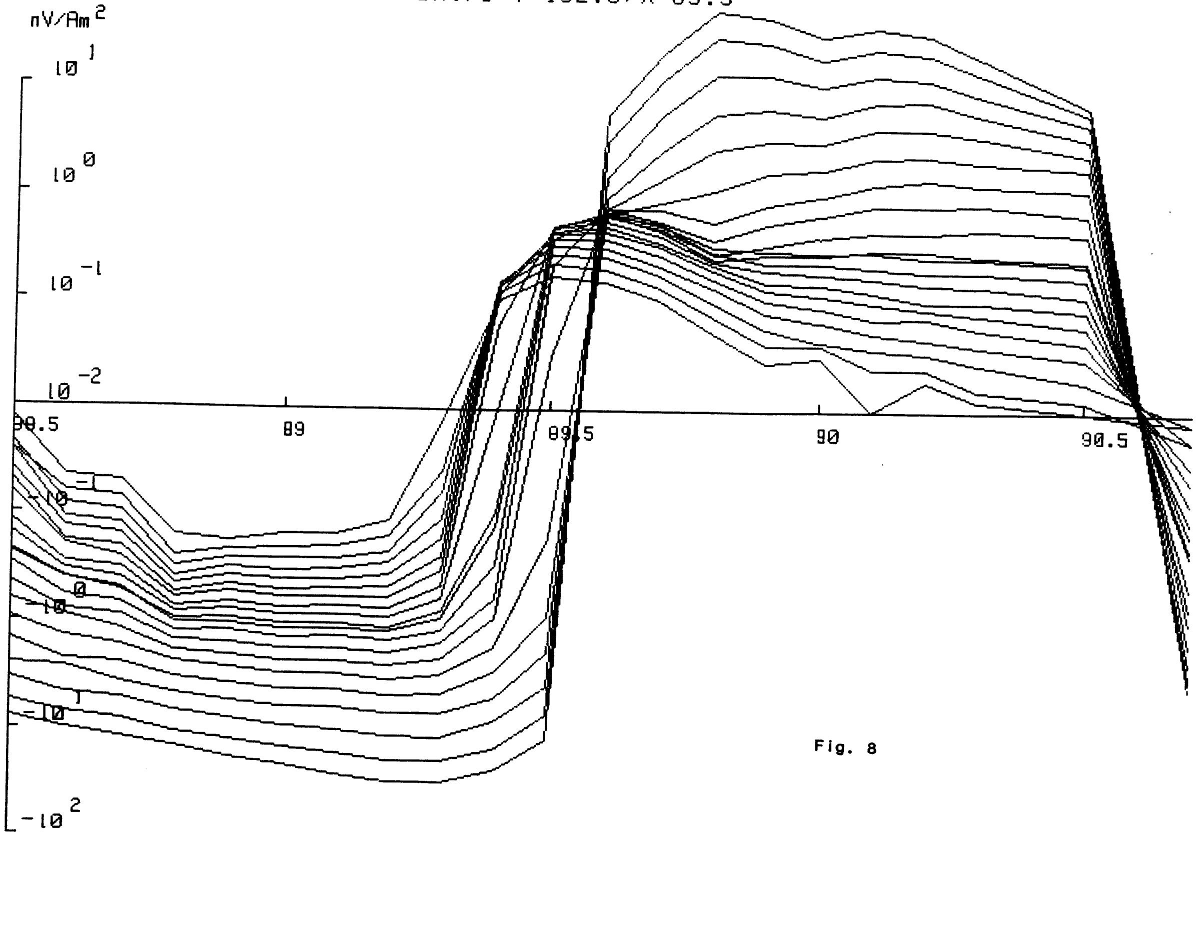

Fig. 8

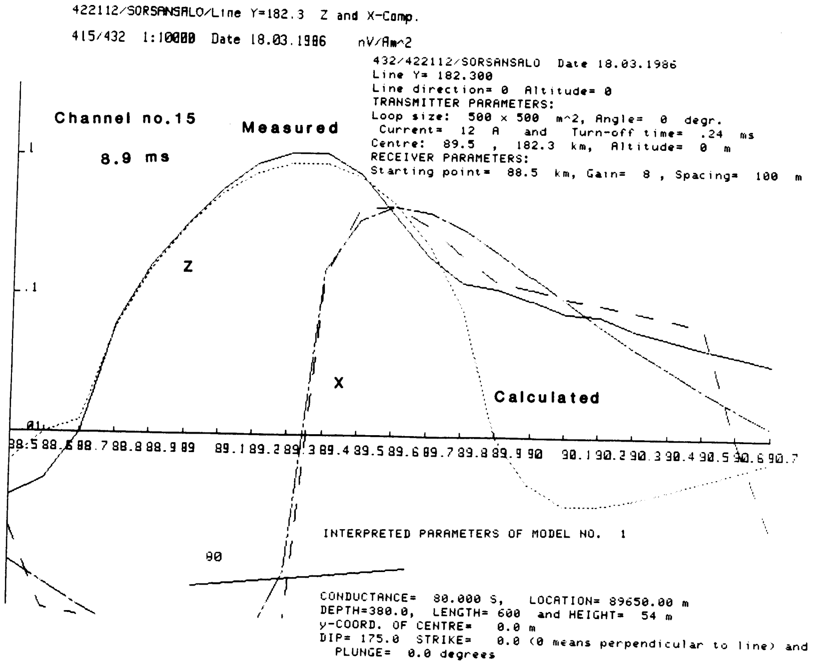

Fig. 9

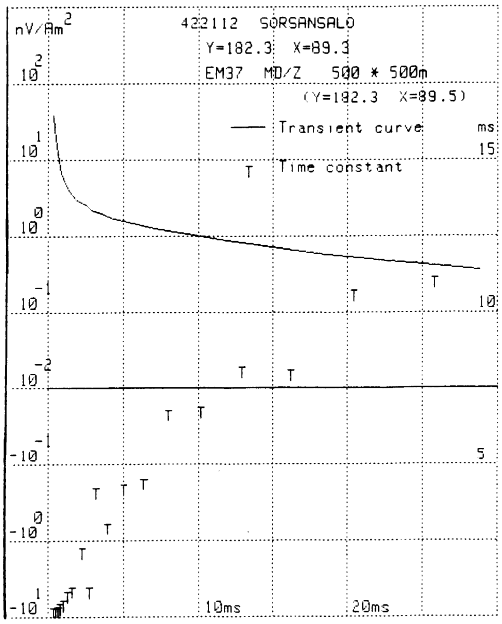

Fig. 10

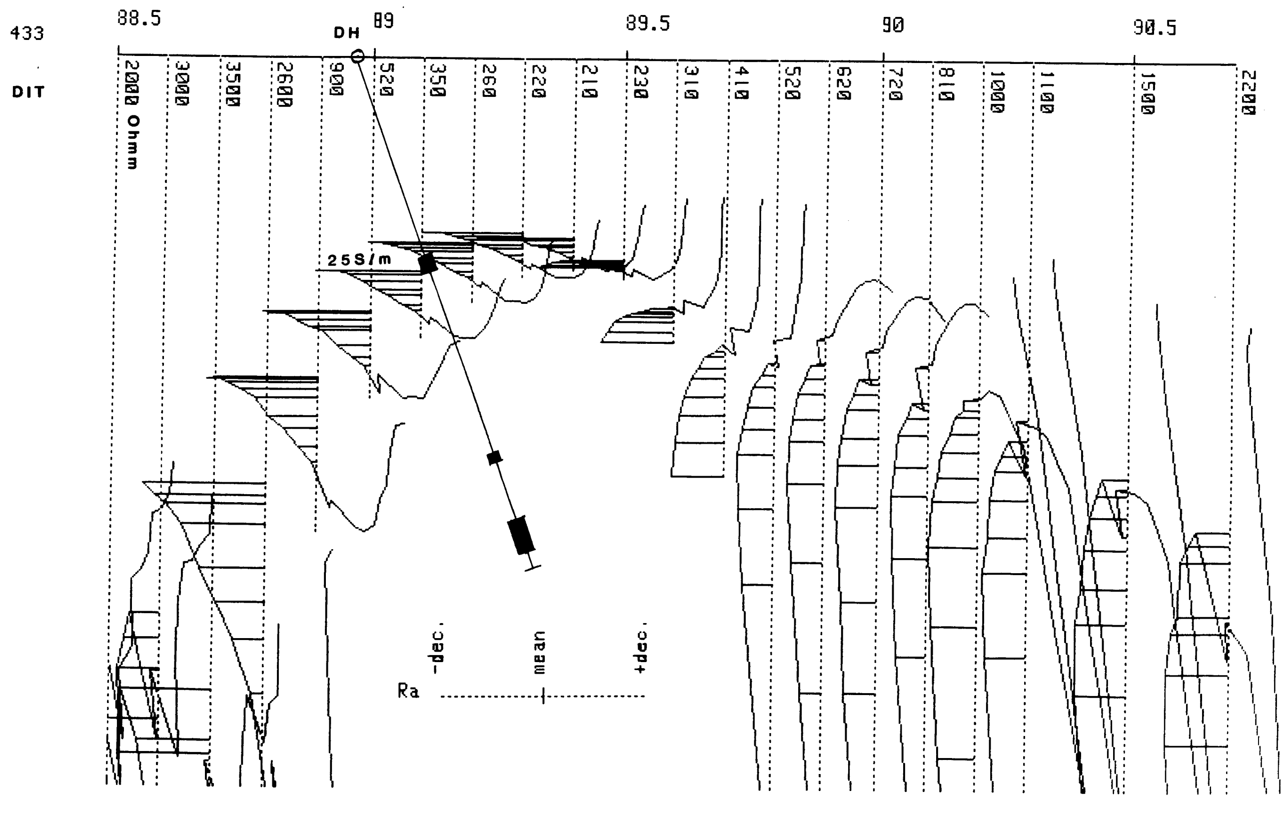

Fig. 11

A SUCCESSFUL APPLICATION OF THE TRANSIENT METHOD

Ensio Lakanen, Outokumpu Oy, Exploration,
P.O.Box 27, SF-02201 Espoo 20, FINLAND

ABSTRACT

The Kalliokylä sulphide orebody, which was found in 1959, has been studied several times geophysically. Since 1979 electric deep sounding, AMT, TDEM and mise-à-la-masse measurements have been performed to establish the depth extensions of the highly conductive sulfide plate. Because of the high contrast and quite gentle dip the results are satisfactory even when the data are interpreted with simple models. A new way of inversing the TDEM results is described.

INTRODUCTION

The discovery of the Kalliokylä orebody in Kiuruvesi in 1959 is one of the few made with an airborne EM method in Finland (Rotary field, Ketola et al., 1972), although a couple of years earlier some sulfides had been found in a nearby outcrop. After the airborne survey studies proceeded rapidly. In the same year, ground surveys and the subsequent drilling localized a pyrrhotite and pyrite mineralization with some zinc and copper. The orebody increased as studies progressed and soon it was found marginal for economic exploitation. In the late 1970s interest was focused to trace the extensions of the orebody. More drilling, deep EM soundings and a special structural study were undertaken (Koistinen, 1984). One aim was to discover a portion more enriched in zinc and copper.

Geology

The orebody is located at the contact between altered rocks (cordierite-anthophyllite) and gneisses (Fig. 1A). The Ruostesuo orebody has been estimated to contain 1.7 Mt of ore grading 35 % S, 2.5 % Zn and 0.36 % Cu down to about 150 m level. The total length of the orebody exceeds two kilometres, but little is known about the extensions at depth; there is room for ore reserves of even 10 Mt.

Outcrops are poor but 134 drill holes provide information on the shallow parts of the formation. There is only one deeper hole (350 m), drilled in 1983. According to Koistinen (1984), the structure is as shown in Fig. 1B. F2 is the predominant major deformation phase, and F1 consists of small, isoclinal folds with amplitudes no longer than a few tens of metres. The NW component of F3 may be significant locally, whereas the NE component is casual. F4 is rare, weak and local; other phases have not been observed. The intensity of F1 obviously controls the thickness of the ore, and it is mostly weak.

Petrophysics

The rocks in the area are not complicated in physical properties. The ore contains abundant pyrrhotite, rendering it moderately magnetic. However, the altered rocks contain magnetite showings in which the susceptibility may be up to one SI unit. In places the mafic volcanite is magnetized to some extent. The mica gneisses are neutral and no black schists have been encountered. The ore exceeds 4000 kg/m^3 and the altered rocks are c. 3000 kg/m^3 in density, a local increase being due to garnet. The density of mafic volcanite is also c. 3000 kg/m^3 and that of acid volcanite and gneisses 2700 - 2800 kg/m^3. The ore is many orders of magnitude more conductive (up to 1000 S/m) than the other rocks of the area.

Magnetic survey permits the altered rocks to be located, but mostly the orebody can be detected, too. The gravity correlates with the magnetized area, indicating an increase in the garnet abundance or the thickness of the altered rocks. The ore can be located unambiguously only by electric and EM methods, but the grade of Zn and Cu cannot be estimated.

Measurements

Various geophysical surveys have been carried out in the area, the older ones being reported by Laurila (1963). In the early 1980s, 73 stations with AMT, 200 stations with TDEM coincident loop 100 x 100 m (Sirotem), and 100 stations with a fixed transmitter loop 400 x 600 m (EM 37) were surveyed. Three holes totalling c. 600 m were measured with a Sirotem borehole probe. The sparsely spaced profiles covering the whole area and nine holes were measured with the mise-à-la-masse method (or charged potential = CP).

RESULTS

The magnetic map (Fig. 2A) is complicated because of so many sources, but anomalous continuations marked A, B and C towards SE are interesting possibly indicating extensions of ore. HLEM (Slingram) outlines the ore outcrops (Fig. 2B). At the eastern end there is a separate smaller anomaly. CP result is not very informative (Fig. 2B). The whole area of altered rocks is at the same potential. There are but few details. The boundary is sharp to south and west but gradual towards north and east. Extensions A and B can be noticed. The borehole data demonstrated that the ore intersections are at the same potential, which changes smoothly towards the country rock indicating large extensions (see Fig. 3A).

TDEM with a coincident loop (Fig. 2C) produced more details than CP. The ore outcrops are well defined. There is an anomaly-free part in the middle of the area, and extensions A and B are clearly visible. Profile X = 54.4 passes over the extension A. Three shallow holes intersect the 2 - 10 m thick sulfide plate, the deepest one suggesting more gentle dip. TDEM results also suggest that the plate continues quite deep (Fig. 3B). The reliability of the interpretation, however, is reduced by the separate eastern conductor (cf. HLEM result) masking the anomaly of deeper parts of the known orebody. Both seem to dip gently to east. Two other parallel profiles measured at intervals of 200 m are similar (not shown); the orebody continues for at least 300 - 400 m eastwards. The two-layer modeling result looks nice, and the DIT, the principle of which is described in the appendix, shows the same behaviour except that the conductivity is abruptly reduced at Y = 69.2.

The same profiles were surveyed with AMT in the late autumn, which was not very favourable timing thinking of the intensity of the natural source fields. The results are poorly compatible with the assumed structure, and there is no suggestion of a gently dipping target (Fig. 3C). The easternmost conductor can be seen at higher frequencies and possibly as elevated depth values at Y = 69.1 and 69.2. The result is obviously distorted also by the 3D effects. The structural model does suggest an anticlinal fold whose axis plunges to ESE diagonally to the profiles.

A deep hole (No. 134) collared at Y = 69.25 was drilled in section X = 54.4 to test the interpretation. It intersected the easternmost conductor at a depth of about 60 m, a thin sulfide body. The next intersection was anticipated at a depth of less than 200 m but was encountered at almost 300 m deep. Petrophysical checking, however, pinpointed a narrow conductive zone (1 S/m) at a depth of slightly less than 200 m, but it was not the right sort of rock.

CP and TDEM measurements in the drill hole (Figs. 3A and 3D) showed that the deepest intersection belongs to the extension of the known orebody, and hence the ground TDEM result must have been biased subtly by the response of the eastern conductor, which also dominates the TDEM borehole data. According to the interpretation of the borehole data the extension of the lower plate might continue less than 100 m, but the used plate of algorithm is not accurate and very suitable for the intersected bodies.

After drilling, EM 37 survey was carried out with a large transmitter loop, 400 x 600 m in size, and with the centre at X = 54.4, Y = 69.175, i.e. above the eastern conductor. The result from profile X = 54.4 can be interpreted with a single conductive plate, which corresponds fairly accurately to the intersections (Fig. 4A). The DIT, which is distorted close to the surface, because that site is outside the transmitter loop (cf. appendix), gives a value about 50 m too shallow over the deepest intersection. There is no sudden decrease in the conductivity and it suggests that the plate continues eastwards for at least 200 m from the deepest drilled intersection. The influence of the overlying conductor is noticed as a sign reversal of the early channels, and an increase in the amplitude. This case shows the need for a model that takes the mutual inductance into consideration. The DIT of transversal profile Y = 69.1 (Fig. 4B) is surprisingly uniform, demonstrating that the upper edge of the plate is fairly wide (200 m) and even, but the depth estimate is again 50 m too shallow. A sharp boundary is situated in the south side, but gentle dip northwards for another 200 m. The plate model interpretation gives a total width of up to 700 m also too shallow. Drill hole 134 intersects the plate close to its centre in X direction, for the hole is known to deviate northwards by 50 m. The time constant of the conductor was calculated to be about 10 ms.

There are no deep drill holes in the west of the area and hence those results are beyond the scope of the present paper.

SUMMARY

The extensions of the orebody, which differs clearly from the environment in conductivity, can be traced to a depth of 200 - 400 m by TDEM. It suggests a marked augmentation of the potential ore reserves in the area. On account of the complex structures, the estimates are not reliable everywhere. Even then, new information has been obtained on the behaviour of the meth-

ods. TDEM with a coincident loop reveals details in the central parts of the area. The deep hole drilled in the east of the area demonstrates that the depth estimates based on the layered earth model are too shallow. Borehole data and their interpretation, however, fits well to the assumed structure. The fixed loop system gave better depth estimates when the large transmitter loop had been placed over the eastern interfering conductor to eliminate its influence.

DEPTH INVERSION TECHNIQUES, DIT

It is very laborious to model electromagnetic methods. Even the layered earth model, or 1D, may take minutes to compute, and 2D and 3D calculations much more. For routine interpretation of observed readings we need various short-cuts, or rules of thumb. One of the most popular ways is asymptote approximation, for instance Niblett-Bostick transformation (Hjelt et al. in this publication) for the plane wave case.

First, the geometry due to the method must be eliminated by calculating a suitable parameter, the apparent resistivity most commonly. Each observed reading is transformed to a respective apparent resistivity, which corresponds to a value of some homogeneous earth. To determine a minimum thickness of the homogeneous layer, necessary to ensure that any resistivity variations deeper than it do not influence the result, one could use the skin depth estimate (e.g. Kaufman and Keller, 1981, Fig. 17.3 or Macnae and Lamontagne, 1984), but more precisely and quite easily it can be obtained from the two-layer model curves of the desired method. The asymptote is the tangent line of the model curve set intersecting the horizontal axis. However, the real influence starts somewhat earlier, because the model curves approach the horizontal axes more gently. The intersection gives the thickness or depth estimate required! The model curves may also oscillate around the horizontal axes, and some methods and geometries produce so-called overshooting, which means that the model curves first change to an opposite direction, compared to the resistivity contrast.

Plotting the apparent resistivities suitably scaled along the horizontal axis and the corresponding calculated depth estimate along the vertical axis transforms the sounding curve readily into the depth curve, i.e. DIT. Deflections from the vertical trend indicate a resistivity contrast, and the respective depth is the true one to some accuracy. DIT applies even for a multilayer case when the successive layer has a conductance large enough compared with previous ones. Deflections of apparent resistivity can be enhanced by taking the gradient of the apparent resistivity (compare to the Niblett-Bostick transformation). Some modifications have been reported by Jones and Foster (1983) and by Gamble (1983). Absolute resistivities are seldom obtained; the thickness should be exceptionally large. DIT results of adjacent soundings are plotted as profiles on a suitable distance scale. Certain tricks, for instance, the static correction and automatic gain as presented by Warner et al. (1983) can be used to improve readability.

DIT has been applied to dipole-dipole multifrequency (Maxiprobe system) soundings by Sinha (1979). Apparent resistivity is obtained from the ratio of the vertical to radial component of the magnetic field. Other possibilities described by Kaufman and Keller (1981, p. 145) have been used by Valla and Gasnier (1984). In this case the correctness of the DIT for the multilayer situation has not been derived; it has only been tested with the calculated 1D models. The users of the Maxiprobe system have noticed that it is possible to discriminate successive layers if their conductance is more than 10 % of the sum conductance of the overlying layers. DIT has recently gained popularity in processing airborne electric data (to eliminate the geometry of the system, e.g. Peltoniemi, 1982 and Mundry, 1984), but the number of frequencies available is too small to locate the layer boundaries. Similar processing could be derived for the HLEM and other EM methods as well.

DIT has not been applied for the TDEM in Western countries, but it has long been a common method in the Soviet Union. It is well known that the apparent resistivity can be calculated for the coincident loop geometry channel by channel (Lee and Lewis, 1974 and more accurately Raiche and Spies, 1981). The Soviet geophysicists have derived a following late-time approximation for the conductance:

$S = 474\sqrt{t/\rho_a(t)}$ (Kvashnin, 1984, pers. comm.)

where t in seconds, is the time since the cut off of the transmitted pulse and $\rho_a(t)$ is the respective apparent resistivity in ohmmeters.

DIT is completed simply by calculating the thickness

$h(t) = S \cdot \rho_a(t)$

The accuracy and applicability of the formula is still to be checked. A real DIT nomogram was constructed (Fig. 5), using the two-layer model curves made by Spies (1980). It is unfortunate that, on the contrary to the frequency domain methods, the resistivity contrast affects considerably the depth estimate of the time domain data. Moreover, an isolating layer starts bending the sounding curve sooner than a conductor at the same depth. The difference can be marked; an isolator located twice as deep shows up in the same time channel. One of the reasons for the contrast dependancy is that the response is a sum of many frequencies at every moment of time. However, it is affected more strongly by the overshoot, which increases in length when the conductivity of the lower layer increases.

Lee and Lewis (1974) have published 1D calculations. A three-layer case, where the second layer is much more conductive than the others, $\sigma_2/\sigma_1 = 400$, the thickness of the first one, $h_1 = 100$ m, h_2 not given, was tested with DIT. The Soviet formula gave a depth of 70 m to the conductive layer; only 60 m was obtained from the nomogram with large contrast. However, in the early channels, time 0.5 ms, the depth was 25 m more, which must be due to overshooting. If the contrast were about 50 the depth estimate would be correct (the conductance ratio is 50 if $h_2 = 12.5$ m). A four-layer case: $\sigma_1 = 0.1$ S/m, $h_1 = 20$ m, $\sigma_2 = 0.01$, $h_2 = 155$, $\sigma_3 = 1$, $h_3 = 5$ m and $\sigma_4 = 0.01$ was also studied. The third most conductive layer is weakly observable from the bending of the DIT curve, starting at the correct depth when using the Soviet formula or nomogram. These and other tests have shown that the use of DIT is not straightforward.

Real massifs can seldom be regarded as 1D models. The following examples have been taken from the small-scale model results of Ogilvy (1983) (Fig. 6). For a vertical plate DIT behaves so that the upper edge of the inversed curves on both sides of the plate descend rapidly ($>45^{o}$). The thicker is the plate, the better is the depth estimate at the middle of the plate. The dip is easy to see, because on the hanging wall side the DIT curves incline at a much slower rate and the depth estimates correspond approximately to the perpendicular distance from the centre of the loop to the plate. The more gentle is the dip, the better are the estimates, and even the depth extension may be noticed. With a horizontal plate wider than the loop size the estimates are surprisingly correct and the boundaries are clearly visible (Fig. 6D). The conductive overburden does not jeopardize the DIT result, but it is almost impossible to estimate the thickness of the plate with this technique. Finally the DIT result for the cylinder is shown (Fig. 6F) with a conductive overburden. These examples show that DIT can be used for 2D and even for 3D situations to obtain the first estimate to the upper surface of a conductive body. Together with the plate approximation derived by Nabighian (published by Barnett, 1984 and McNeill et al., 1984) it is possible to make serious and yet fast interpretations.

The success of using DIT for TDEM depends greatly on the way the apparent resistivity is calculated. Accurate formulas are cumbersome to calculate. That is why the late time approximation is commonly used. The vertical primary moment is also provided. This is true at the middle of the transmitter loop, but applies roughly almost throughout the inner part of the loop. Because of the smoke-ring phenomenon (Nabighian, 1979), the primary current loop expands as a function of time, and in a resistive ground it propagates rapidly. Hence even a station outside the initial loop can be treated the same way during the late times. Studies are being carried out at certain universities to find more general ways of calculating apparent resistivities.

REFERENCES

Barnett, C.T. 1984, Simple inversion of time-domain electromagnetic data. Geophysics, Vol. 49, p. 925-933.

Bostick, F.X., Jr. 1977, A simple and almost exact method of MT analysis. Abstract: Workshop on electrical methods in geothermal exploration, Utah.

Gamble, I.D. 1983, Simple one-dimensional magnetotelluric inversions. Expanded abstract: Presented at the 53rd Annual International SEG Meeting, Las Vegas, September 11-15, 1983.

Jones, A.G., Foster, J.H. 1983, An objective real-time data adaptive technique for efficient in-field model resolution improvement in magnetotelluric studies. Expanded abstract: Presented at the 53rd Annual International SEG Meeting, Las Vegas, September 11-15, 1983.

Kaufman, A.A., Keller, G.V. 1981, The magnetotelluric sounding method. Amsterdam, Elsevier.

Ketola, M., Laurila, M., Suokonautio, V. 1972, On a digital two-plane rotary field airborne system and its use in conjunction with the magnetic method in Finland. Geoexploration, Vol. 10, p. 203-220.

Koistinen, T. 1984, Kiuruveden Kalliokylän geologiset tutkimukset. Malmin ja ympäristön rakennegeologiaa. Unpublished report, Outokumpu Oy, 10 p. (in Finnish).

Laurila, M. 1963, The geophysical "case history" of Kalliokylä sulfide deposit. Geoexploration, Vol. 1, p. 16-24.

Lee, T., Lewis, R. 1974, Transient EM response of a large loop on a layered ground. Geophys. Prosp., Vol. 22, p. 430-444.

Macnae, J.C., Lamontagne, Y. 1984, Data processing techniques for EM sounding and prospecting. Expanded abstract: Presented at the 54th Annual International SEG Meeting, Atlanta, December 2-6, 1984.

McNeill, J.D., Edwards, R.N., Levy, G.M. 1984, Geophysics, Vol. 49, p. 918-924.

Mundry, E. 1984, Geoelectrical model calculations for two-dimensional resistivity distributions. Geophysical Prospecting, Vol. 32, p. 124-131.

Nabighian, M.N. 1979, Quasi-static transient response of a conducting half-space - An approximate representation. Geophysics, Vol. 44, p. 1700-1705.

Ogilvy, R.D. 1983, A model study of the transient electromagnetic coincident loop technique. Geoexploration, Vol. 21, p. 231-264.

Peltoniemi, M. 1982, Characteristics and results of an airborne EM-method of geophysical surveying. Geol. Survey of Finland, Bull. 321, 229 p.

Raiche, A.P., Spies, B.R. 1981, Coincident loop TEM master curves for interpretation of two-layer earths. Geophysics, Vol. 46, p. 53-64.

Sinha, A.K. 1979, Maxiprobe EMR - 16, A new wide-band multi-frequency ground EM system. Current research, Part B, Geological Survey of Canada, Paper 79-1B, p. 23-26.

Spies, B.R. 1980, TEM in Australian conditions. Ph.D. thesis, Macquarie University.

Valla, P., Gasnier, S. 1984, Broadband frequency electromagnetic soundings with absolute phase reference. Expanded abstract: Presented at the 54th Annual International SEG Meeting, Atlanta, December 2-6, 1984.

Warner, B.N., Bloomquist, M.G. and Griffith, P.G 1983, Magneto-telluric interpretations based upon new processing and display techniques. Expanded abstract: Presented at the 53rd Annual International SEG Meeting, Las Vegas, September 11-15, 1983.

Figure captions

Fig. 1. The geology of the area. A) ground projection, B) structural model by Koistinen with the assumed deformation phases.

Fig. 2. Geophysical countour maps of the area. A) magnetic, B) HLEM and CP and C) Sirotem channel 5 = 2 ms. The extensions are marked with letters A, B and C. Also marked is profile X = 54.4.

Fig. 3. Sections of profile X = 54.4: A) CP result, B) TDEM coincident loop result, 2-layer interpretation and DIT, C) AMT result and Bostick inversion and D) TDEM borehole result with plate model interpretation.

Fig. 4. TDEM fixed loop system results; A) profile X = 54.4 and B) profile Y = 69.1. Also included are the DIT and plate interpretation of channel 17 = 14.4 ms.

Figure 5. Depth inversion techniques (DIT) nomogram for TDEM coincident loop with derivation of apparent resistivity. The use of the nomogram is straightforward: The observed reading, Bz, normalized by current in μV/A is multiplied by time in ms and divided by the loop radius in m. This value is plotted on the left-hand vertical axis and lined horizontally to intersect the ρ-curve (this is a late-time approximation). The apparent resistivity can now be read from the horizontal axis with the normalizing factors. At the same time the intersection of the desired curve, h_R for the Soviet formula or different conductivity contrasts, gives the depth in m from the right-hand vertical axis with the loop radius as a normalizing factor. δ-line (dashed) is the equivalent of the skin depth when the frequency is replaced by 1/t. Apparent resistivity can be obtained in some other ways as well and for a square loop an equivalent radius must be calculated.

Figure 6. 3D models of the small scale measurements taken from Ogilvy (1983), and DIT results, h_R-curve applied. A) corresponds to Ogilvy's Fig. 15, B) to Fig. 5, C) to Fig. 6, D) to Fig. 24, E) to Fig. 23 and F) to Fig. 22. The strike length is 2L (L is a loop diameter).

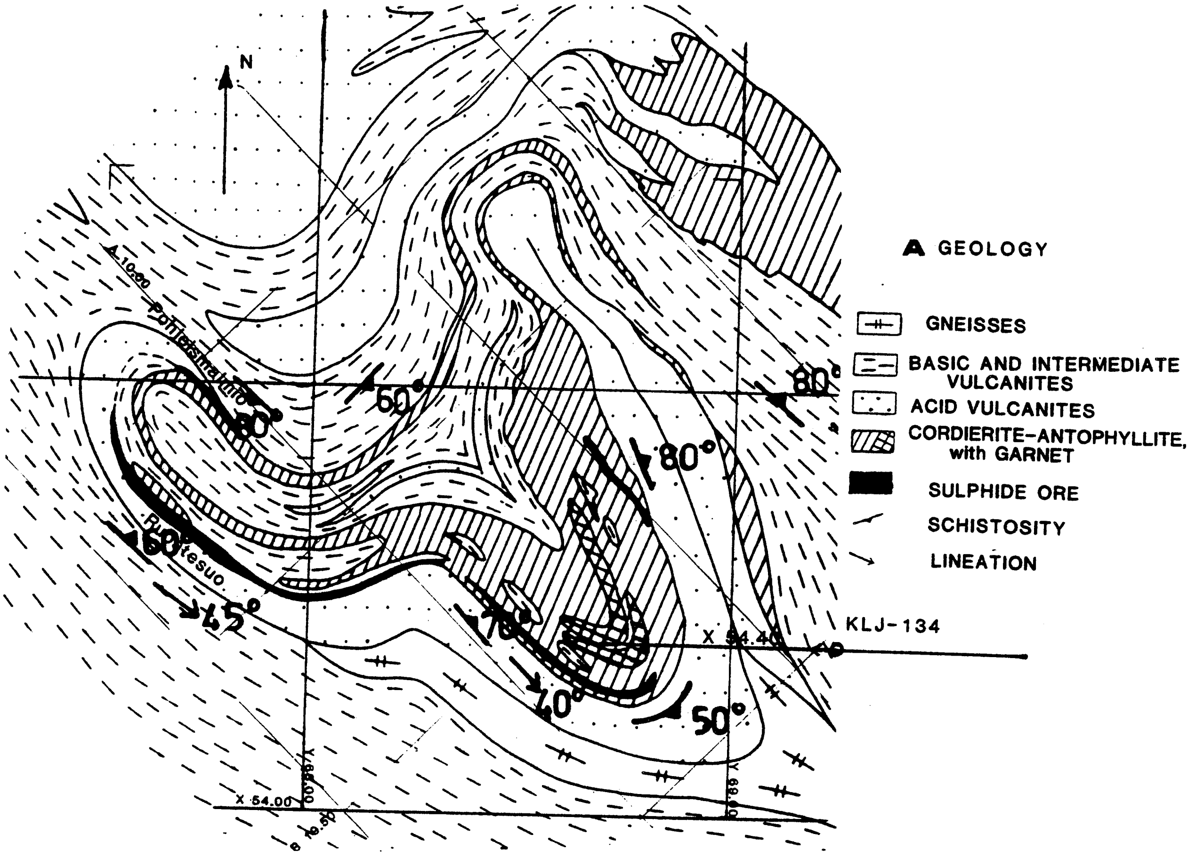

B TECTONIC INTERPRETATION

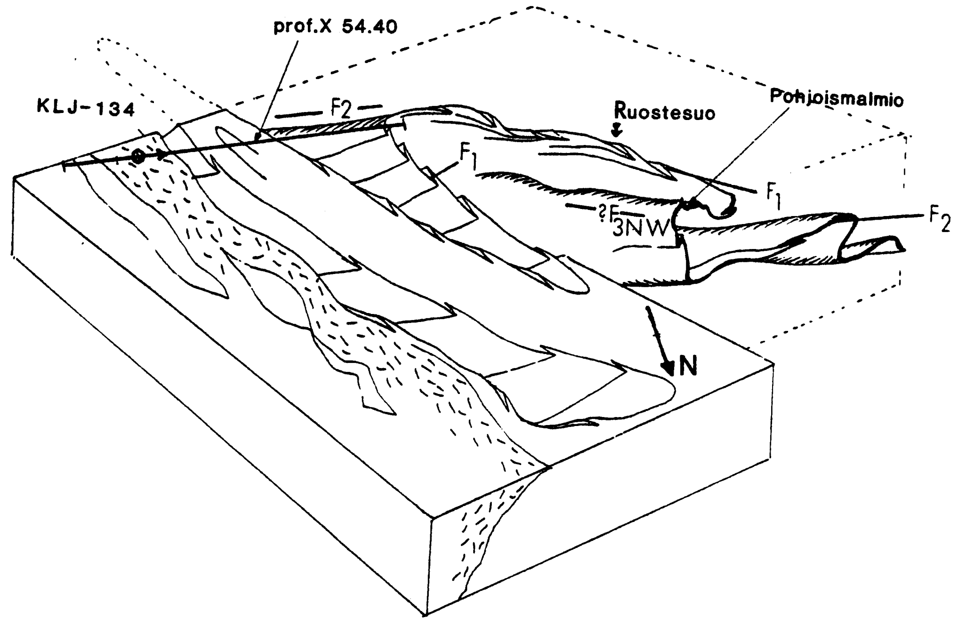

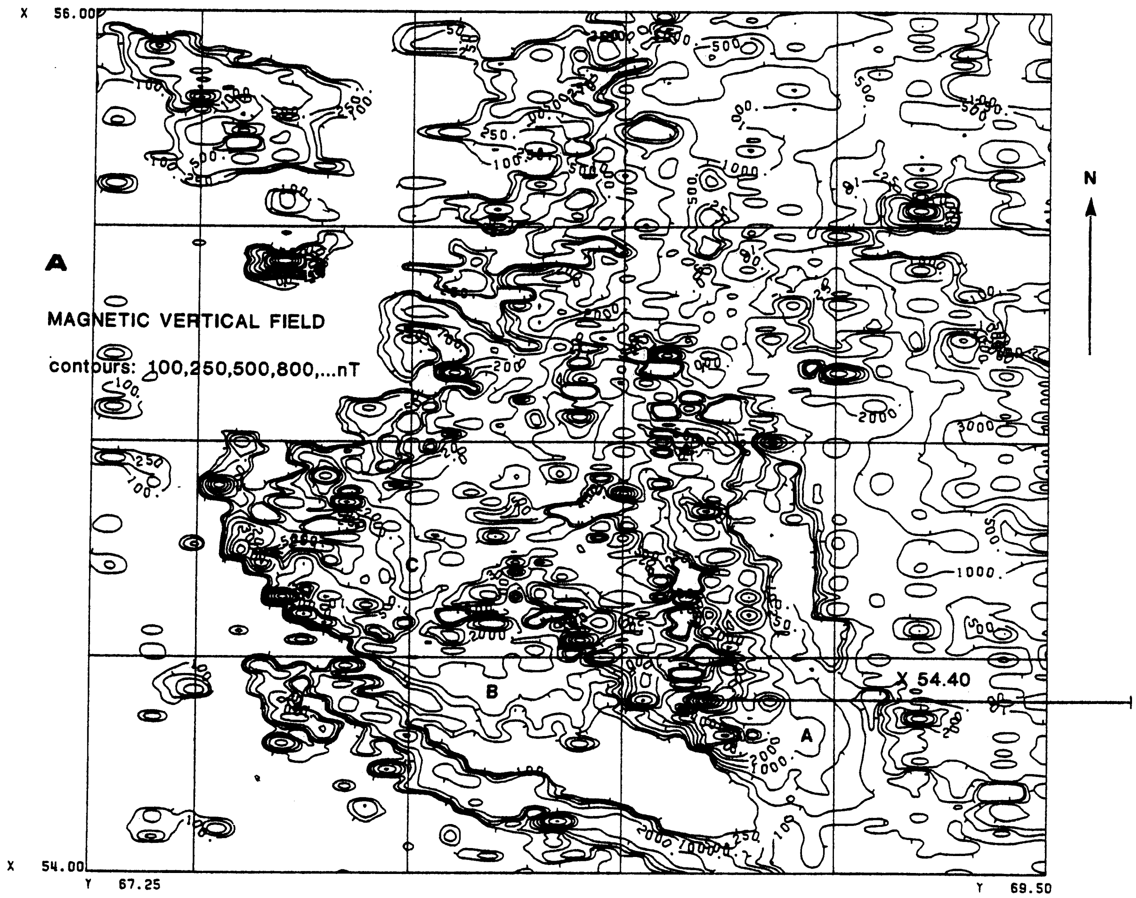

A
MAGNETIC VERTICAL FIELD
contours: 100,250,500,800,...nT
X 56.00
X 54.00
Y 67.25
Y 69.50
N
X 54.40
A
B
C

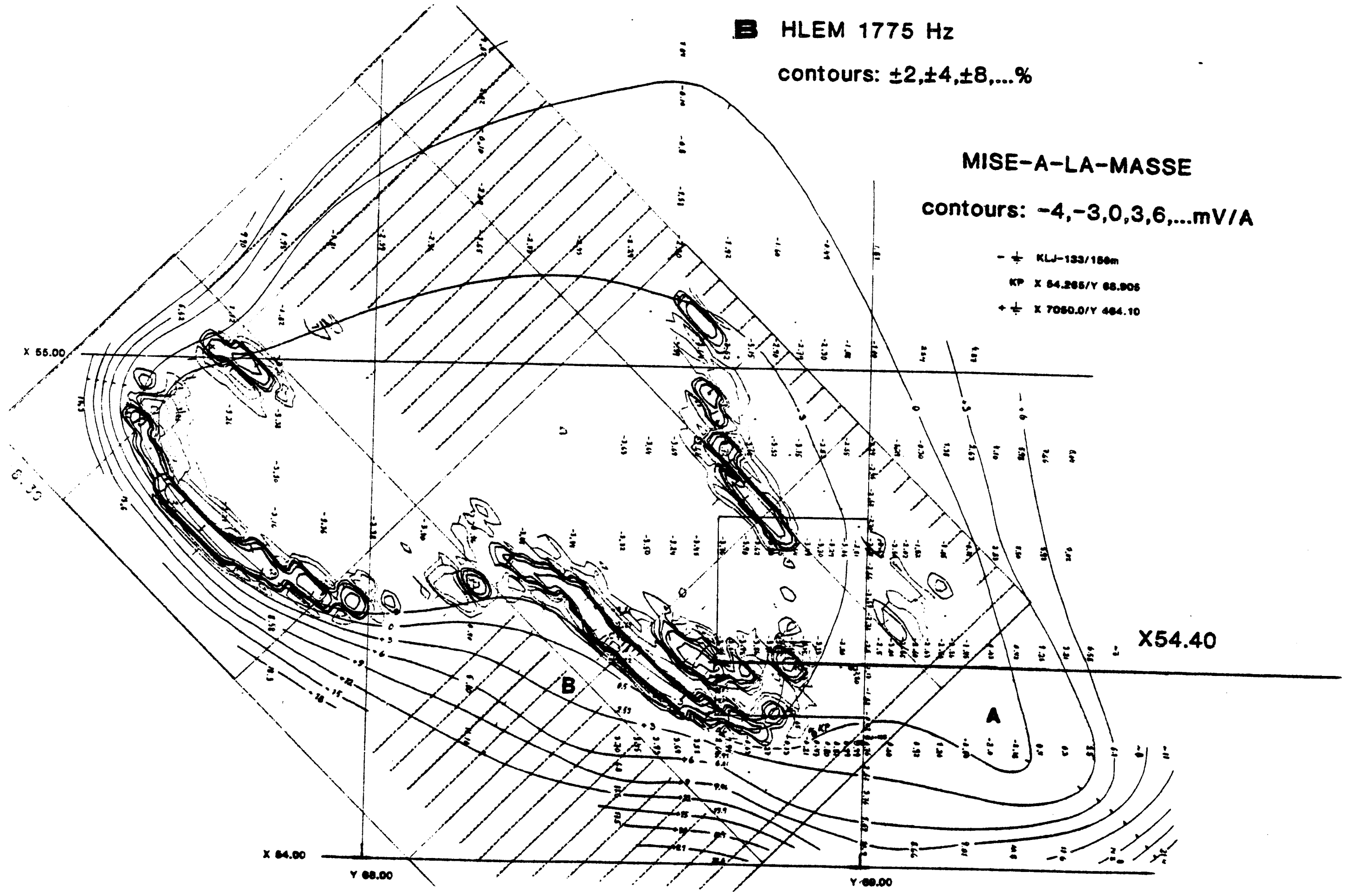
B HLEM 1775 Hz
contours: ±2,±4,±8,...%
MISE-A-LA-MASSE
contours: -4,-3,0,3,6,...mV/A
KLJ-133/156m
KP X 54.265/Y 68.905
X 7050.0/Y 464.10
X 55.00
X54.40
A
B
X 54.00
Y 68.00
Y 69.00

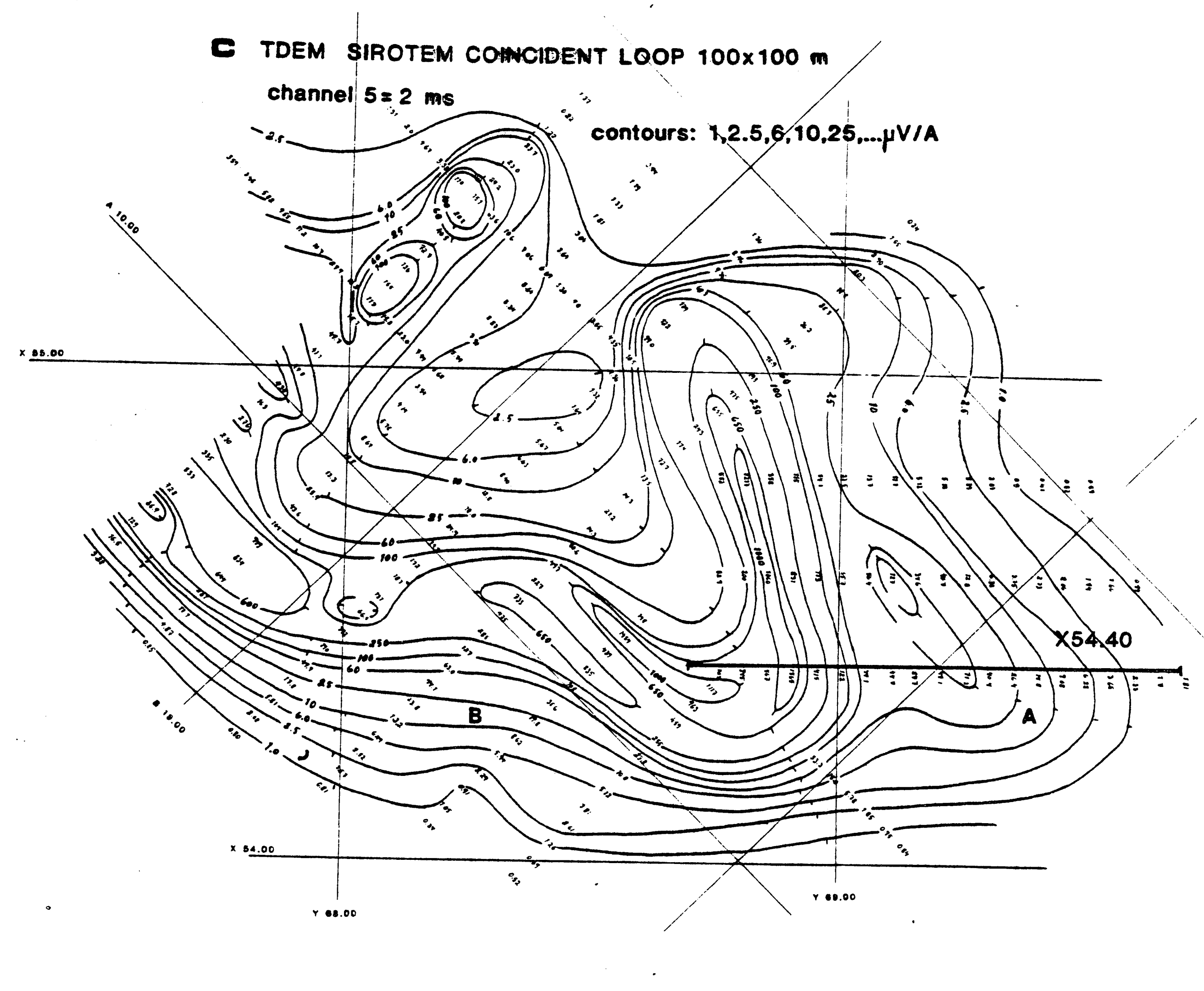
C TDEM SIROTEM COINCIDENT LOOP 100x100 m
channel 5 = 2 ms
contours: 1,2.5,6,10,25,...μV/A
A 10.00
X 55.00
X54.40
A
B
B 10.00
X 54.00
Y 68.00
Y 69.00

SECTION X 54.40

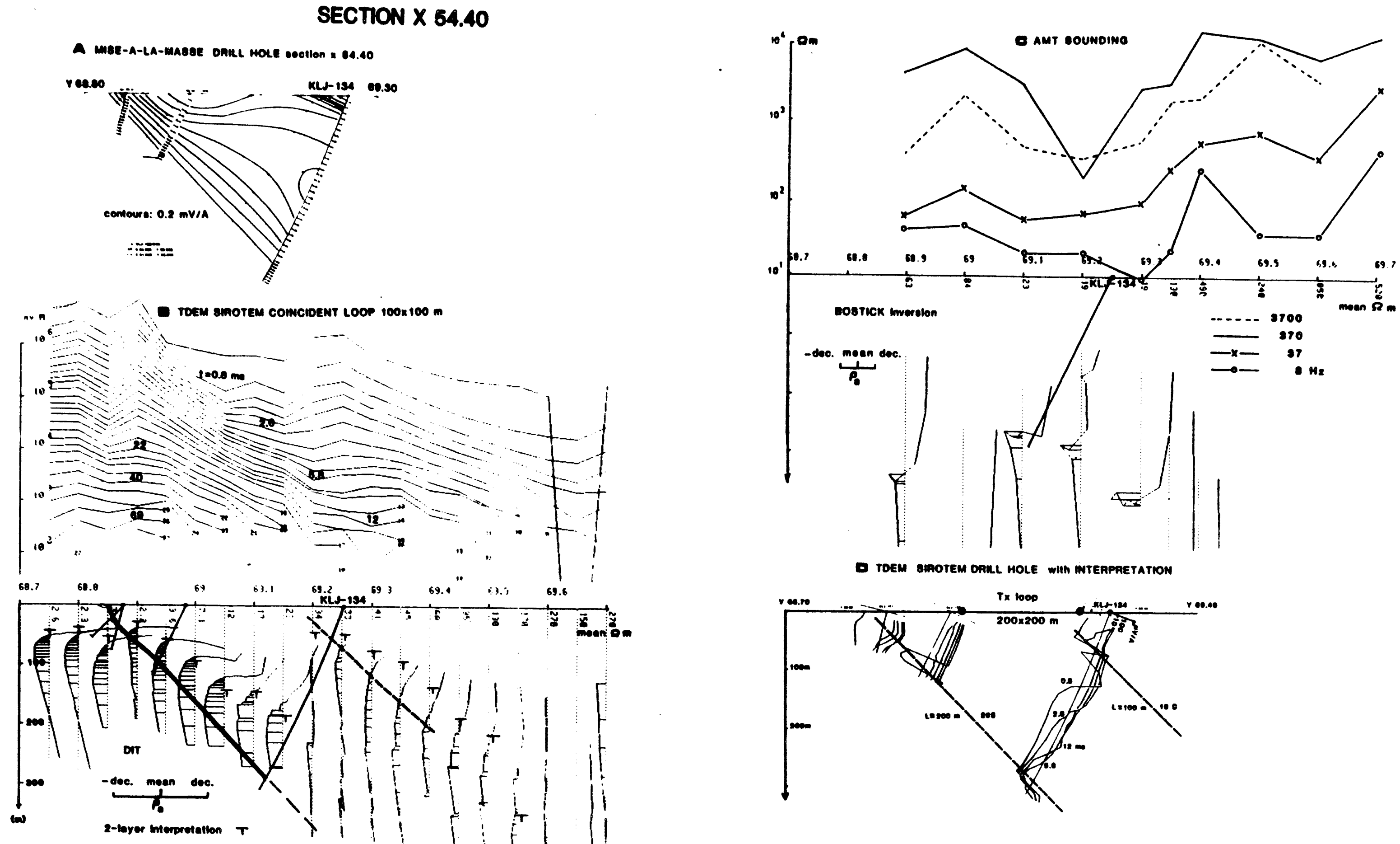

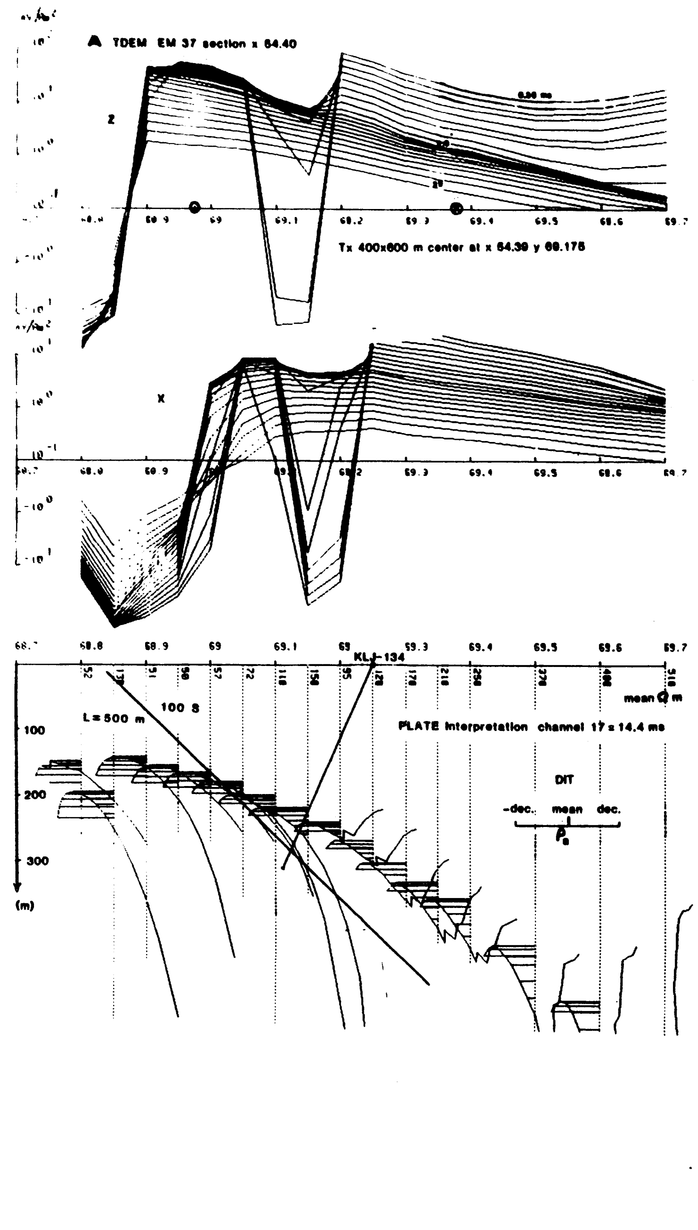
A TDEM EM 37 section x 64.40
Tx 400x600 m center at x 64.38 y 69.175
Z
X
KLJ-134
100 S
L=500 m
PLATE interpretation channel 17=14.4 ms
DIT
-dec. mean dec.
mean Ω m
(m)

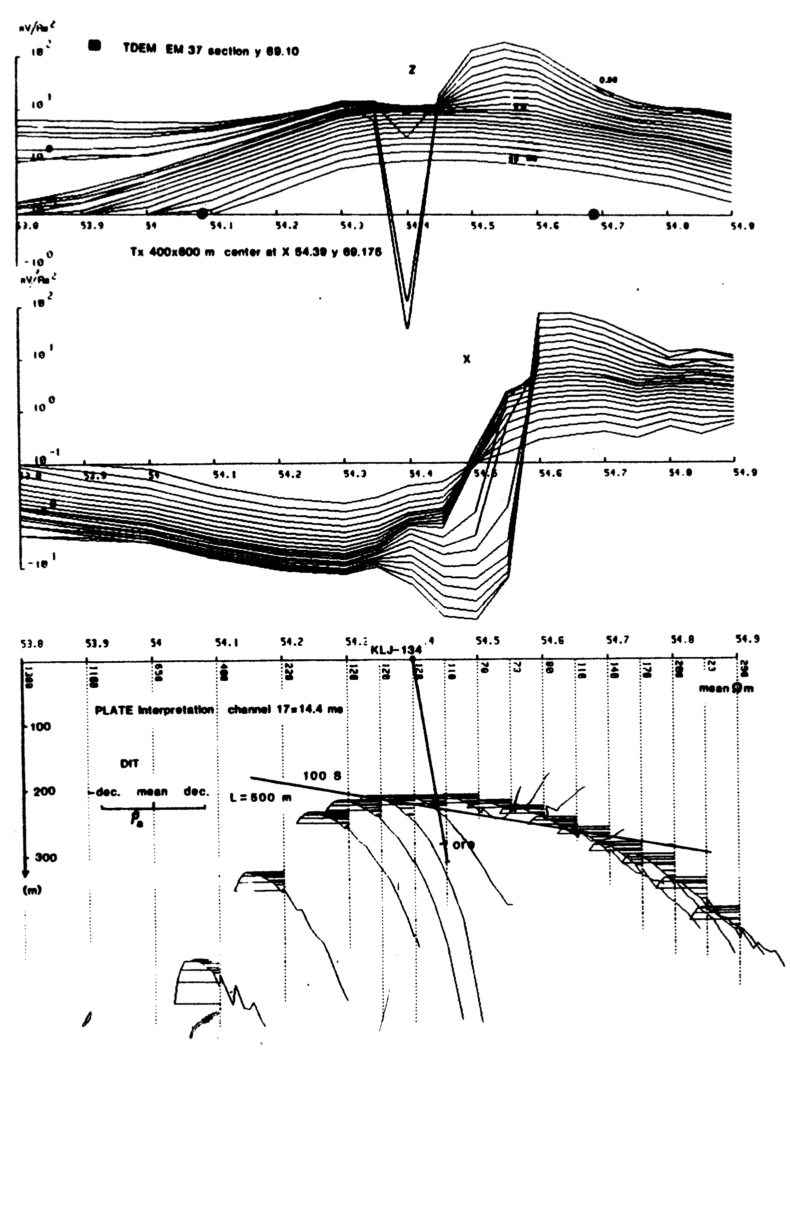
B TDEM EM 37 section y 69.10
Tx 400x600 m center at X 64.38 y 69.175
Z
X
KLJ-134
100 S
L=500 m
PLATE interpretation channel 17=14.4 ms
DIT
-dec. mean dec.
ore
mean Ω m
(m)

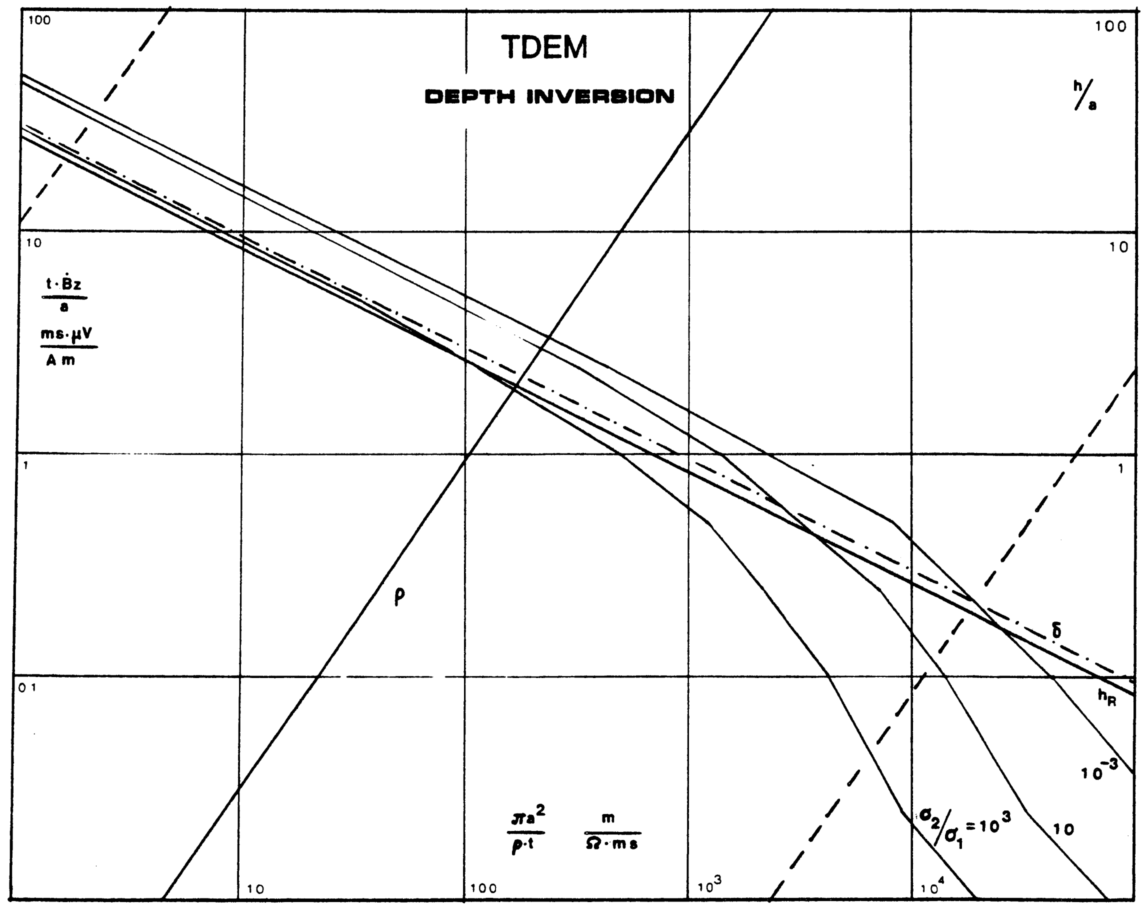
TDEM
DEPTH INVERSION
h/a
t·Ḃz / a
ms·µV / A m
ρ
δ
h_R
10^-3
10
σ2/σ1 = 10^3
πa^2 / ρ·t
m / Ω·ms
100
10
1
0.1
10^3
10^4

TDEM COINCIDENT LOOP

SMALL-SCALE MODELS and DIT

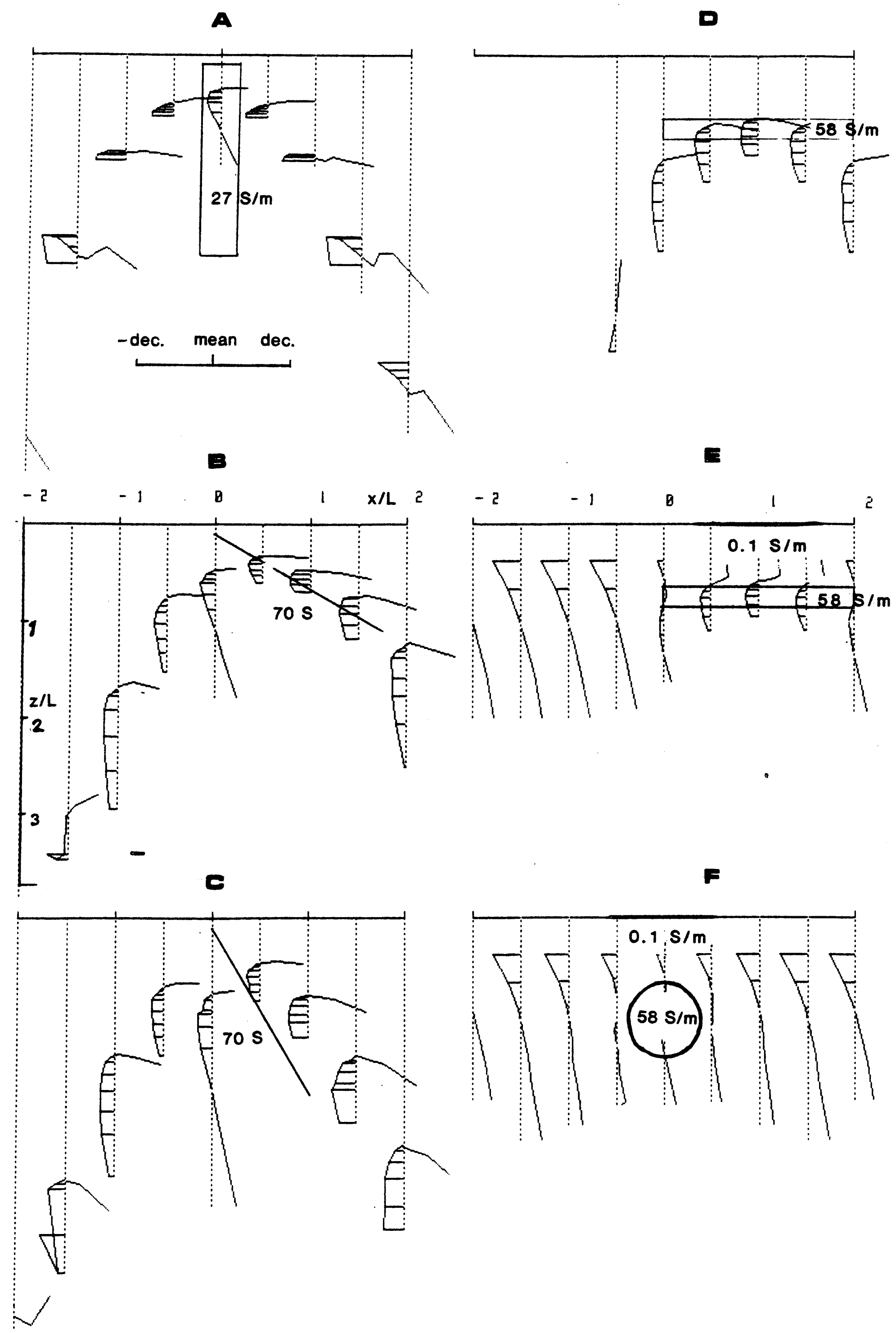

GEONICS LIMITED

TECHNICAL NOTE TN-12

APPLICATION OF SIMPLE LOOP MODELS TO THE INTERPRETATION OF TRANSIENT ELECTROMAGNETIC SURVEYS IN A RESISTIVE ENVIRONMENT

1. INTRODUCTION

In the spring of 1983 demonstration surveys using the EM37 transient EM system were carried out in Sweden, Finland, and Norway at the sites shown in Figure 1. In all cases the terrain was known beforehand to be resistive. Before each survey the target, as described by the client, was simulated with a simple loop model and the response calculated as a function of transmitter loop size and position. This information was used to locate the actual transmitter loop.

For each of the three surveys it was possible to accurately match the measured survey profiles of dB/dt (at late time) with the response from a loop model which in turn agreed well with the known geology. The survey decay curves were also integrated numerically to produce profiles of the magnetic field B (rather than its time derivative) to illustrate the feasibility of this technique.

This short note briefly describes the simple loop program, discusses the merits of numerical integration of the transient response to generate B, and illustrates both features with data from the three surveys.

Simple exponential decay over the later portion of the transient response is often seen in surveys carried out in relatively resistive environments.

There were thus good reasons for determining which plate parameters controlled the late time response. A parametric study was performed using calculated results from the University of Toronto program supplemented by actual physical measurements of the response from a series of model plates.

The results of the study (McNeill, 1982) demonstrated that the late stage response is a simple function of the plate parameters. Indeed if a and b are the minor and major dimensions of the full plate, it can be replaced by a single rectangular loop of wire of dimensions 0.7a and 0.7b centered on the plate, as long as the response is not measured in close proximity to the plate. The wire loop carries a current described by $I_o \exp(-t/\tau)$, where I_o is essentially a function of the product of the primary magnetic field H_o averaged over the plate and a. The late-stage time constant τ is determined by the product of S, the plate conductance (also called the conductivity-thickness) and a.

The surprisingly simple dependence of the plate response on S and a facilitates survey interpretation. The fact that the response can be relatively accurately approximated by that from an appropriate wire loop permits use of a simple fast computer algorithm to calculate the late stage plate response. In the Geonics approximate plate program I_o and τ are given by

$$I_o = 0.64 \; a \; H_o \; f_1 \; (b/a)$$

$$\tau = [\mu_o \; Sa \; f_2 \; (b/a)]/10$$

where μ_o is the permeability of free-space, f_1 (b/a) and f_2 (b/a) are empirically derived, slowly varying functions of (b/a) as experience has shown that this should be the case).

(5) Examine the survey profiles at time greater than the calculated late-stage time constant to ensure that their shape is no longer varying with time - i.e. that the target currents are now stationary and simply decaying with time.

(6) Using trial and error, match the profiles generated by the plate program to the survey profiles. This can generally be achieved to satisfactory accuracy in about six tries as long as a plate model is appropriate.

3. TARGET IMPULSE AND STEP RESPONSES

The EM37-3 and most other transient electromagnetic systems generate a target response by causing an essentially static magnetic field at the target to be abruptly terminated. They are said to measure the target impulse response since the induced emf which drives the vortex eddy currents is, in resistive ground, proportional to the time derivative of the primary magnetic field (and the transmitter current) and is thus an impulse function.

On the other hand the UTEM system employs a triangular transmitter current waveform, the time derivative of which is a step function, and this system is said to measure the step response of a target.

There are some significant differences between the impulse and step response. For example if the target is confined it is easy to show that at the late stage the impulse response is proportional to $(1/\tau) \exp(-t/\tau)$ whereas the step response is proportional to $\exp(-t/\tau)$. Therefore the impulse response from targets with short time-constant will be relatively enhanced compared with the step response. This is an advantage if we are searching for poor conductors, but a disadvantage if we are searching for good conductors located in close proximity to poor ones. It is apparent that it will sometimes be useful to obtain both the impulse and the step response.

Fortunately linear systems theory shows that the target step response loop whilst maintaining a finite voltage across the loop terminals. Our solution has been to design the transmitter so that the current turn-off exhibits a rapid linear-ramp decay with time. This results in a target emf which is accurately rectangular rather than an impulse function.

Although the duration of the rectangular pulse is short (typically 450μsec for a 300 x 600 meter transmitter loop carrying a peak current of 30 amperes) the finite length can cause distortion of the target response. This distortion is appreciable for short time constant targets at all measurement time, and for homogeneous and layered earth response at early time. For both situations, removal of the distortion is necessary in order to compare survey results with theoretical modeling based on an infinitely fast transmitter turn-off. To solve the problem Geonics has developed a computer algorithm which employs as input both the measured values of dB/dt at each survey point along the profile and the known transmitter turn-off time. The program calculates profiles of B and dB/dt, both corrected for finite turn-off time. As will be seen in the following case histories it is routinely used for survey interpretation.

5. SURVEY RESULTS AND INTERPRETATION

All of the surveys were carried out with a standard EM37, for which the location of the various time gates is shown in Table 1. The gates are sufficiently narrow that no correction for finite gate width is necessary.

Table 1. EM37 Gate Center Locations

Channel	Location(msec)	Channel	Location(msec)
1	0.089	11	0.876
2	0.110	12	1.087
3	0.140	13	1.40
4	0.177	14	1.77
5	0.220	15	2.21
6	0.280	16	2.82
7	0.355	17	3.57

location of the plate is in reasonable agreement and the geometry and depth in excellent agreement. It must be remembered that in this case the approximate dimensions of the body were known beforehand and used as inputs to the model. For example the measured data from a single survey line with only two field components could not be expected to yield an accurate strike length.

SURVEY #2: Hannukainen (Kolari, Finland)

Figure 7 shows a plan view of the survey area. The Kivivuopio orebody is a gently dipping, strata-bound, skarn iron-ore deposit located at a depth of 300 - 700m. It had been detected and outlined by magnetics and extensive AMT surveying as well as other geophysical methods (Pietilä and Hattula, 1982), and confirmed by drilling as indicated. Again the bedrock is resistive; thickness of the deposits in this region ranges from a few meters to 40 m. An objective of the survey was to determine whether the body continued down-dip to the west.

Raw survey profiles are shown in Figure 8, profiles corrected for finite transmitter turn-off time in Figure 9, profiles of B in Figure 10, and the transient decay curve again in Figure 5. The latter indicates exponential decay commencing at about 3 msec, with a time constant of 3.66 msec. Late stage behaviour beyond this time is confirmed by the profiles of Figure 8 (the continuing change of the profile at the east end of the line is thought to be due to the adjacent conductor).

The two "glitches" at the transmitter wire appear to have been caused by operator error. However they offer an interesting example of the effect of correcting for finite transmitter turn-off. Since they are of low time constant (less than the transmitter turn-off time of 210 μsec), correcting for the turn-off time substantially enhances their response (Figure 9), whereas integrating to produce profiles of B reduces their response as well as reducing the overall dynamic range required to plot the data (Figure 10).

the modeling suggested that the drill would just intersect the top of the target at a distance of 110m; a few weeks later drill intersections were confirmed at 108-111m and 113-116m, with no further intersections to 160m.

SUMMARY

The survey data presented in this short note demonstrates the usefulness of a simple loop model for interpreting the results of transient EM surveys using large loop Turam-type transmitters, as long as neither the source nor the receiver is close to the plate, and the ground is reasonably resistive (in excess of a few hundred ohm-meters). Furthermore the loop must not be much larger than the transmitter, although the data from Hannukainen suggest that it can still be reasonably large.

Arguments and data are presented which indicate the usefulness of numerically integrating the transient curves so as to obtain profiles of the magnetic field as well as its time derivative, and thus of the target step response as well as the impulse response.

ACKNOWLEDGEMENTS

The authors would like to acknowledge the assistance given by Boliden Aktiebolag (Malå), Rautaruukki Oy (Hannukainen), and Prospektering A/S (Kautokeino). These companies helped in carrying out the surveys, supplied geological and geophysical data about the sites and gave permission to publish the results.

The work described herein was partially funded by National Research Council of Canada IRAP Grant TES 666.

LIST OF ILLUSTRATIONS

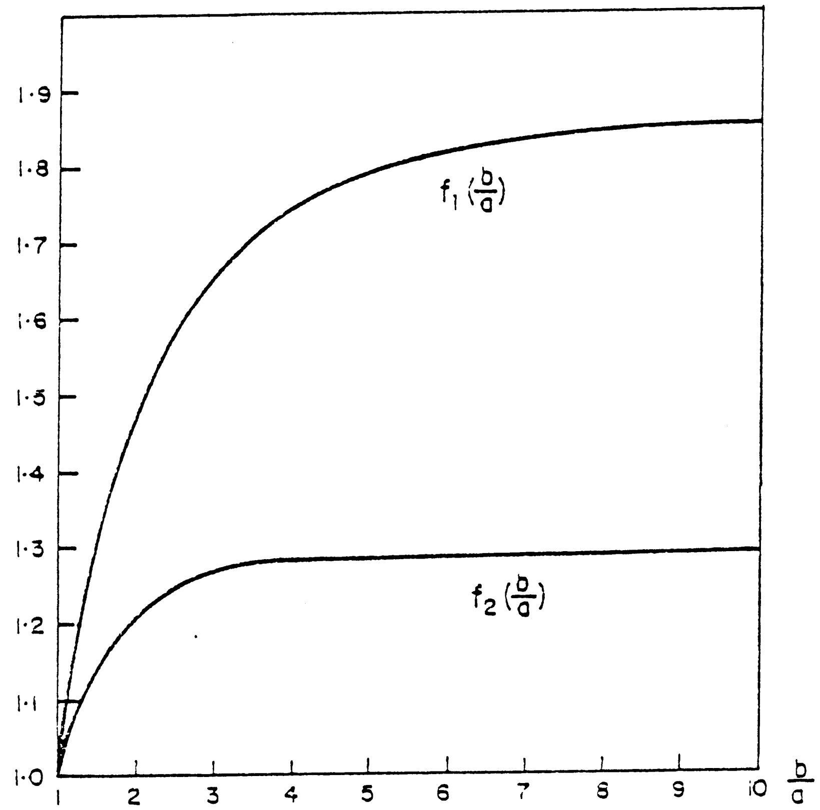

Figure 2.

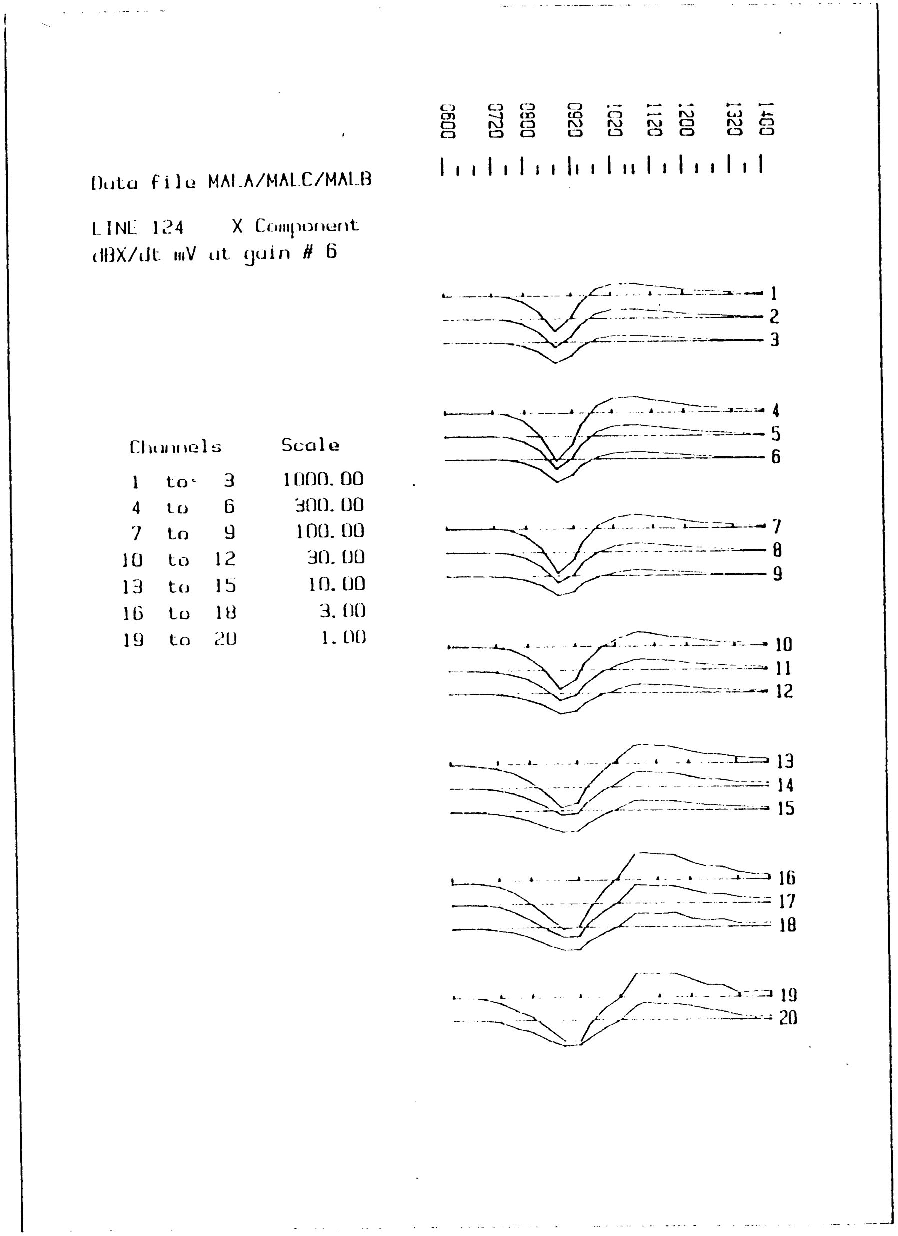

Data file MALA/MALC/MALB
LINE 124 X Component
dBX/dt mV at gain # 6
0600 0720 0800 0920 1020 1120 1200 1320 1400
Channels Scale
1 to 3 1000.00
4 to 6 300.00
7 to 9 100.00
10 to 12 30.00
13 to 15 10.00
16 to 18 3.00
19 to 20 1.00
1 2 3 4 5 6 7 8 9 10 11 12 13 14 15 16 17 18 19 20

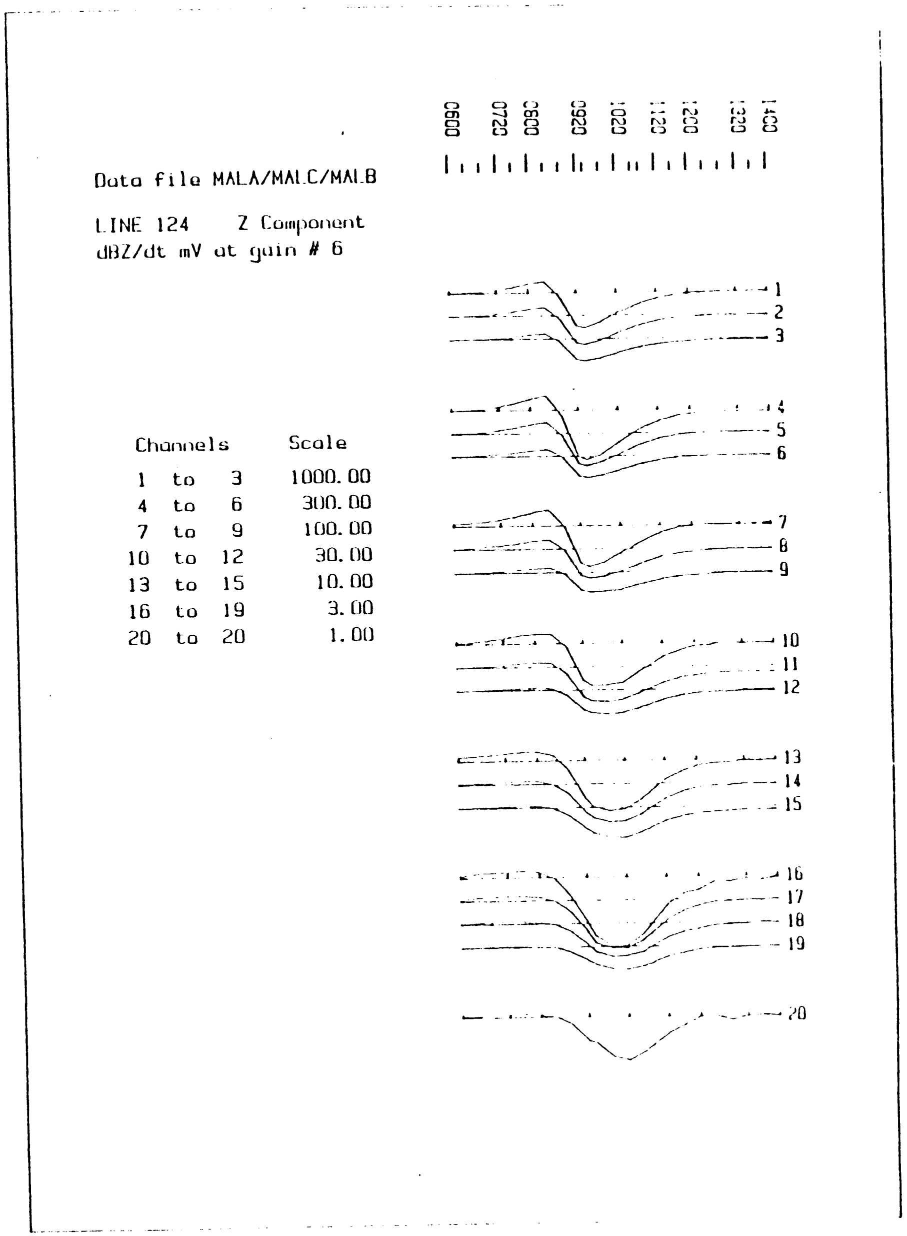

Data file MALA/MALC/MALB
LINE 124 Z Component
dBZ/dt mV at gain # 6
0600 0720 0800 0920 1020 1120 1200 1320 1400
Channels Scale
1 to 3 1000.00
4 to 6 300.00
7 to 9 100.00
10 to 12 30.00
13 to 15 10.00
16 to 19 3.00
20 to 20 1.00
1 2 3 4 5 6 7 8 9 10 11 12 13 14 15 16 17 18 19 20

Figure 4.

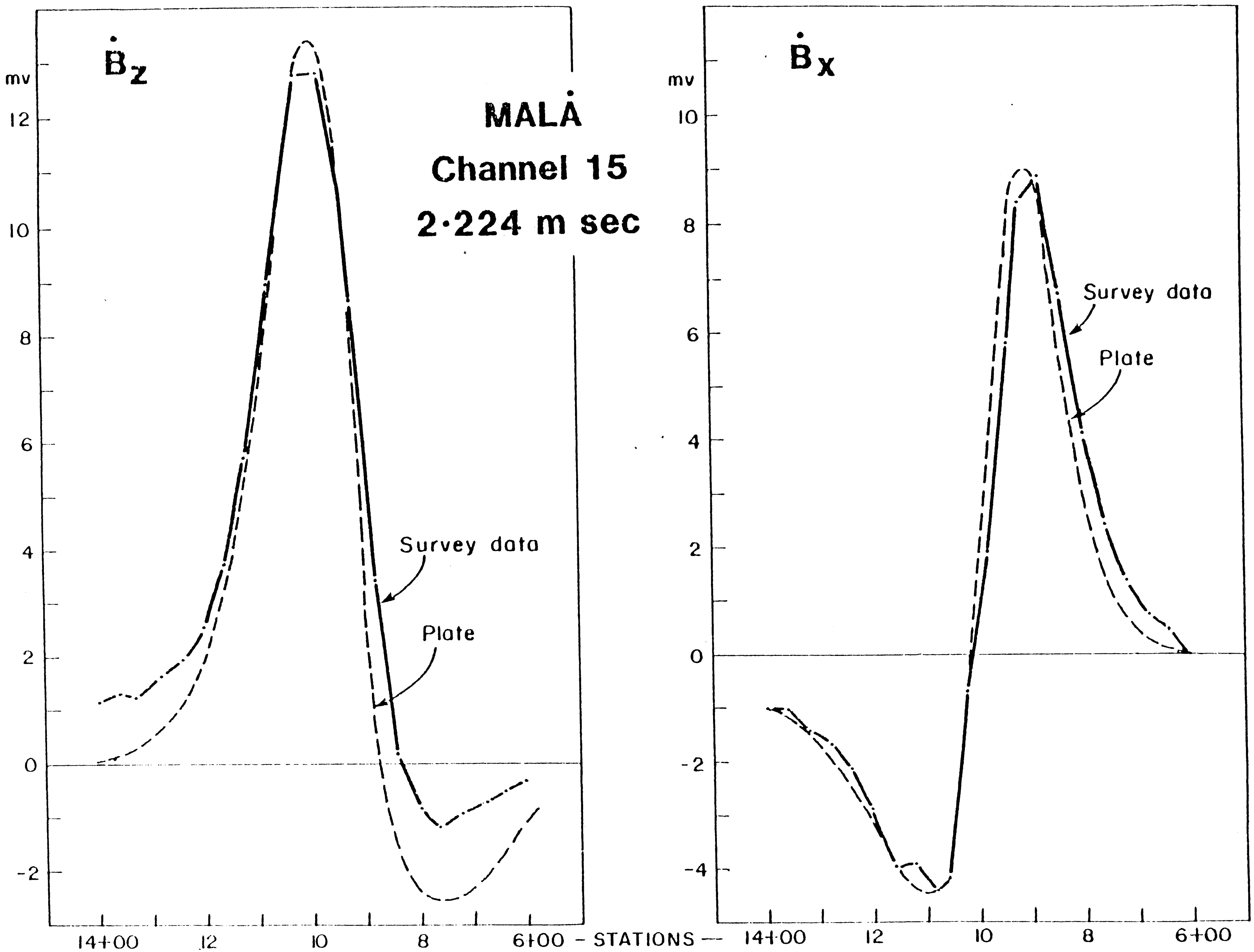

Ḃz
mv
12
10
8
6
4
2
0
-2
MALÀ
Channel 15
2·224 m sec
Survey data
Plate
14+00
12
10
8
6+00 - STATIONS —
Ḃx
mv
10
8
6
4
2
0
-2
-4
Survey data
Plate
14+00
12
10
8
6+00

Figure 6.

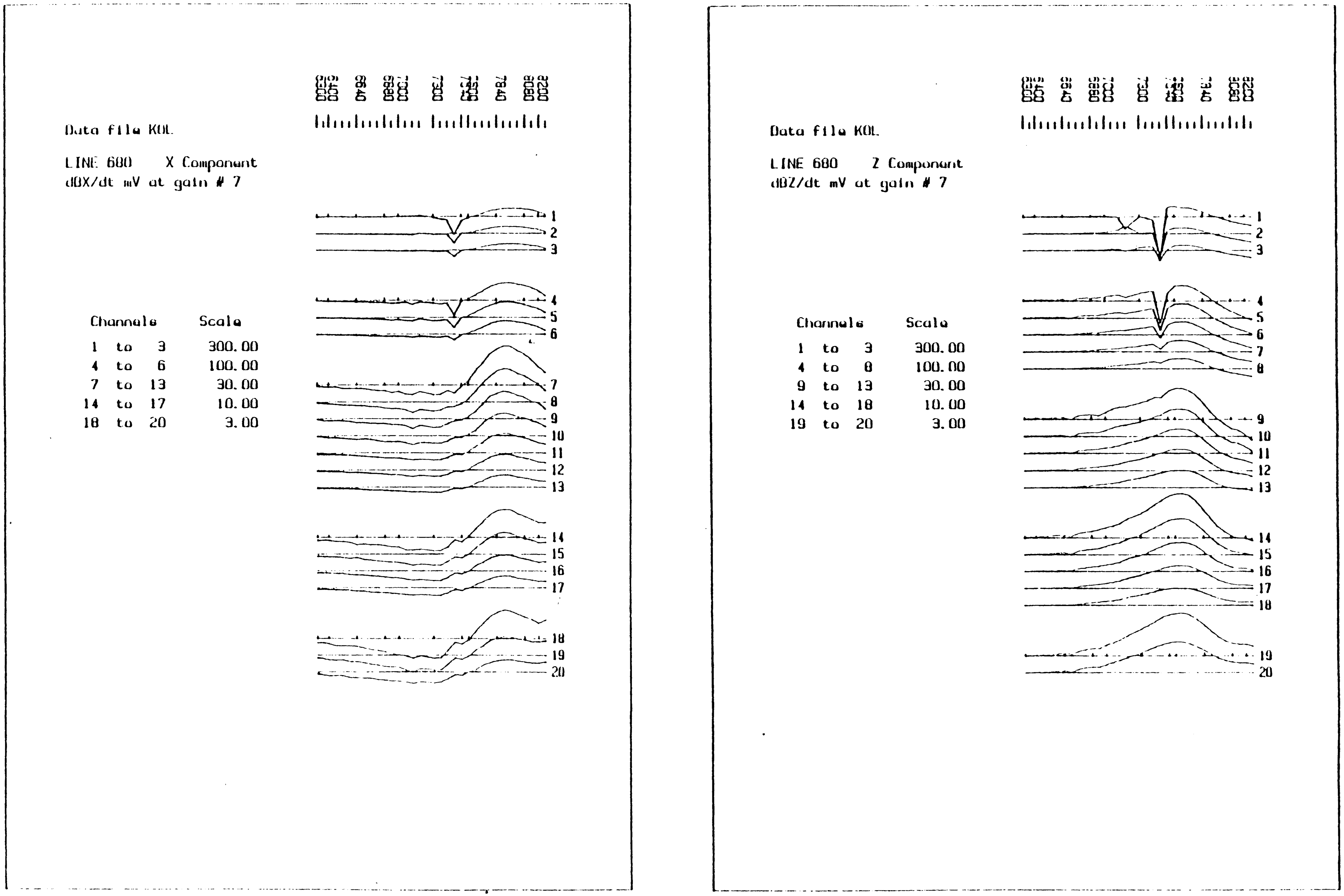

Data file KOL
LINE 680 X Component
dBX/dt mV at gain # 7
Channels Scale
1 to 3 300.00
4 to 6 100.00
7 to 13 30.00
14 to 17 10.00
18 to 20 3.00
1 2 3 4 5 6 7 8 9 10 11 12 13 14 15 16 17 18 19 20
Data file KOL
LINE 680 Z Component
dBZ/dt mV at gain # 7
Channels Scale
1 to 3 300.00
4 to 8 100.00
9 to 13 30.00
14 to 18 10.00
19 to 20 3.00
1 2 3 4 5 6 7 8 9 10 11 12 13 14 15 16 17 18 19 20

Figure 8.

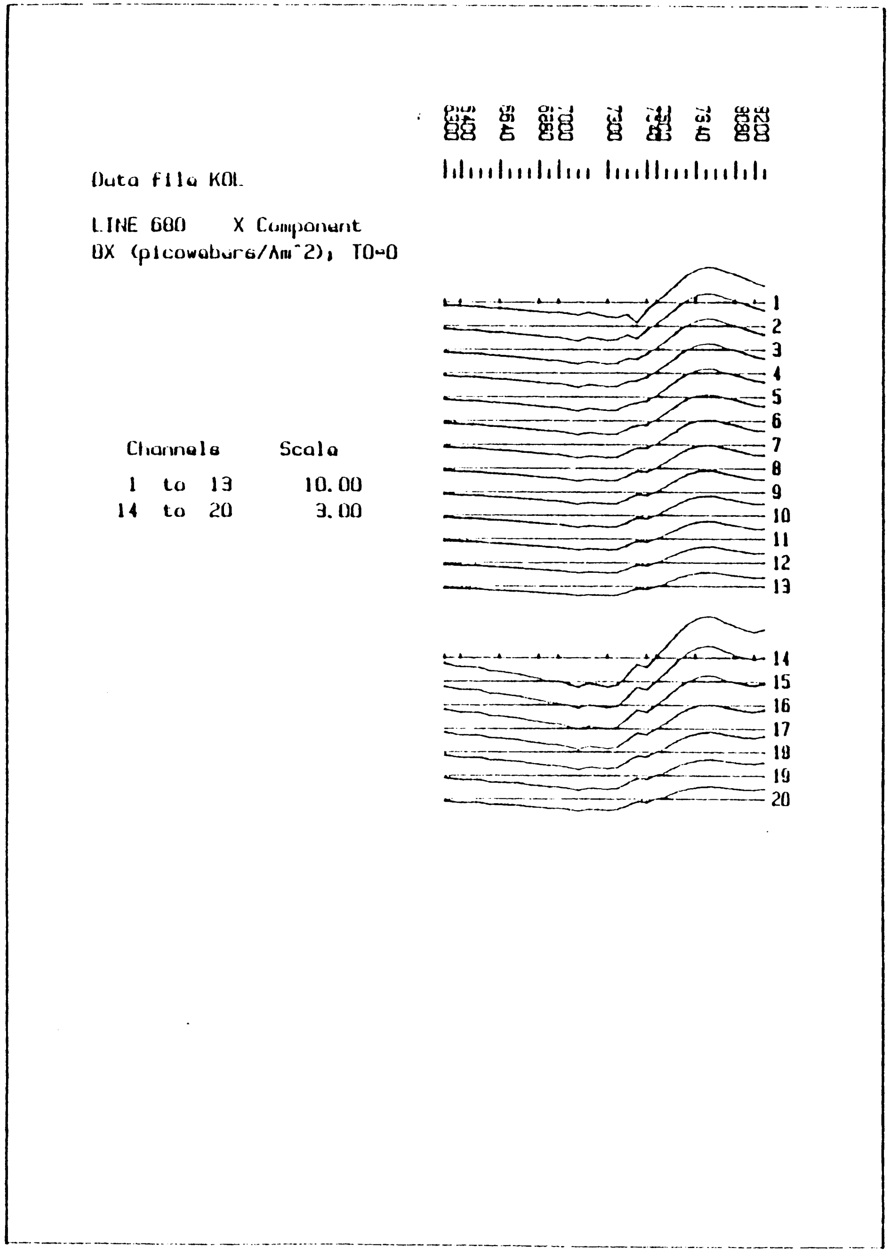
Data file KOL
LINE 680 X Component
BX (picowebers/Am^2), T0=0
Channels Scale
1 to 13 10.00
14 to 20 3.00
1
2
3
4
5
6
7
8
9
10
11
12
13
14
15
16
17
18
19
20

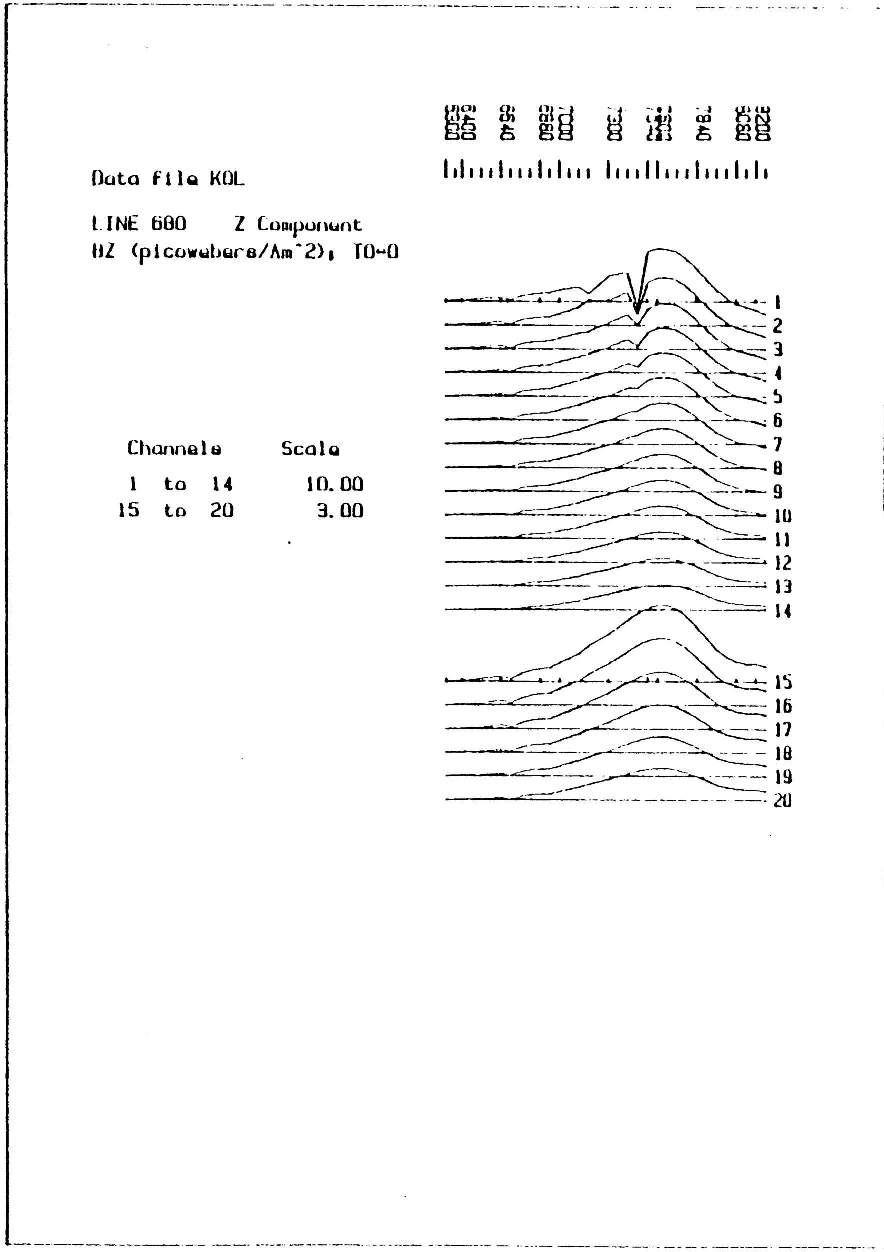
Data file KOL
LINE 680 Z Component
BZ (picowebers/Am^2), T0=0
Channels Scale
1 to 14 10.00
15 to 20 3.00
1
2
3
4
5
6
7
8
9
10
11
12
13
14
15
16
17
18
19
20

Figure 10.

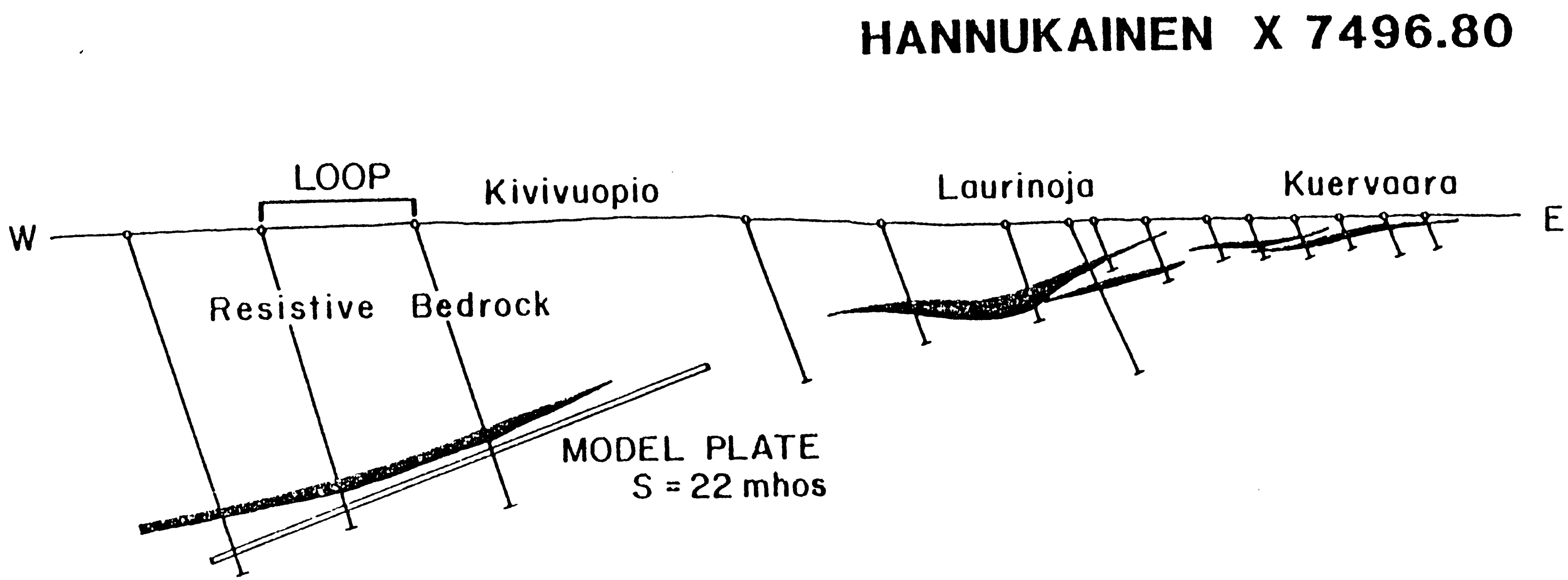
HANNUKAINEN X 7496.80
LOOP
Kivivuopio
Laurinoja
Kuervaara
W
E
Resistive Bedrock
MODEL PLATE
S = 22 mhos
0
500 m

Figure 12.

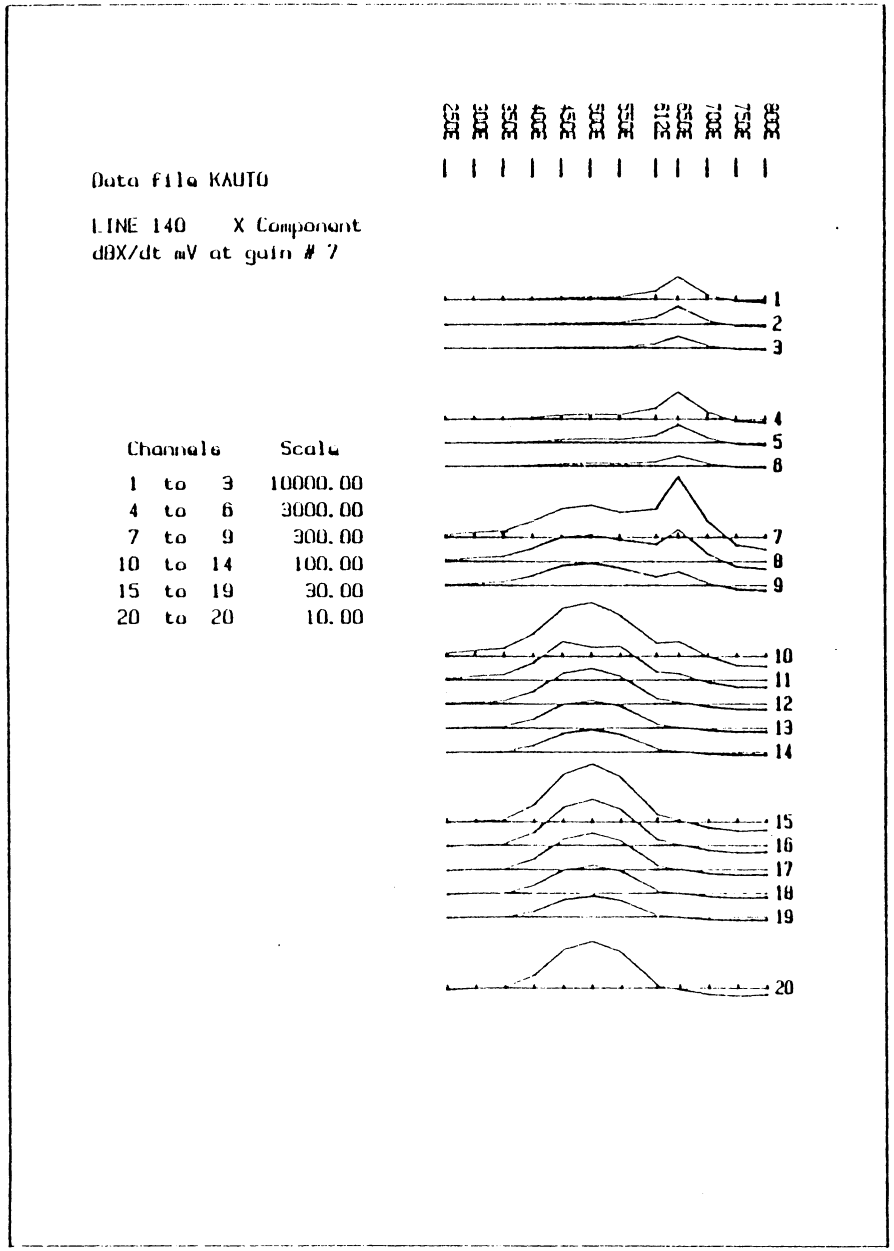
Data file KAUTO
LINE 140 X Component
dBX/dt mV at gain # 7
Channels Scale
1 to 3 10000.00
4 to 6 3000.00
7 to 9 300.00
10 to 14 100.00
15 to 19 30.00
20 to 20 10.00
250E 300E 350E 400E 450E 500E 550E 612E 650E 700E 750E 800E

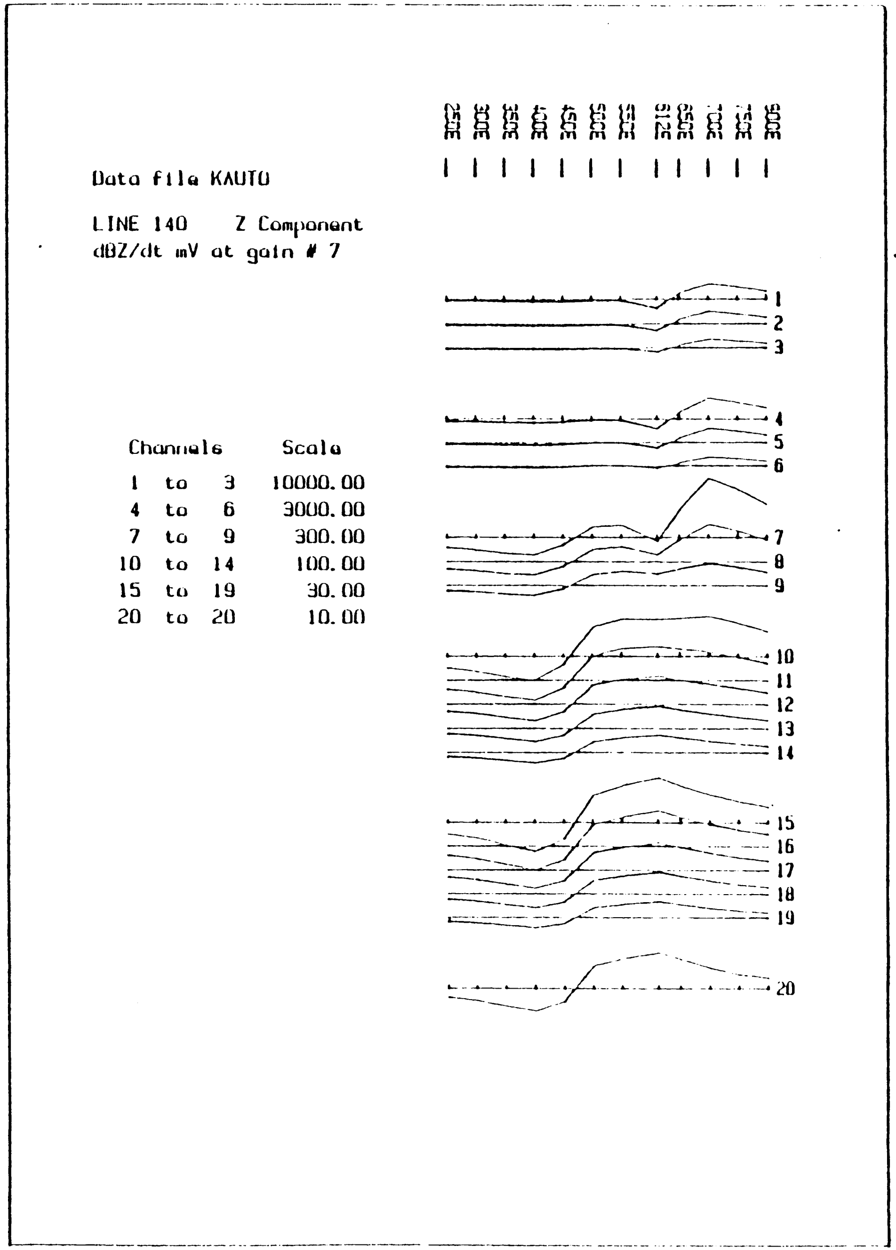
Data file KAUTO
LINE 140 Z Component
dBZ/dt mV at gain # 7
Channels Scale
1 to 3 10000.00
4 to 6 3000.00
7 to 9 300.00
10 to 14 100.00
15 to 19 30.00
20 to 20 10.00
250E 300E 350E 400E 450E 500E 550E 612E 650E 700E 750E 800E

Figure 14.

KAUTOKEINO Channel 19 5·7 m sec

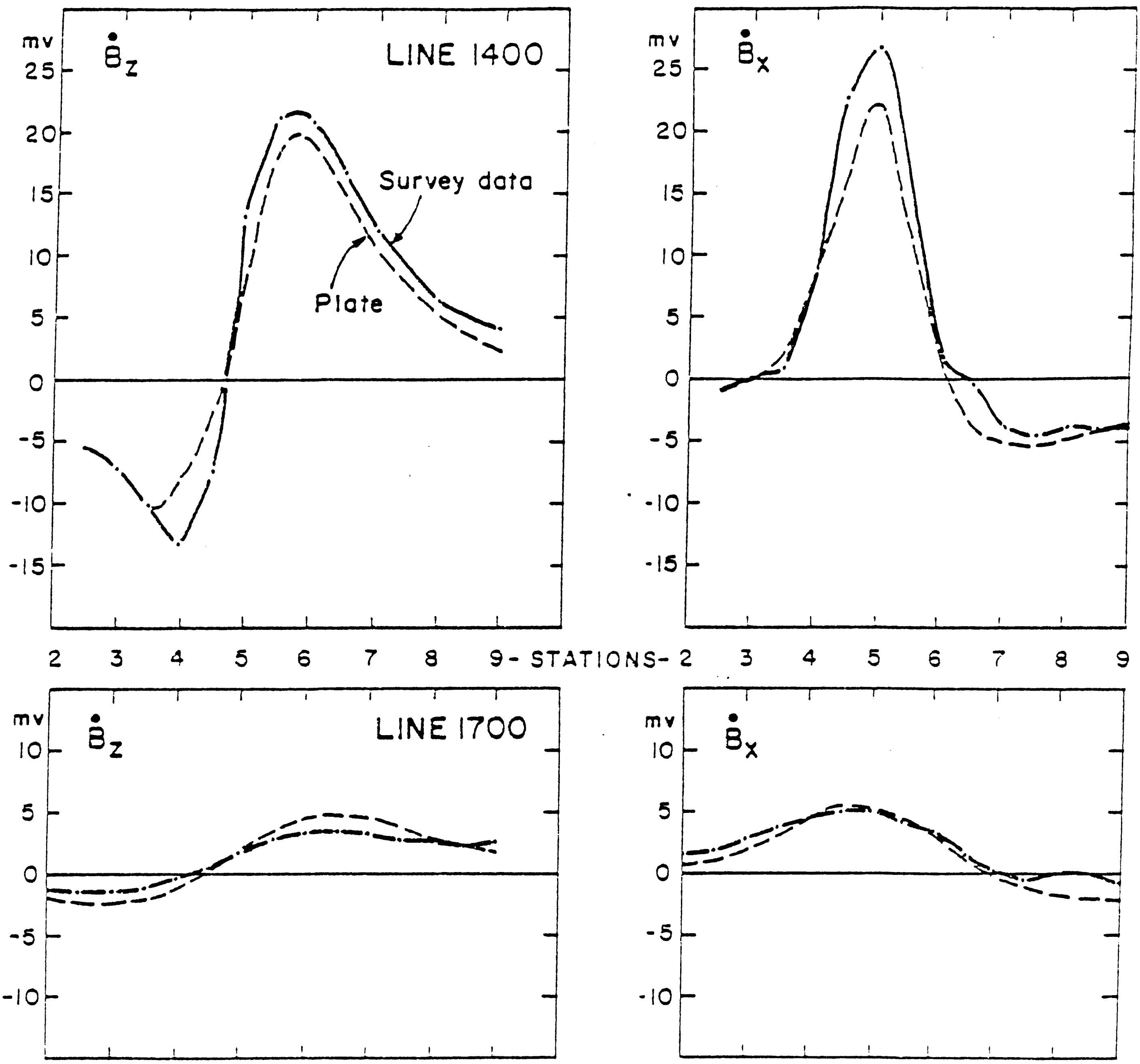

Figure 16.

DESCRIPTION OF THE SURVEY DETAILS

Equipment was transported from Espoo Finland to Løkken by the Finnish technician, Jouko Longi, who taught the local crew to use it and supervised the survey all the time. Geophysicist Ensio Lakanen was present from 15th to 23rd of August.

Equipment

The ground transient EM device EM37-3 is manufactured by Geonics Ltd., Canada. This instrument was first introduced in 1980, but has been updated so that this unit is the latest No. 3 version delivered in 1984.

Transmitter consists of a console weighing 20 kg and power unit with 5 HP Honda gasoline engine coupled to 120 V, 3-phase, 400 Hz alternator weighing 60 kg. Output power is 2.8 kW, maximum current 30 A and voltage 150 V. The transmitter loop was built up with 4 mm^2 isolated copper wire; 9 reels with 400 m, 20 kg each were available. The current waveform in the transmitter consists of alternating bipolar current pulses with a slow exponential turn-on and a rapid linear shut-off (turn-off) time depending on the loop size and current, normally less than 0.5 ms. The repetition rate can be set at 2.5 or low, 6.25 or medium, and 25 Hz or high.

Receiver consists of a console weighing 22 kg and air-cored 100 cm dia. coil weighing 8 kg. A coil holder is supplied to facilitate measurement, along three axes. The measured quantity is the time rate of decay of magnetic flux at 20 logarithmically spaced time channels covering range from 0.08 at high to 80 ms at low repetition rate. 4 digits plus sign LED display is used and integration time can be selected from 2^n (n = 4, 6, 8, 10, 12, 14) cycles at 25 Hz. The effective area of the coil is about 100 m^2. Synchronization of receiver to transmitter can be maintained with oven controlled high stability quartz crystals. Receiver energy is taken from 12 V rechargeable NiCd batteries of 20 Ah.

At the receiver the induced voltage in the coil is measured in millivolts. The reading is normalized by dividing with the effective area of the coil and the current in the transmitter loop and is written in nanovolts per A x meter^2 (nV/Am^2).

Survey

The fixed or large loop mode of measurement was used meaning that the transmitter is located in a fixed position feeding a large loop, here 400 x 400 m^2 or more, and the receiver with the coil moves from station to station along survey line. One or more lines or profiles are measured with one transmitter position, and they cross the loop continuing outside of it as far as the field is strong enough, which equals about the perpendicular length of the loop. Then the transmitter is moved to another location.

Altogether 20 transmitter locations were needed to cover the desired area in the surroundings of Løkken, 18 loops 400 x 400 m^2 in size and two double sized loops. Survey lines, numbering 30 were spaced 250 or 500 m apart so that two or one lines per loop were measured respectively, three with one double sized loop. The length of the lines varied from 0.9 to 2.6 km totalling 46.35 km. Point spacing was mostly 100 m (occasionally 50 or 200 m), 429 stations or points were measured. There were two men crew measuring and two extra men were laying the next loop beforehand except the double sized loops. Two components along Z (vertical) and X (along the line) axes were recorded, and in one profile also Y.

Repetition rate of 25 Hz or high was mainly used, one profile with medium frequency. Integration time n = 10 and gain N = 7 (quite high indicating resistive environment) were used. Power lines and inhabited areas caused some trouble and some places had to be dismissed. One power line from west to Astrup shaft was totally switched off during the measurements close to it. Only one instrument failure occurred, when measuring the last profile the eighteenth channel was lost; it was later noticed to be caused by moisture. The weather was mostly favourable, but rains got heavier in September. The average of 13 stations occupied per working day can be regarded satisfactory in the rough terrain with long carrying distances.

The survey has been divided to 10 separate areas introduced from west to east (appendix 2/1).

Svinsås (appendix 3)

Two transmitter loops 400 x 400 m^2 centered at

1: 600 (m) W(est), 150 N(orth) (local coordinates)

2: 50 W, 275 S(outh)

Two profiles in south - north direction

1: 600 W, 700 S to 800 N

2: 150 W, 800 S to 500 N

Point spacing 100 m

Total 2.8 km 30 p(oints)

Blokkum (-Marka) (app. 4)

Transmitter loop 400 x 400 m^2 centered at

Y = 30.4, X = 98.65 (east and north resp.)

Profile in south-north direction

Y = 30.4, X = 99.3 - 100.8

Point spacing 100 and 200 m

Total 1.5 km 14 points

Moen (app. 5)

Transmitter loop 700 x 900 m^2 centered at

0, 0 (local coordinates)

Profile in southsouthwestern - northnortheastern direction

0, 1300 S to 1000 N

Point spacing 100 and 200 m

Total 2.3 km 18 p.

Damlia (app. 6)

Transmitter loop 400 x 400 m^2 centered at

Y = 31.85, X = 98.65 (regional coordinates)

Profile in south - north direction

Y = 31.75, X = 97.9 - 99.3

Point spacing 100 m

Total 1.4 km 15 p.

Högåsen (app. 7)

Transmitter loop 800 x 800 m^2 centered at

Y = 33.0, X = 98.95

Three profiles in south - north direction

1: Y = 32.5, X = 97.7 - 99.9

2: Y = 33.0, X = 97.6 - 100.2

3: Y = 33.5, X = 97.6 - 99.8

Point spacing 100 m and 200 m

Total 7.0 km 53 p.

Björnli (app. 8)

Transmitter loop 275 x 525 m^2 centered at

120 W, 150 N (local coordinates)

Two profiles in about southwest - northeast direction

1: 0, 400 S to 650 N

2: 250 W, 400 S to 700 N

Point spacing 50 and 100 m

Total 2.15 km 28 p.

Mogset (app. 9)

Transmitter loop 400 x 400 m^2 centered at

Y = 33.25, X = 102.05

Profile in south - north direction

Y = 33.35, X = 101.2 - 102.7

Point spacing 100 and 200 m

Total 1.5 km 14 p.

Høydal (app. 10)

Four transmitter loops 400 x 400 m^2 centered at

1: Y = 36.9, X = 99.35

2: Y = 37.4, X = 99.25

3: Y = 37.87, X = 99.25

4: Y = 38.5, X = 99.15

Nine profiles in south - north direction

1: Y = 36.75, X = 98.8 - 99.8 (loop No. 1)

2: Y = 37.0, X = 98.6 - 100.2 (loop No. 1)

3: Y = 37.25, X = 98.6 - 100.1 (loop No. 2)

4: Y = 37.5, X = 98.5 - 100.1 (loop No. 2)

5: Y = 37.75, X = 98.5 - 100.0 (loop No. 3)

6: Y = 38.0, X = 98.5 - 100.0 (loop No. 3)

7: Y = 38.25, X = 98.4 - 100.0 (loop No. 4)

8: Y = 38.5, X = 98.4 - 99.9 (loop No. 4)

9: Y = 38.75, X = 98.4 - 99.9 (loop No. 4)

Point spacing 100 and 200 m

Total 13.3 km 134 p.

Urvatnet (app. 11)

Seven transmitter loops 400 x 400 m^2 centered at

1: Y = 40.0, X = 98.75

2: Y = 40.5, X = 98.85

3: Y = 41.0, X = 98.65

4: Y = 41.55, X = 98.85

5: Y = 42.0, X = 98.65

6: Y = 42.5, X = 98.65

7: Y = 43.0, X = 98.45

Seven profiles in south - north direction

1: Y = 40.0, X = 98.0 - 99.6 (loop No. 1)

2: Y = 40.5, X = 98.1 - 99.5 (loop No. 2)

3: Y = 41.0, X = 97.9 - 99.2 (loop No. 3)

4: Y = 41.55, X = 98.0 - 99.4 (loop No. 4)

5: Y = 42.0, X = 97.8 - 99.4 (loop No. 5)

6: Y = 42.5, X = 97.7 - 99.3 (loop No. 6)

7: Y = 43.0, X = 97.6 - 99.1 (loop No. 7)

Point spacing 100 and 200 m

Total 10.4 km 91 p.

Åmot (app. 12)

Two transmitter loops 400 x 400 m^2 centered at

1: Y = 41.25, X = 100.4

2: Y = 42.05, X = 100.35

Three profiles in south - north direction

1: Y = 41.0, X = 99.8 - 101.0 (loop No. 1)

2: Y = 41.5, X = 99.5 - 100.6 (loop No. 1)

3: Y = 42.0, X = 99.5 - 101.0 (loop No. 2)

Point spacing 100 and 200 m

Total 3.8 km 31 p.

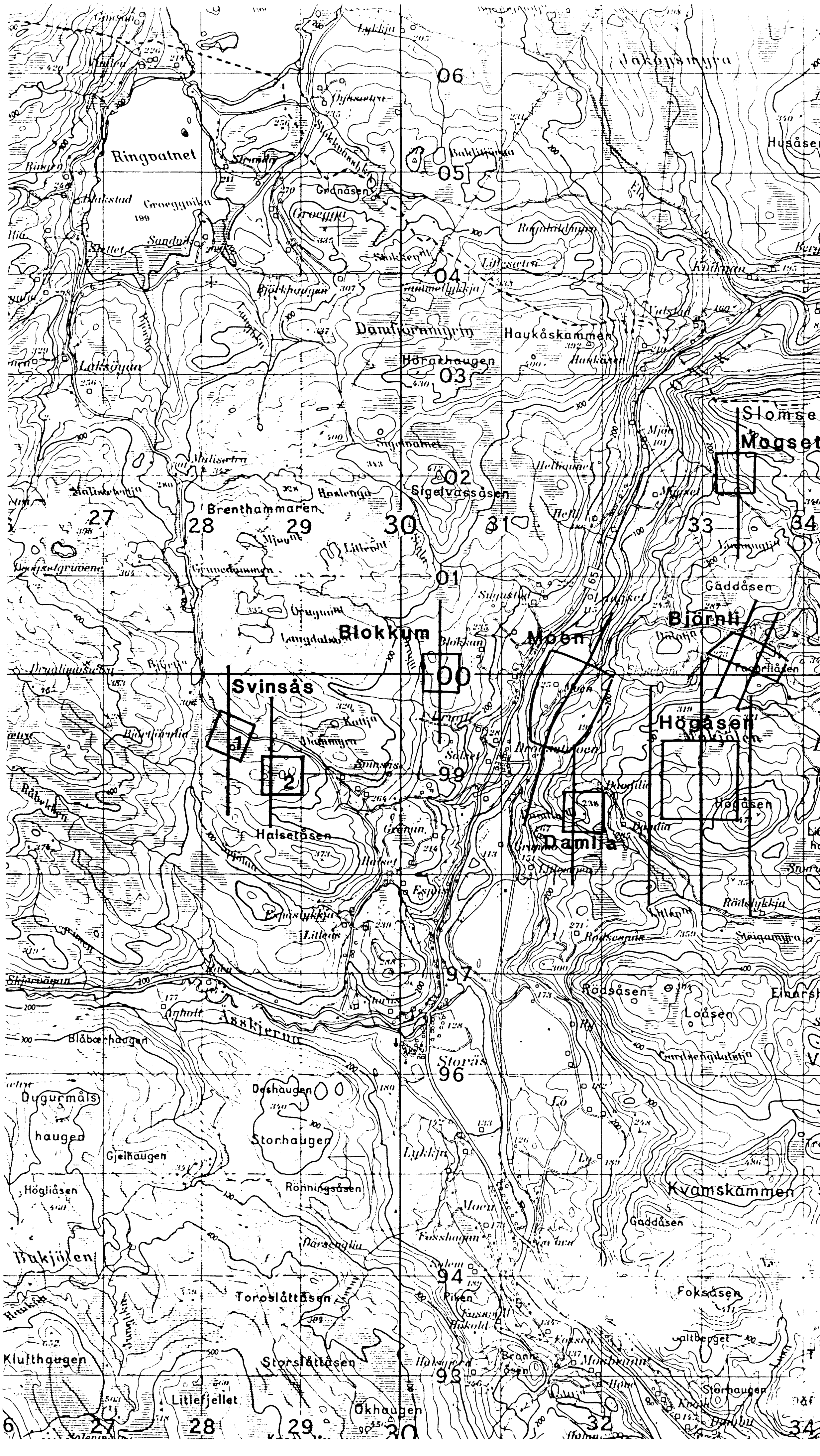

Ringvatnet
Jakobsmyra
Husåsen
Granåsen
Damtjörnmyra
Haukåskammen
Hörarhaugen
Slomsetra
Mogset
Brenthammaren
Sigelvassåsen
Gäddåsen
Bjärnli
Blokkum
Moen
Svinsås
Högåsen
Halsetåsen
Damlia
Rödsåsen
Loåsen
Einarsh
Blåbærhaugen
Dugurmåls
haugen
Deshaugen
Storhaugen
Gjelhaugen
Rönningsåsen
Högliåsen
Kvamskammen
Gaddåsen
Bukjölen
Toroslåttåsen
Foksåsen
Klufthaugen
Storslåttåsen
Storhaugen
Litlefjellet
Okhaugen
06
05
04
03
02
01
00
99
97
96
94
93
27
28
29
30
31
32
33
34
1
2

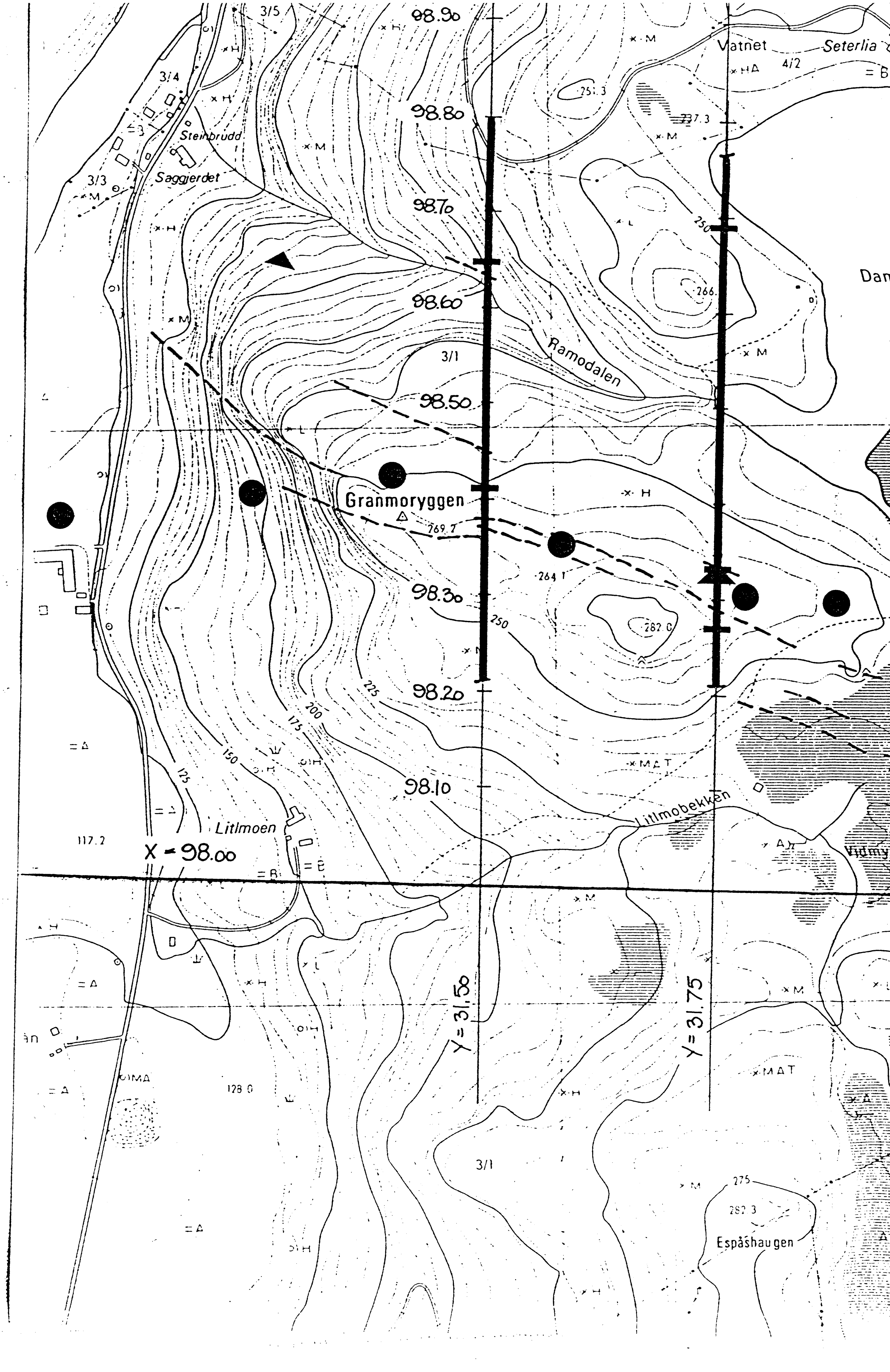
98.90
98.80
98.70
98.60
98.50
98.30
98.20
98.10
X = 98.00
Y = 31.50
Y = 31.75
Vatnet
Seterlia
4/2
3/5
3/4
3/3
3/1
Steinbrudd
Saggjerdet
Ramodalen
Granmoryggen
269.7
264.1
282.0
250
225
200
175
150
125
Litlmobekken
Litlmoen
117.2
128.0
275
282.3
Espåshaugen

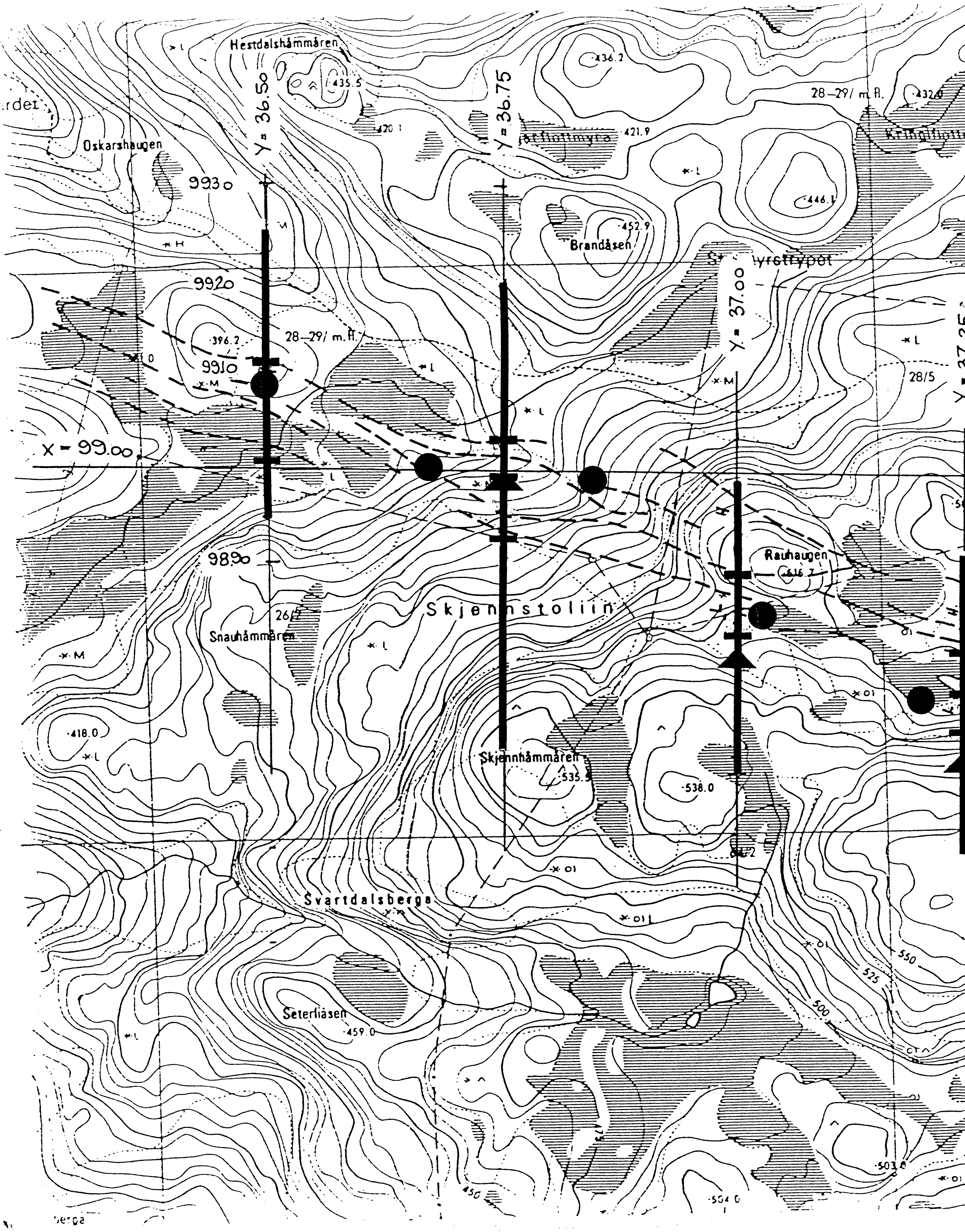

Hestdalshåmmåren
435.5
436.2
28–29/ m.fl.
Oskarshaugen
420.1
421.9
Y = 36.50
Y = 36.75
993o
Brandåsen
452.9
446.1
992o
396.2
28–29/ m.fl.
991o
Y = 37.00
28/5
X = 99.00
989o
Rauhaugen
26/2
Snauhåmmåren
418.0
Skjennhåmmåren
535.5
538.0
Svartdalsberga
Seterliåsen
459.0
550
525
500
503.0

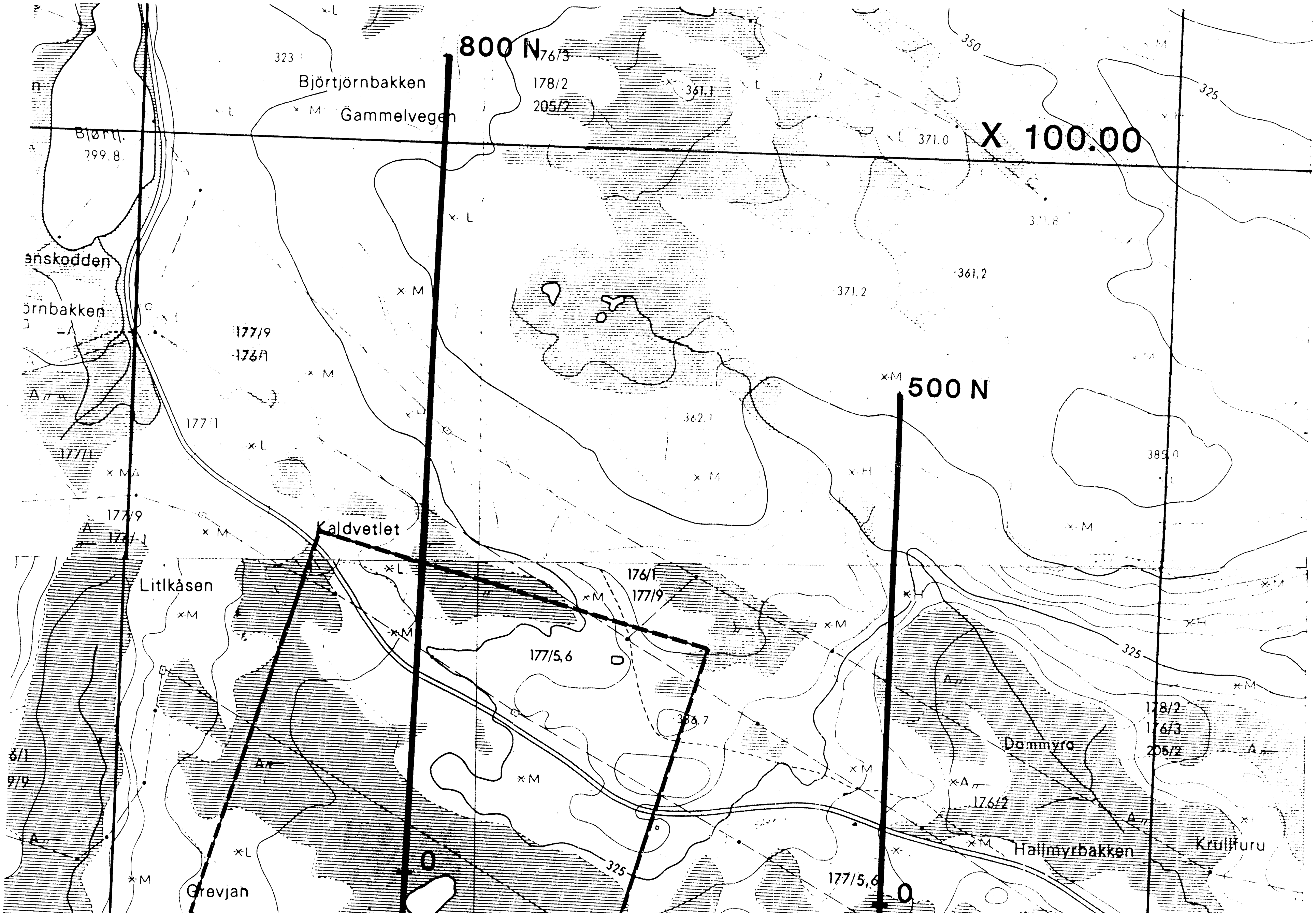

800 N
500 N
X 100.00
Björtjörnbakken
Gammelvegen
Bjørtj.
299.8
323
enskodden
örnbakken
Kaldvetlet
Litlkåsen
Grevjan
Dammyra
Hallmyrbakken
Krullfuru
176/3
178/2
205/2
361.1
371.0
371.2
361.2
362.1
385.0
386.7
177/9
176/1
177/1
177/5,6
176/2
350
325
0

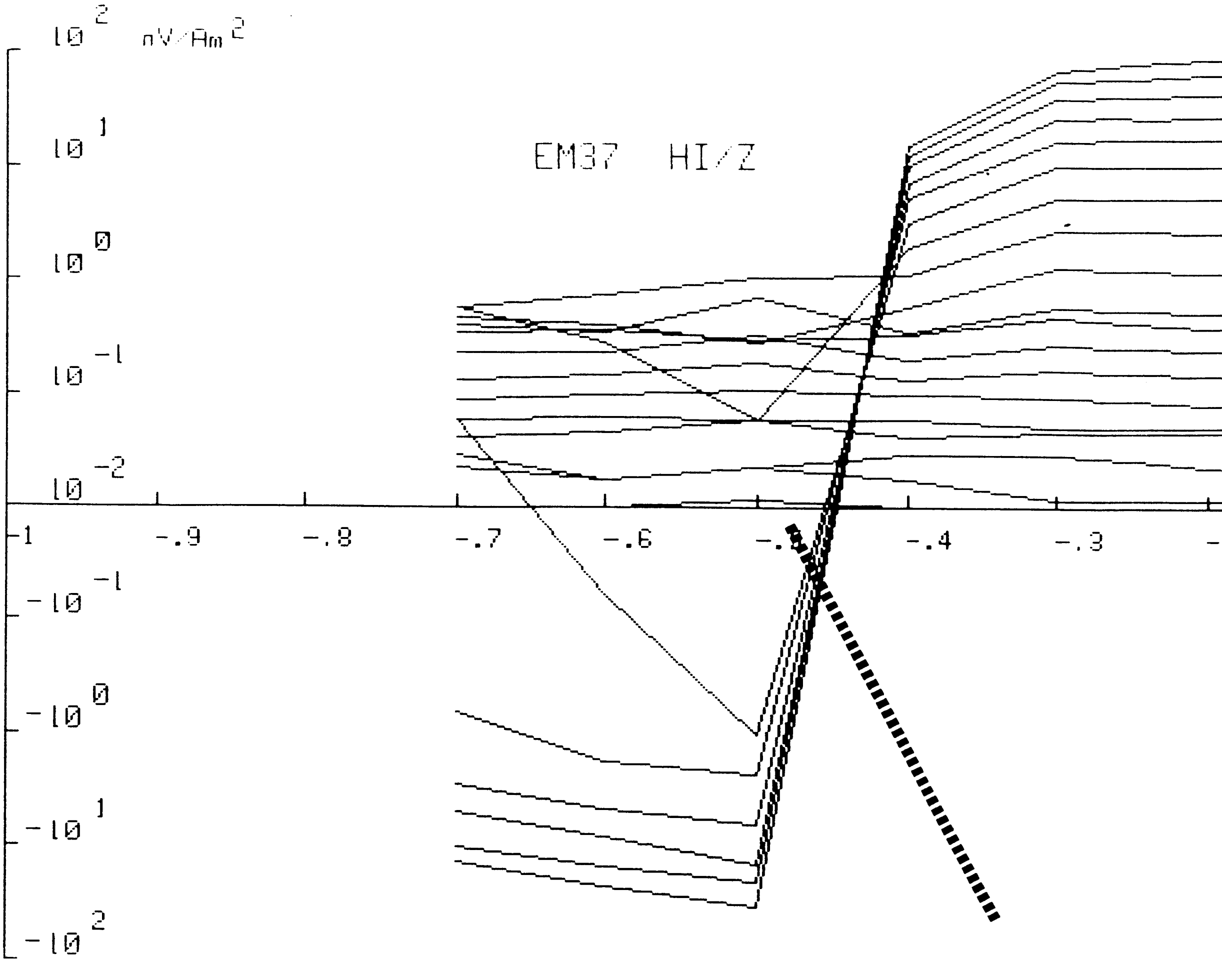

10^2 nV/Am^2
EM37 HI/Z
10^1
10^0
10^-1
10^-2
-1
-.9
-.8
-.7
-.6
-.4
-.3
-10^-1
-10^0
-10^1
-10^2

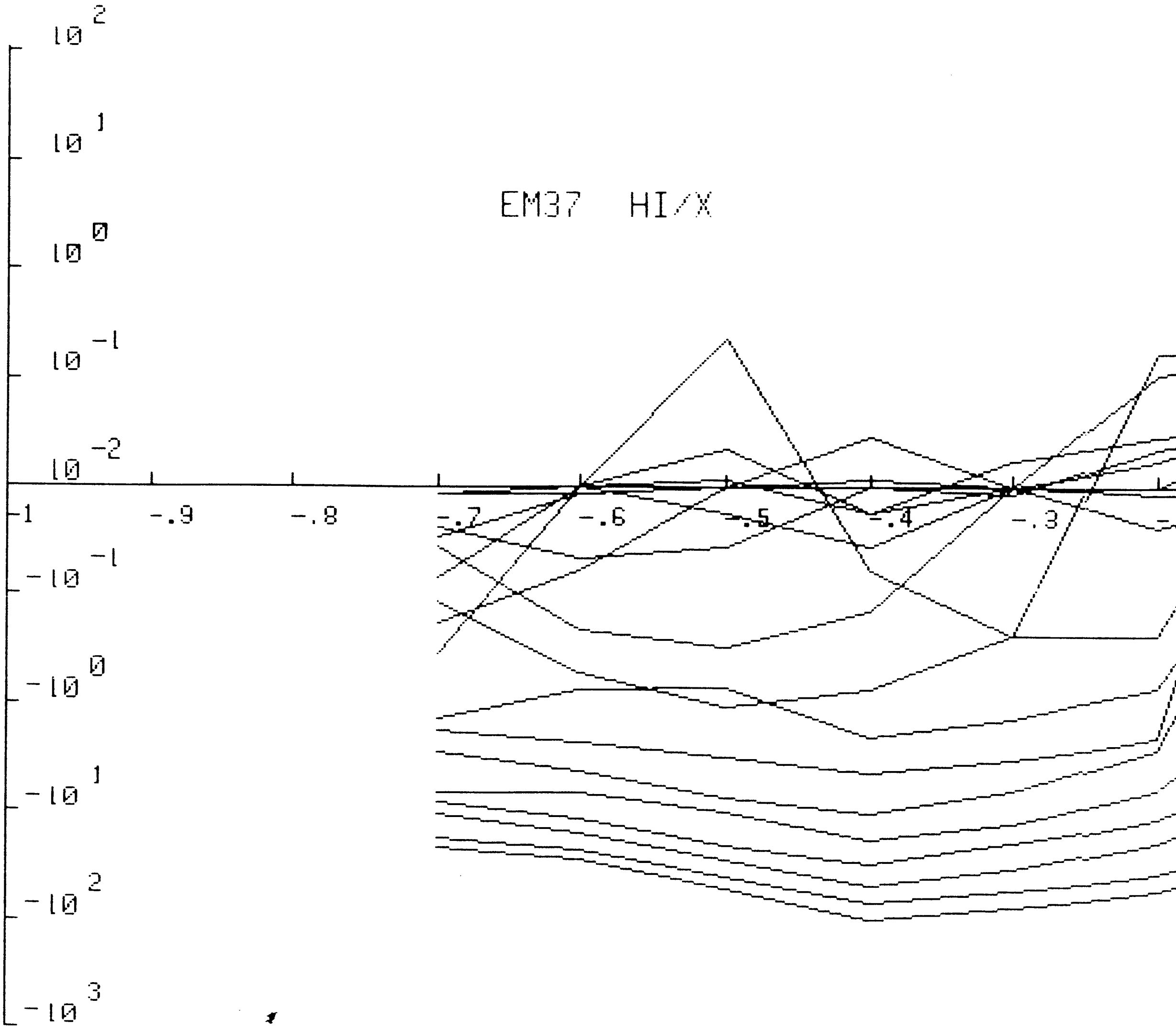

10^2
10^1
EM37 HI/X
10^0
10^-1
10^-2
-1
-.9
-.8
-.7
-.6
-.5
-.4
-.3
-10^-1
-10^0
-10^1
-10^2
-10^3

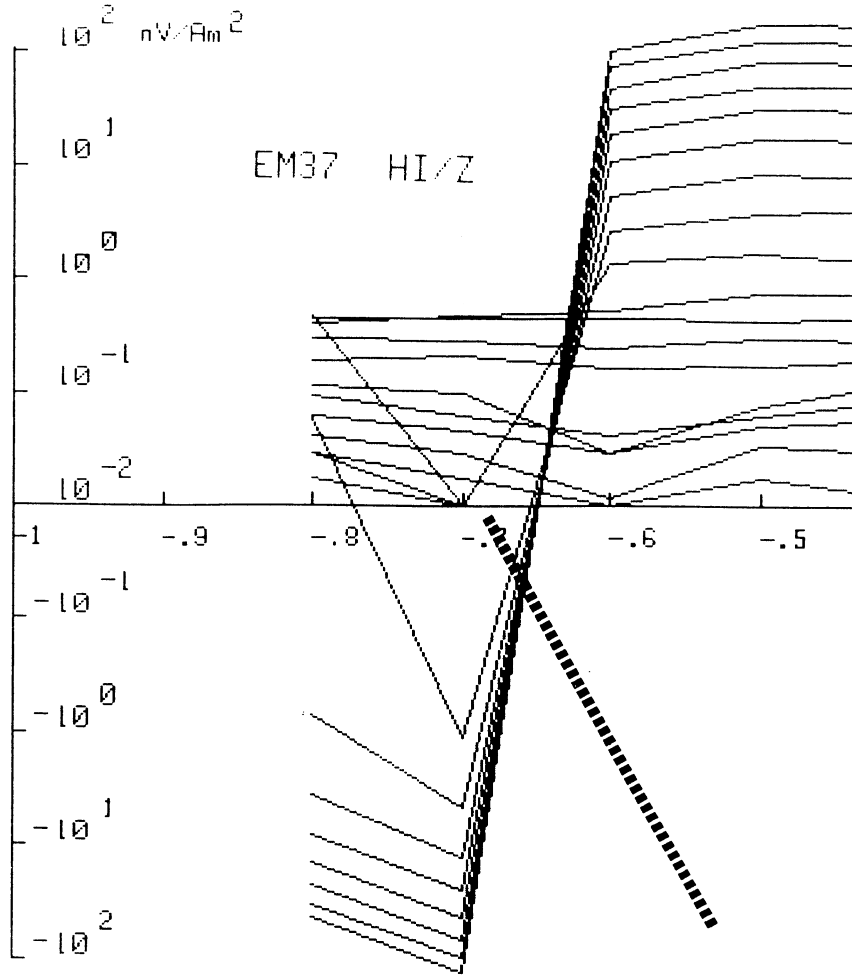

10^2 nV/Am^2
EM37 HI/Z
10^1
10^0
10^-1
10^-2
-1
-.9
-.8
-.6
-.5
-10^-1
-10^0
-10^1
-10^2

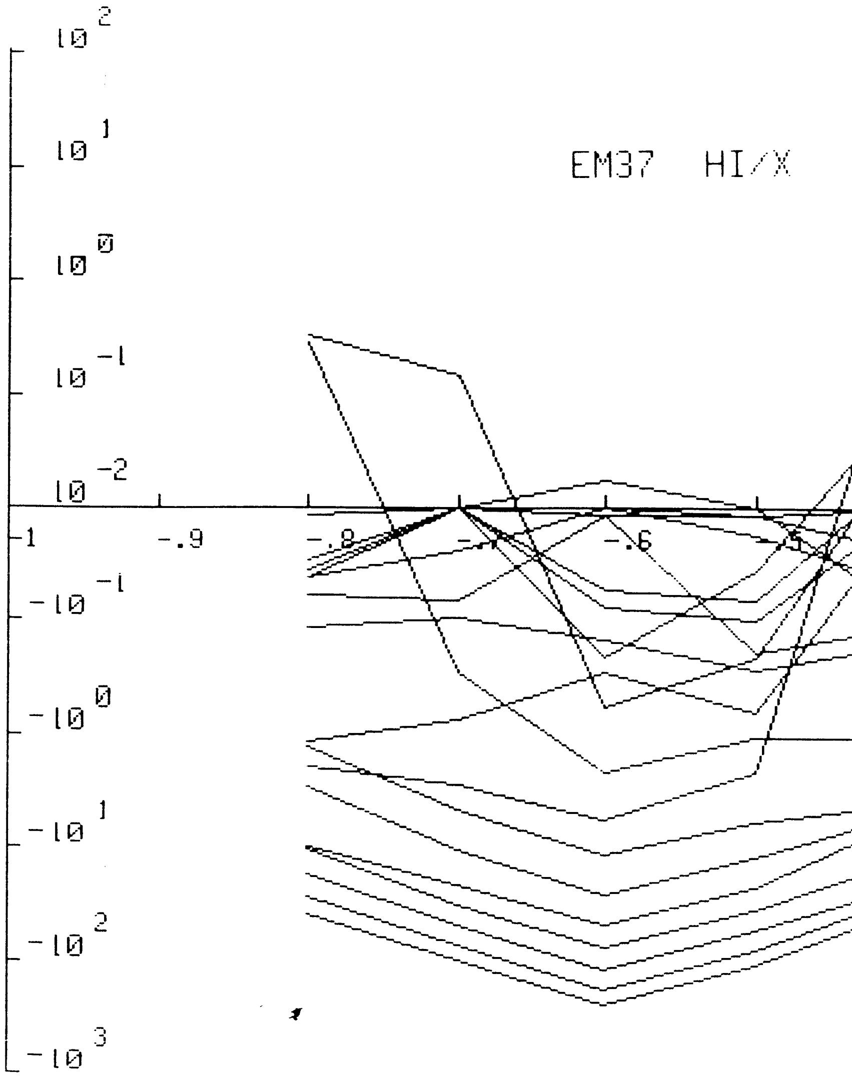

10^2
10^1
EM37 HI/X
10^0
10^-1
10^-2
-1
-.9
-10^-1
-10^0
-10^1
-10^2
-10^3

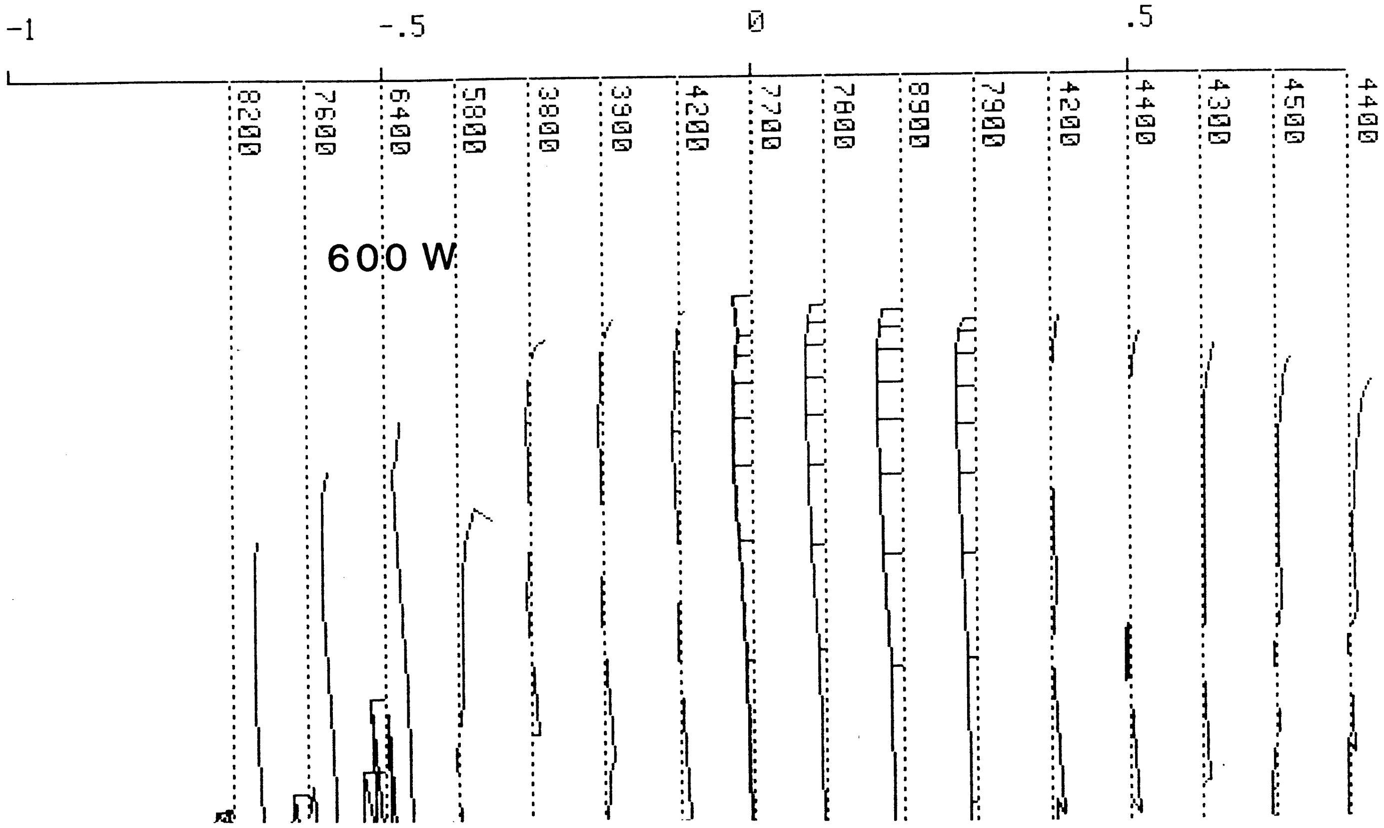

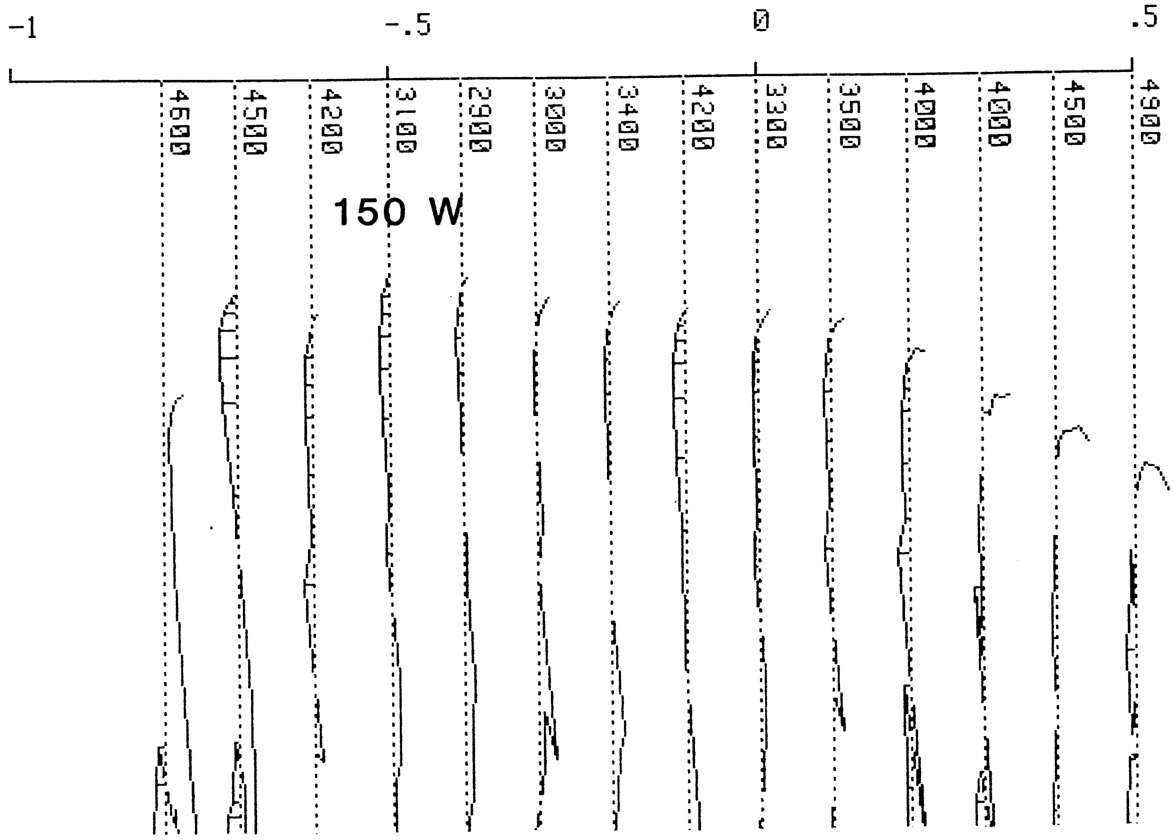

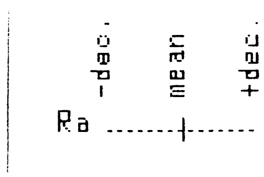

OUTOKUMPU OY Exploration	1:10000	
		JL -85
LÖKKEN , Svinsås		433
DIT-plots 600 W 150 W	App. 3/4	

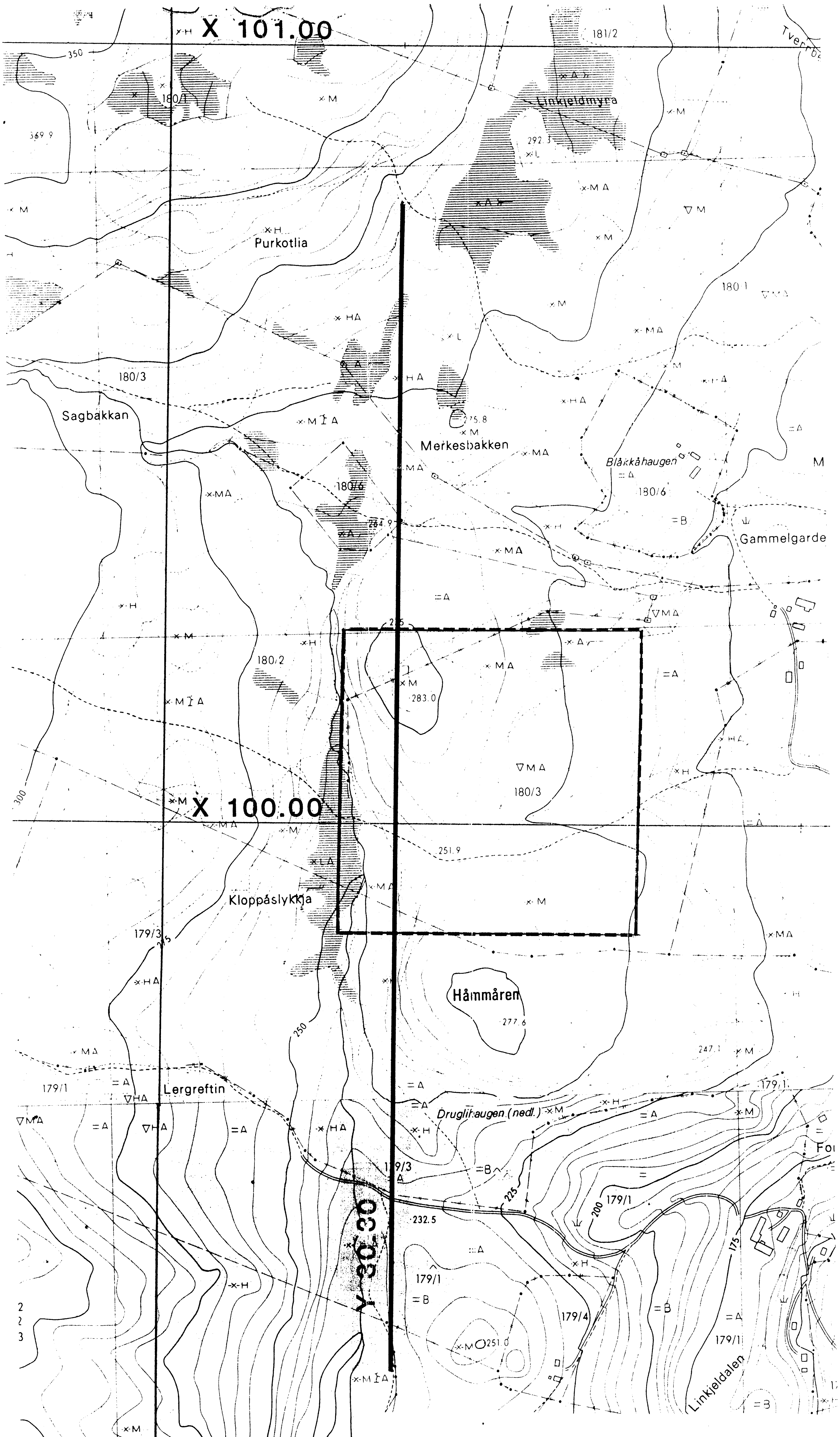

OUTOKUMPU OY Exploration	1:5000
	JL -85
LÖKKEN , Blokkum	
TDEM survey layout	App. 4/1

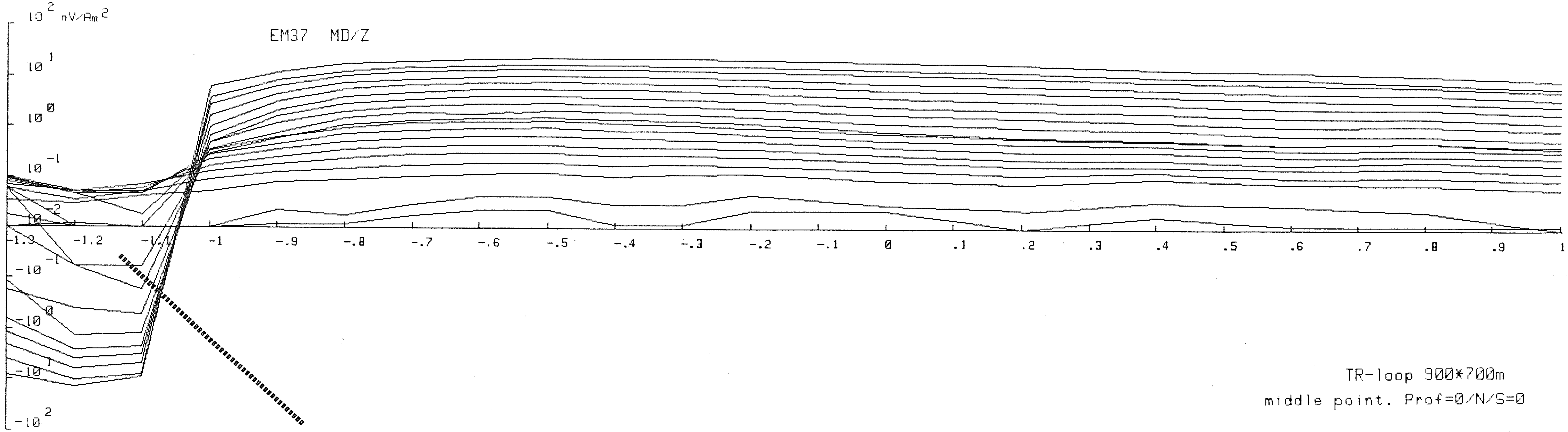

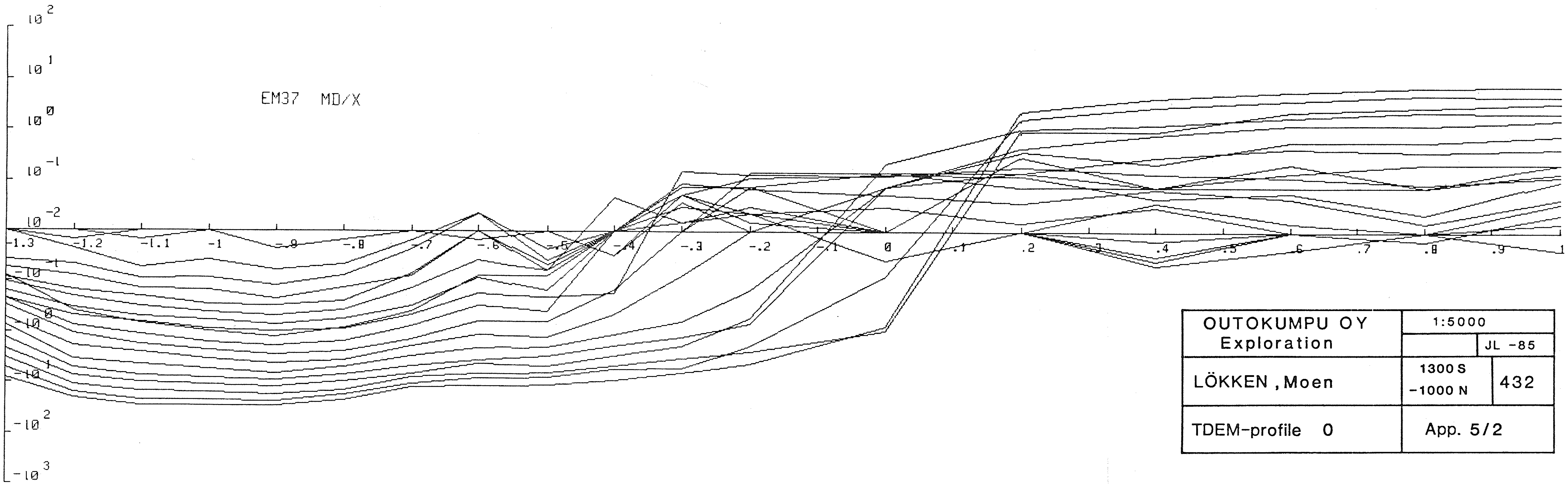

OUTOKUMPU OY Exploration	1:5000 JL -85	
LÖKKEN , Moen	1300 S -1000 N	432
TDEM-profile 0	App. 5/2	

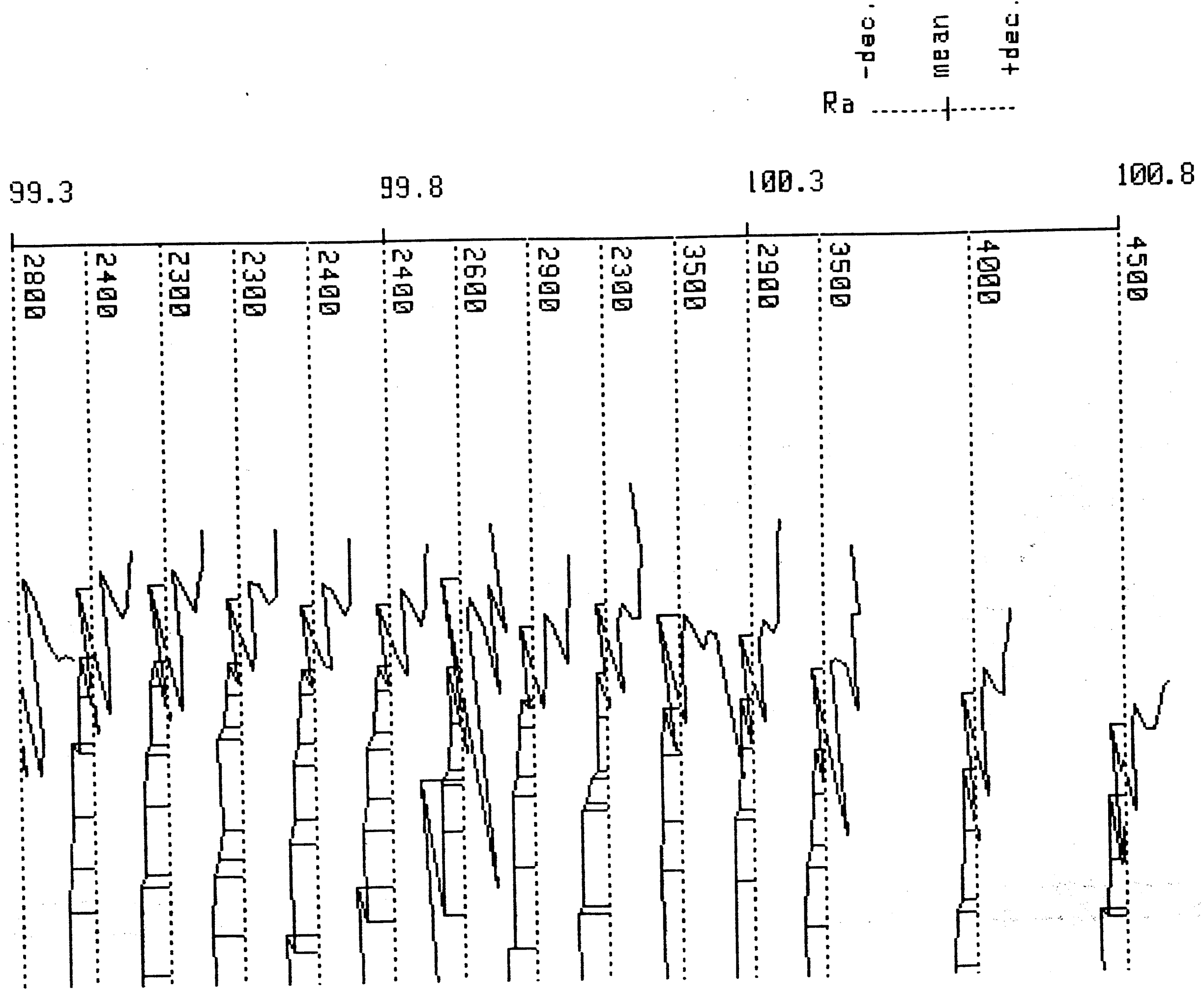

OUTOKUMPU OY Exploration	1:10000	
		JL -85
LÖKKEN , Blokkum		433
DIT-plot Y 30.40	App. 4/3	

Linear plot

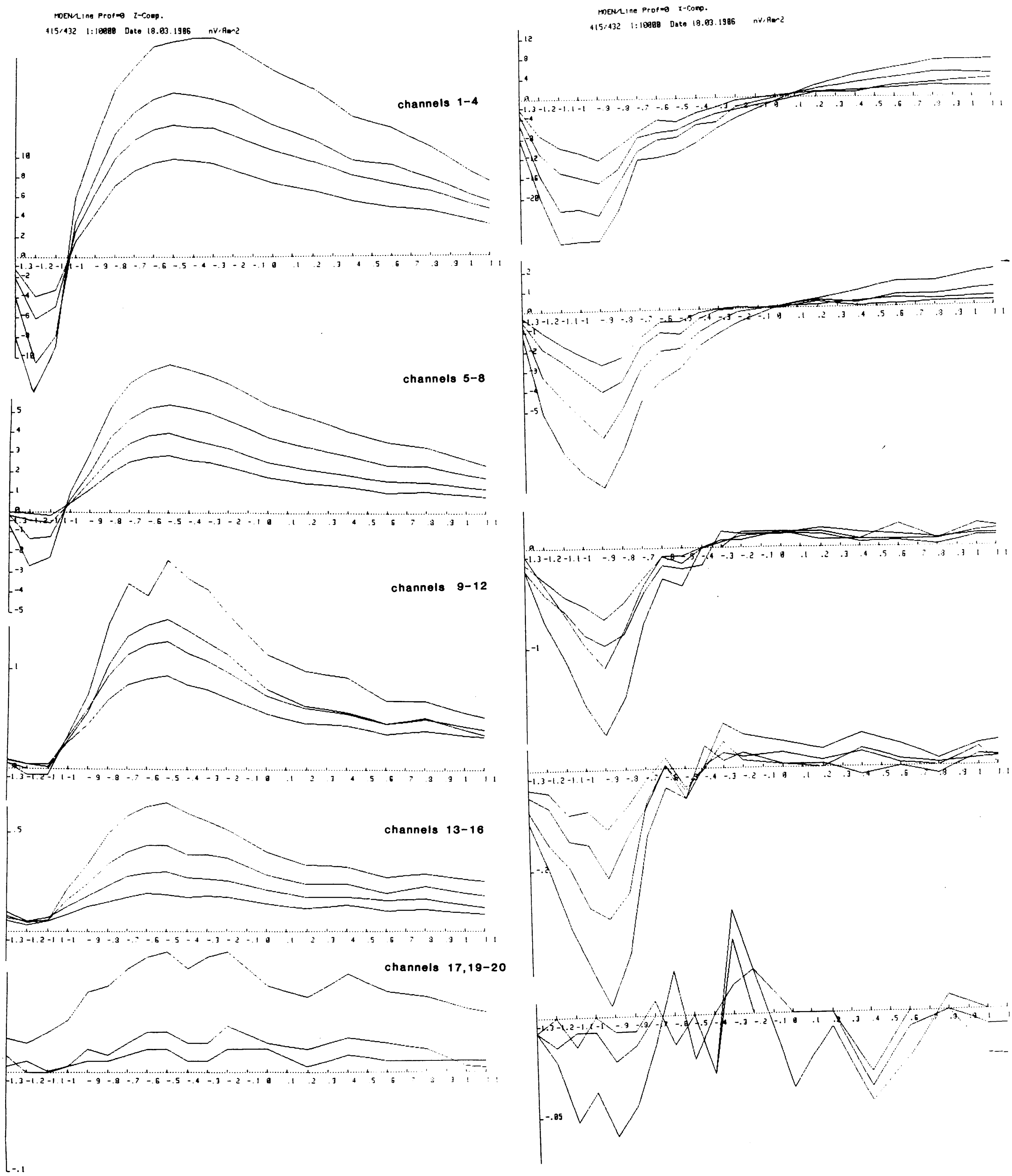
MOEN/Line Prof=0 Z-Comp.
415/432 1:10000 Date 18.03.1986 nV/Am^2
MOEN/Line Prof=0 X-Comp.
415/432 1:10000 Date 18.03.1986 nV/Am^2
channels 1-4
channels 5-8
channels 9-12
channels 13-16
channels 17,19-20

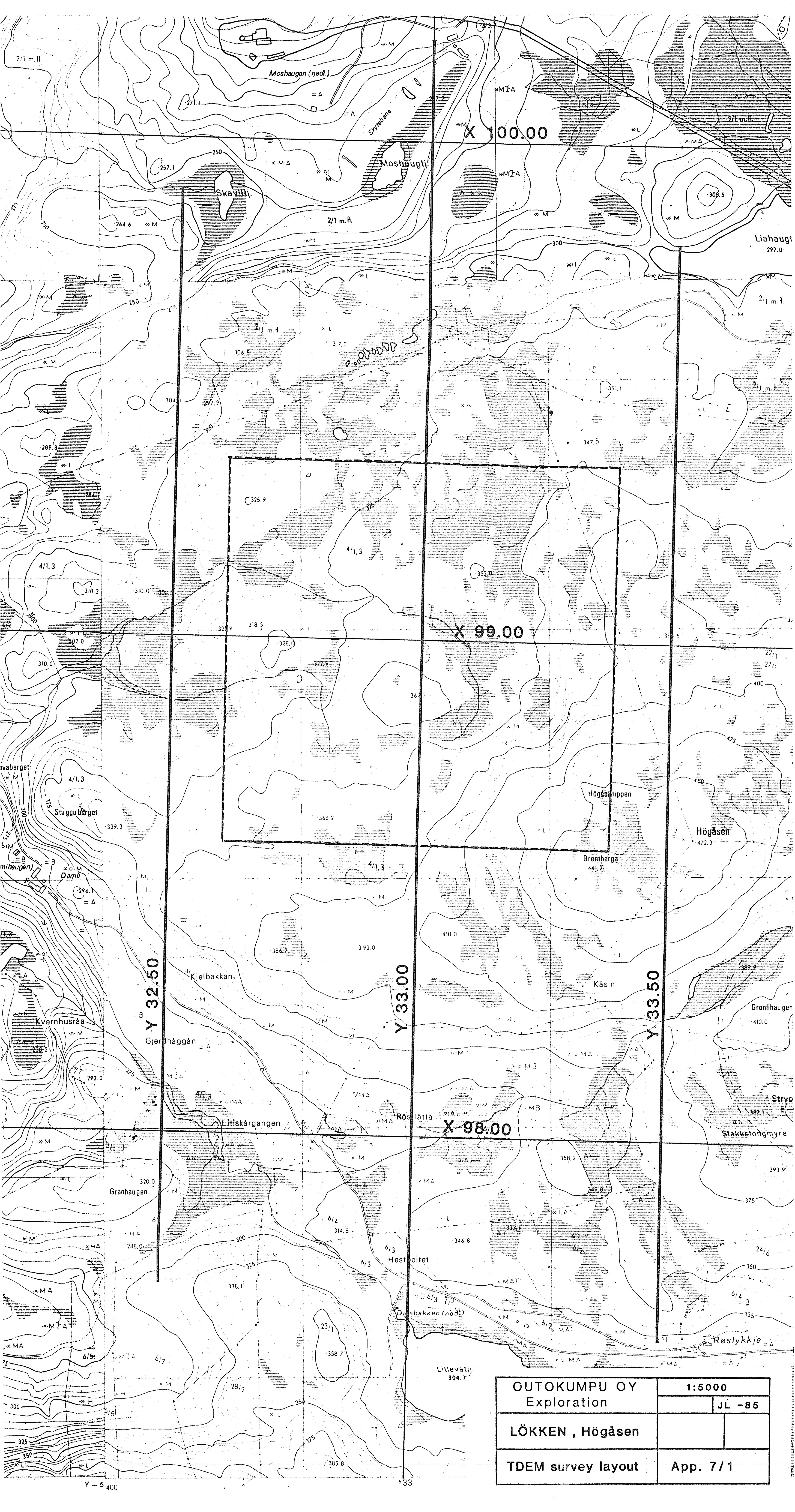

OUTOKUMPU OY Exploration	1:5000	
		JL -85
LÖKKEN , Högåsen		
TDEM survey layout	App. 7/1	

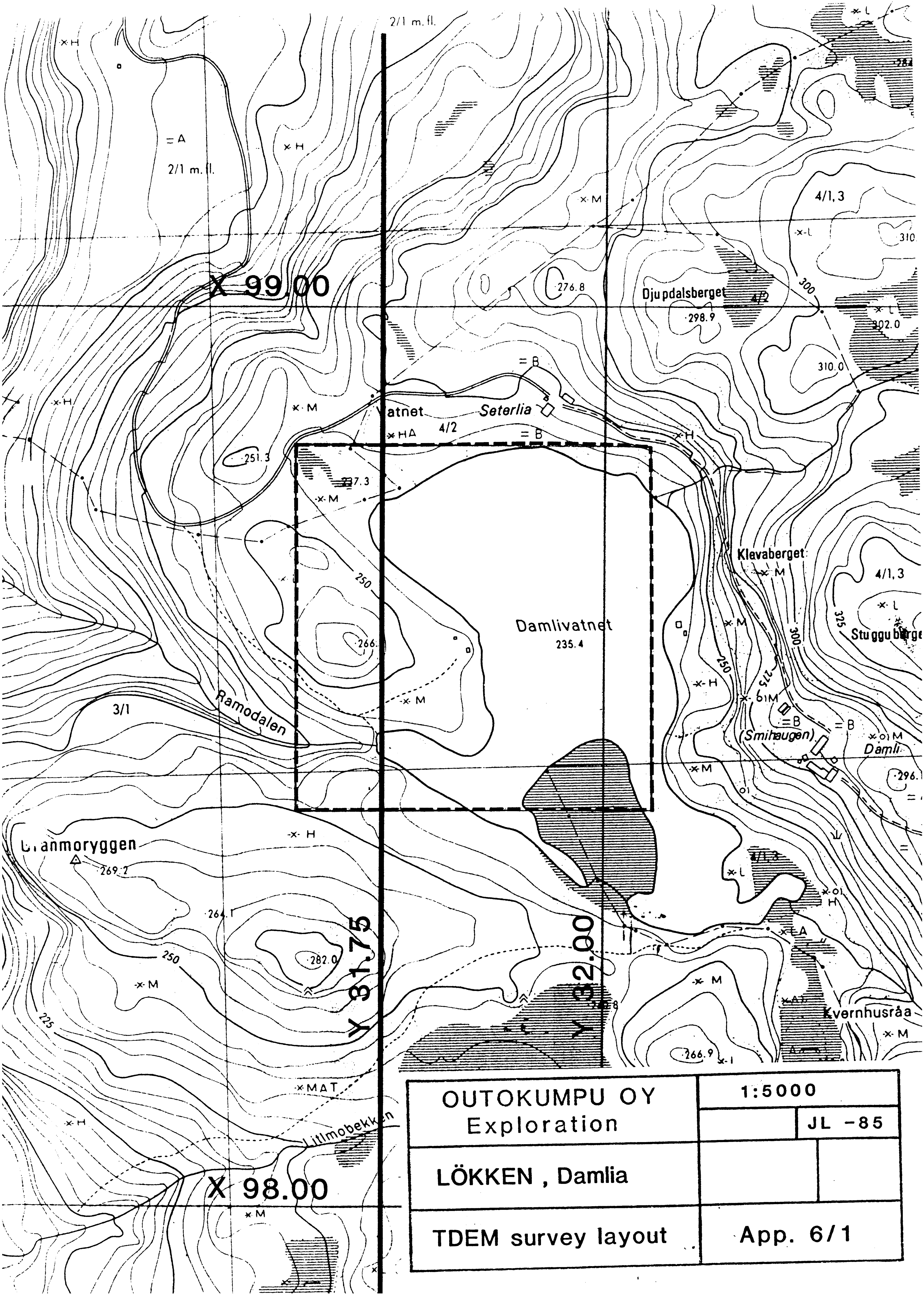

OUTOKUMPU OY Exploration	1:5000 JL -85
LÖKKEN , Damlia	
TDEM survey layout	App. 6/1

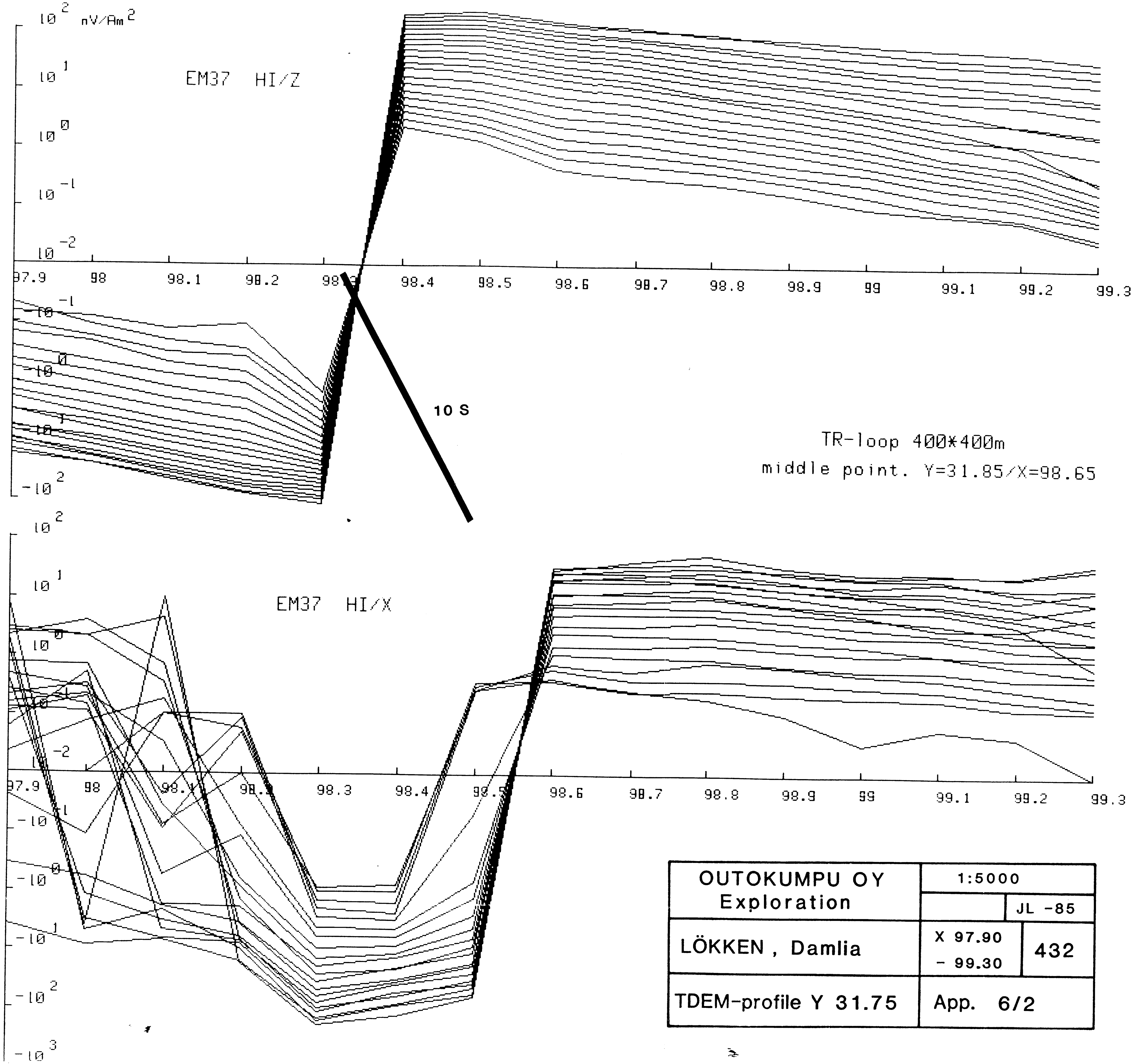

OUTOKUMPU OY Exploration	1:5000	
		JL -85
LÖKKEN , Damlia	X 97.90 - 99.30	432
TDEM-profile Y 31.75	App. 6/2	

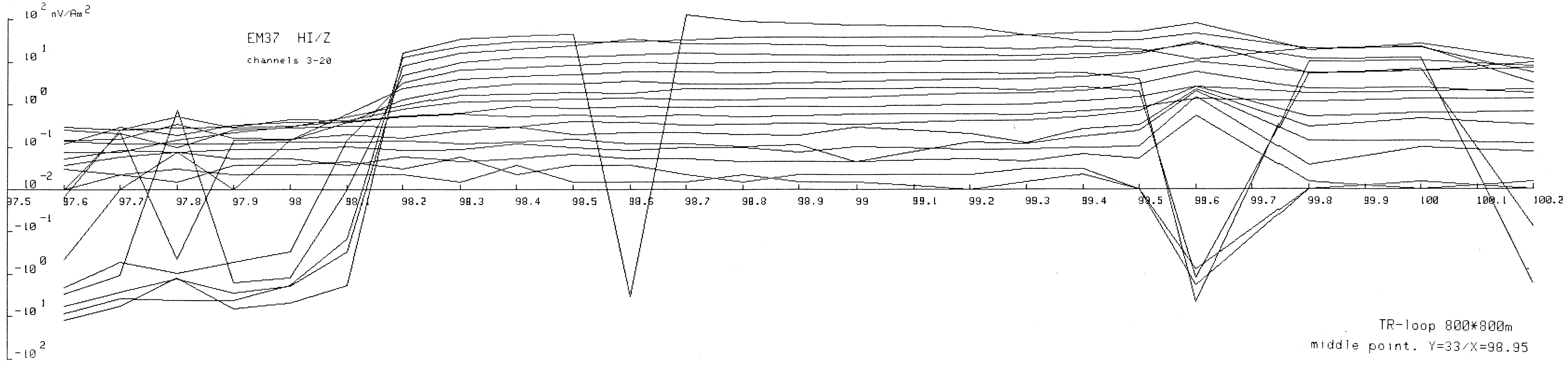

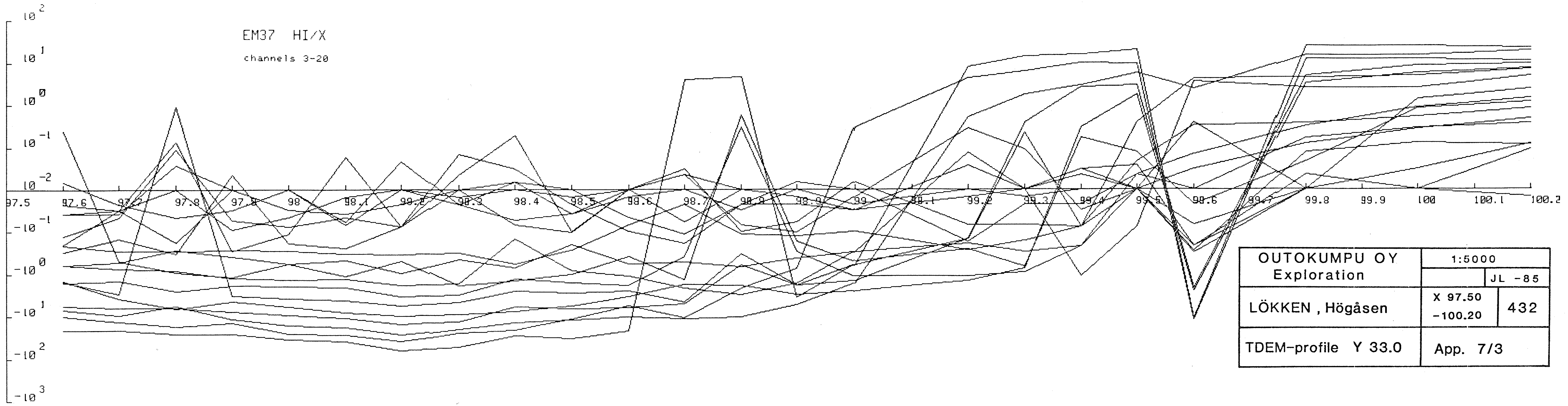

OUTOKUMPU OY Exploration	1:5000	
		JL -85
LÖKKEN , Högåsen	X 97.50 -100.20	432
TDEM-profile Y 33.0	App. 7/3	

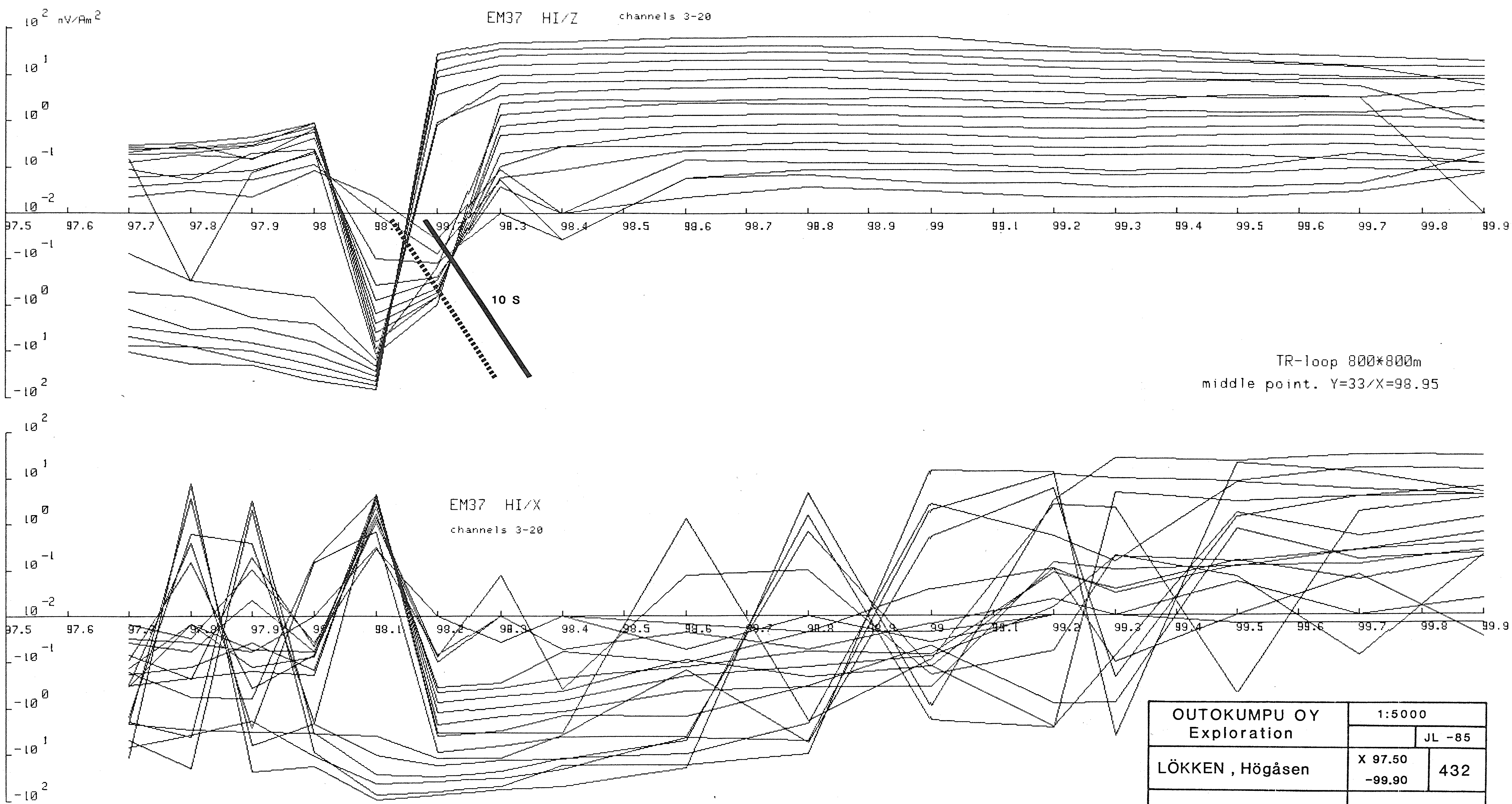

OUTOKUMPU OY Exploration	1:5000	
		JL -85
LÖKKEN , Högåsen	X 97.50 -99.90	432
TDEM-profile Y 32.50	App. 7/2	

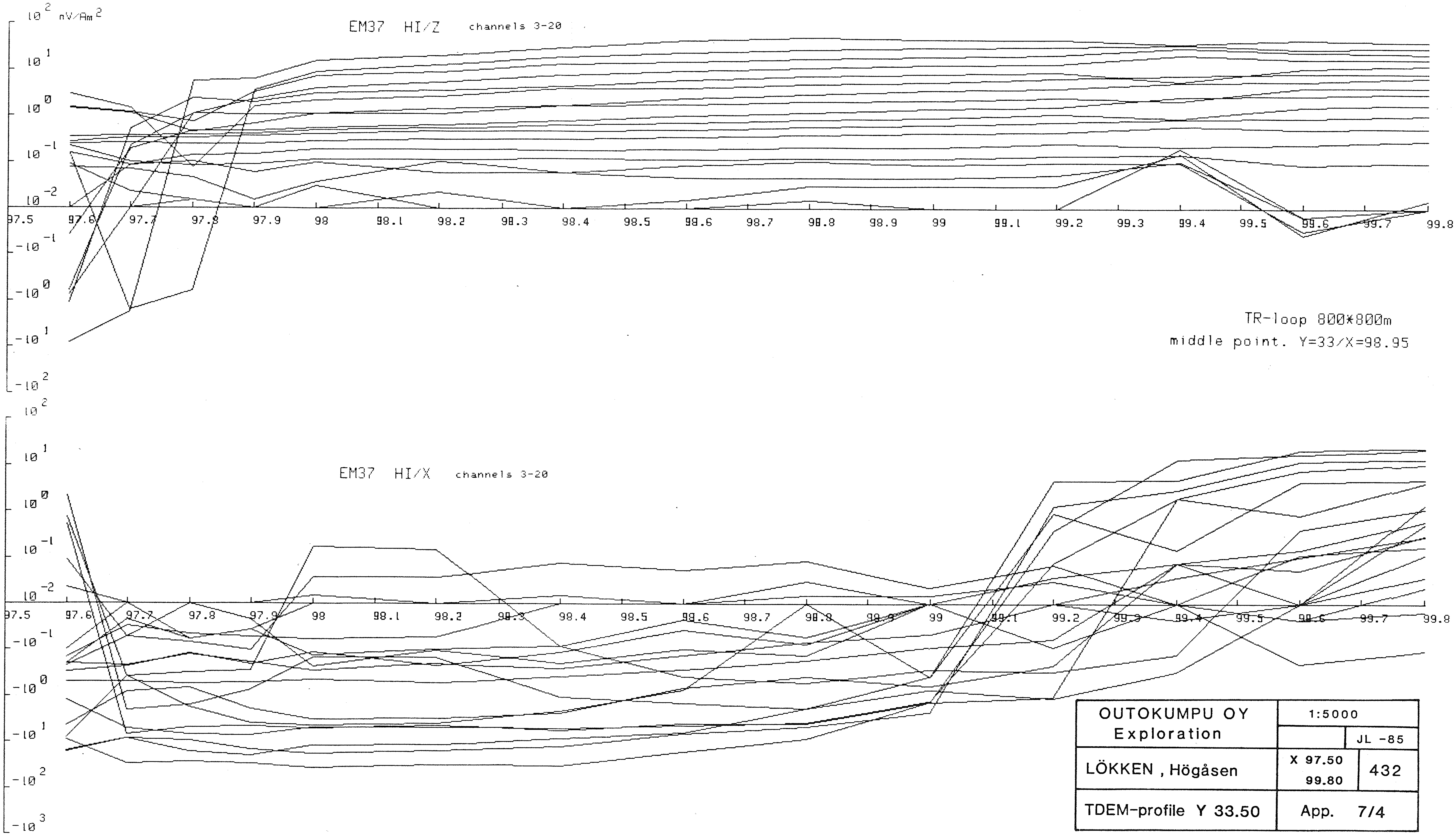

OUTOKUMPU OY Exploration	1:5000	
		JL -85
LÖKKEN , Högåsen	X 97.50 99.80	432
TDEM-profile Y 33.50	App. 7/4	

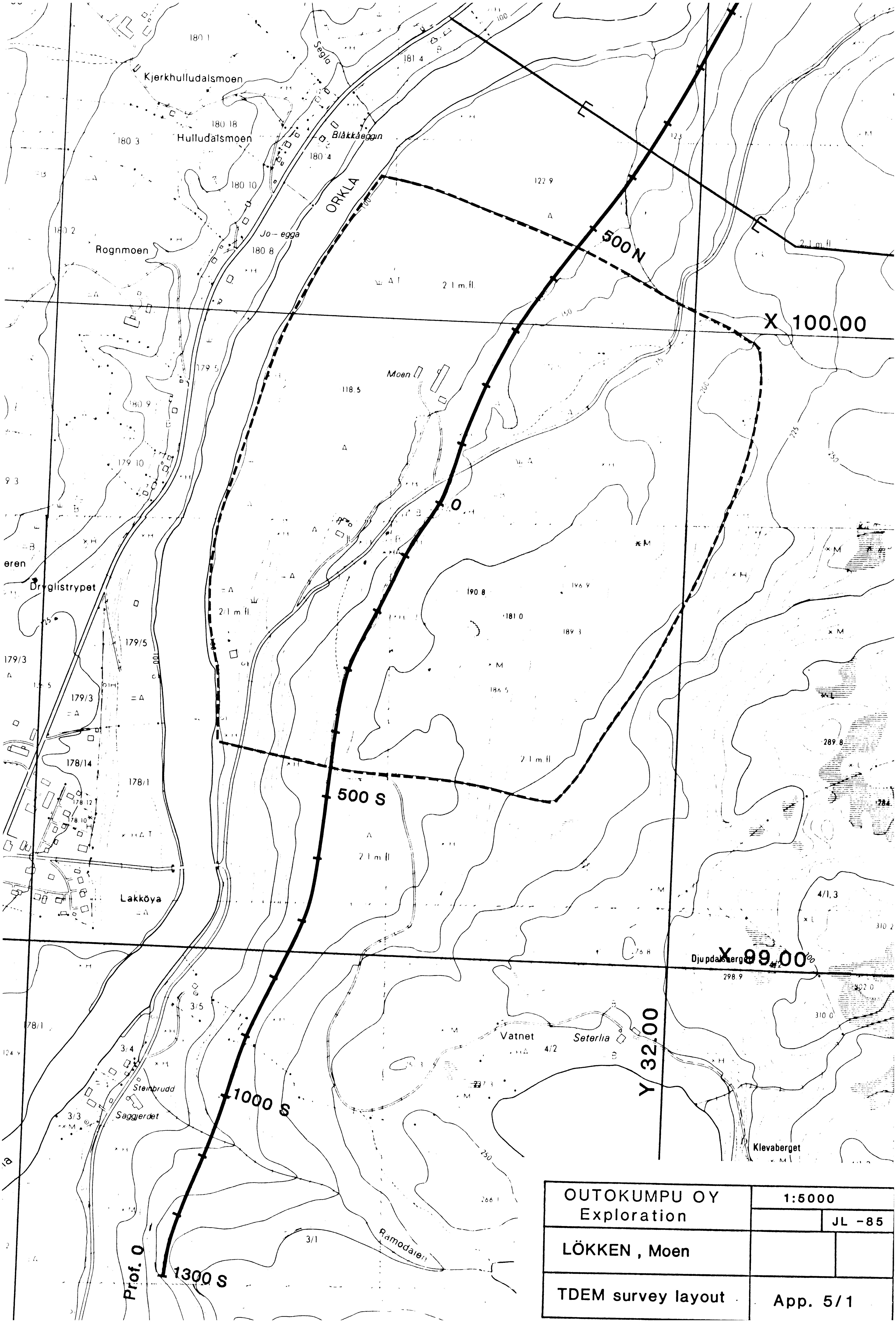

OUTOKUMPU OY Exploration	1:5000	
		JL -85
LÖKKEN , Moen		
TDEM survey layout	App. 5/1	

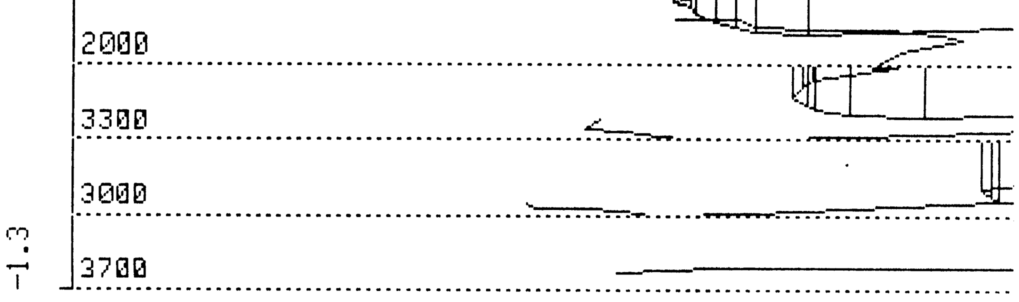
2000
3300
3000
-1.3
3700

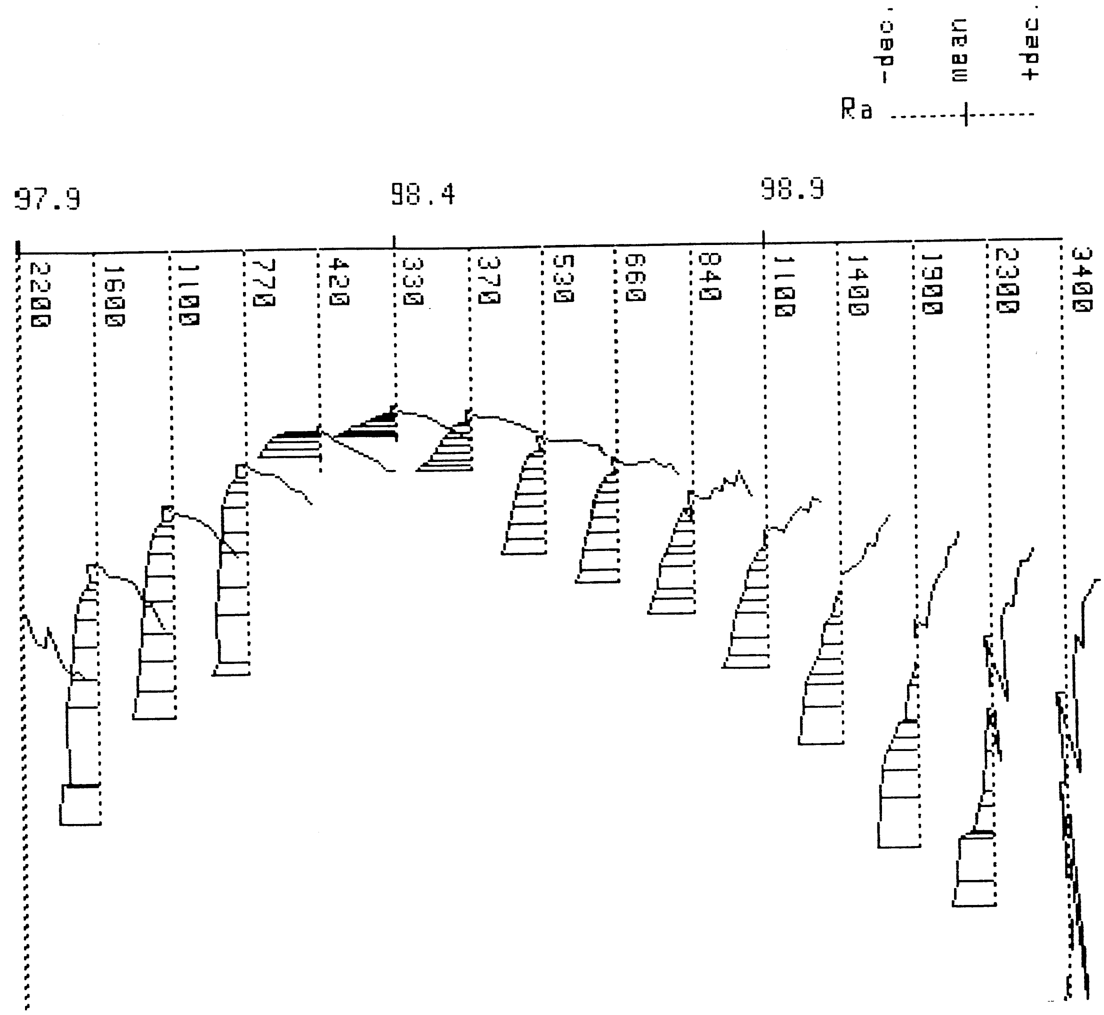

OUTOKUMPU OY Exploration	1:10 000 JL -85
LÖKKEN , Damlia	433
DIT-plot Y 31.75	App. 6/3

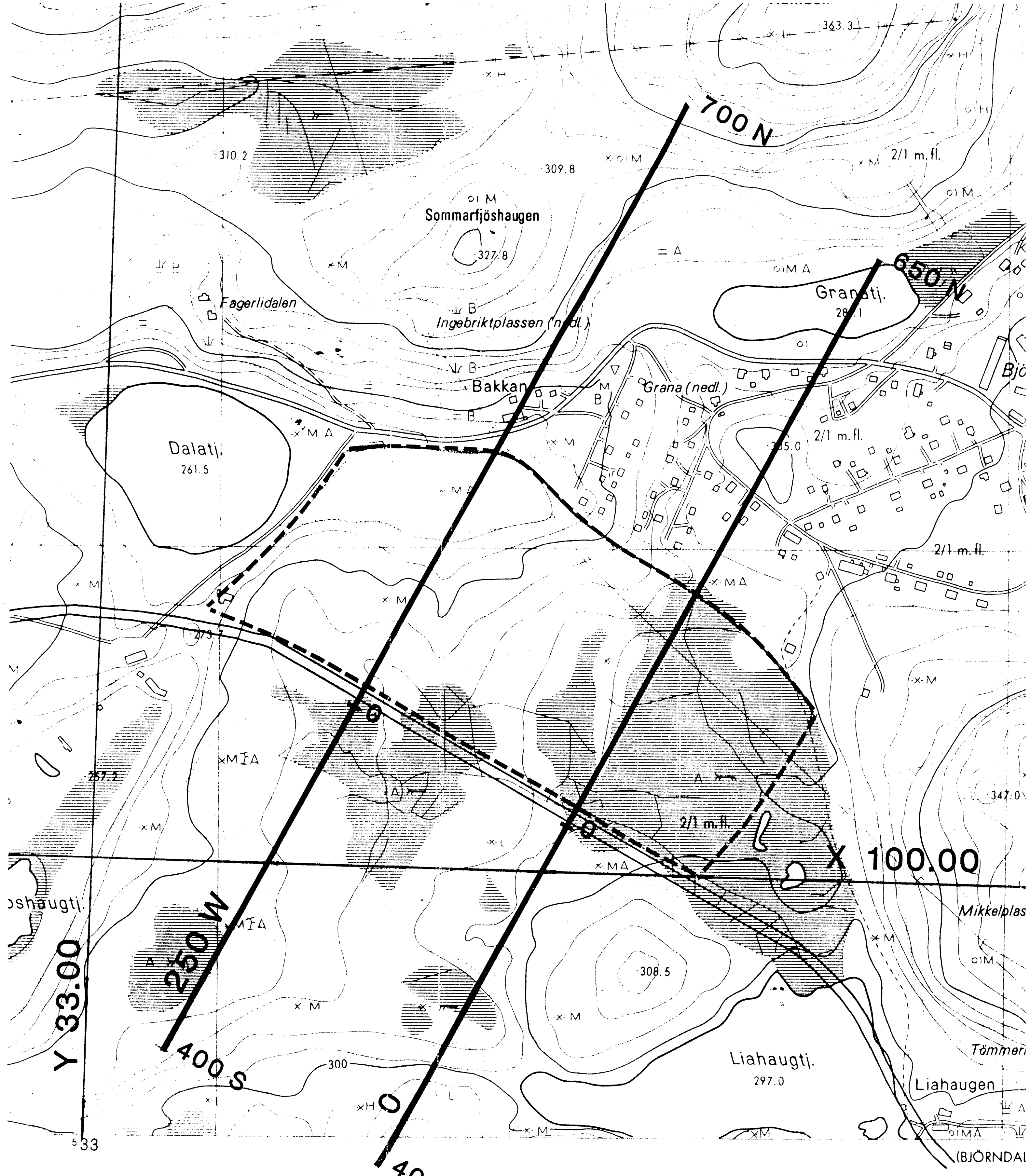

GO, andre
ıtogramm best pkt
st fastmerke, [kompassdrag]
erker betyr
ı.v presisjon, vanlig
:esgrense
e
e, servitutgrense
' eller stein
renserøys, grensepunkt

ndomsgrense
erde m fl
erde m fl ı eiendomsgrense
emur ı eiendomsgrense]

Bygning, [ruin, grunnmur
Riksveg
Fylkesveg (med bro)
Kommunal bilveg
Privat bilveg
Anna veg
Sti
Veg med bom
Busslomme, møteplass, o
Permanent velteplass
Offentlig veg under bygg
Jernbane, enkelt, dobbel
Veg og jernbanetunnel
Større skjæring
Større fylling

OUTOKUMPU OY Exploration	1:5000 JL -85
LÖKKEN , Björnli	
TDEM survey layout	App. 8/1

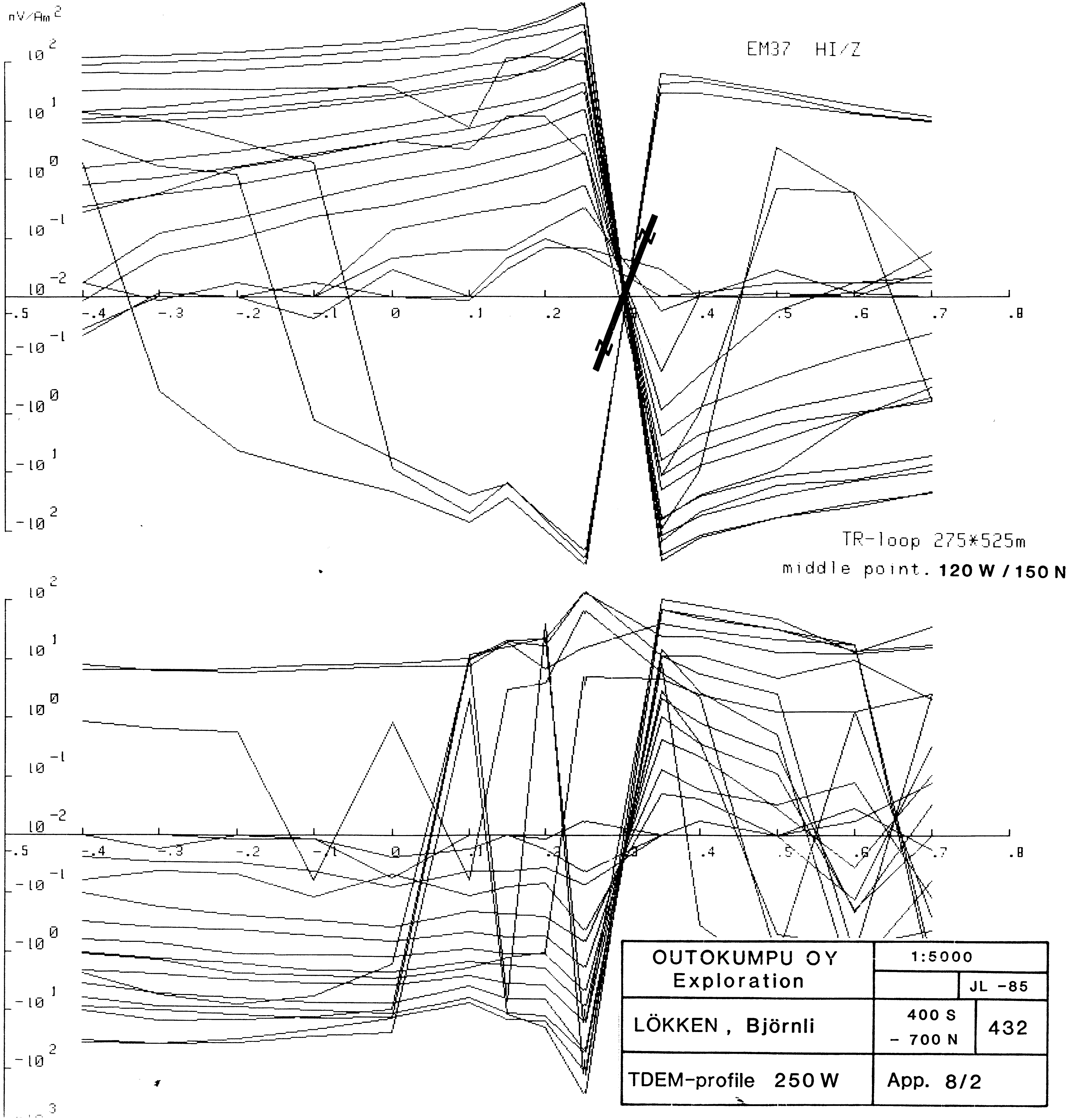

OUTOKUMPU OY Exploration	1:5000	
		JL -85
LÖKKEN , Björnli	400 S - 700 N	432
TDEM-profile 250 W	App. 8/2	

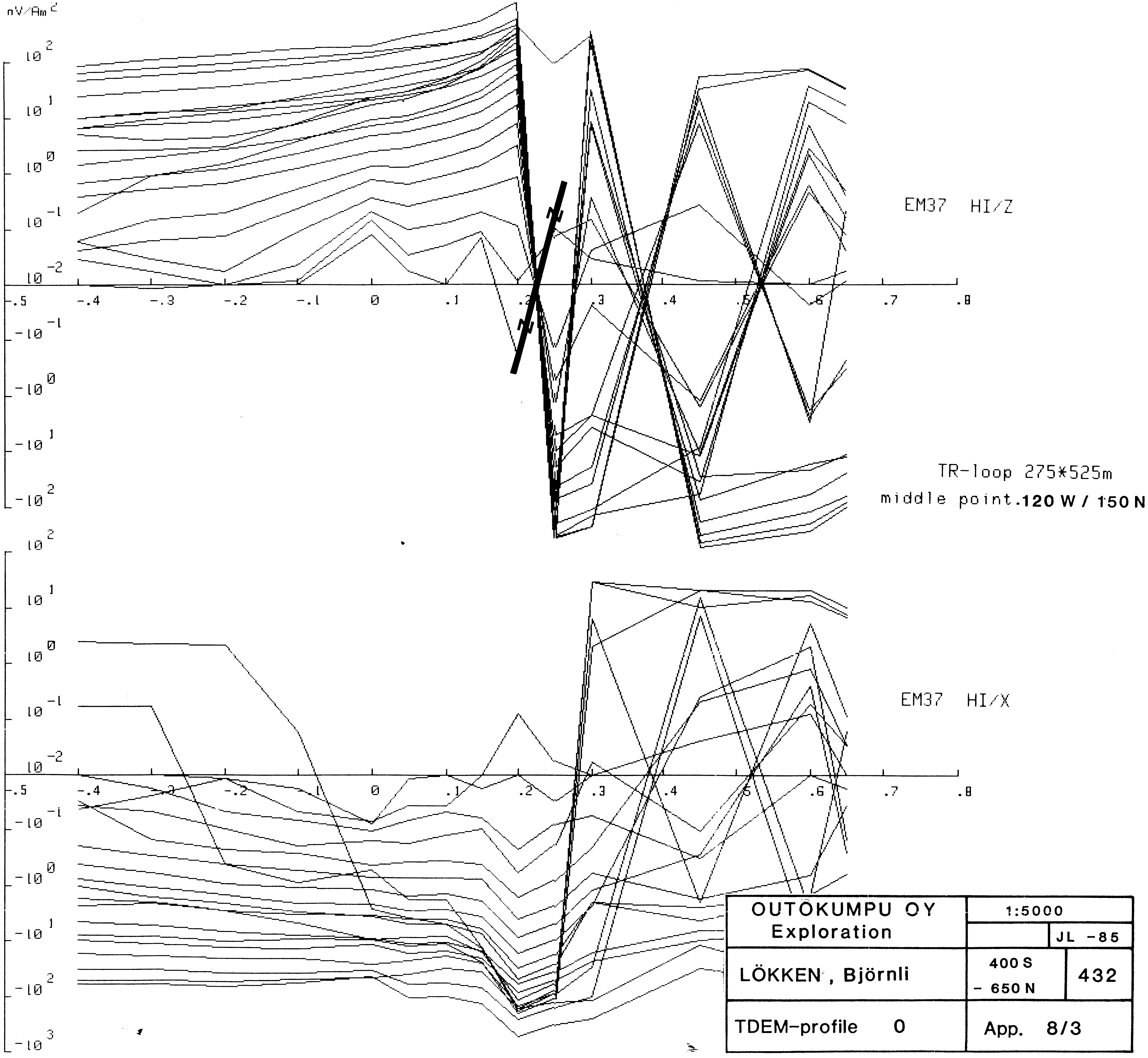

OUTOKUMPU OY Exploration	1:5000	JL -85
LÖKKEN , Björnli	400 S - 650 N	432
TDEM-profile 0	App. 8/3	

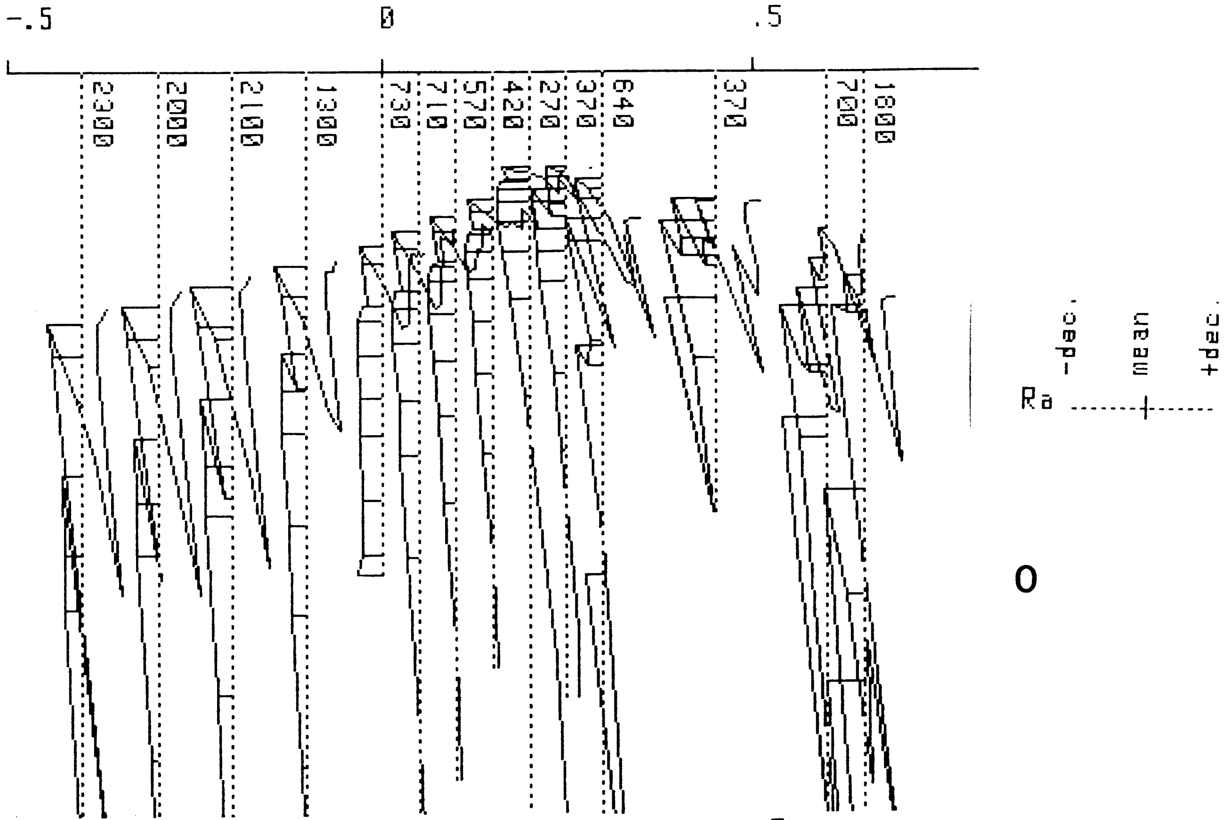

0

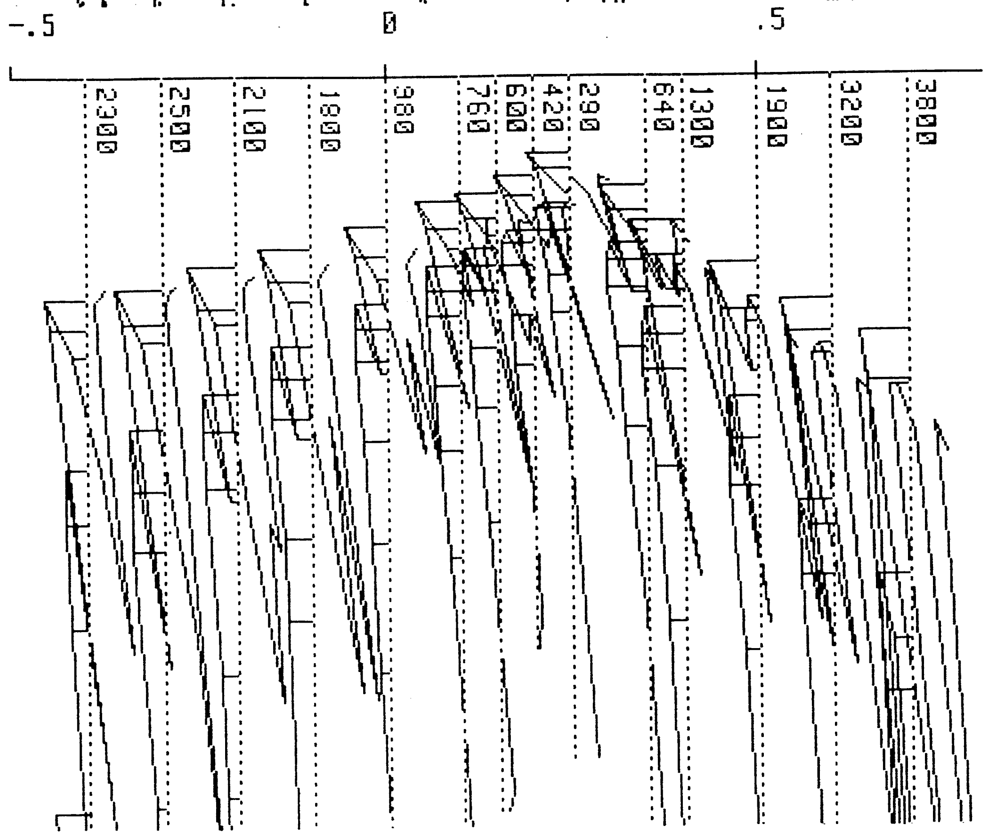

250 W

OUTOKUMPU OY Exploration	1:10 000	
		JL -85
LÖKKEN , Björnli		433
DIT-plots 0 250 W	App. 8/4	

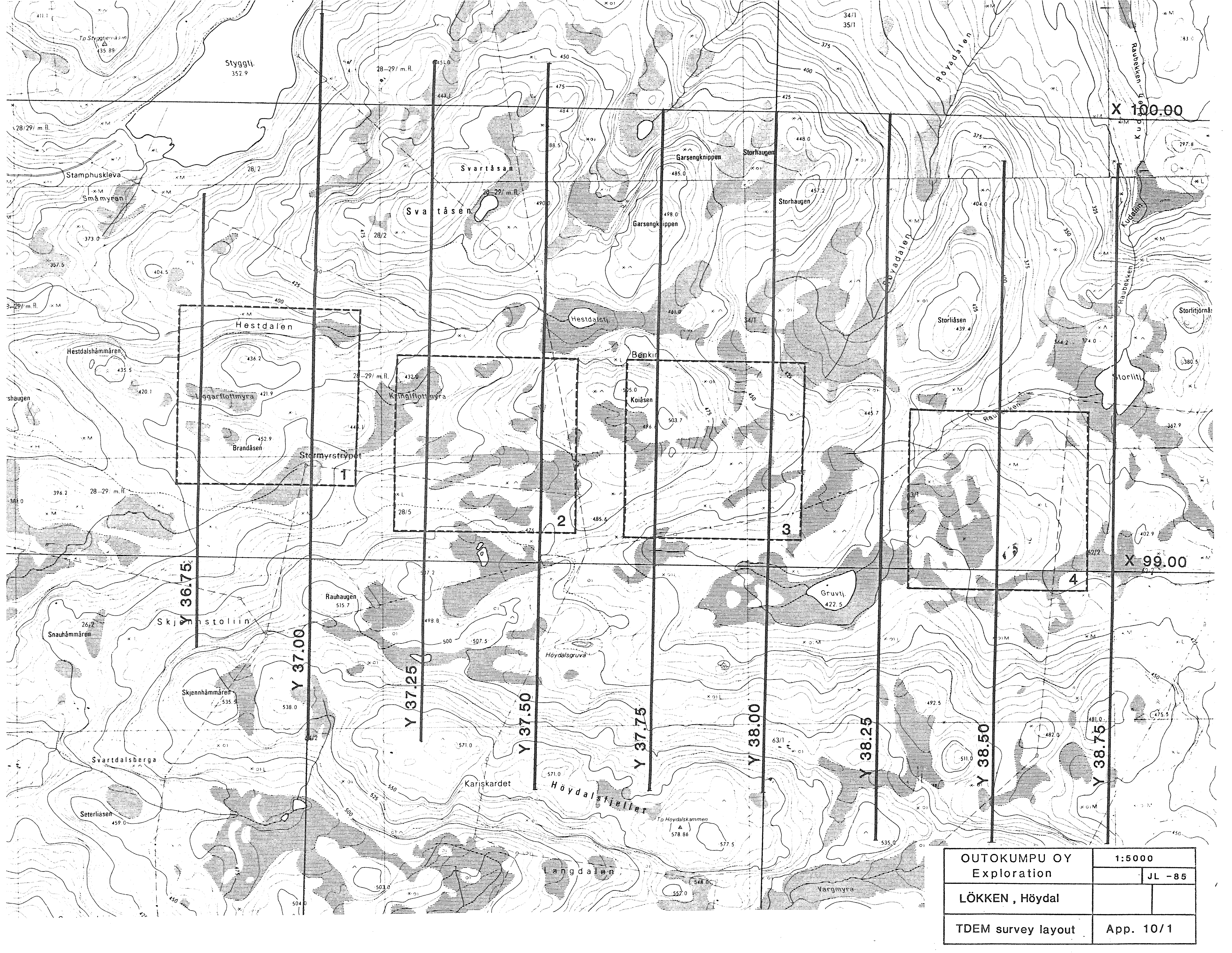

X 100.00
X 99.00
Y 36.75
Y 37.00
Y 37.25
Y 37.50
Y 37.75
Y 38.00
Y 38.25
Y 38.50
Y 38.75
1
2
3
4
Styggtj.
Stamphuskleva
Svartåsan
Svartåsen
Garsengknippen
Storhaugen
Röyadalen
Raubekken
Kudalen
Hestdalen
Hestdalshammaren
Brandåsen
Stormyrstrypet
Hestdalstj.
Koiåsen
Storliåsen
Storlitj.
Rauhaugen
Gruvtj.
Skjennstoliin
Snauhåmmaren
Skjennhåmmaren
Höydalsgruva
Svartdalsberga
Seterliasen
Kariskardet
Höydalsfjellet
Langdalen
Vargmyra
OUTOKUMPU OY
Exploration
1:5000
JL -85
LÖKKEN , Höydal
TDEM survey layout
App. 10/1

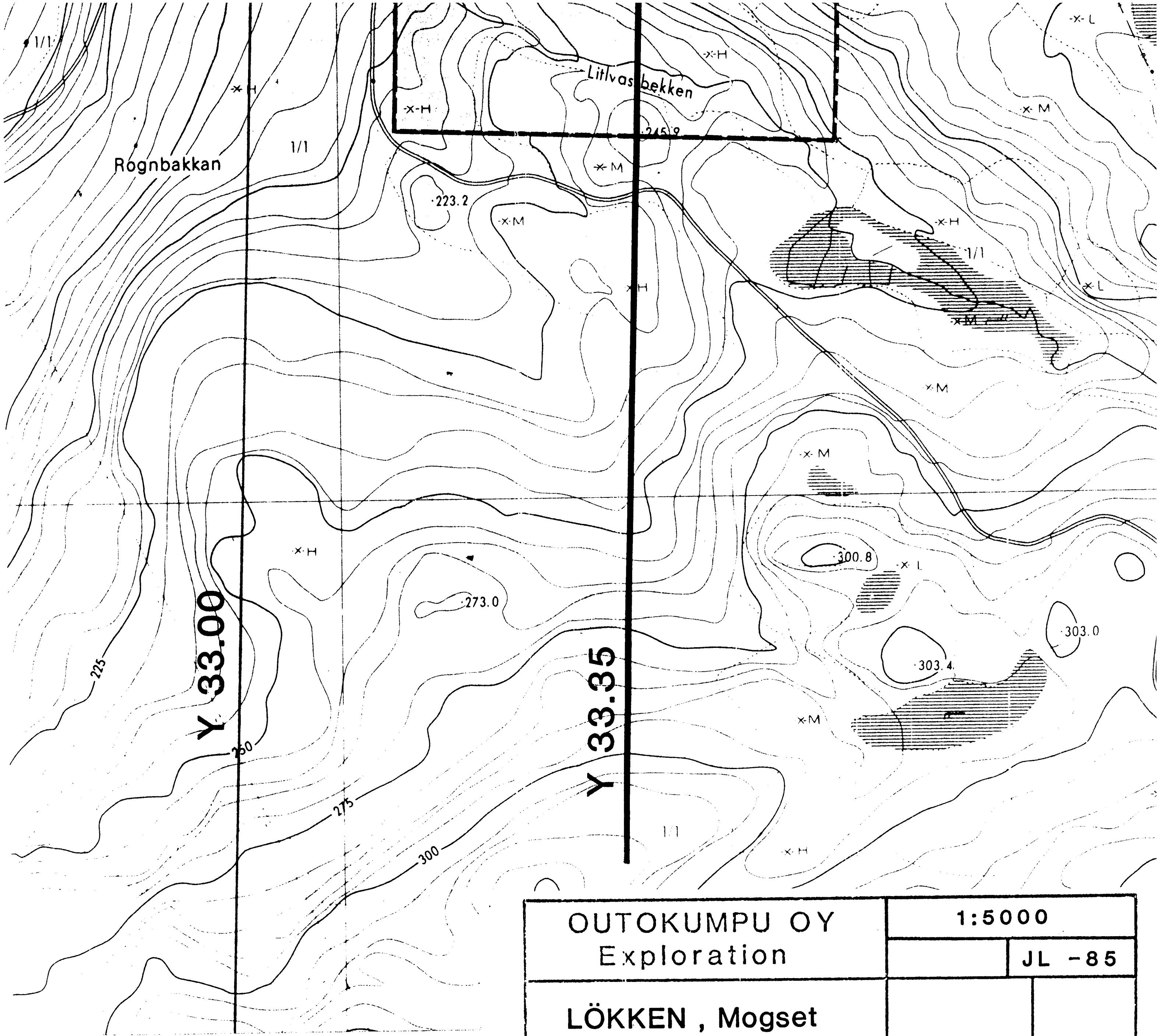

OUTOKUMPU OY Exploration	1:5000 JL -85
LÖKKEN , Mogset	
TDEM survey layout	App. 9/1

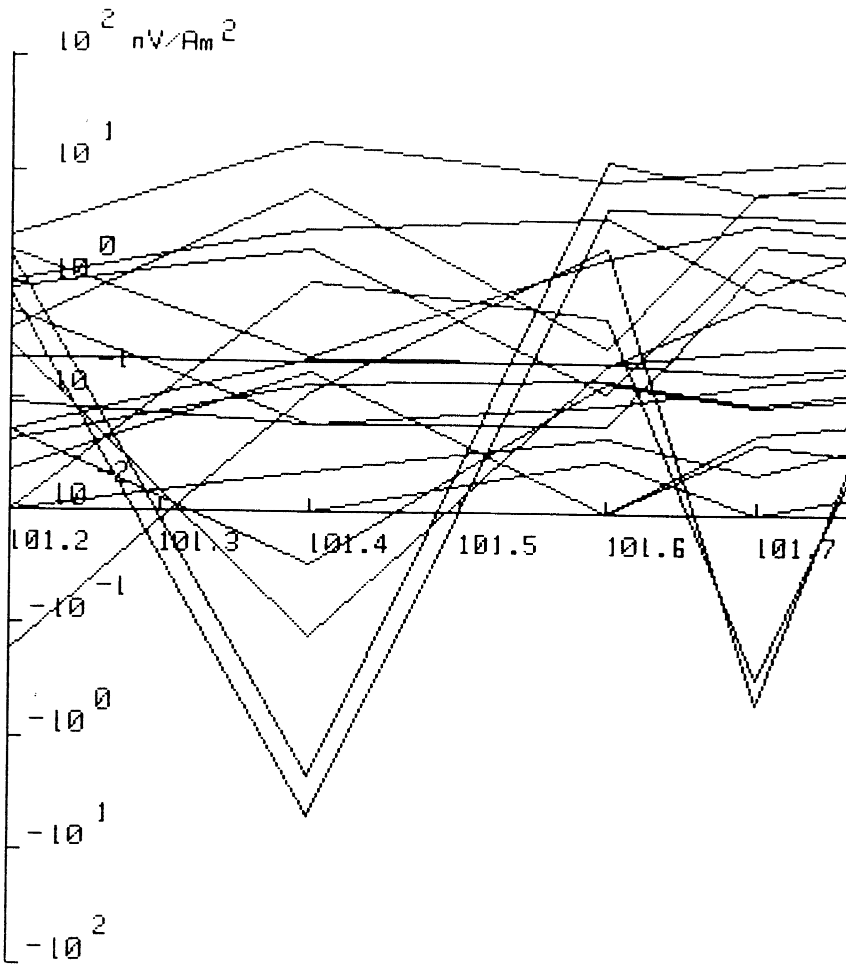

10^2 nV/Am^2
10^1
10^0
10^-1
10^-2
101.2
101.3
101.4
101.5
101.6
101.7
-10^-1
-10^0
-10^1
-10^2

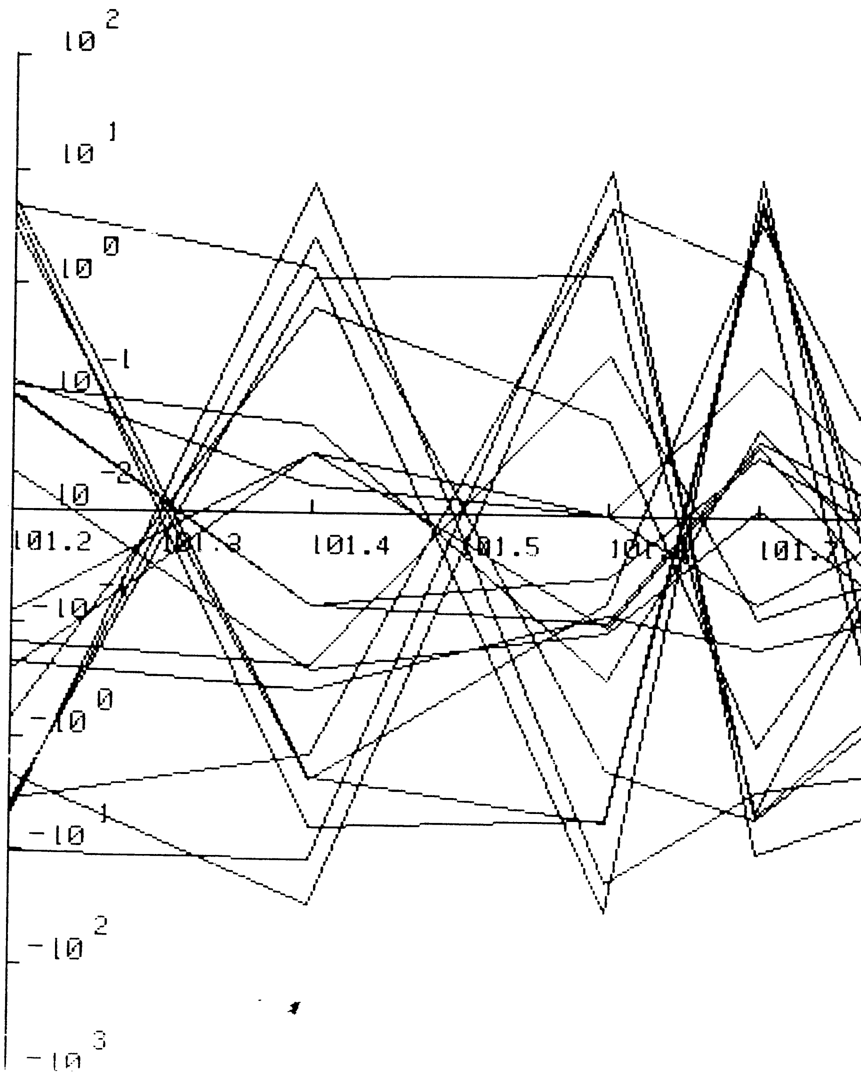

10^2
10^1
10^0
10^-1
10^-2
101.2
101.3
101.4
101.5
-10^0
-10^1
-10^2
-10^3

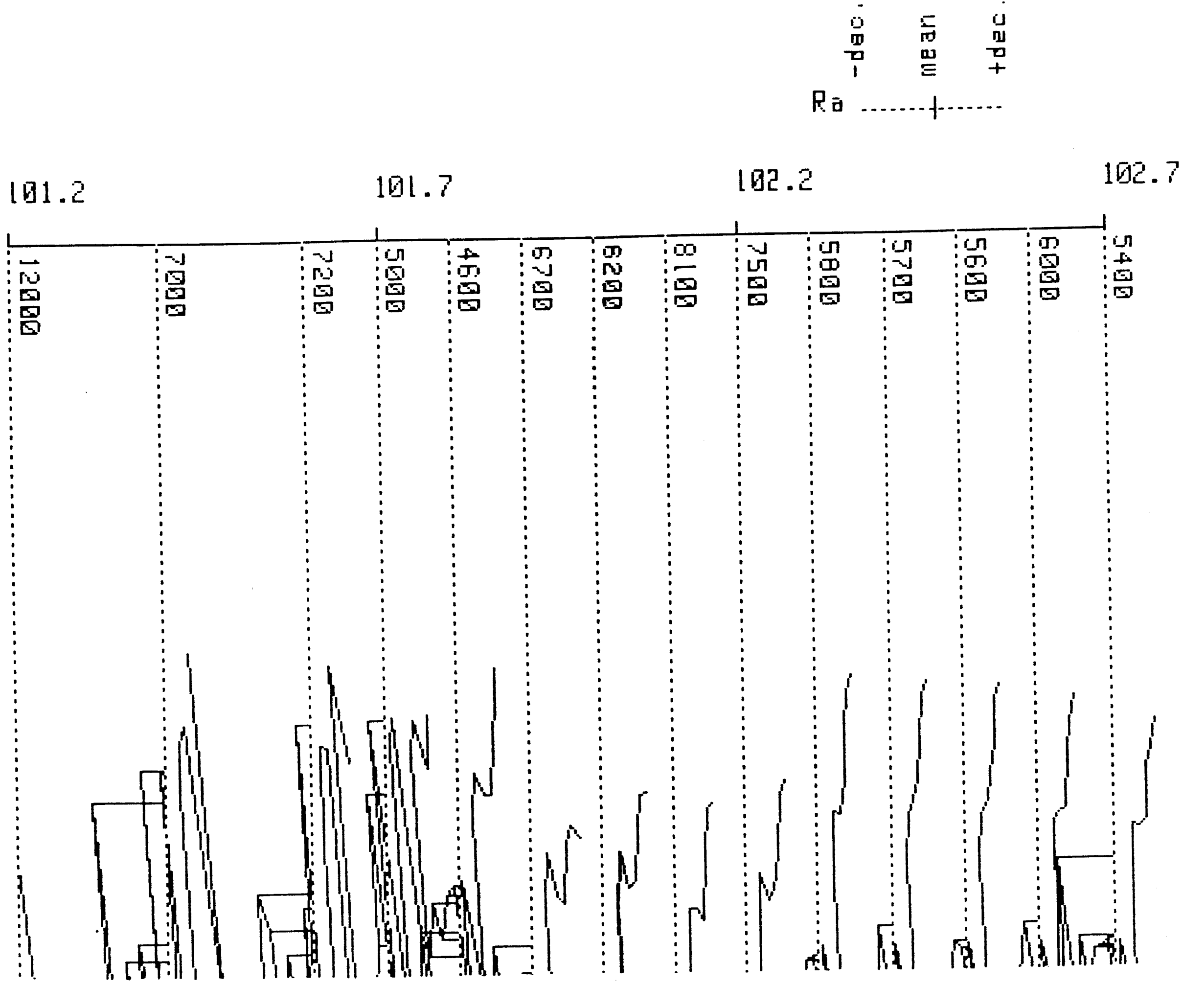

OUTOKUMPU OY Exploration	1:10 000	
		JL -85
LÖKKEN , Mogset		433
DIT-plot Y 33.35	App. 9/3	

OUTOKUMPU OY Exploration	1:5000
	JL -85
LÖKKEN , Urvatnet	
TDEM survey layout	App. 11/1

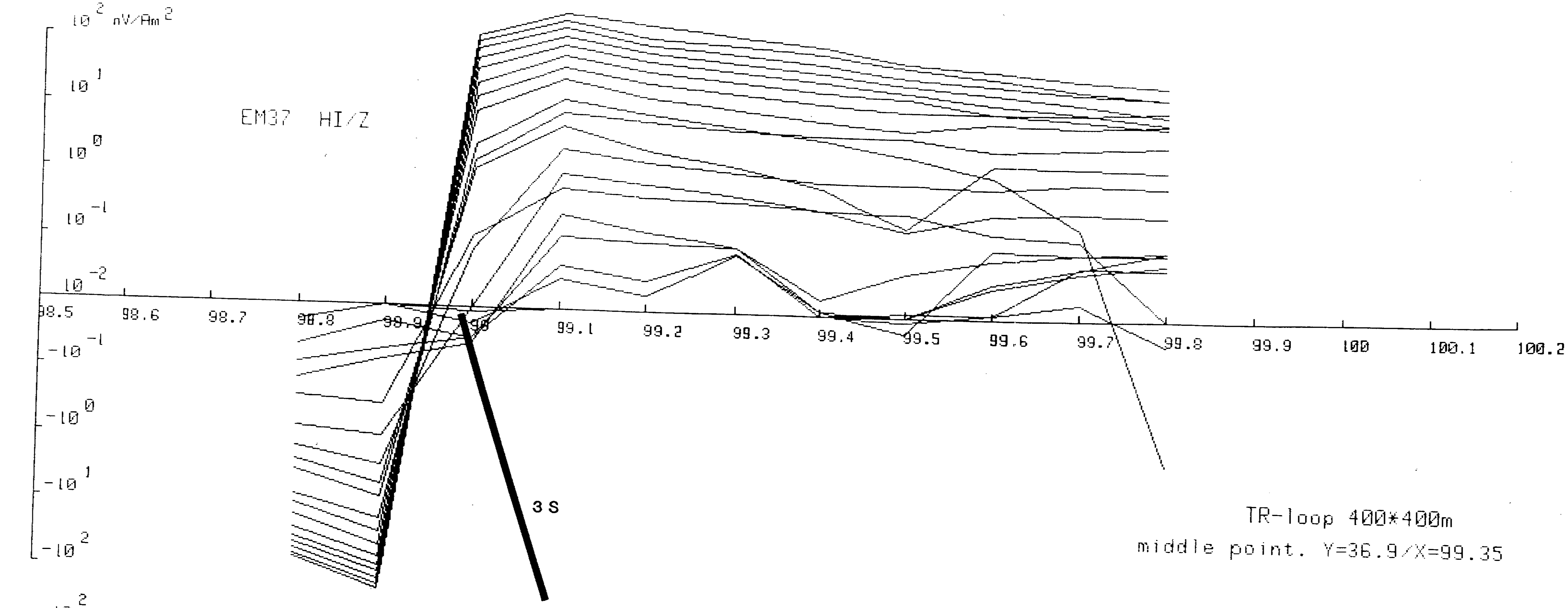

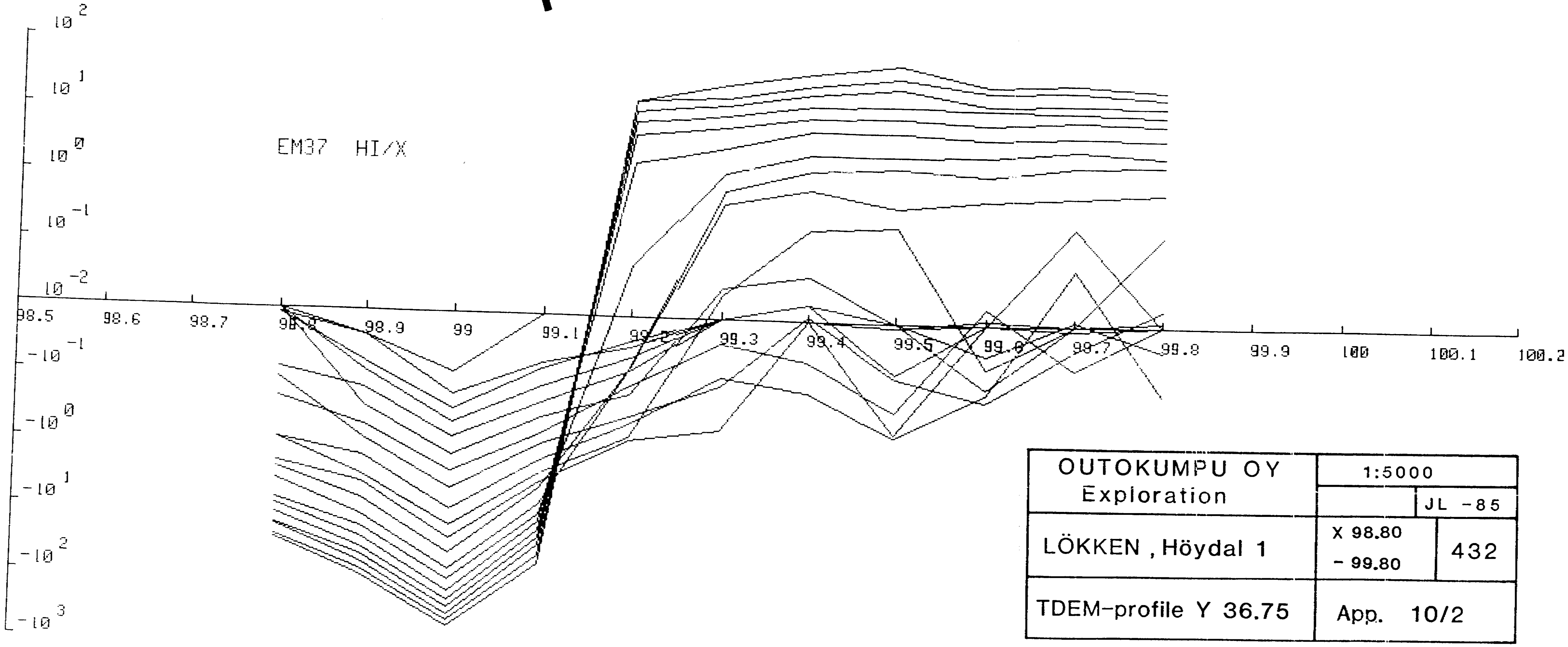

OUTOKUMPU OY Exploration	1:5000	JL -85
LÖKKEN , Höydal 1	X 98.80 - 99.80	432
TDEM-profile Y 36.75	App. 10/2	

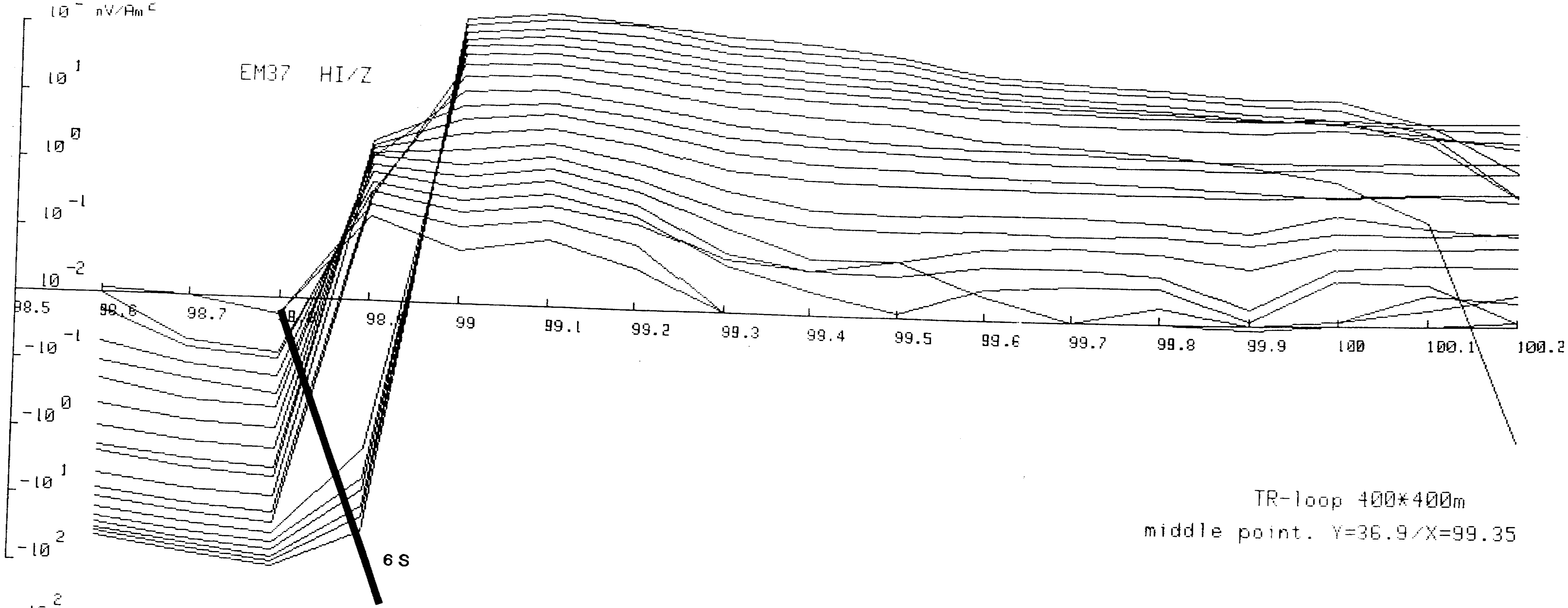

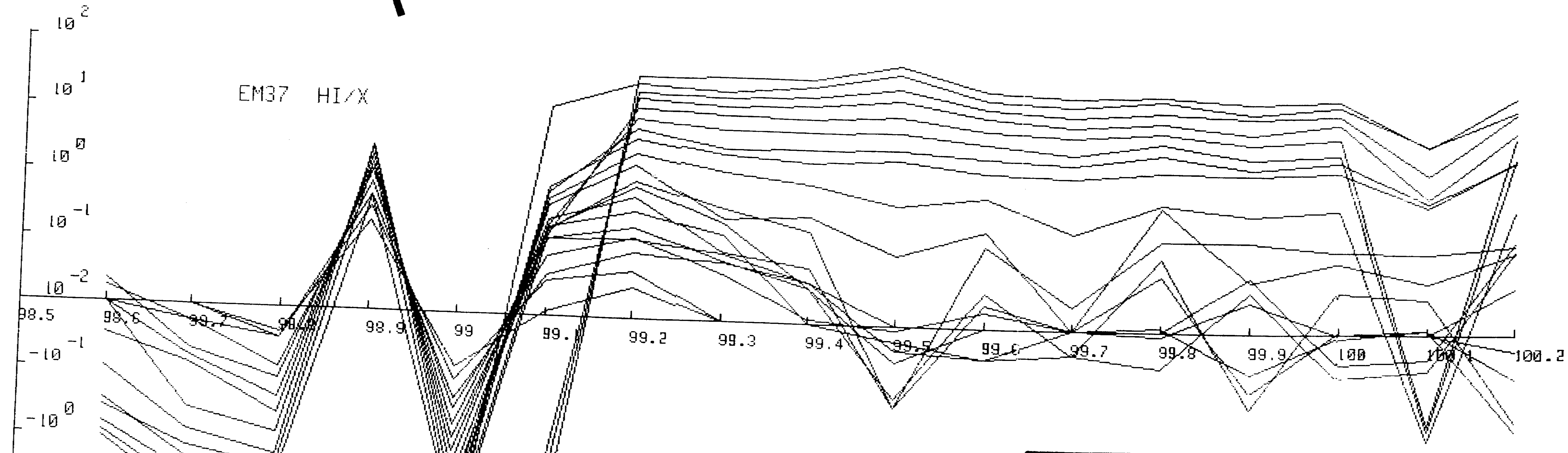

OUTOKUMPU OY Exploration	1:5000	JL -85
LÖKKEN , Höydal 1	X 98.50 - 100.20	432
TDEM-profile Y 37.00	App. 10/3	

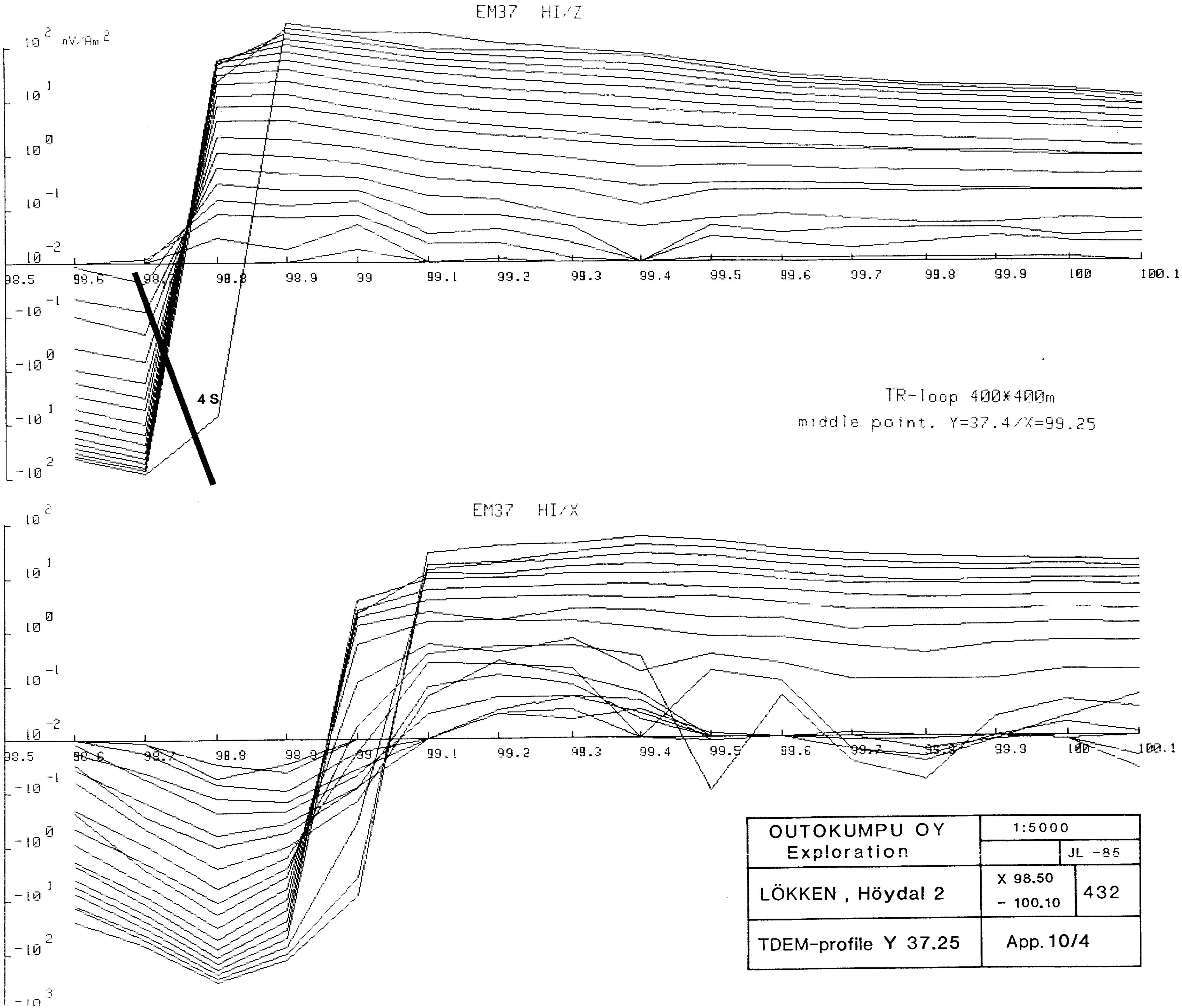

OUTOKUMPU OY Exploration	1:5000	
		JL -85
LÖKKEN , Höydal 2	X 98.50 – 100.10	432
TDEM-profile Y 37.25	App. 10/4	

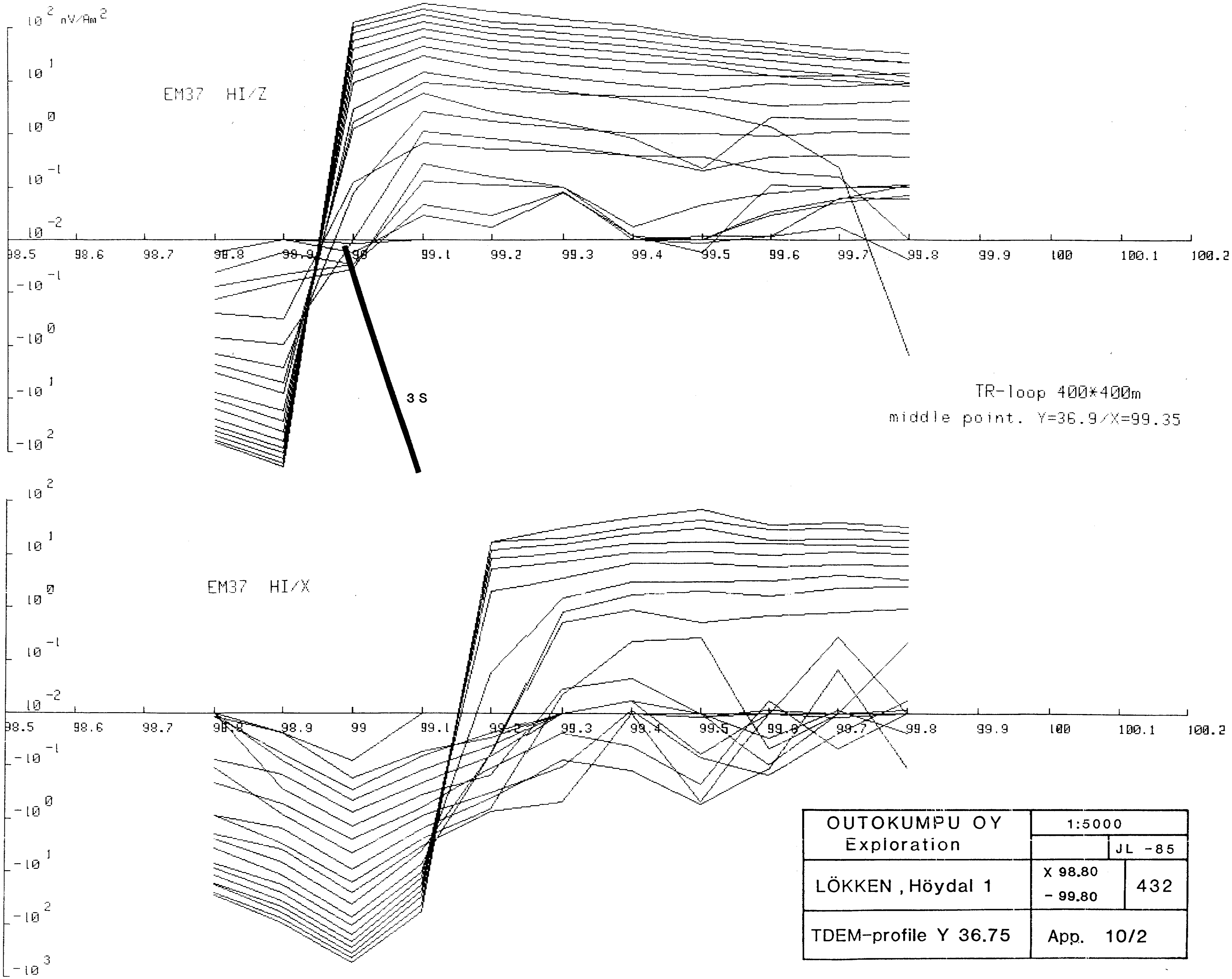

10^2 nV/Am^2
EM37 HI/Z
3 S
TR-loop 400*400m
middle point. Y=36.9/X=99.35
98.5 98.6 98.7 98.8 98.9 99 99.1 99.2 99.3 99.4 99.5 99.6 99.7 99.8 99.9 100 100.1 100.2
EM37 HI/X
OUTOKUMPU OY
Exploration
1:5000
JL -85
LÖKKEN , Höydal 1
X 98.80
- 99.80
432
TDEM-profile Y 36.75
App. 10/2

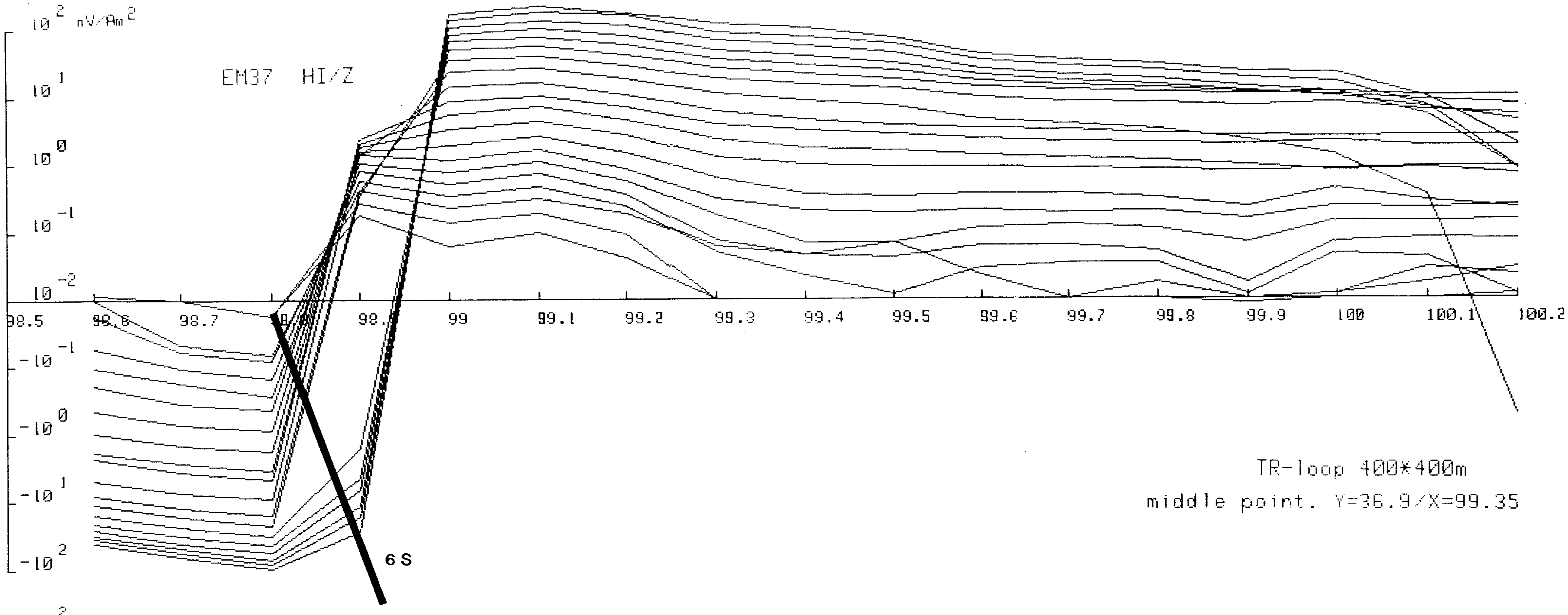

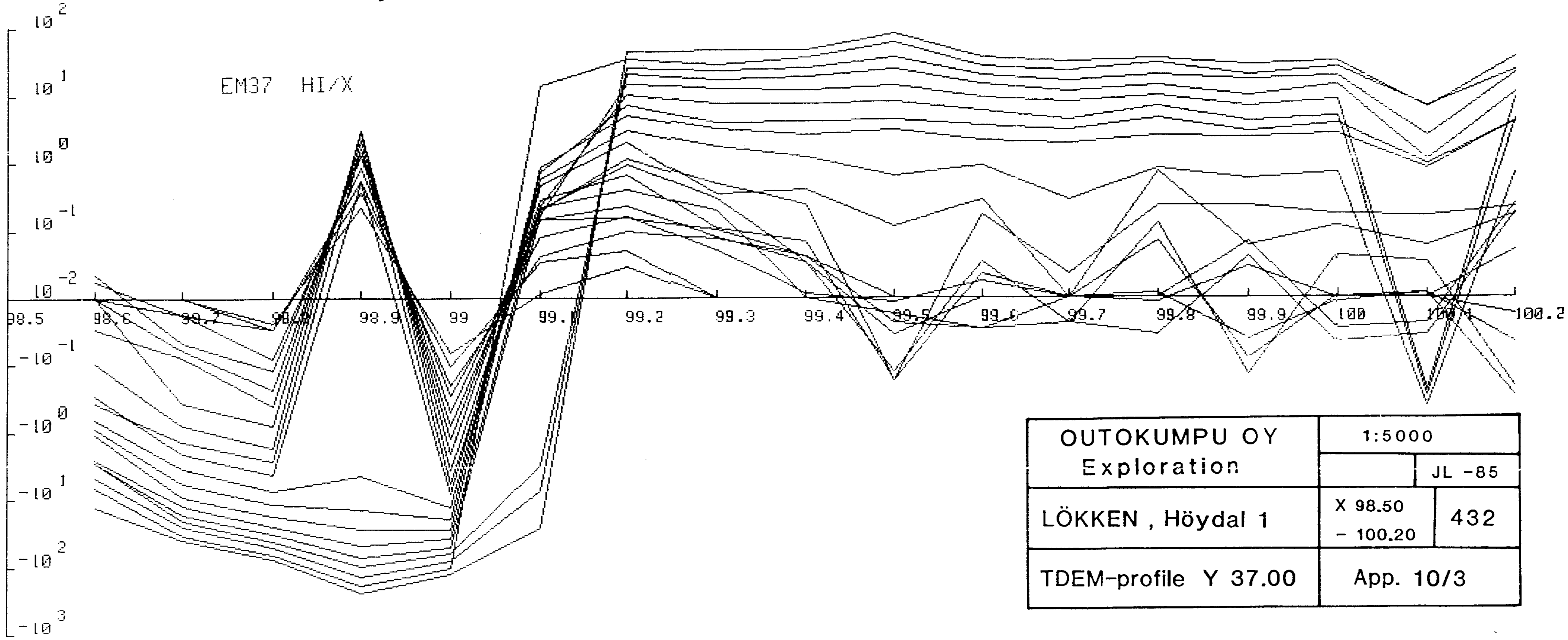

OUTOKUMPU OY Exploration	1:5000	
		JL -85
LÖKKEN , Höydal 1	X 98.50 – 100.20	432
TDEM-profile Y 37.00	App. 10/3	

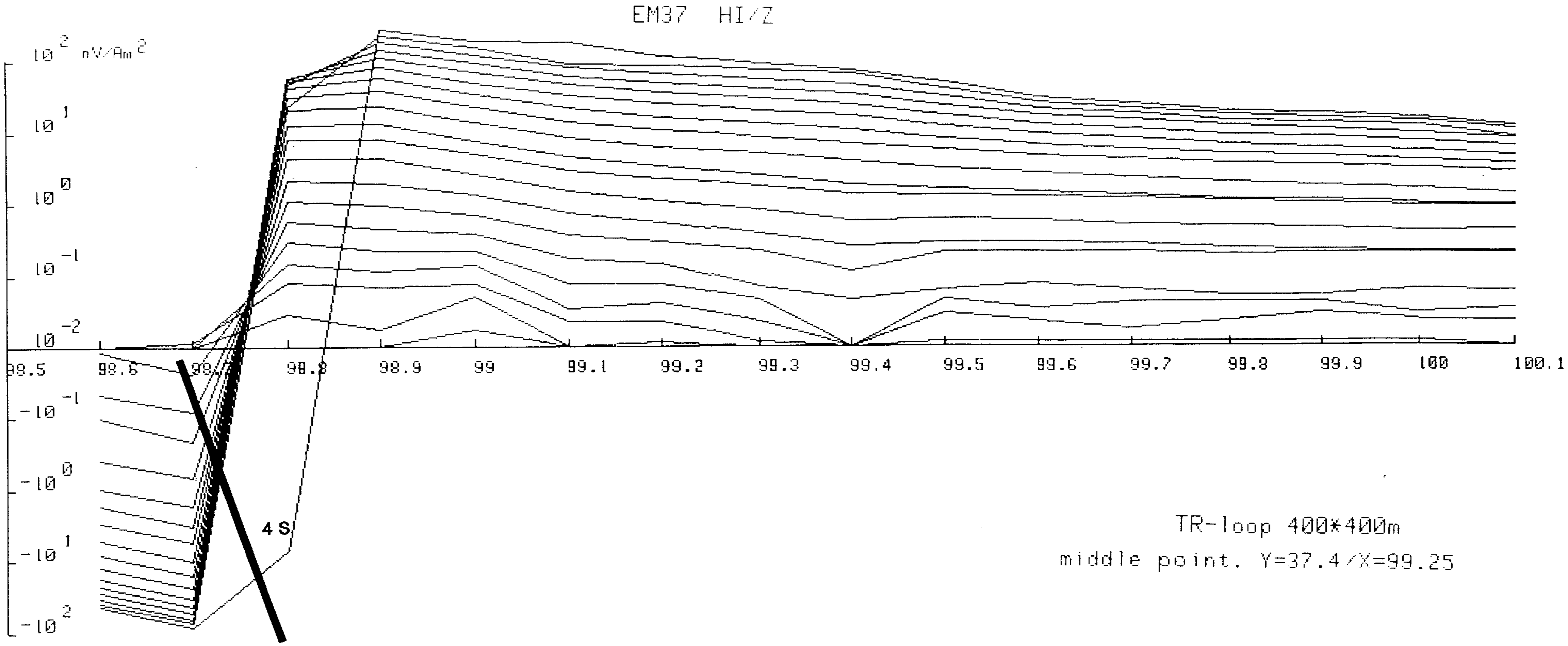

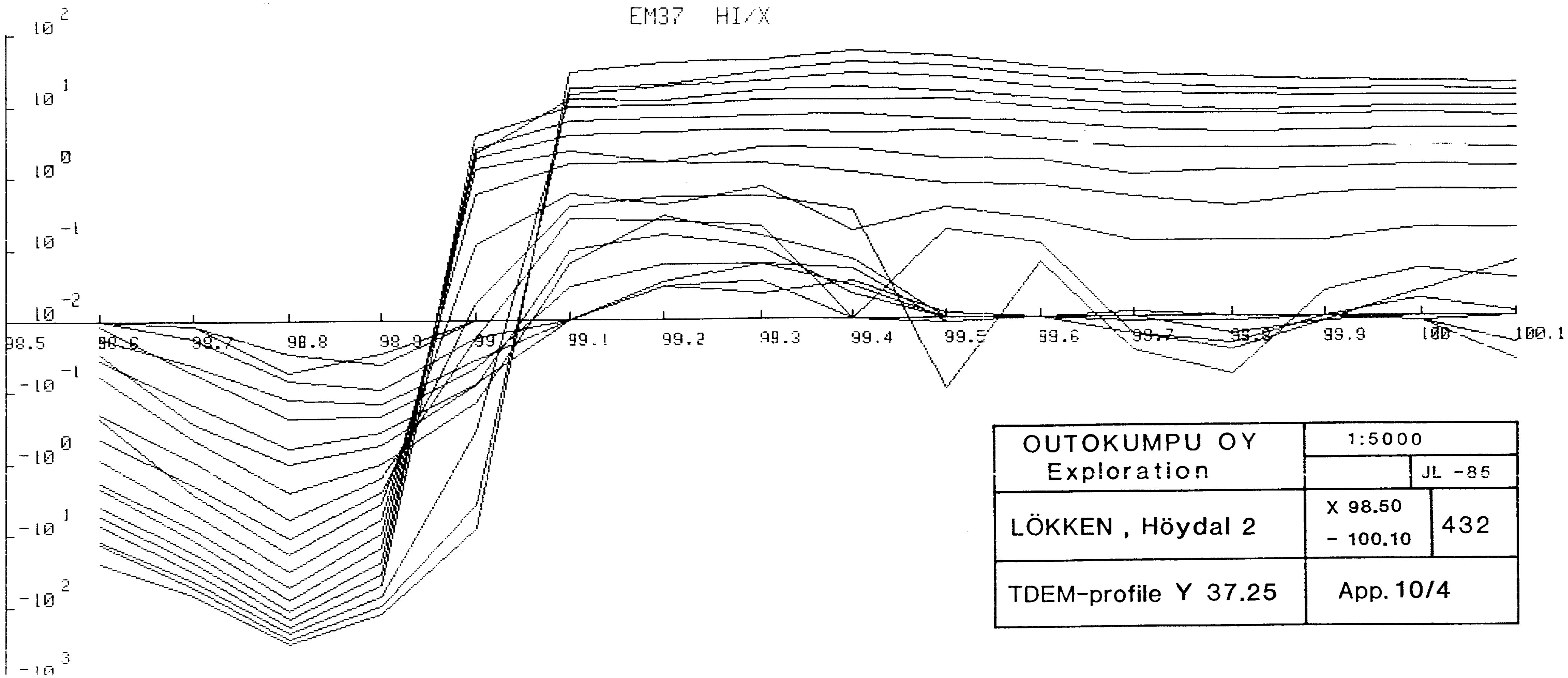

OUTOKUMPU OY Exploration	1:5000 JL -85	
LÖKKEN , Höydal 2	X 98.50 - 100.10	432
TDEM-profile Y 37.25	App. 10/4	

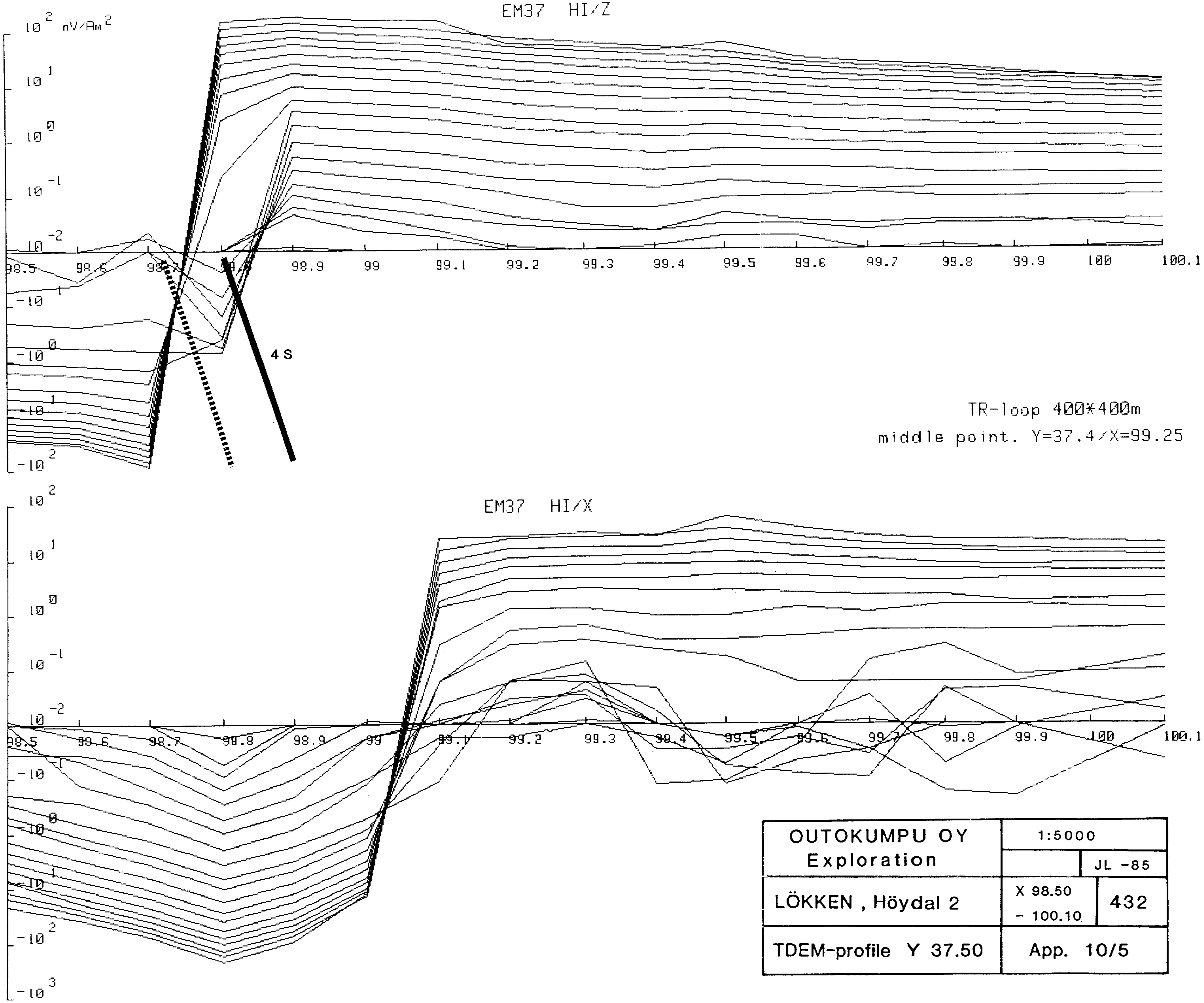

OUTOKUMPU OY Exploration	1:5000	
		JL -85
LÖKKEN , Höydal 2	X 98.50 - 100.10	432
TDEM-profile Y 37.50	App. 10/5	

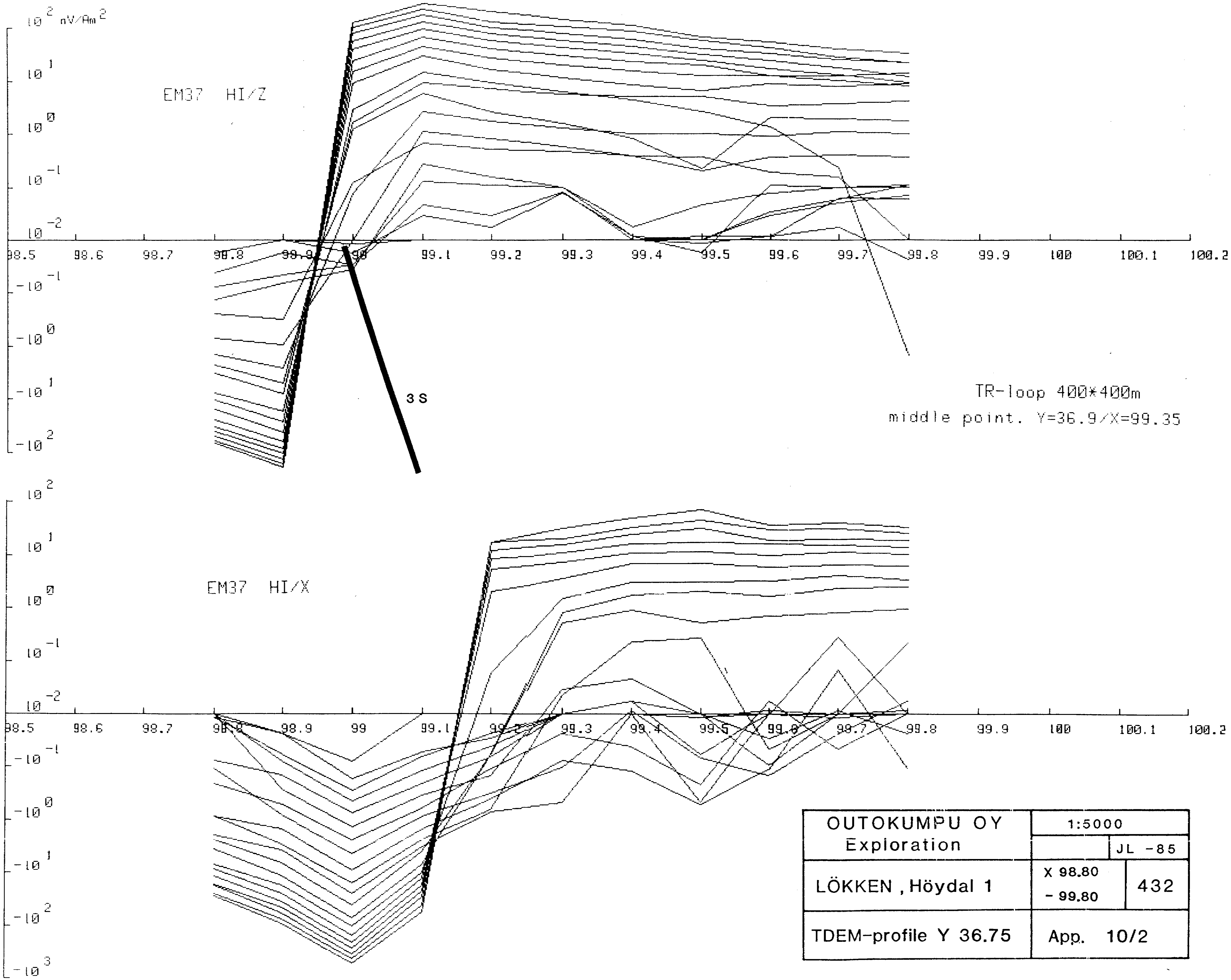

OUTOKUMPU OY Exploration	1:5000	JL -85
LÖKKEN , Höydal 1	X 98.80 - 99.80	432
TDEM-profile Y 36.75	App. 10/2	

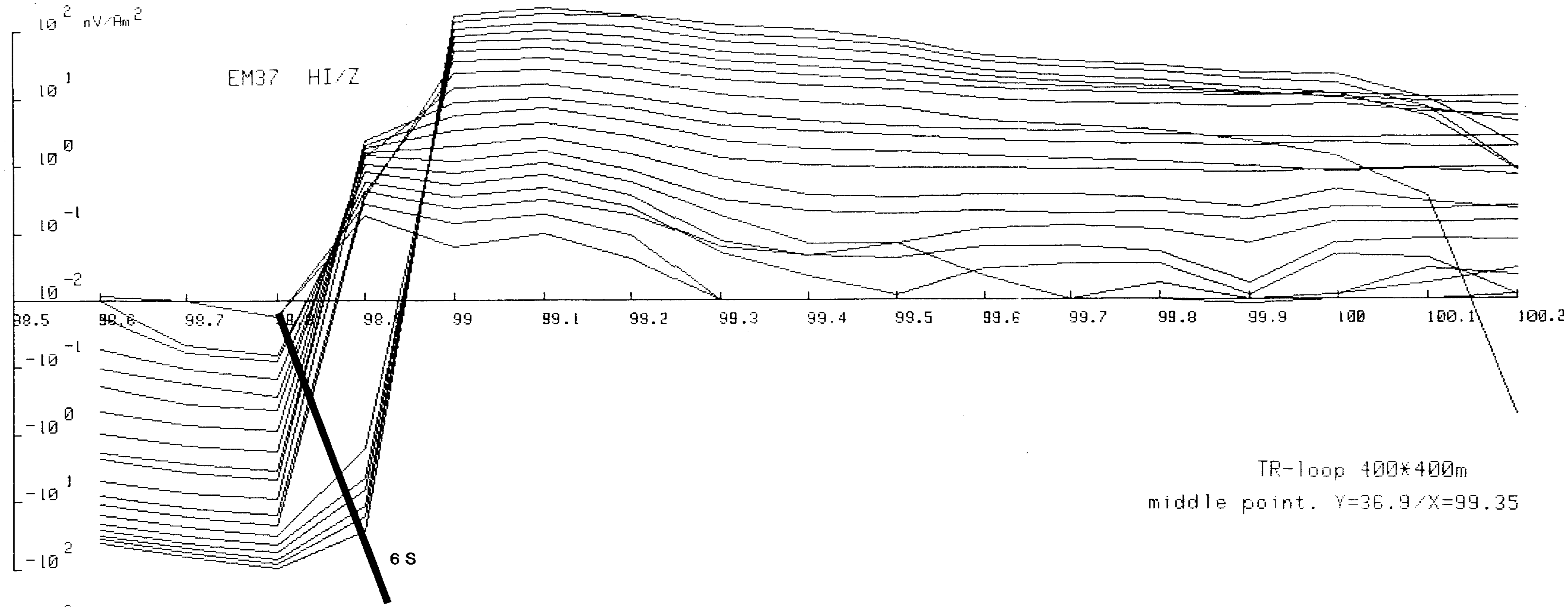

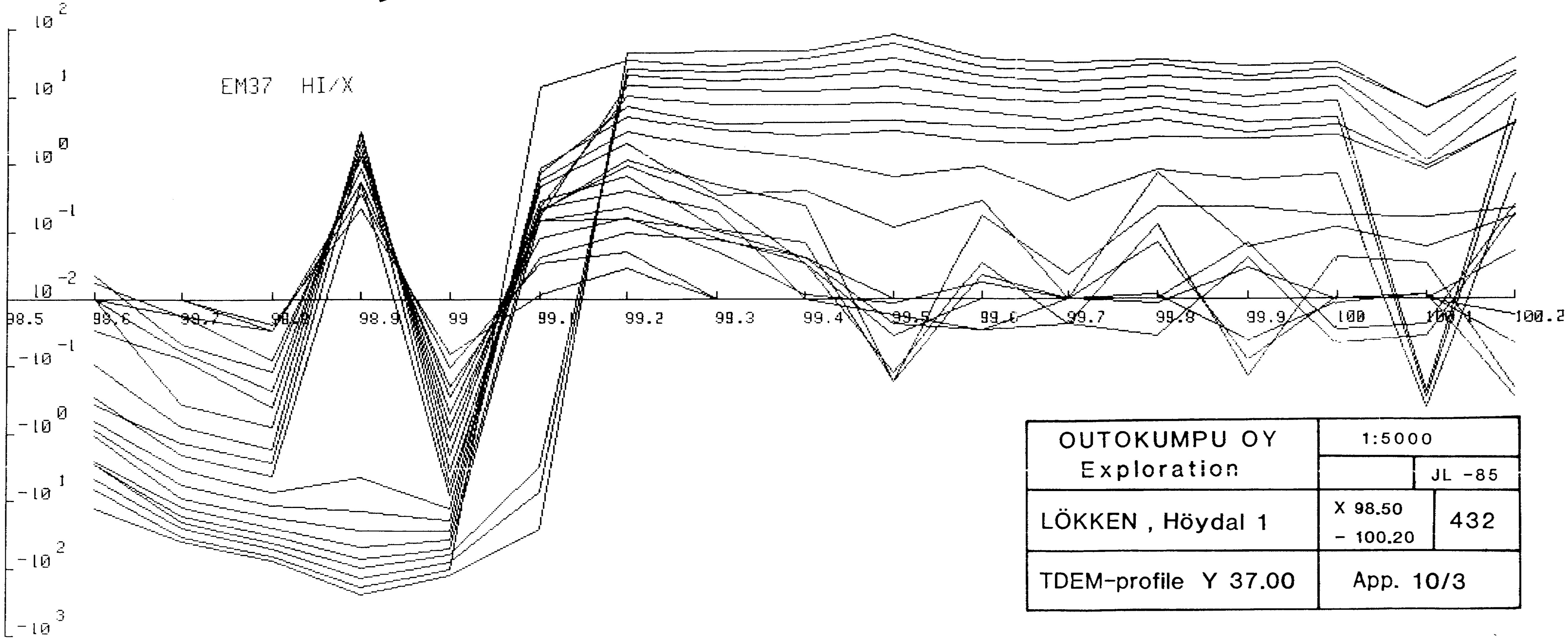

OUTOKUMPU OY Exploration	1:5000	JL -85
LÖKKEN , Höydal 1	X 98.50 - 100.20	432
TDEM-profile Y 37.00	App. 10/3	

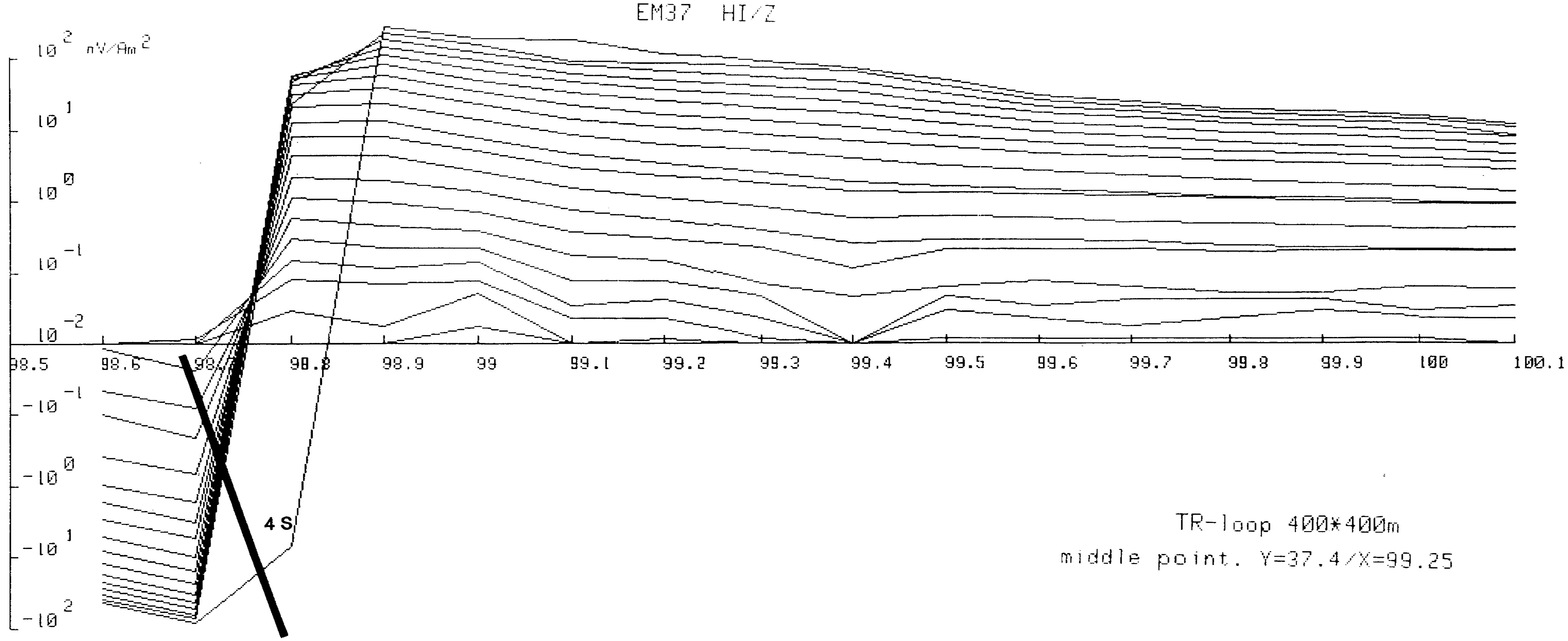

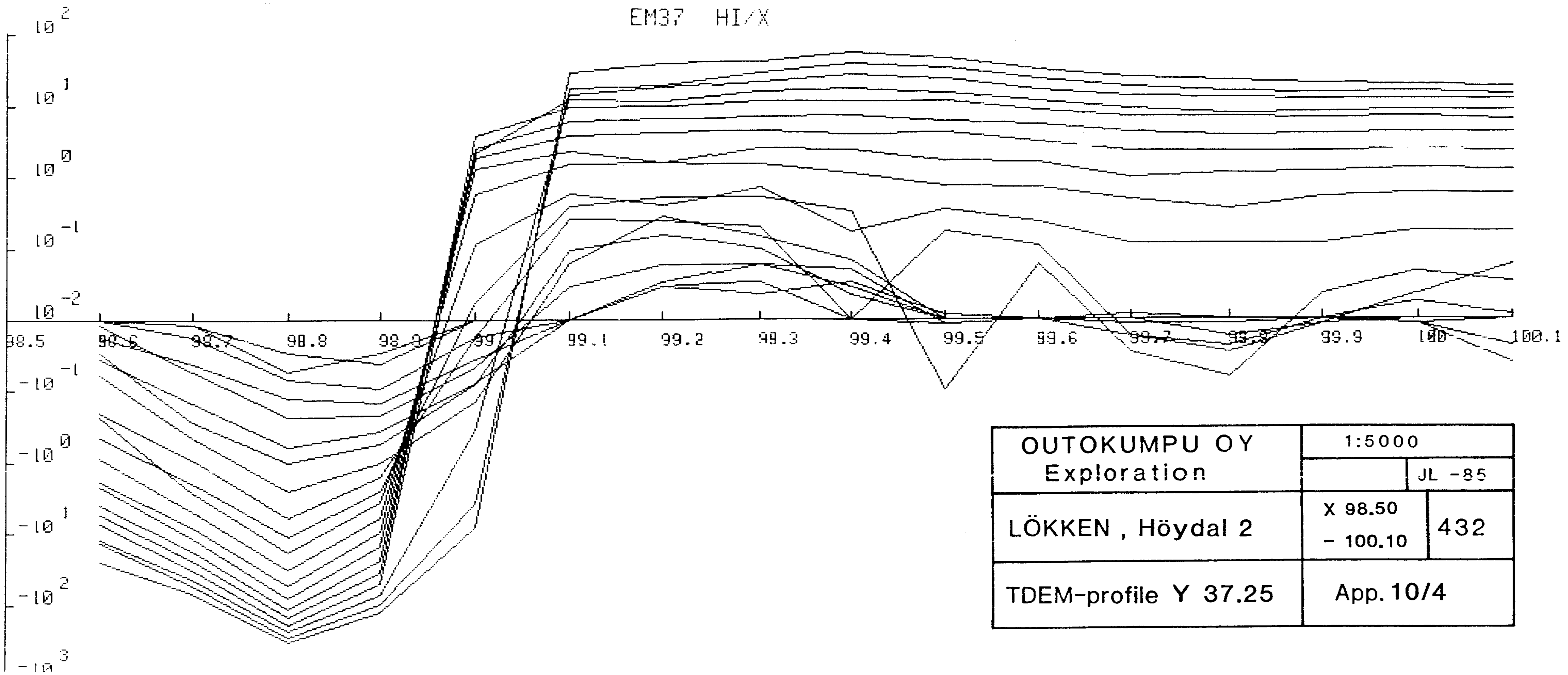

OUTOKUMPU OY Exploration	1:5000	
		JL -85
LÖKKEN , Höydal 2	X 98.50 - 100.10	432
TDEM-profile Y 37.25	App. 10/4	

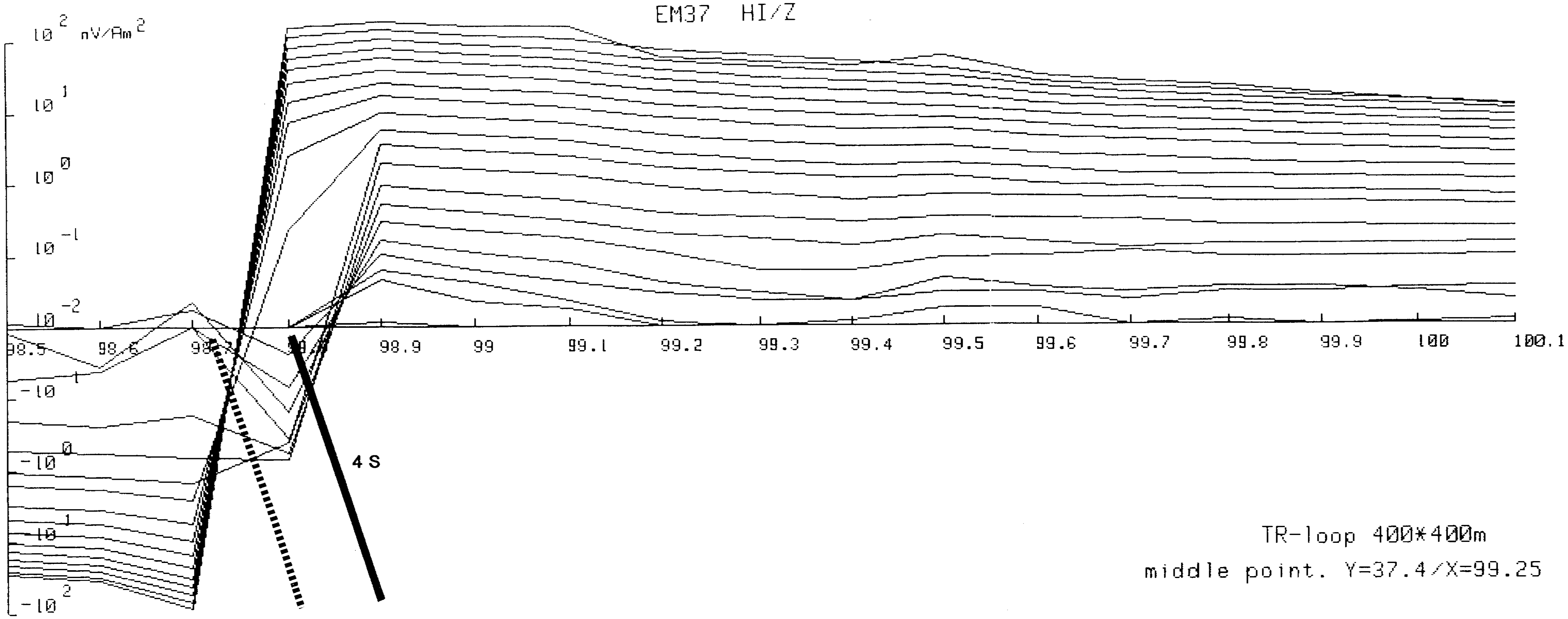

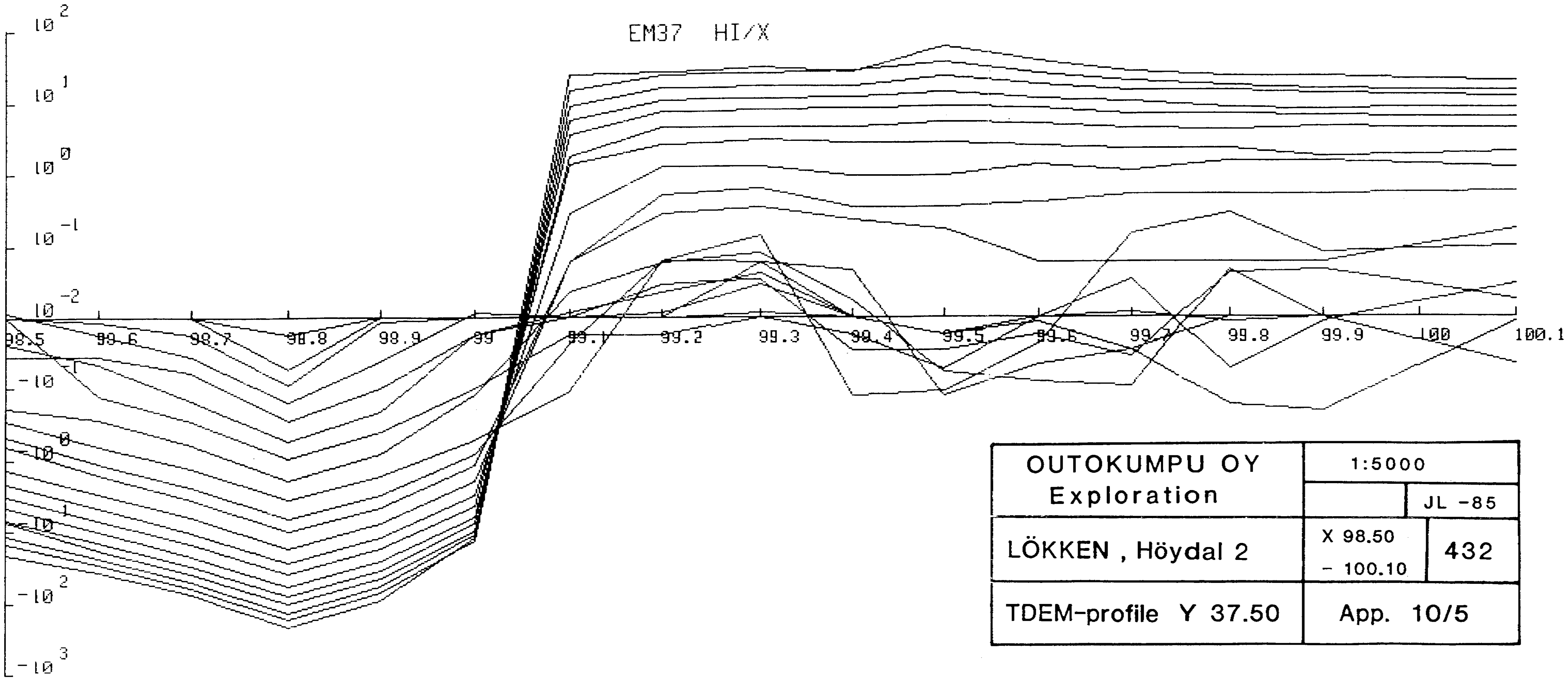

OUTOKUMPU OY Exploration	1:5000	
		JL -85
LÖKKEN , Höydal 2	X 98.50 - 100.10	432
TDEM-profile Y 37.50	App. 10/5	

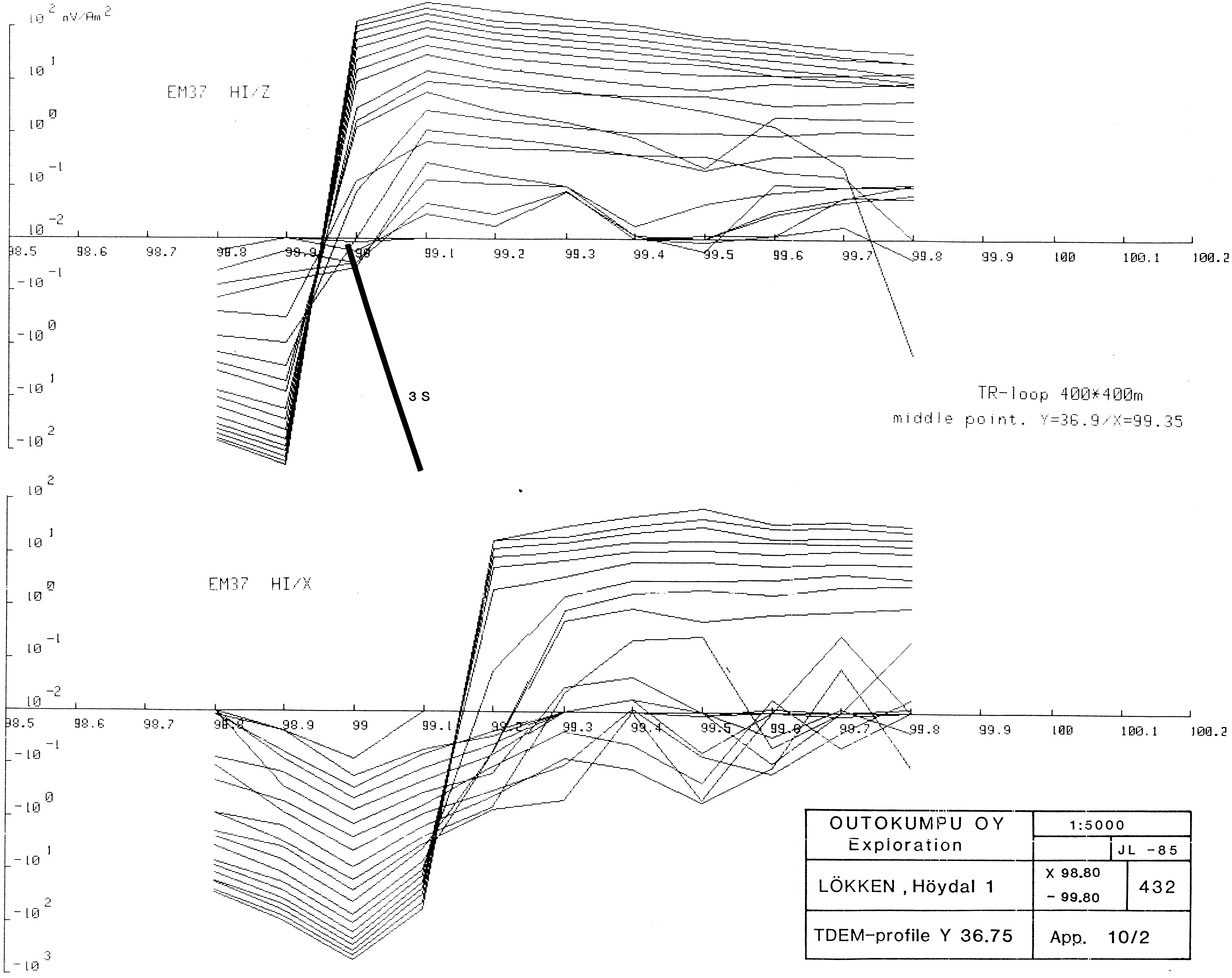

OUTOKUMPU OY Exploration	1:5000	
		JL -85
LÖKKEN , Höydal 1	X 98.80 - 99.80	432
TDEM-profile Y 36.75	App. 10/2	

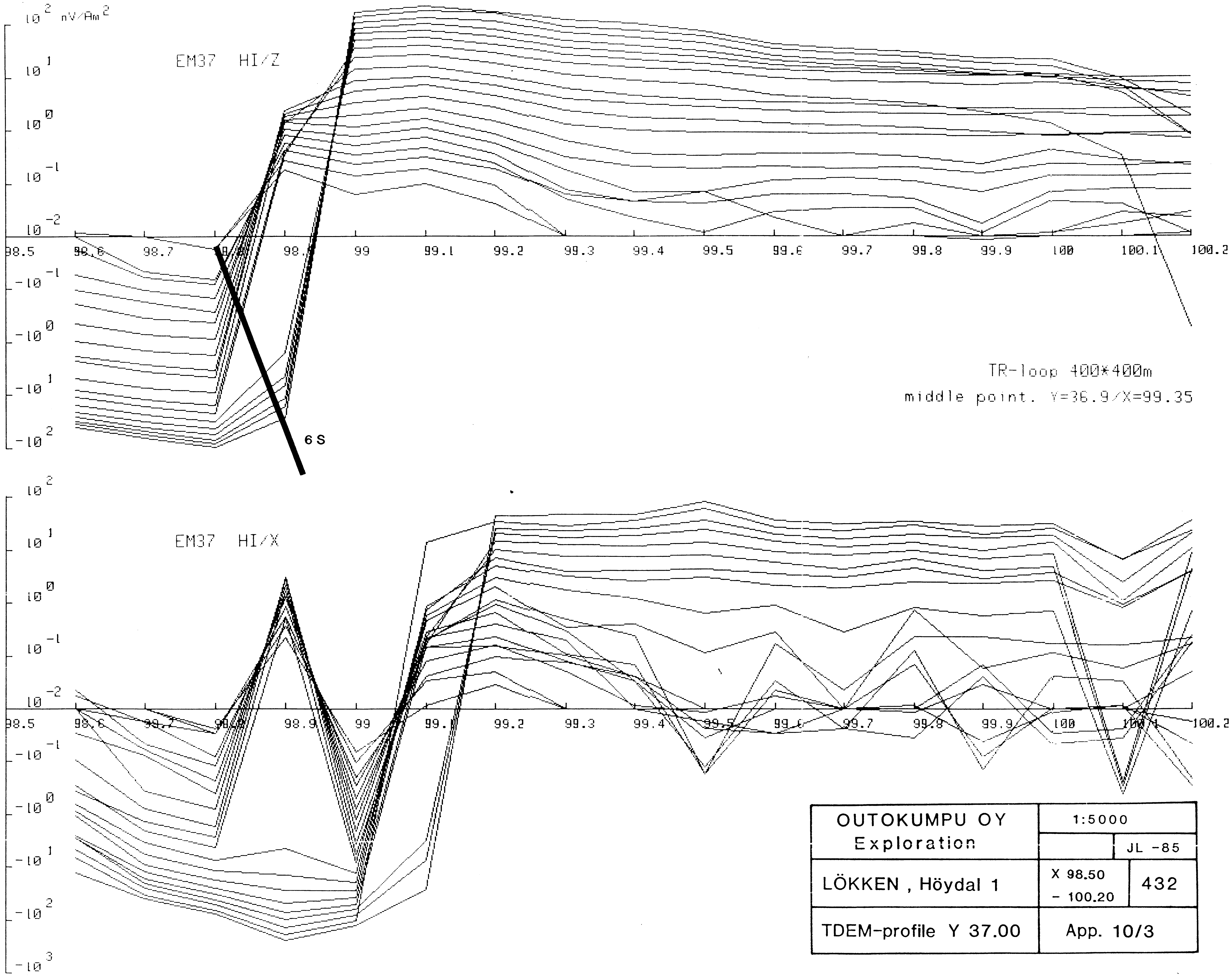

OUTOKUMPU OY Exploration	1:5000	
		JL -85
LÖKKEN , Höydal 1	X 98.50 - 100.20	432
TDEM-profile Y 37.00	App. 10/3	

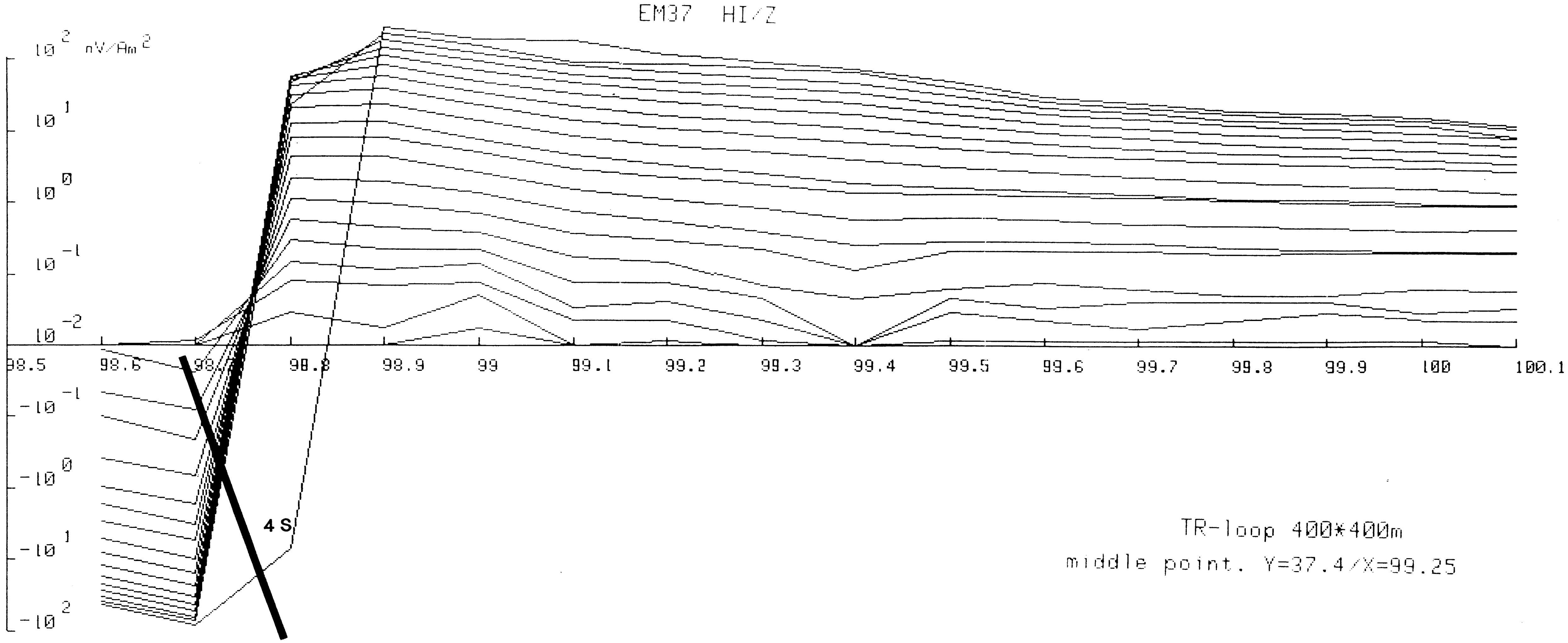

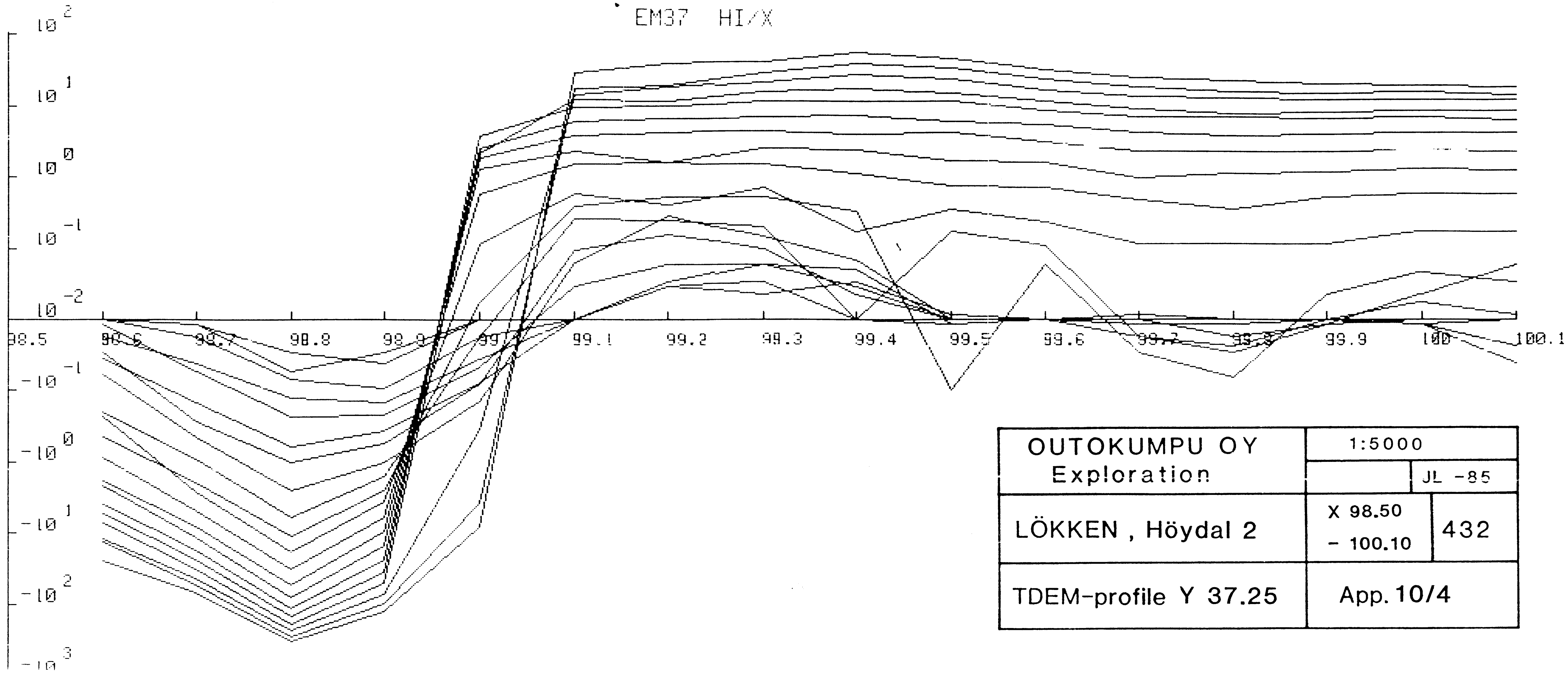

OUTOKUMPU OY Exploration	1:5000 JL -85	
LÖKKEN , Höydal 2	X 98.50 - 100.10	432
TDEM-profile Y 37.25	App. 10/4	

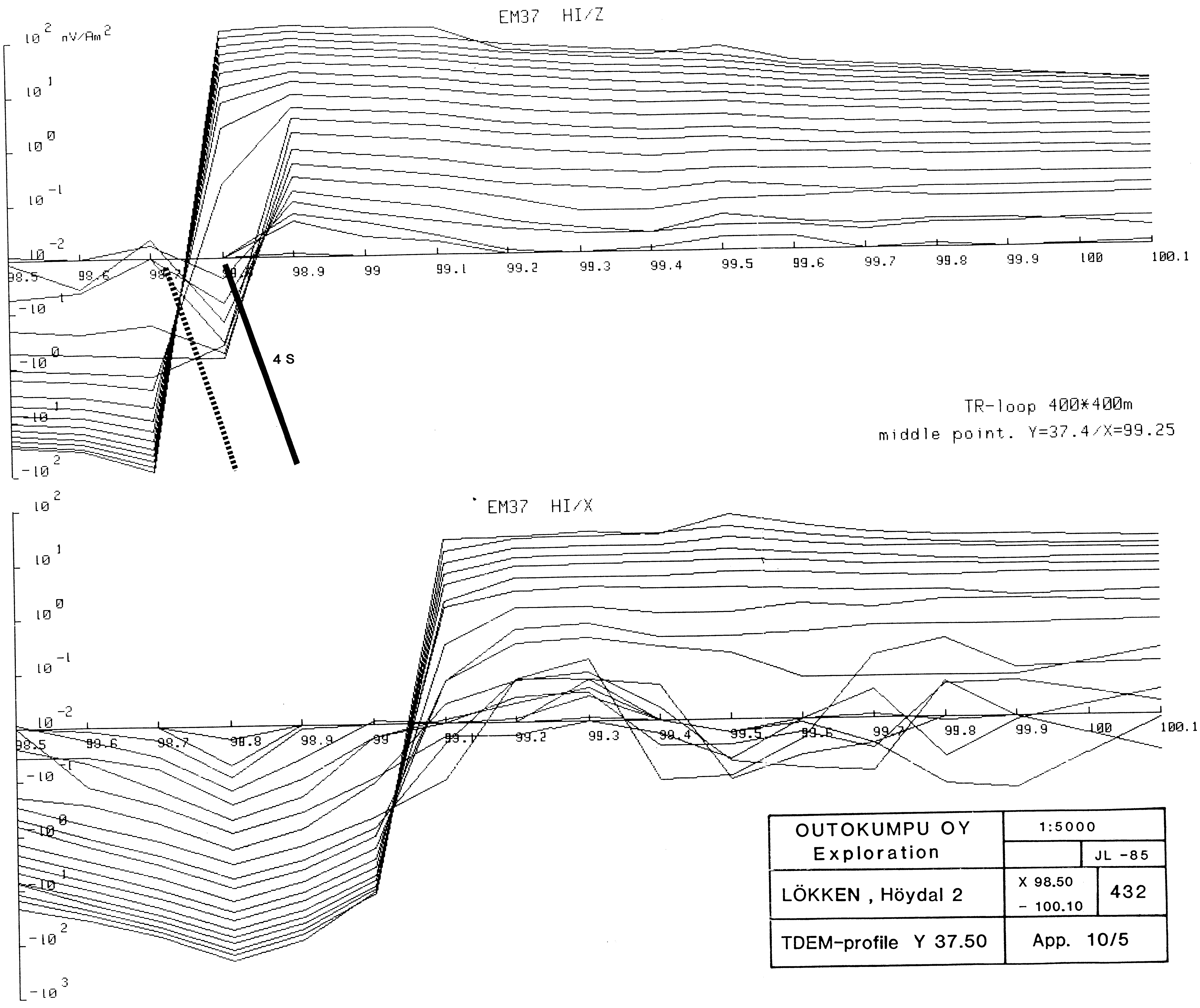

EM37 HI/Z
nV/Am²
4 S
TR-loop 400*400m
middle point. Y=37.4/X=99.25
EM37 HI/X
OUTOKUMPU OY
Exploration
1:5000
JL -85
LÖKKEN , Höydal 2
X 98.50
- 100.10
432
TDEM-profile Y 37.50
App. 10/5

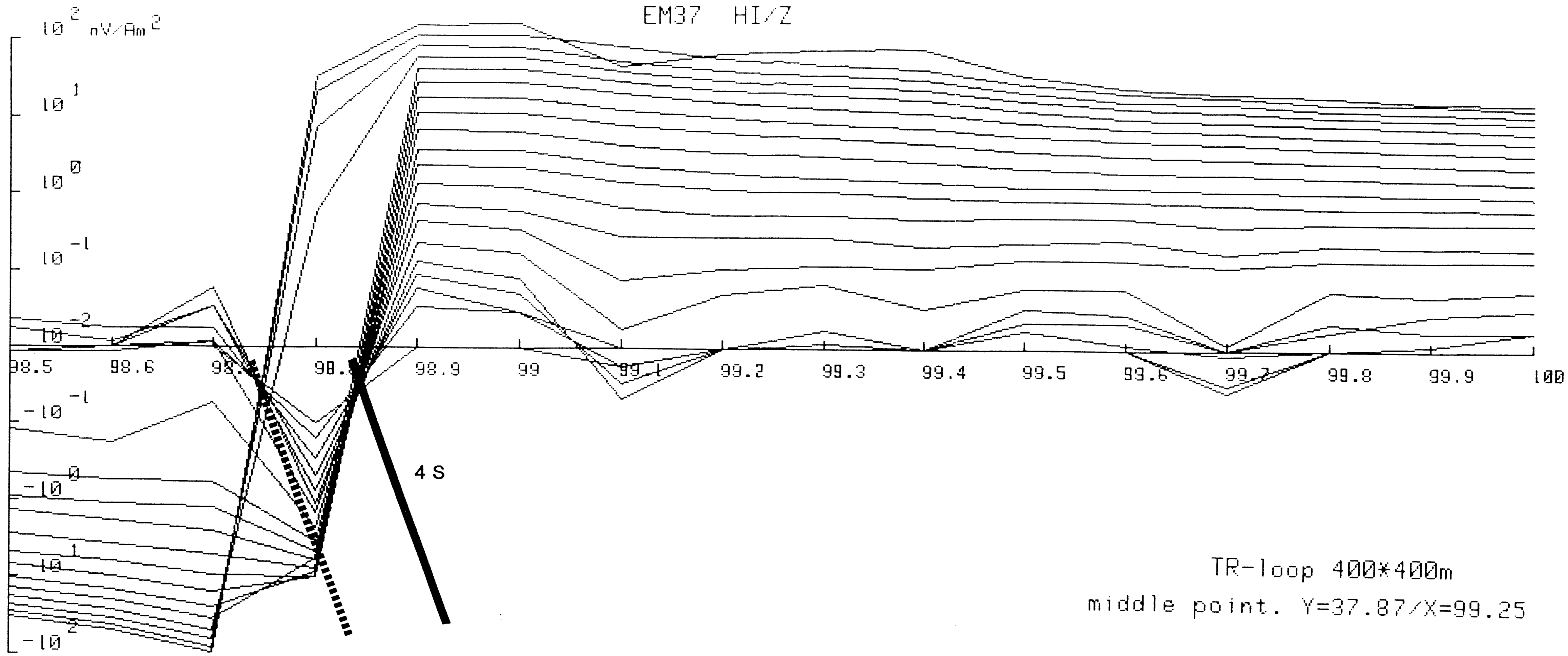

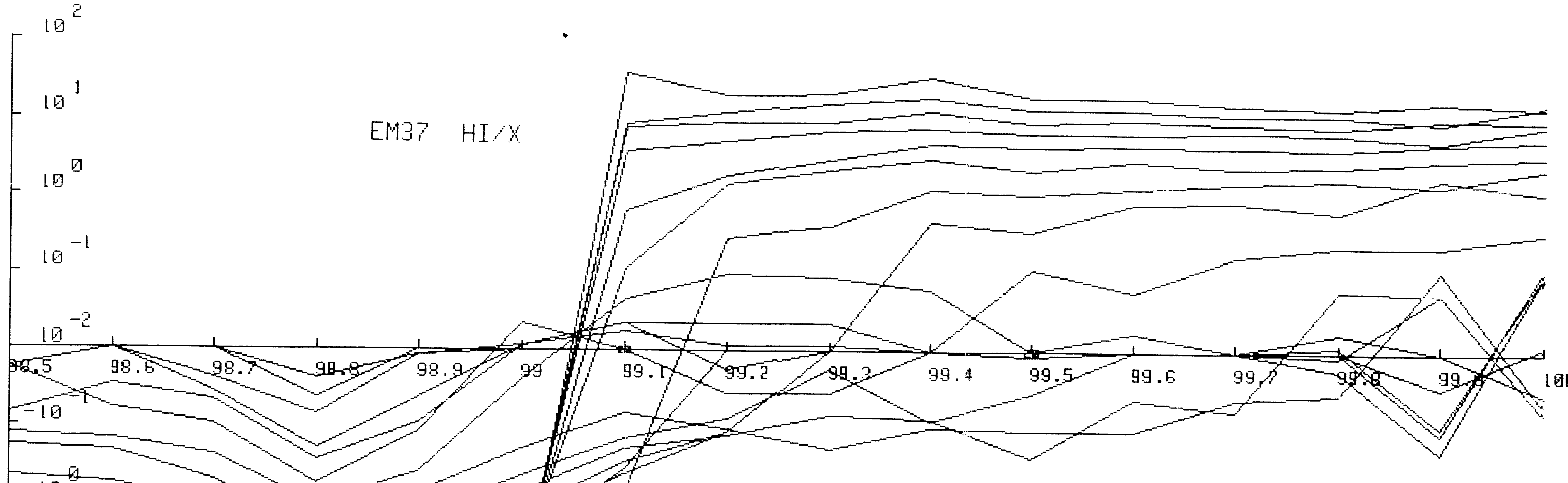

OUTOKUMPU OY Exploration	1:5000 JL -85	
LÖKKEN , Höydal 3	X 98.50 - 100.00	432
TDEM-profile Y 37.75	App. 10/6	

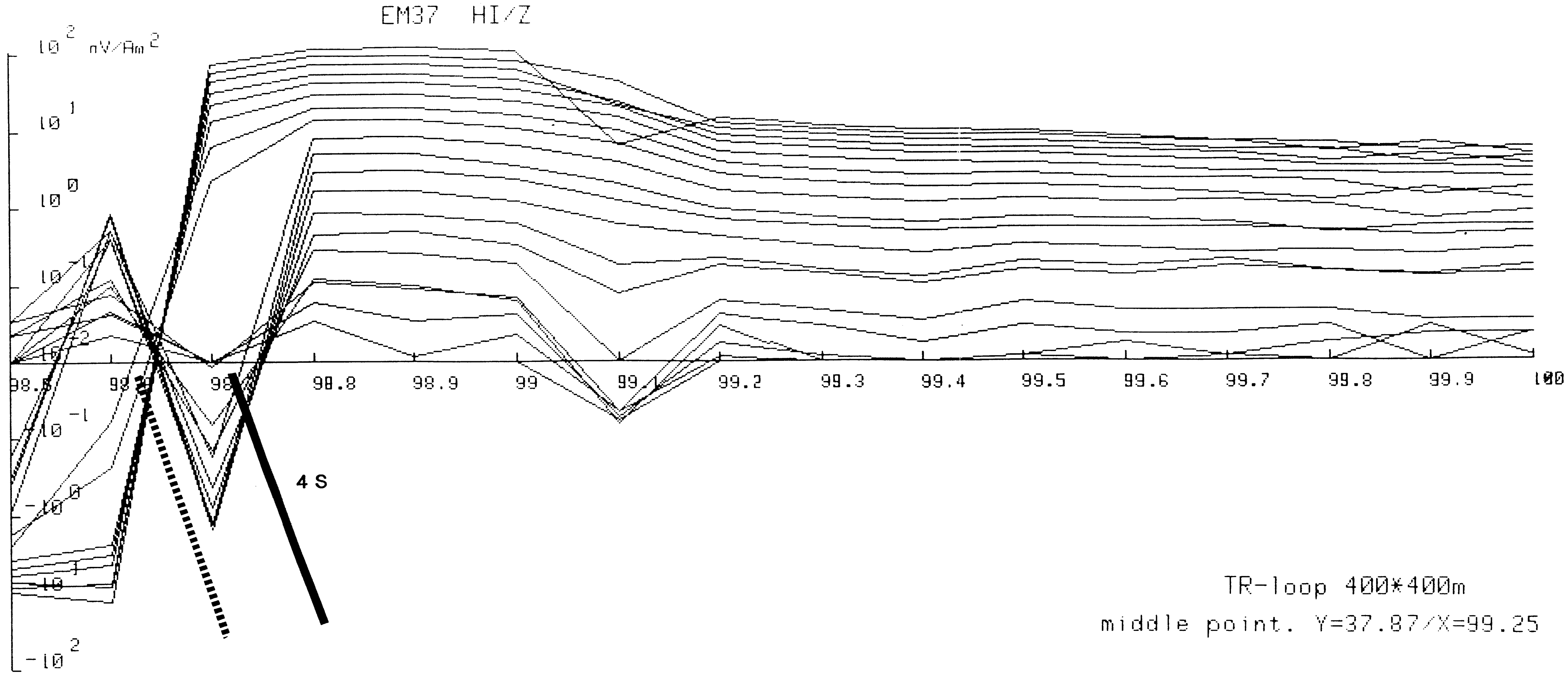

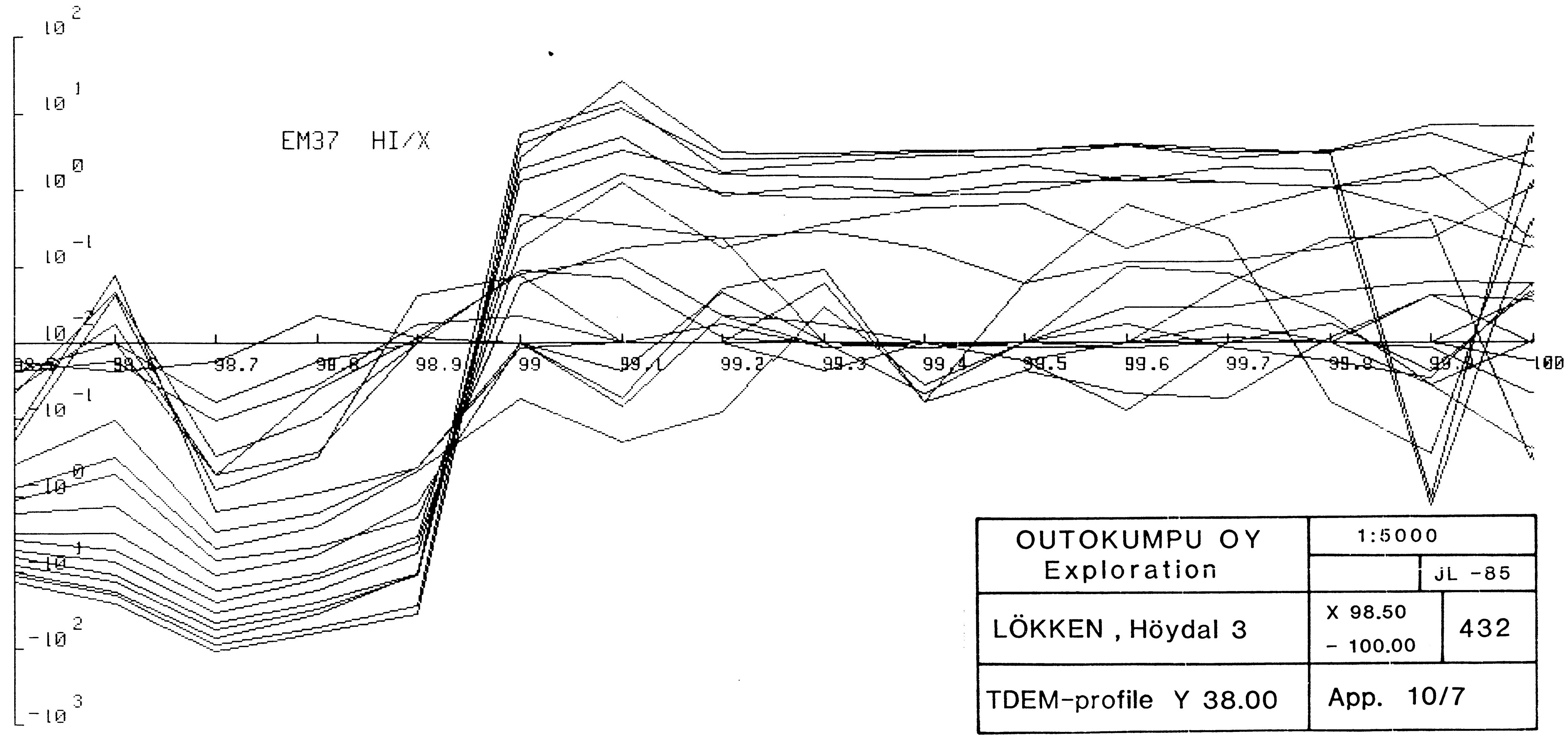

OUTOKUMPU OY Exploration	1:5000 JL -85	
LÖKKEN , Höydal 3	X 98.50 - 100.00	432
TDEM-profile Y 38.00	App. 10/7	

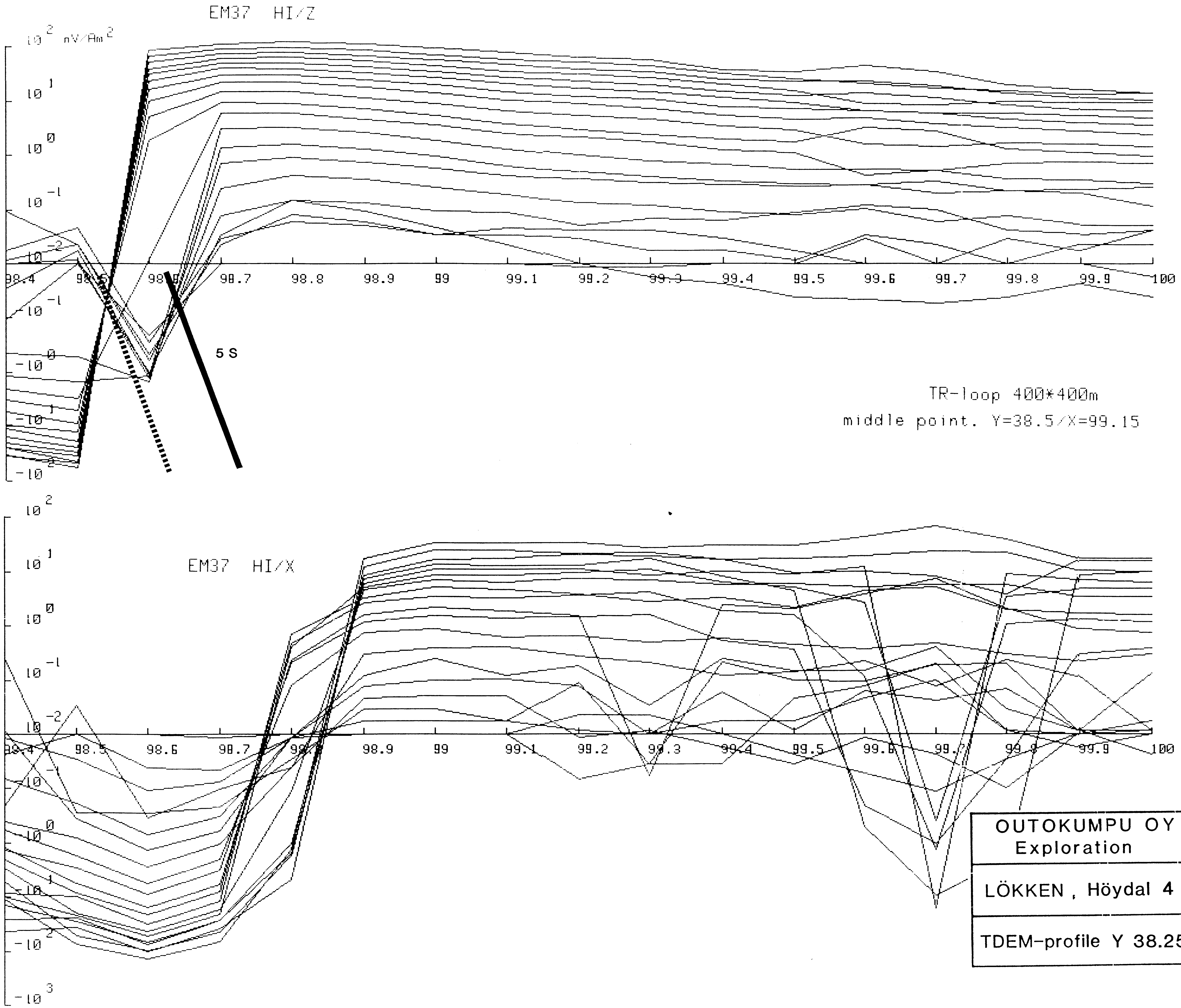

OUTOKUMPU OY Exploration	1:5000	
		JL -85
LÖKKEN , Höydal 4	X 98.40 – 100.00	432
TDEM-profile Y 38.25	App.	10/8

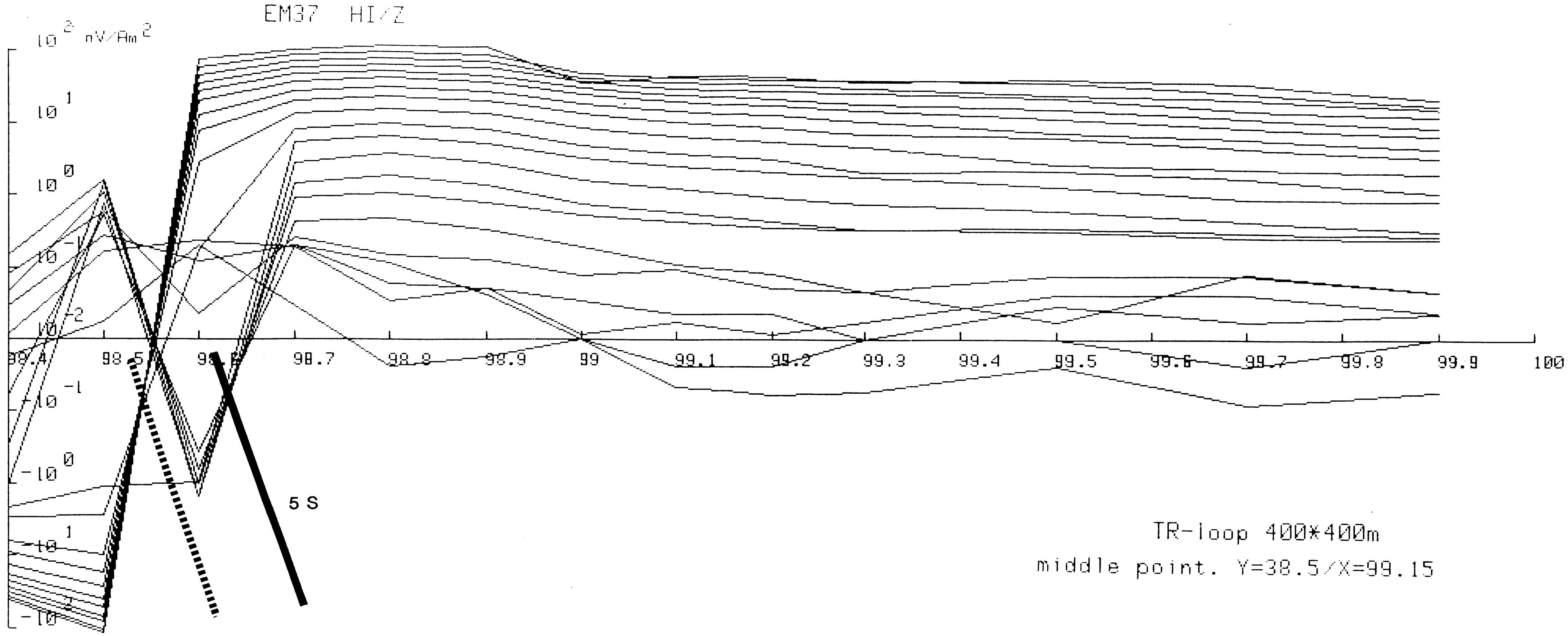

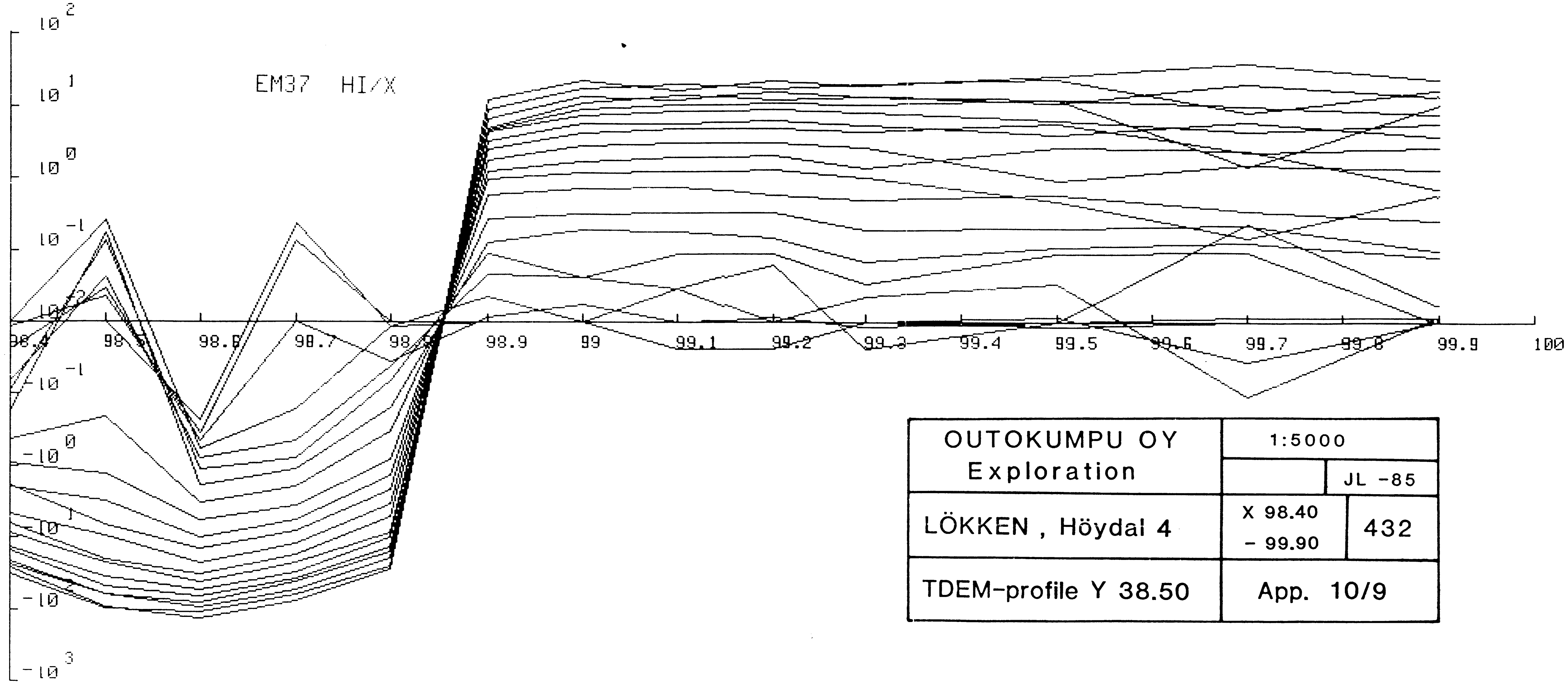

OUTOKUMPU OY Exploration	1:5000	
		JL -85
LÖKKEN , Höydal 4	X 98.40 - 99.90	432
TDEM-profile Y 38.50	App. 10/9	

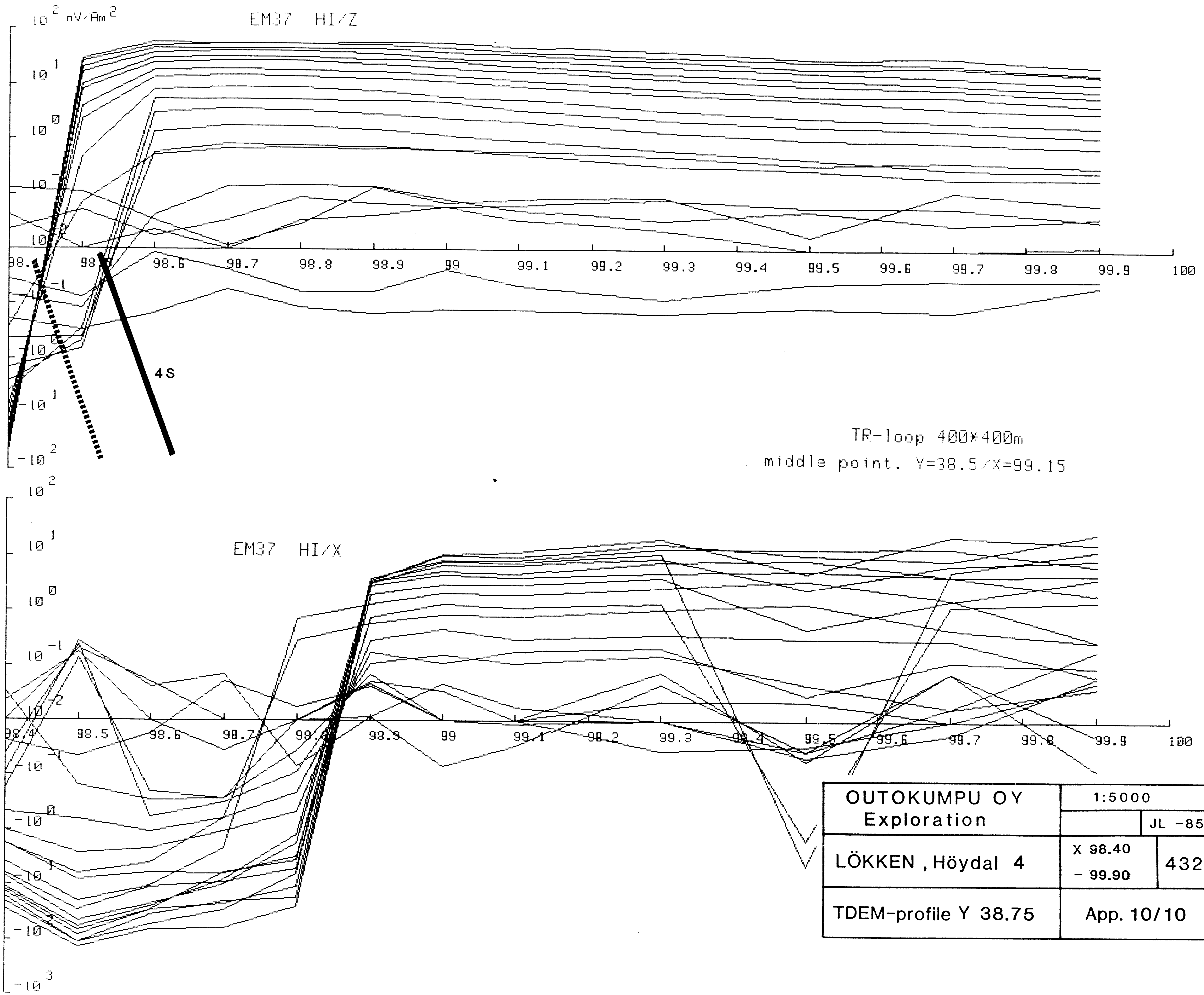

OUTOKUMPU OY Exploration	1:5000	
		JL -85
LÖKKEN , Höydal 4	X 98.40 - 99.90	432
TDEM-profile Y 38.75	App. 10/10	

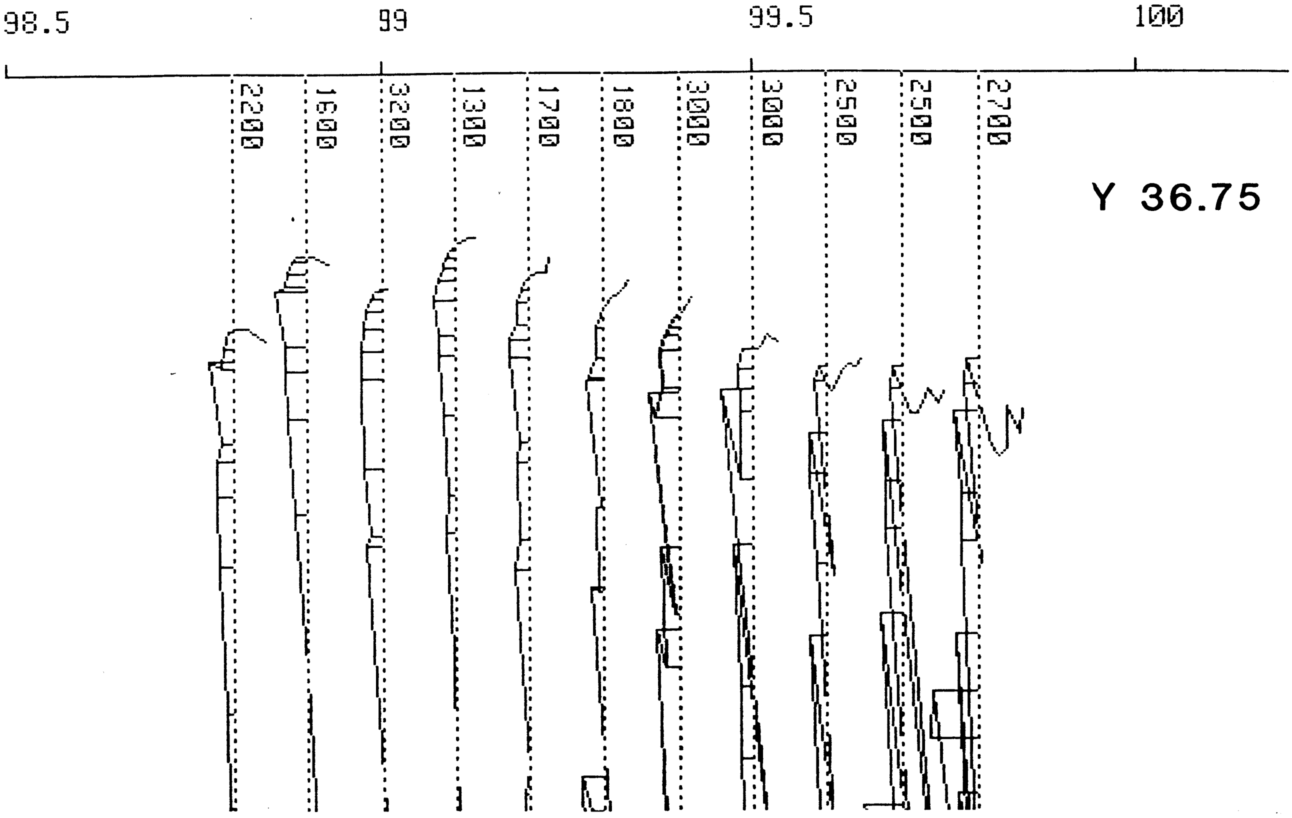

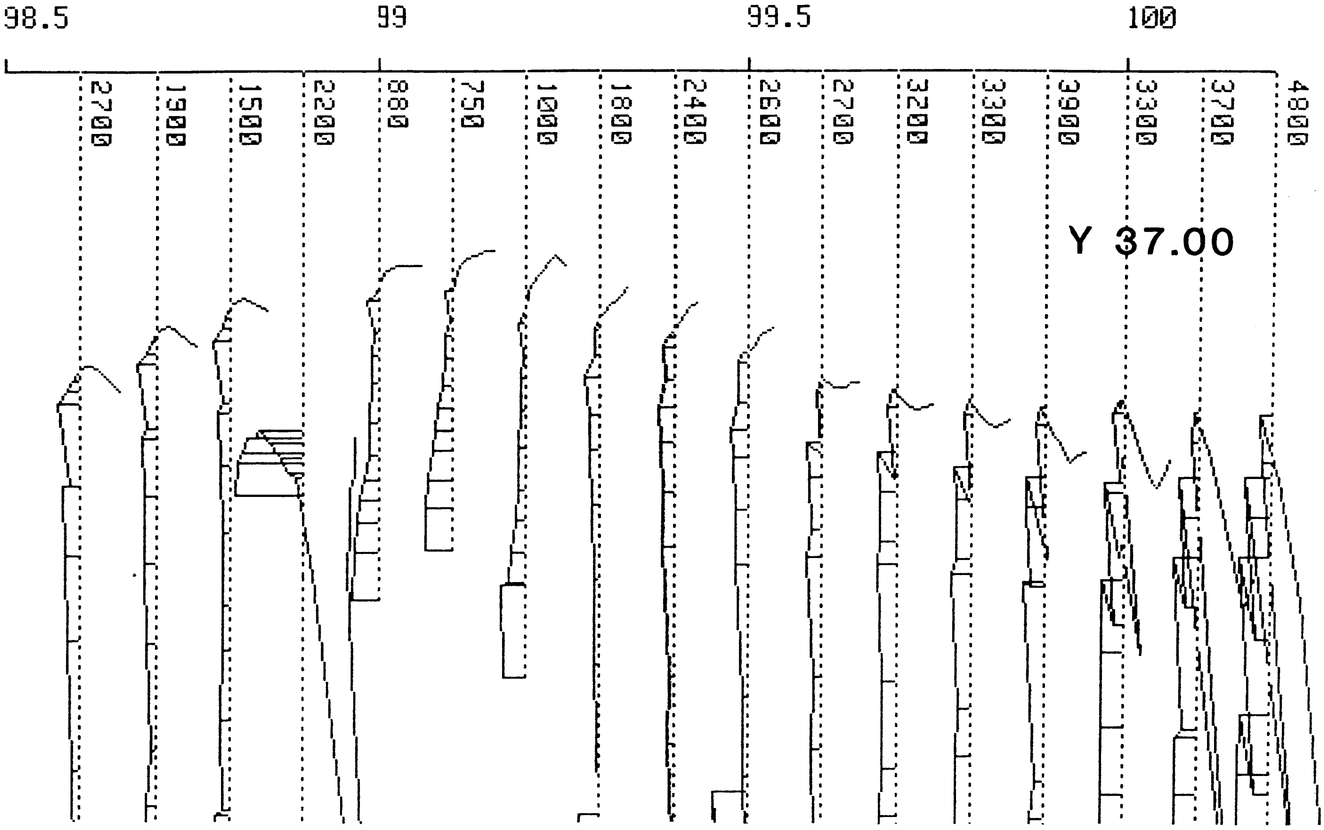

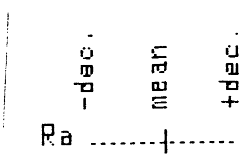

OUTOKUMPU OY Exploration	1:10000	
		JL -85
LÖKKEN , Höydal		433
DIT-plot Y 36.75 Y 37.00	App. 10/11	

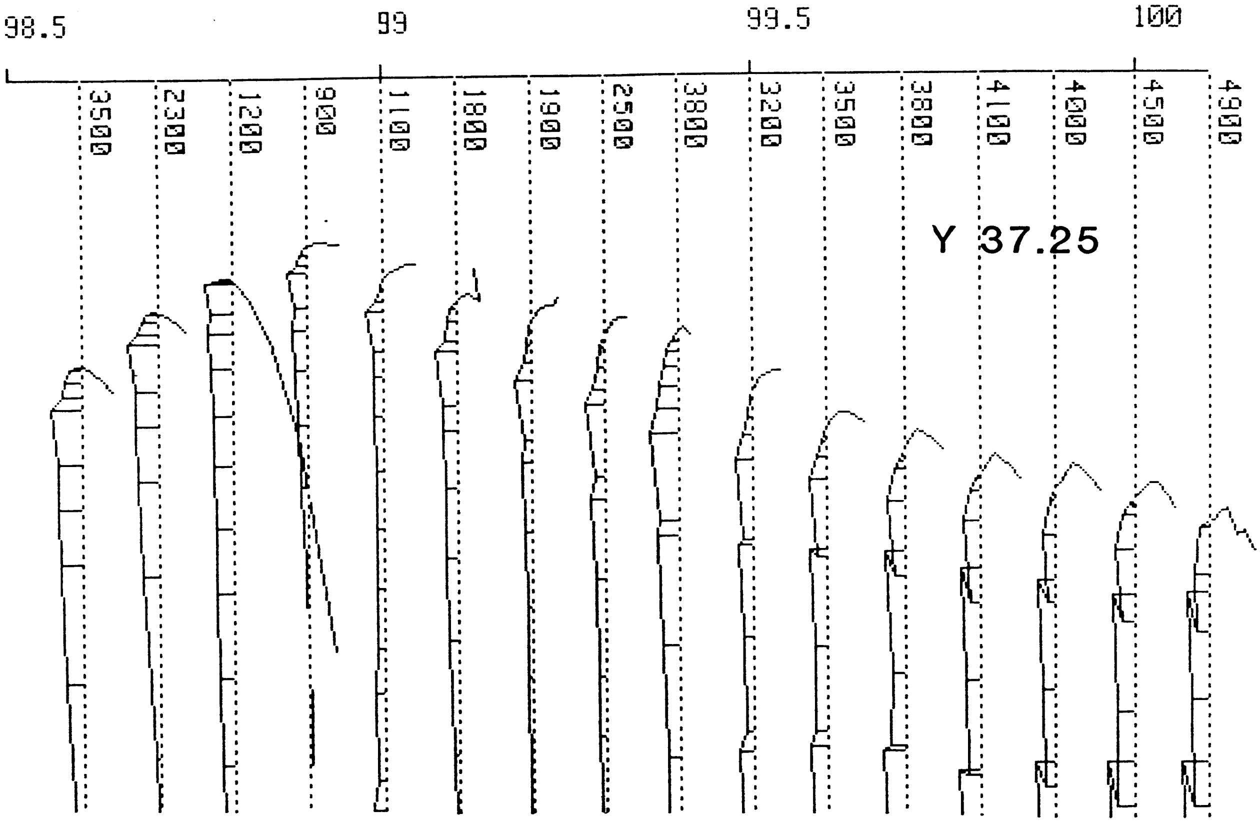

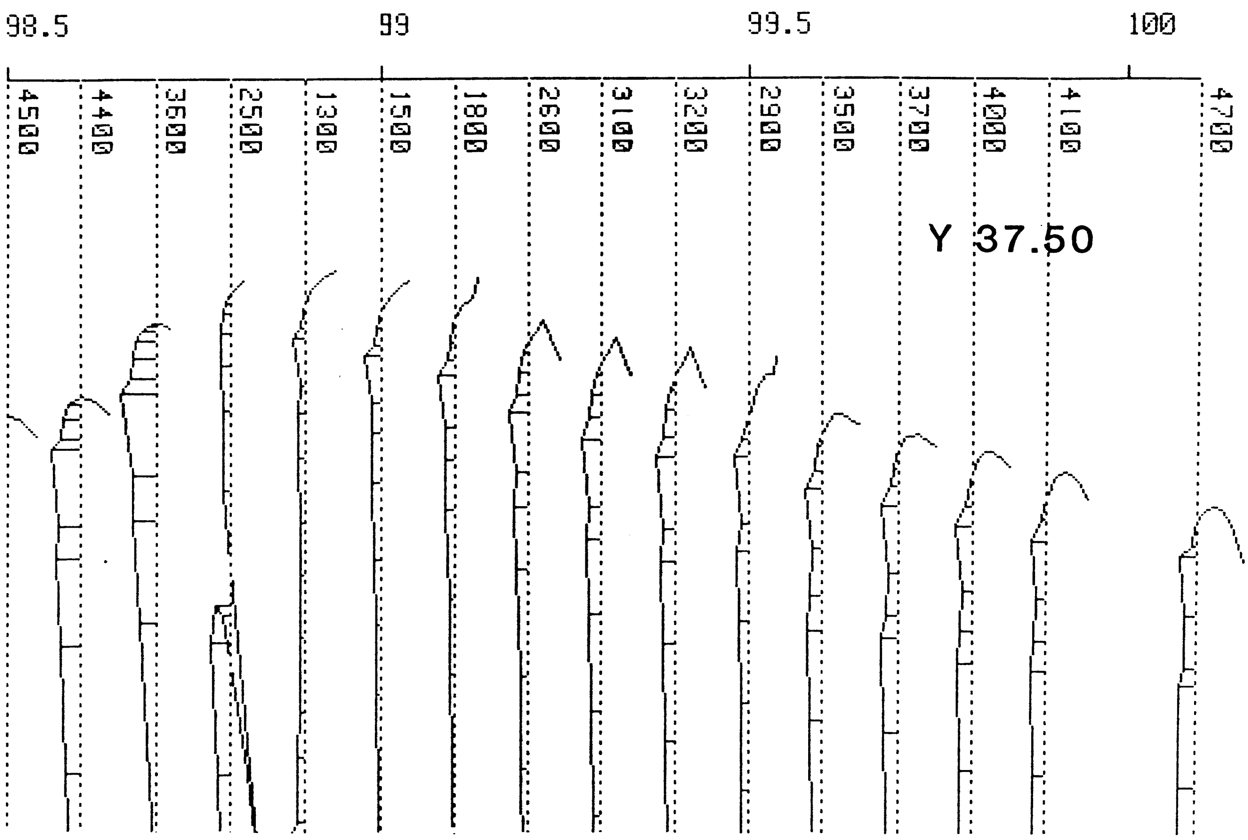

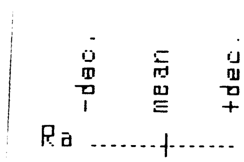

OUTOKUMPU OY Exploration	1:10 000	
		JL -85
LÖKKEN , Höydal		433
DIT-plots Y 37.25 Y 37.50	App. 10/12	

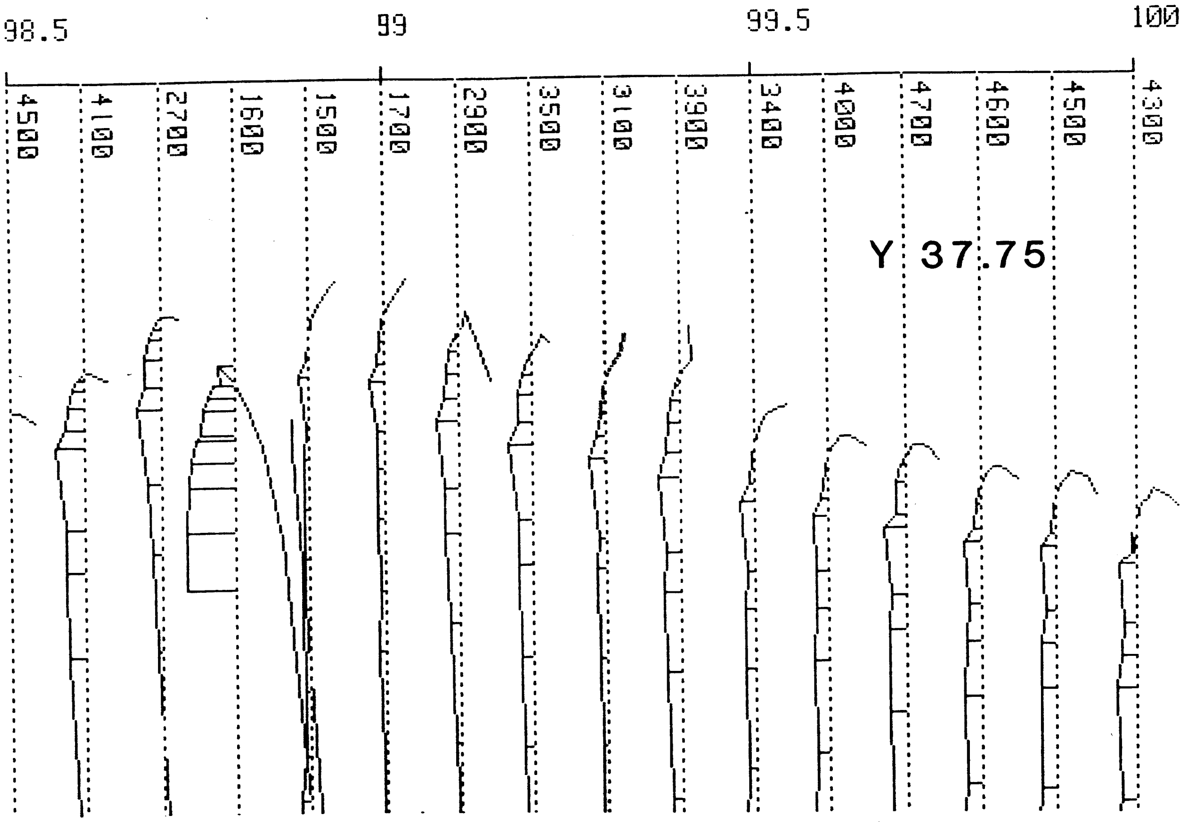

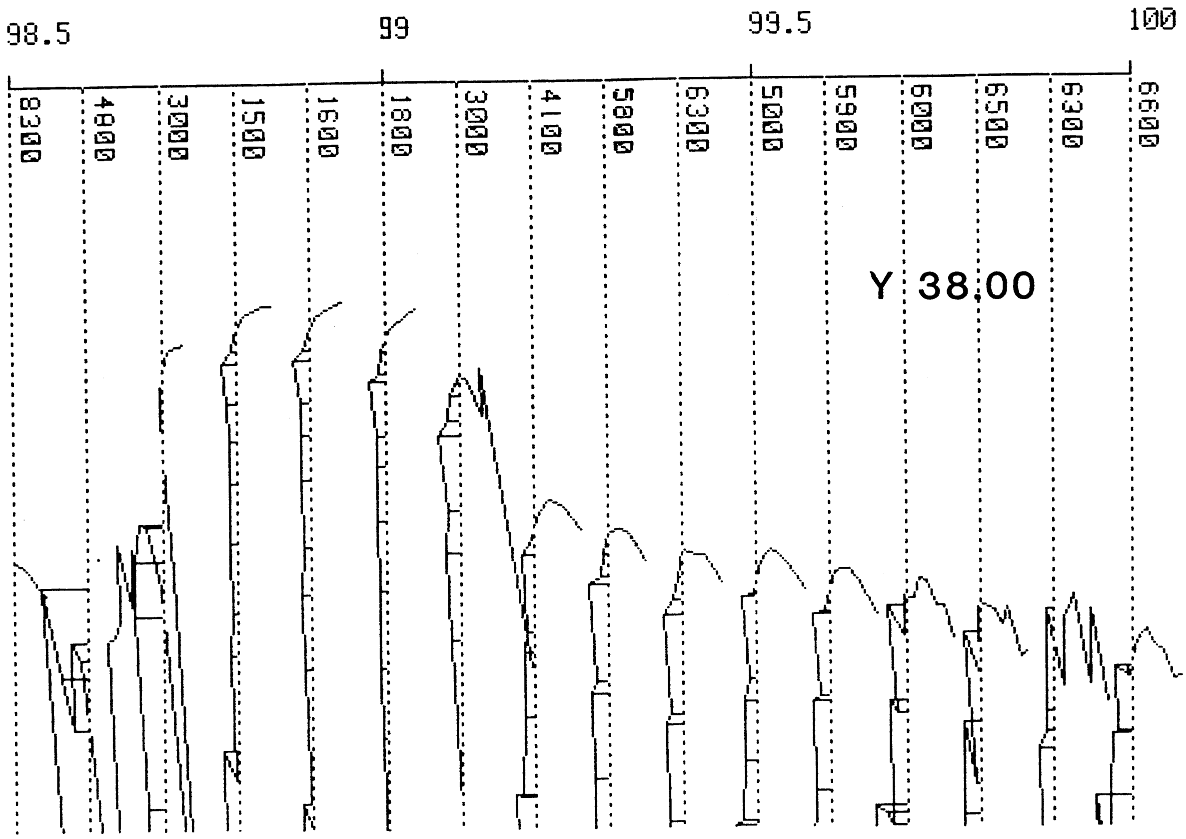

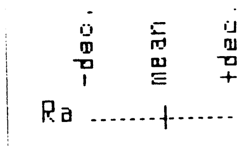

OUTOKUMPU OY Exploration	1:10000	JL -85
LÖKKEN , Höydal		433
DIT-plots Y 37.75 Y 38.00	App. 10/13	

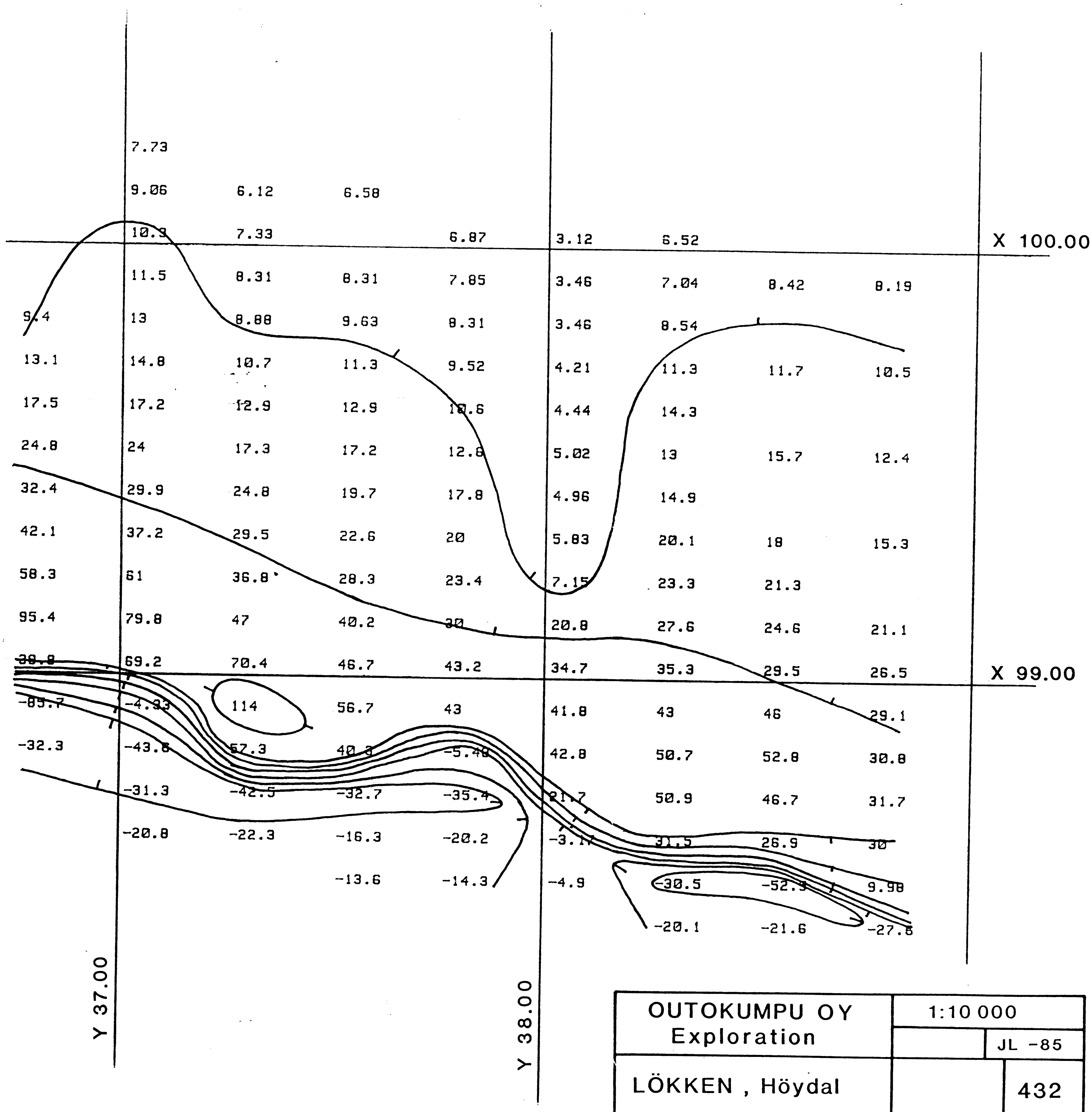

OUTOKUMPU OY Exploration	1:10 000 JL -85
LÖKKEN , Höydal	432
contoured map TDEM/Z-comp. channel no. 5 (.22ms)	App. 10/15

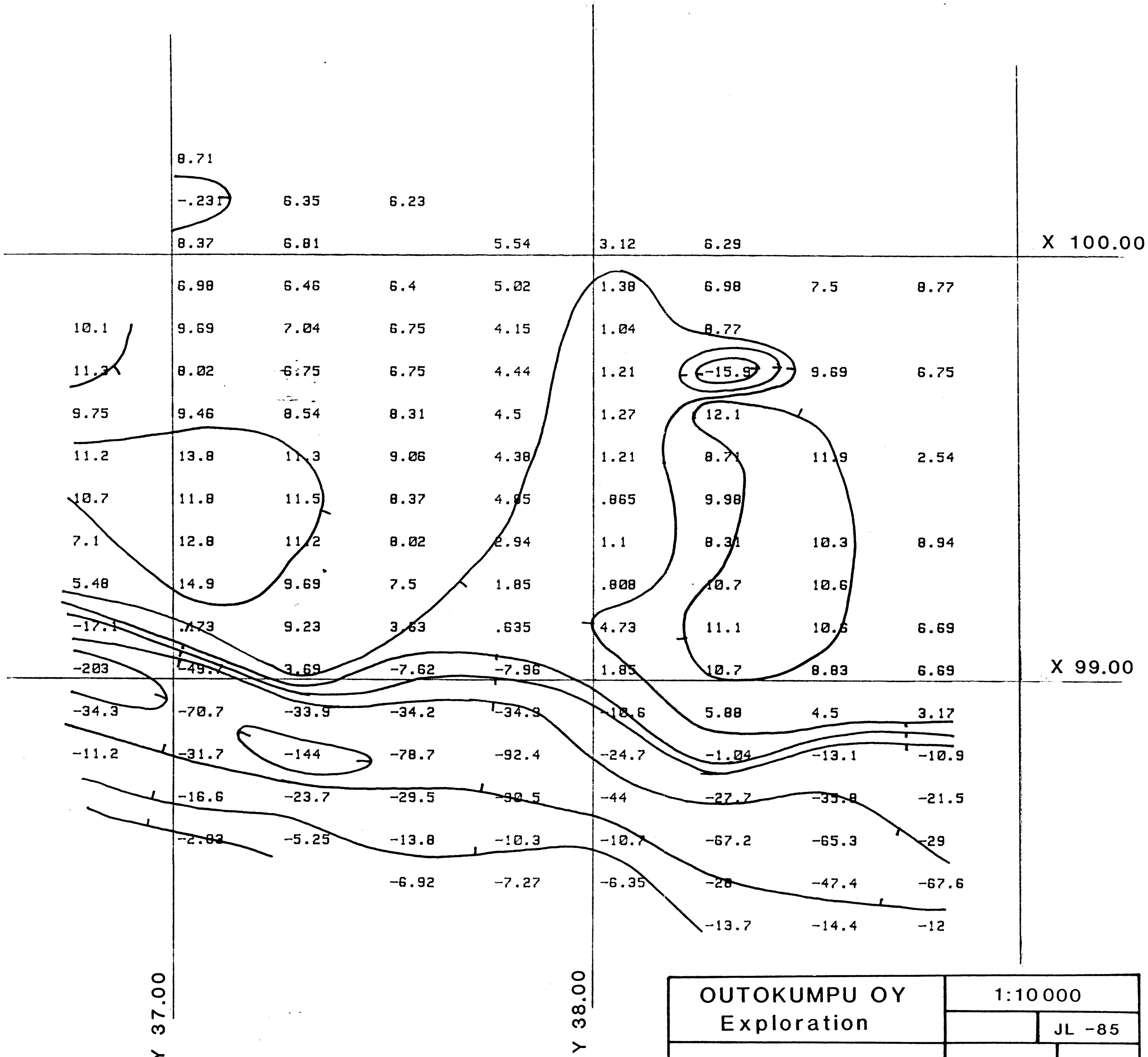

OUTOKUMPU OY Exploration	1:10 000	JL -85
LÖKKEN , Höydal		432
contoured map TDEM/X-comp. channel no. 5 (.22ms)	App. 10/16	

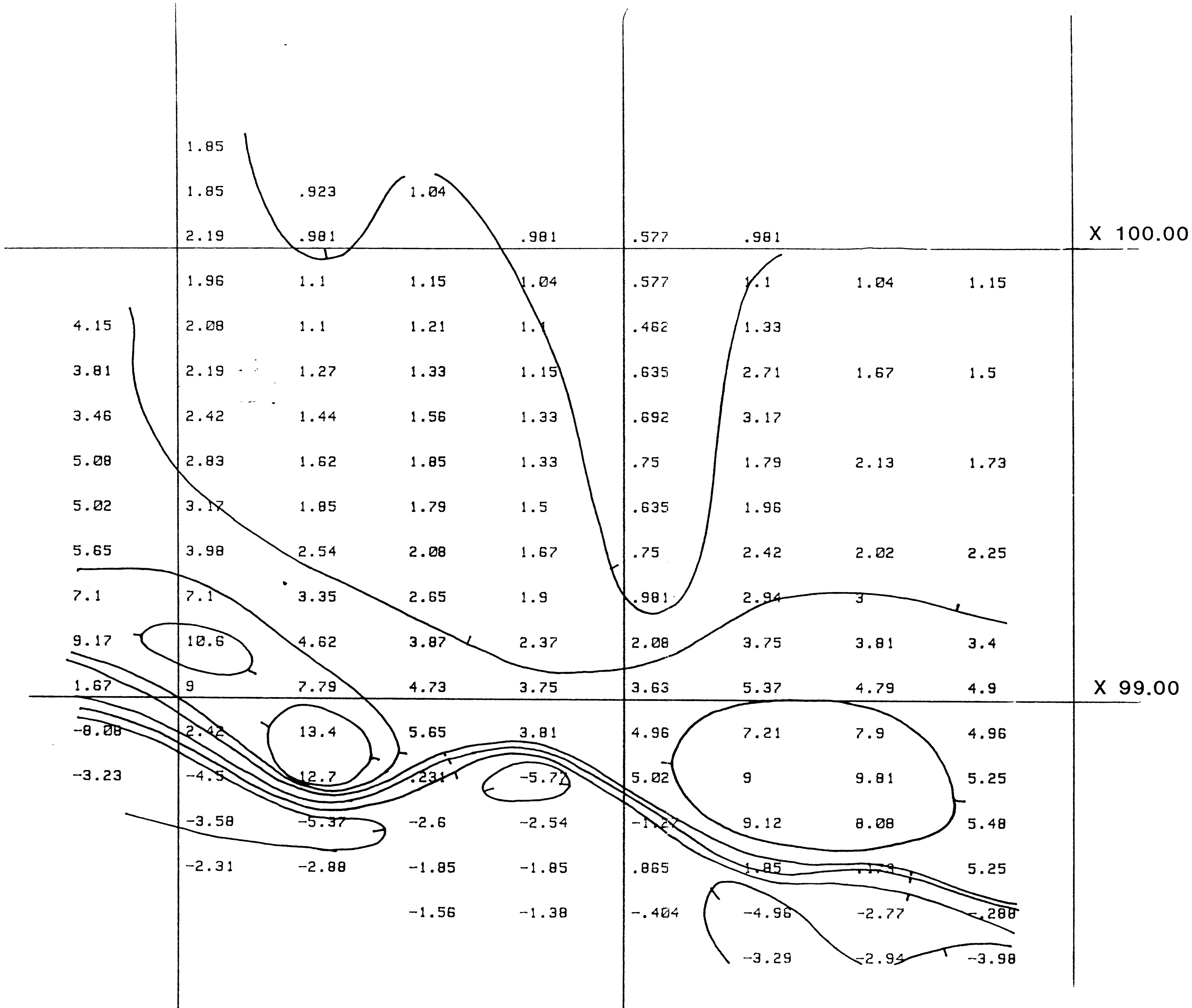

OUTOKUMPU OY Exploration	1:10 000	
		JL -85
LÖKKEN , Höydal		432
contoured map TDEM/Z-comp. channel no. 10 (.71ms)	App. 10/17	

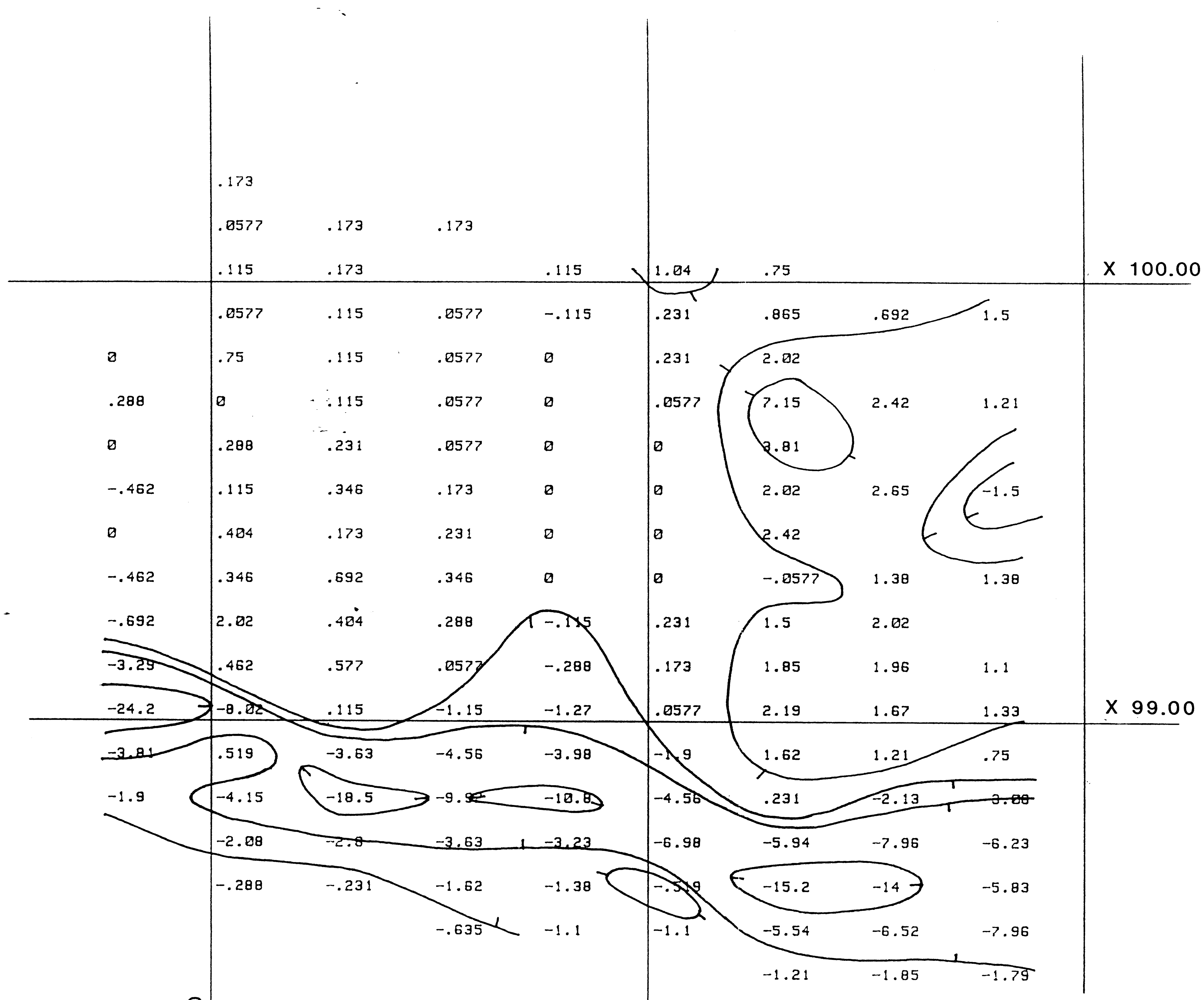

OUTOKUMPU OY Exploration	1:10 000	
		JL -85
LÖKKEN , Höydal		432
contoured map TDEM/X-comp. channel no. 10 (.71ms)	App. 10/18	

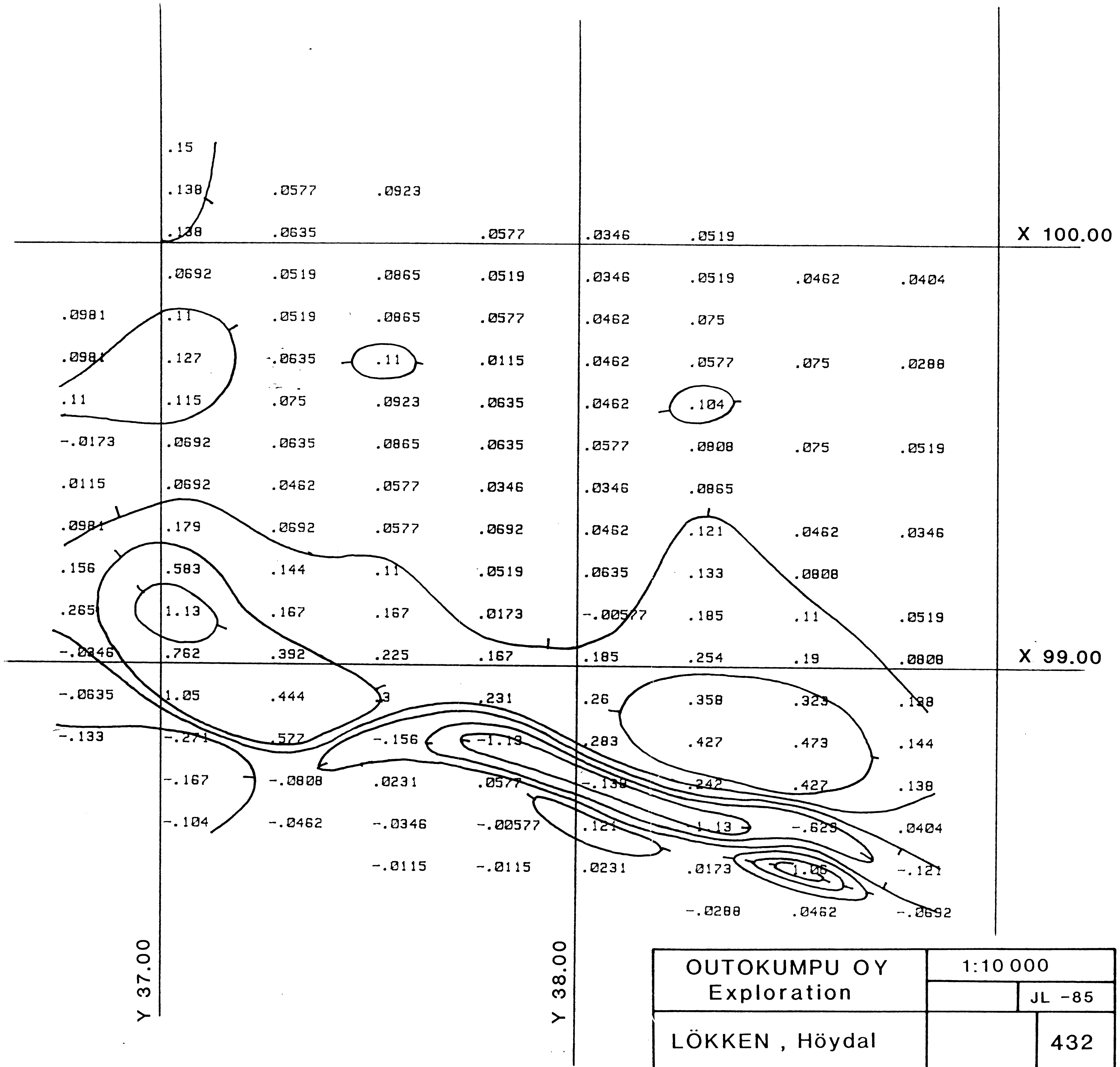

OUTOKUMPU OY Exploration	1:10 000 JL -85
LÖKKEN , Höydal	432
contoured map TDEM/Z-comp. channel no. 15 (2.22ms)	App. 10/19

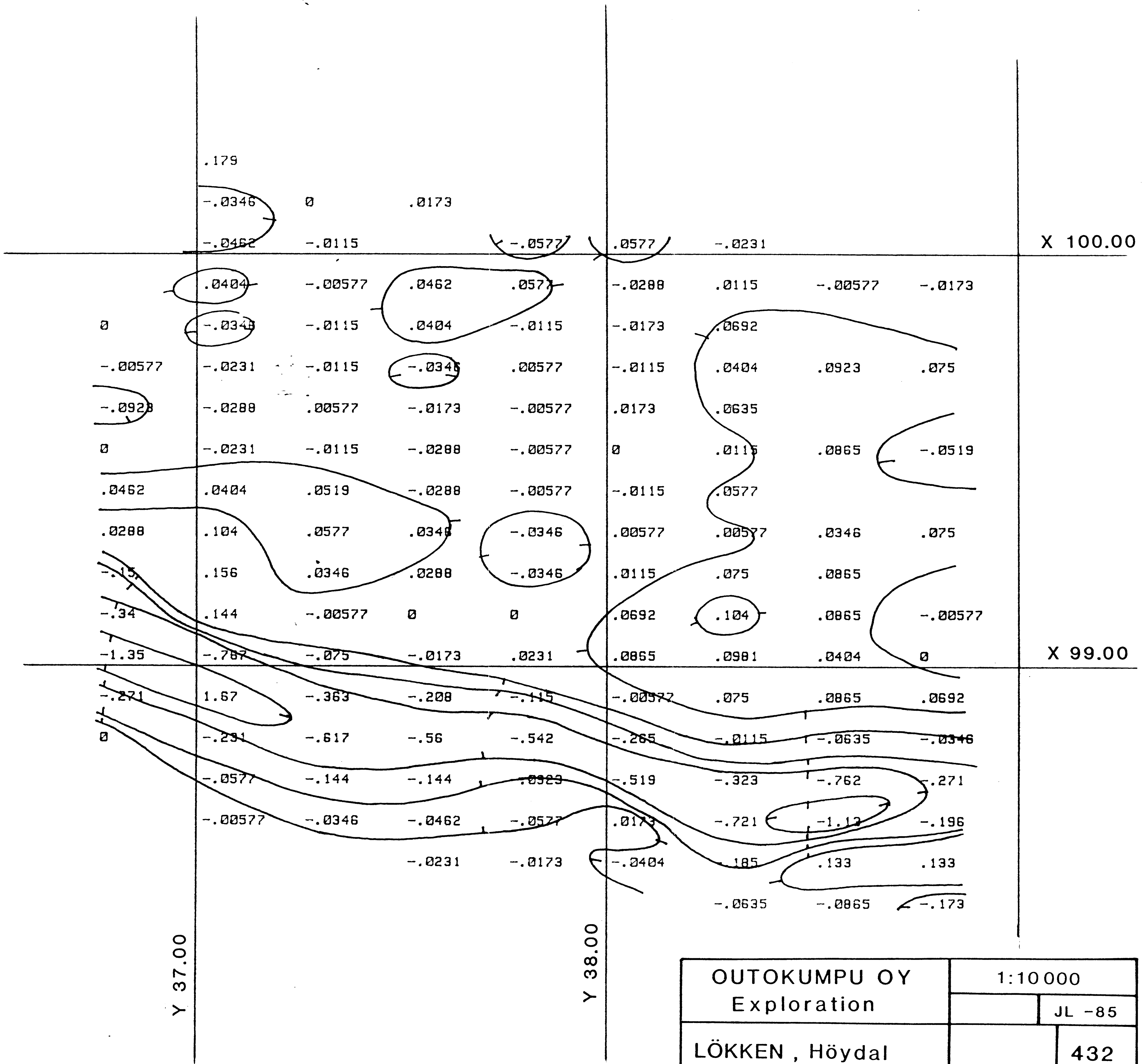

OUTOKUMPU OY Exploration	1:10 000 JL -85
LÖKKEN , Höydal	432
contoured map TDEM/X-comp. channel no. 15 (2.22ms)	App. 10/20

11

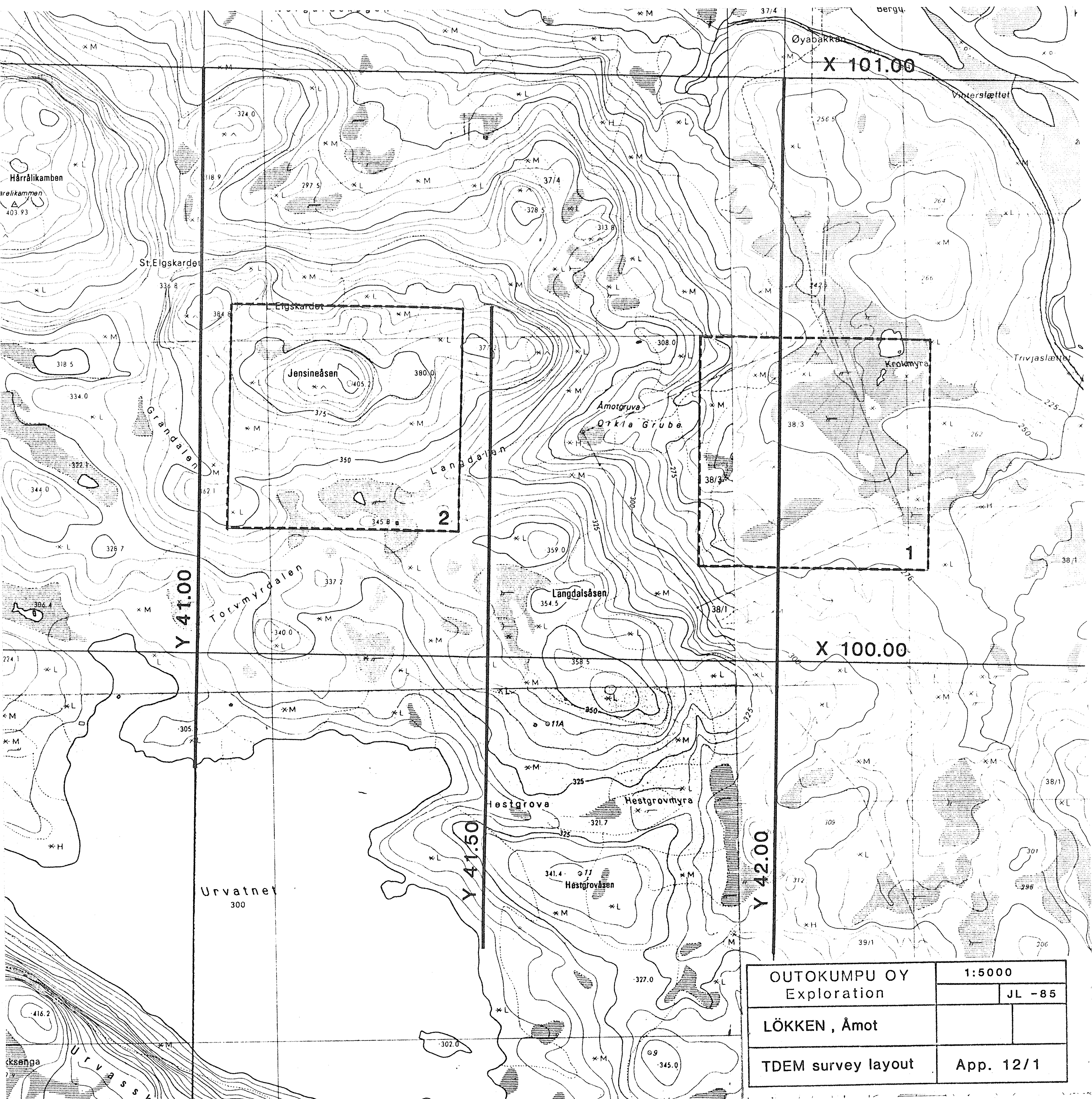

OUTOKUMPU OY Exploration	1:5000	
		JL -85
LÖKKEN , Åmot		
TDEM survey layout	App. 12/1	

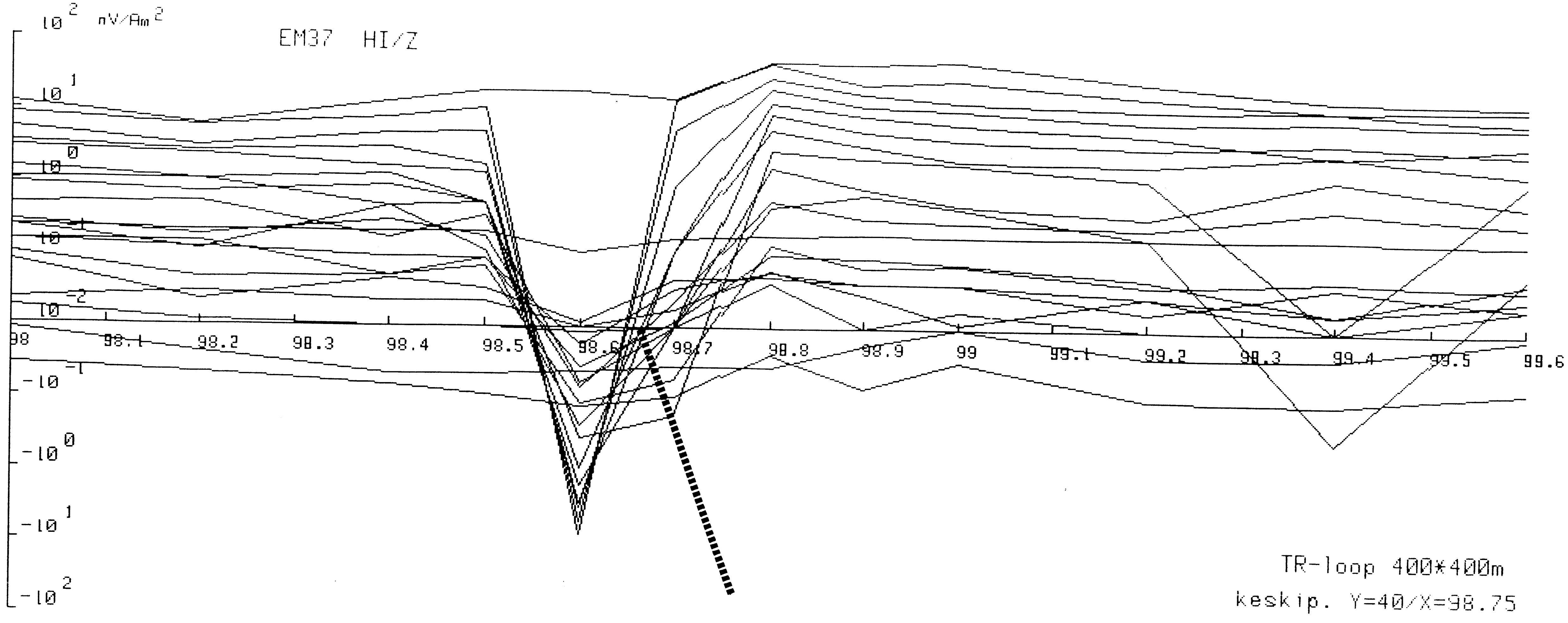

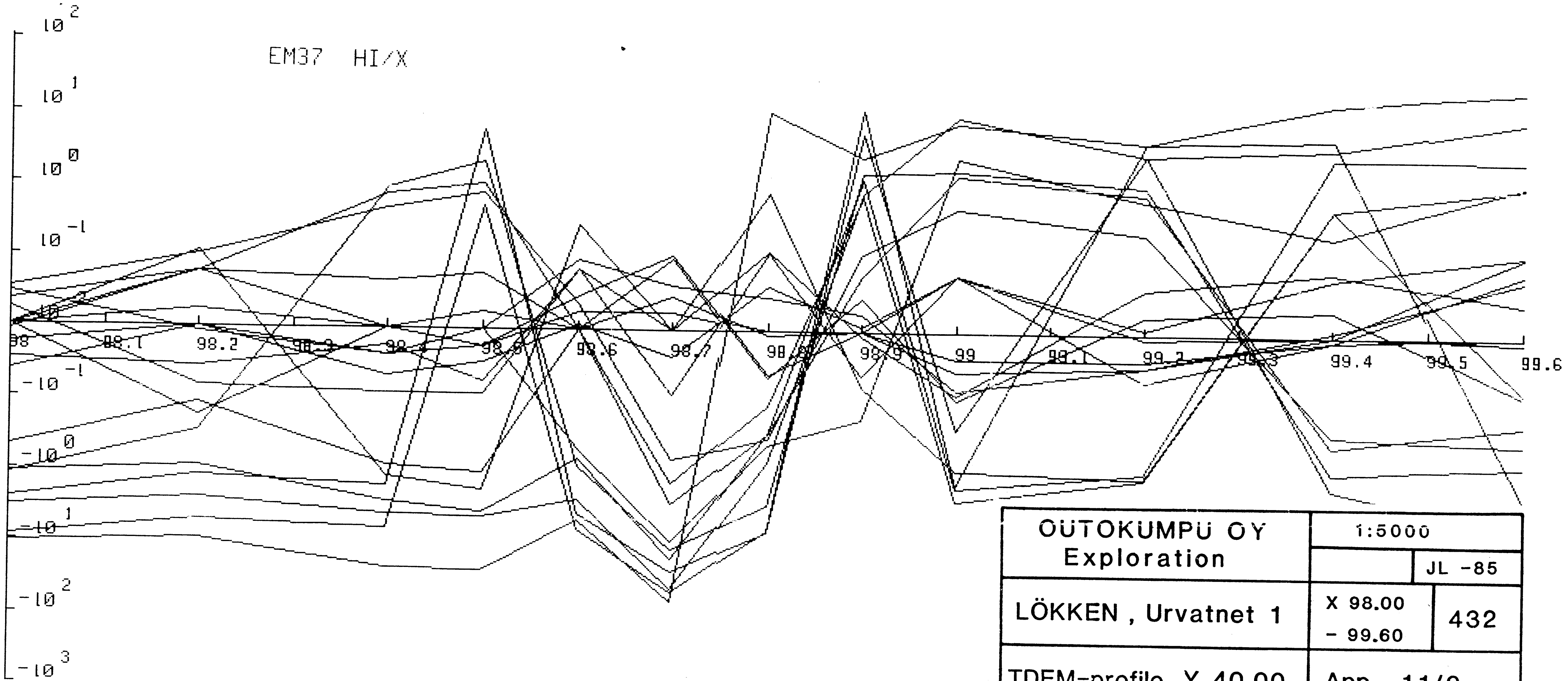

OUTOKUMPU OY Exploration	1:5000	
		JL -85
LÖKKEN , Urvatnet 1	X 98.00 - 99.60	432
TDEM-profile Y 40.00	App. 11/2	

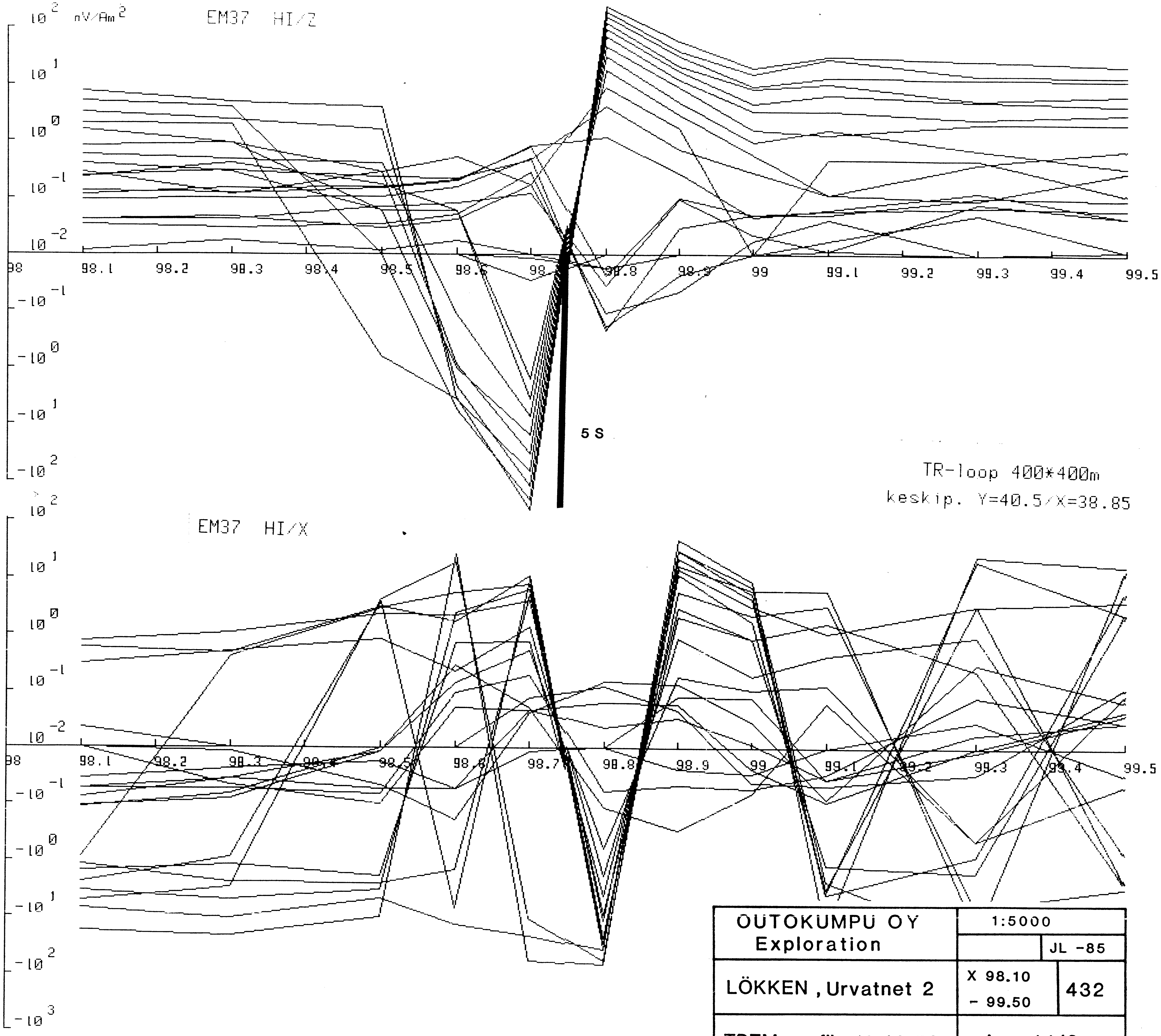

OUTOKUMPU OY Exploration	1:5000	
		JL -85
LÖKKEN, Urvatnet 2	X 98.10 - 99.50	432
TDEM-profile Y 40.50	App. 11/3	

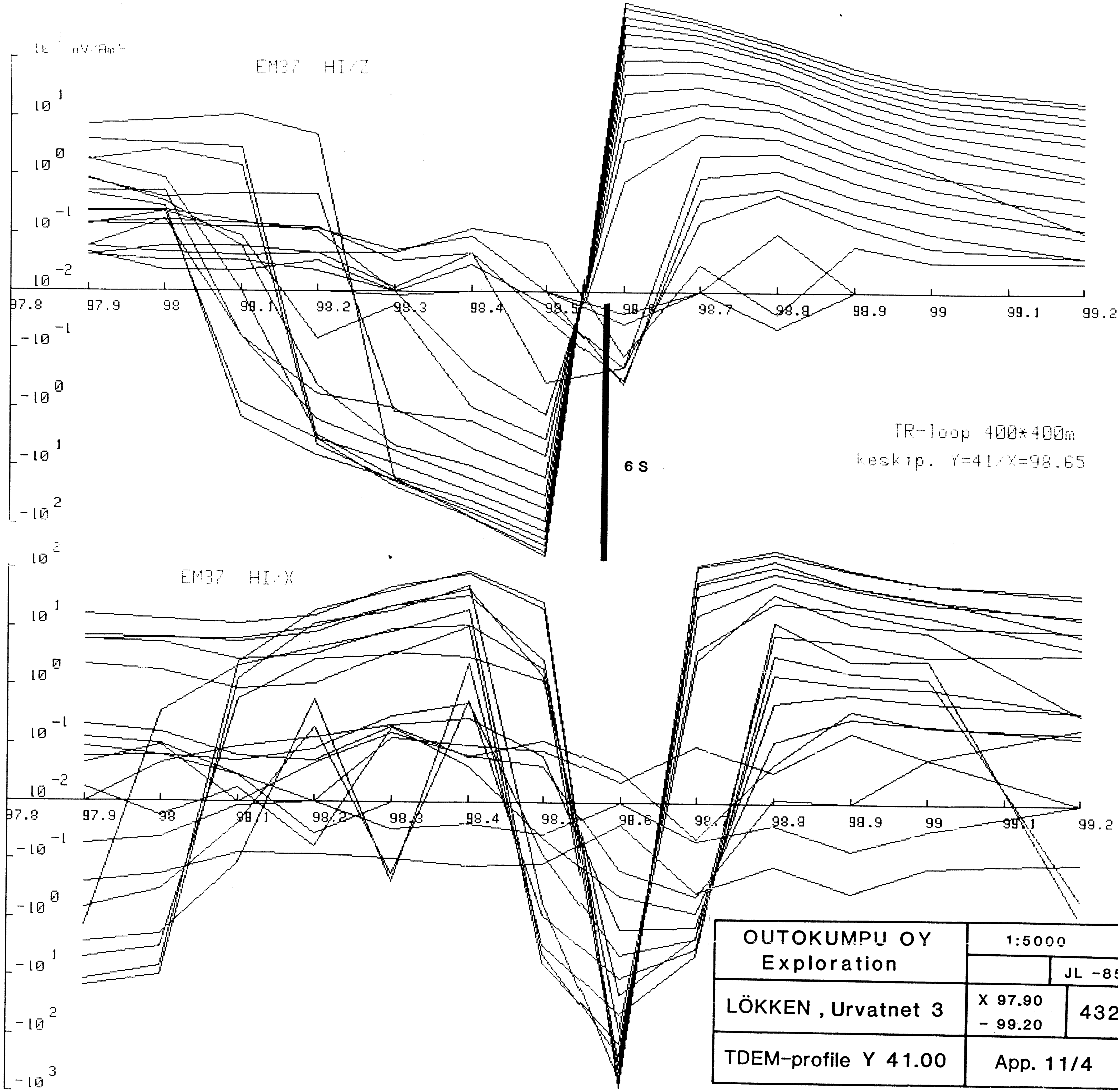

OUTOKUMPU OY Exploration	1:5000	JL -85
LÖKKEN , Urvatnet 3	X 97.90 - 99.20	432
TDEM-profile Y 41.00	App. 11/4	

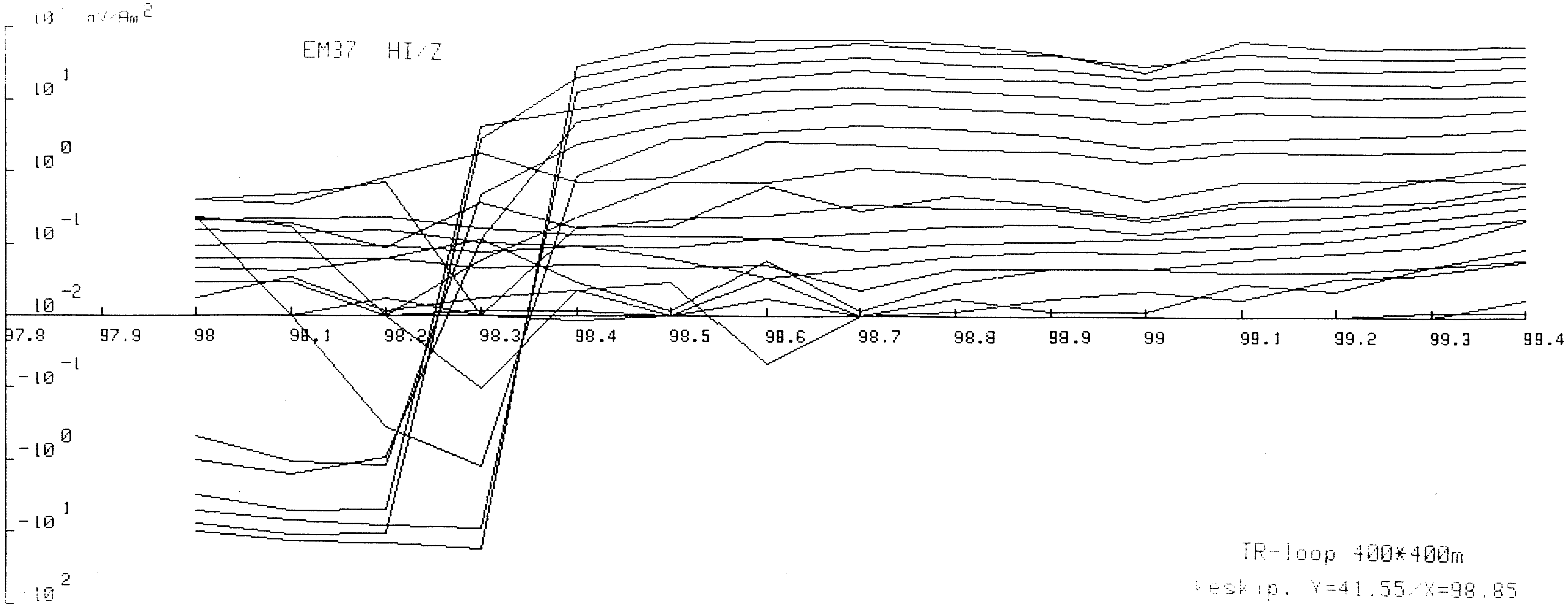

TR-loop 400*400m
Keskip. Y=41.55/X=98.85

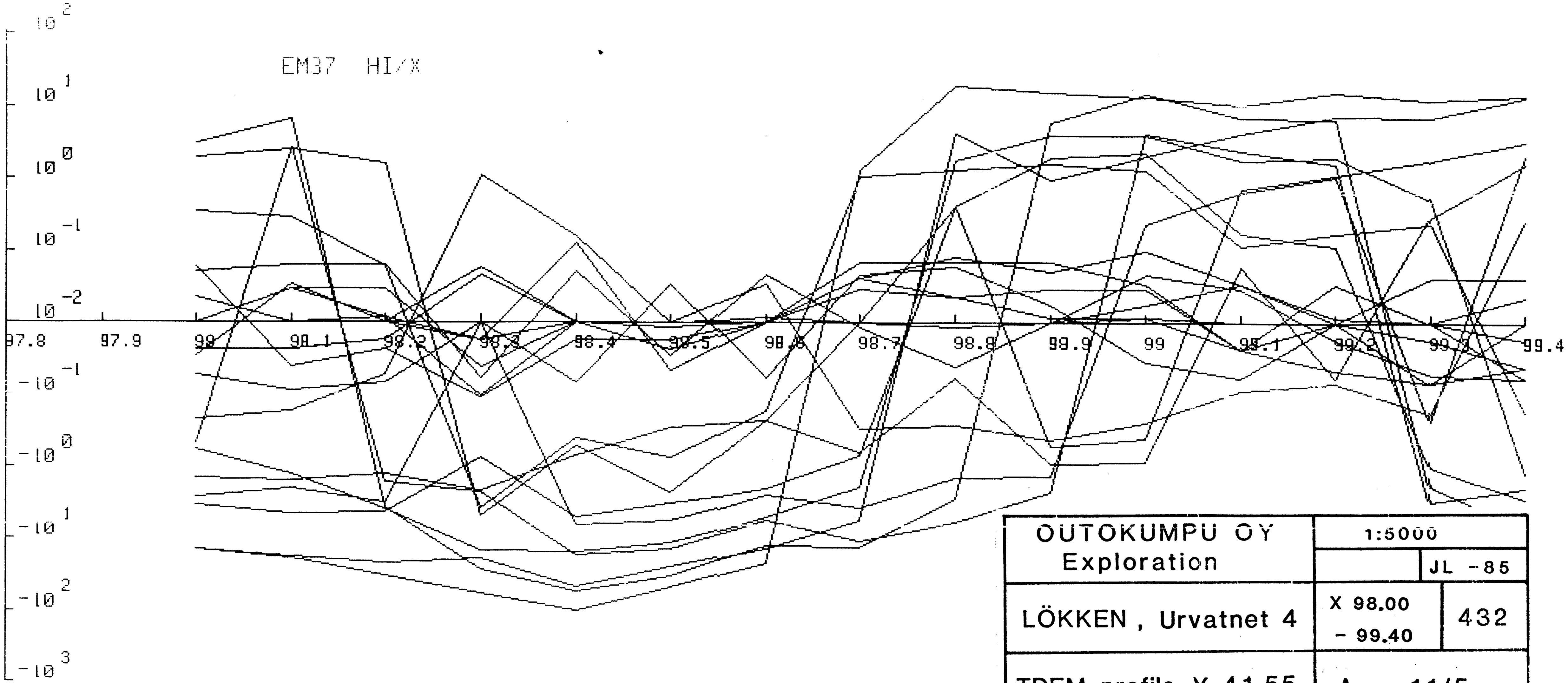

OUTOKUMPU OY Exploration	1:5000	JL -85
LÖKKEN , Urvatnet 4	X 98.00 - 99.40	432
TDEM-profile Y 41.55	App. 11/5	

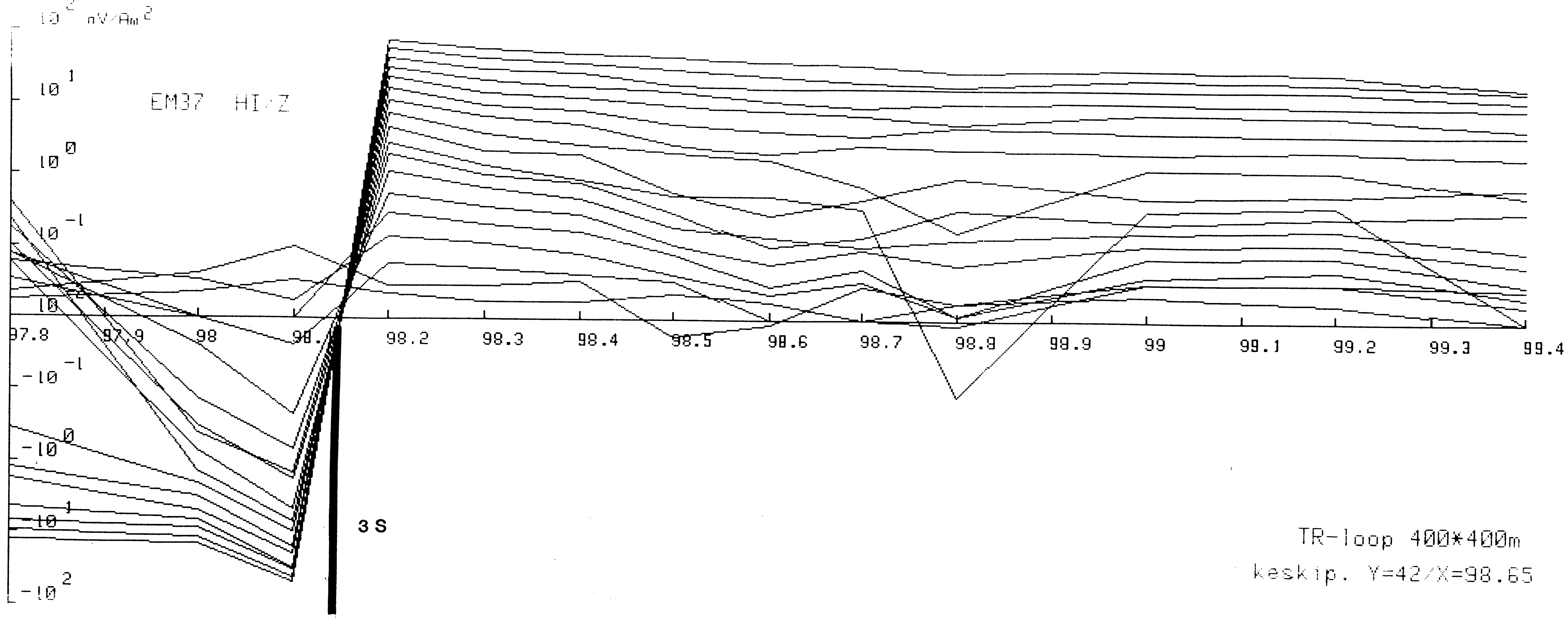

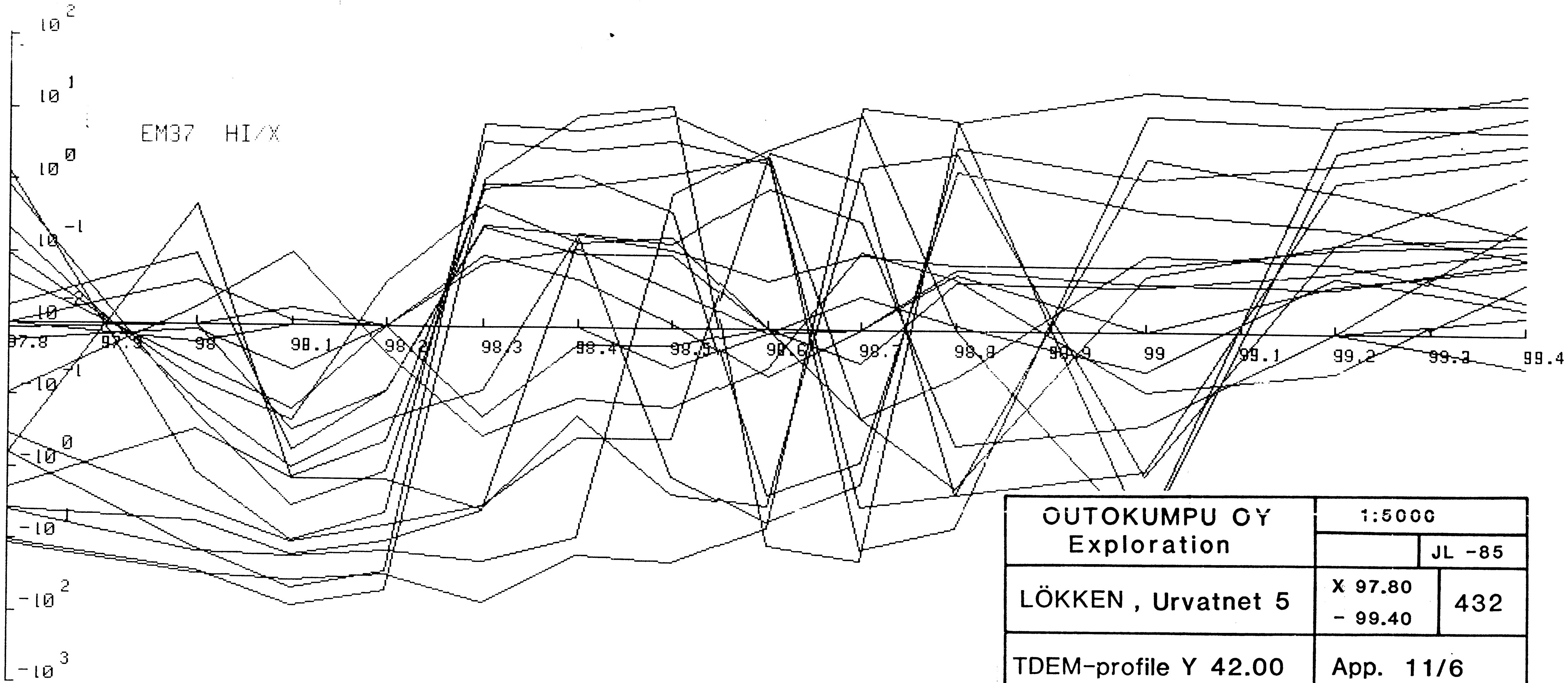

OUTOKUMPU OY Exploration	1:5000	
		JL -85
LÖKKEN , Urvatnet 5	X 97.80 - 99.40	432
TDEM-profile Y 42.00	App. 11/6	

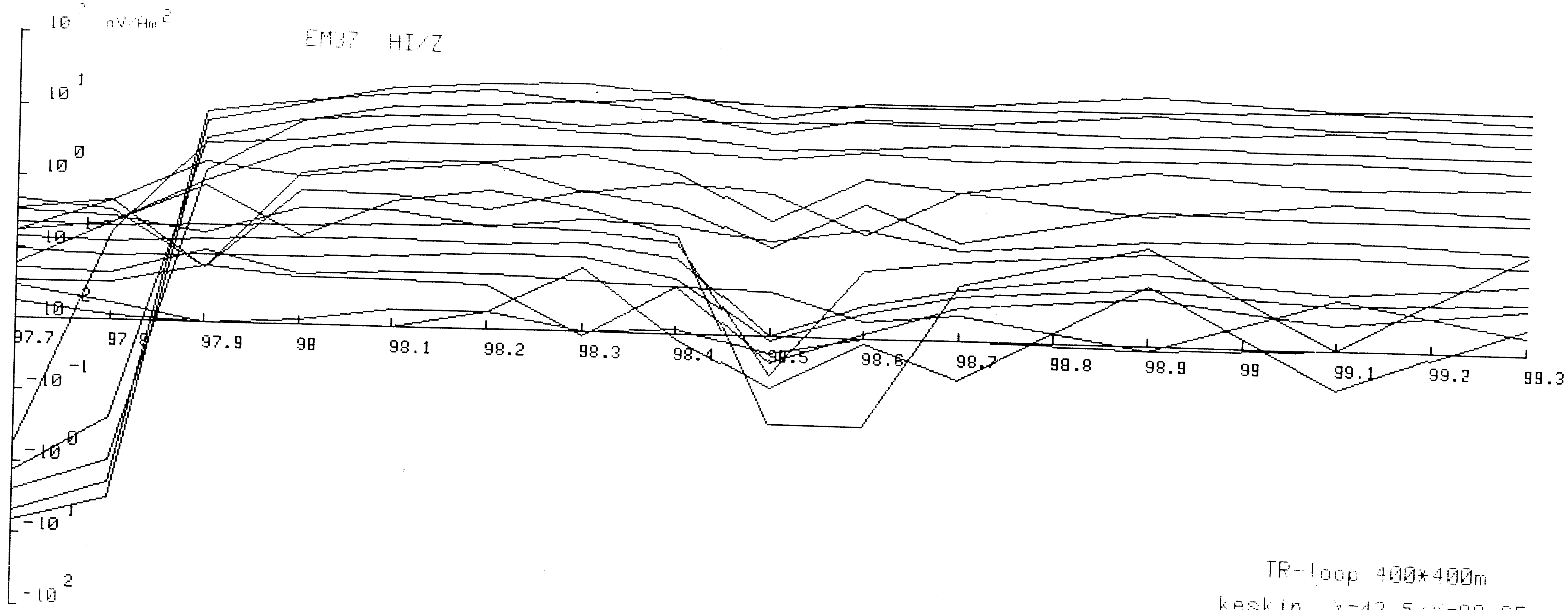

TR-loop 400*400m
keskip. Y=42.5/X=98.65

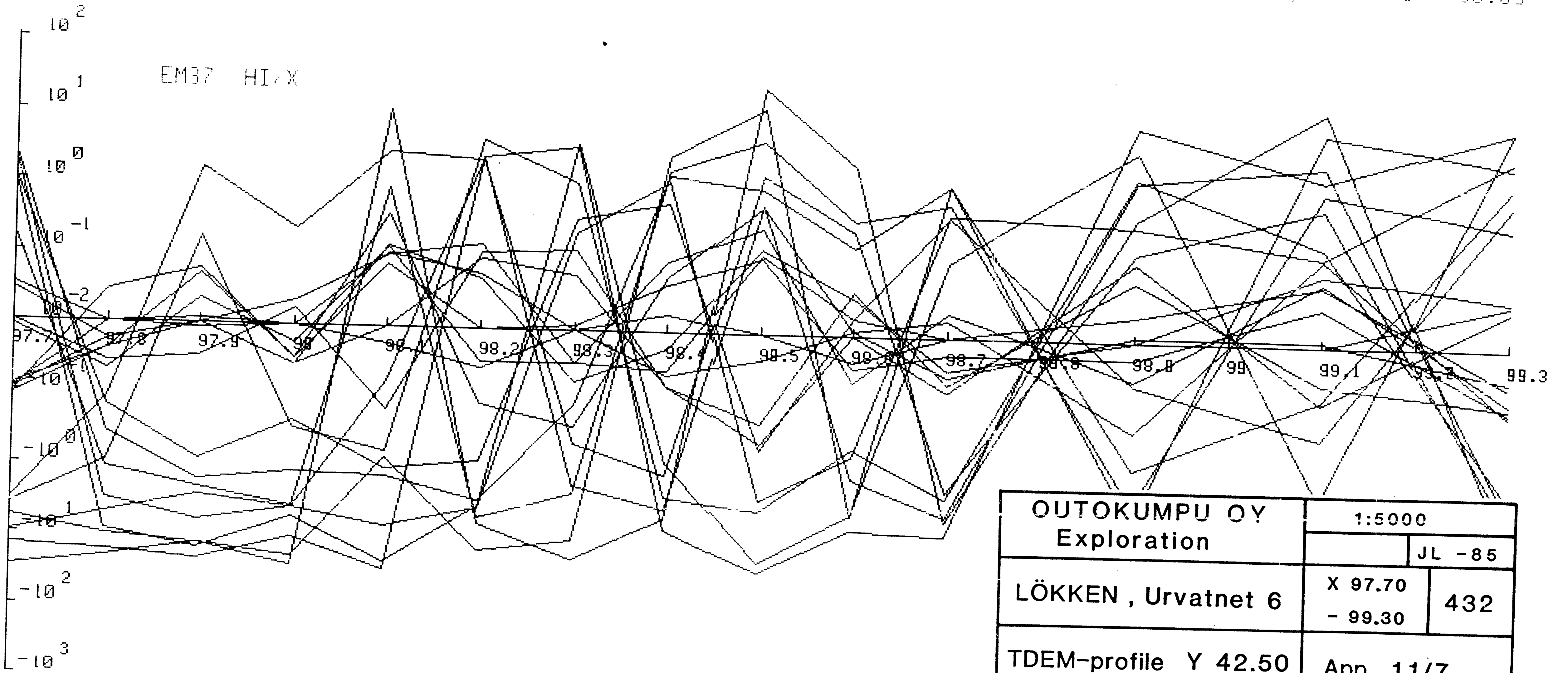

OUTOKUMPU OY Exploration	1:5000	JL -85
LÖKKEN , Urvatnet 6	X 97.70 - 99.30	432
TDEM-profile Y 42.50	App. 11/7	

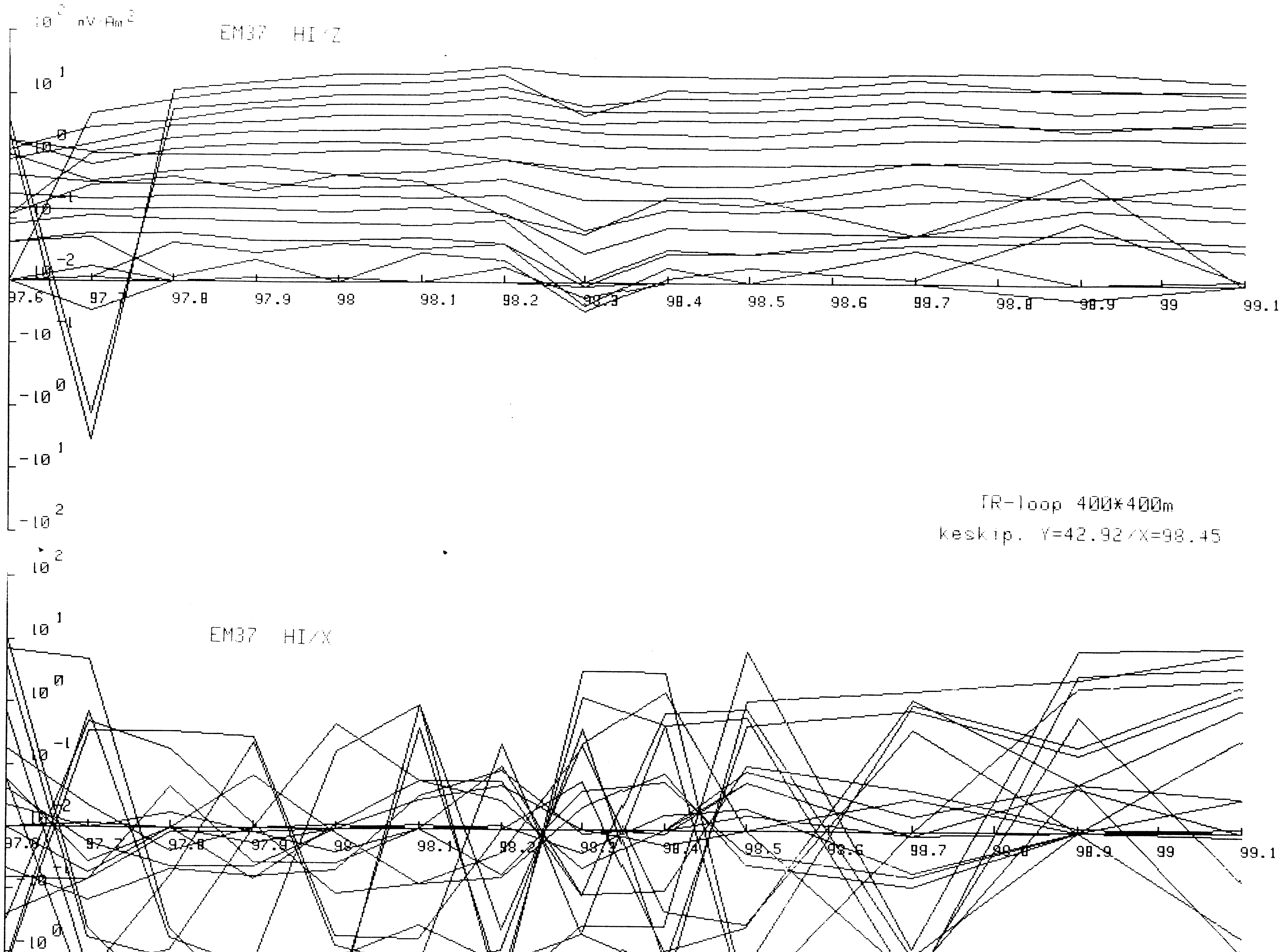

OUTOKUMPU OY Exploration	1:5000	
		JL -85
LÖKKEN , Urvatnet 7	X 97.60 -99.10	432
TDEM-profile Y 43.00	App. 11/8	

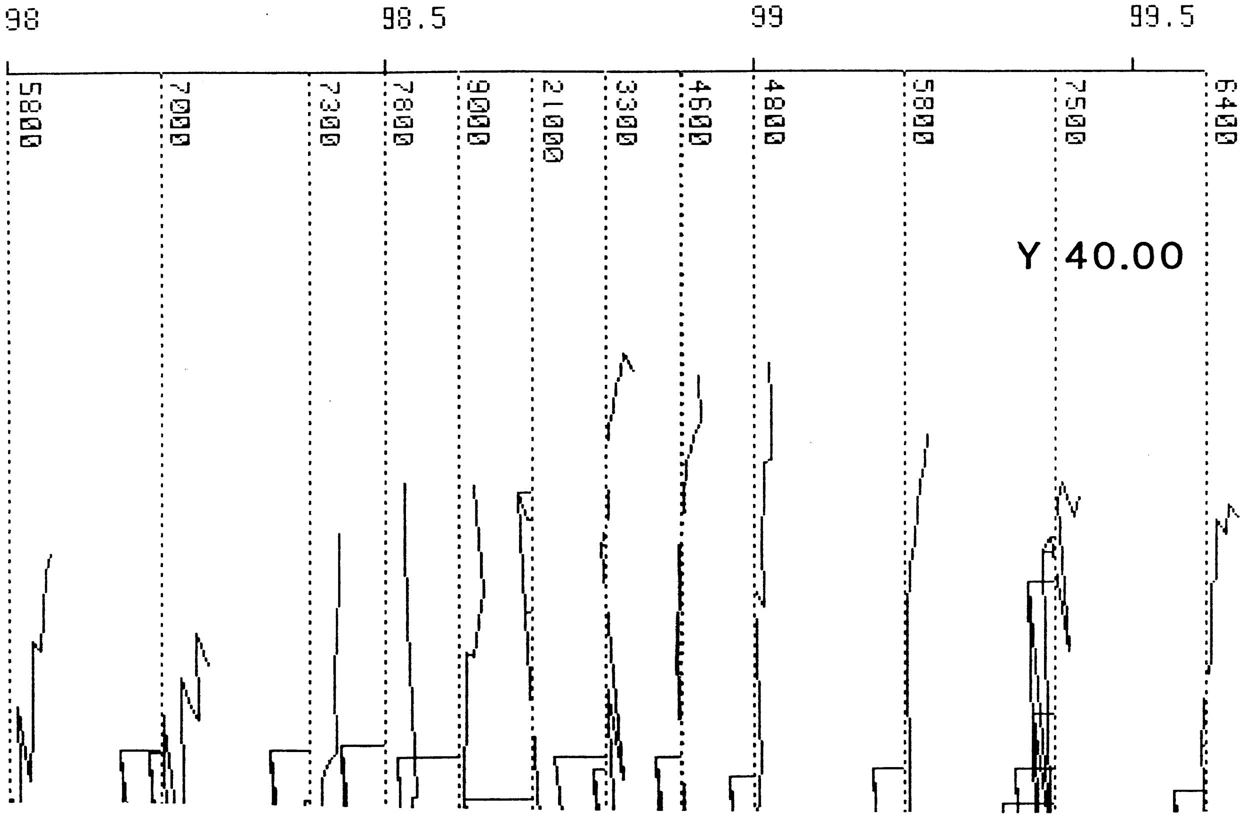

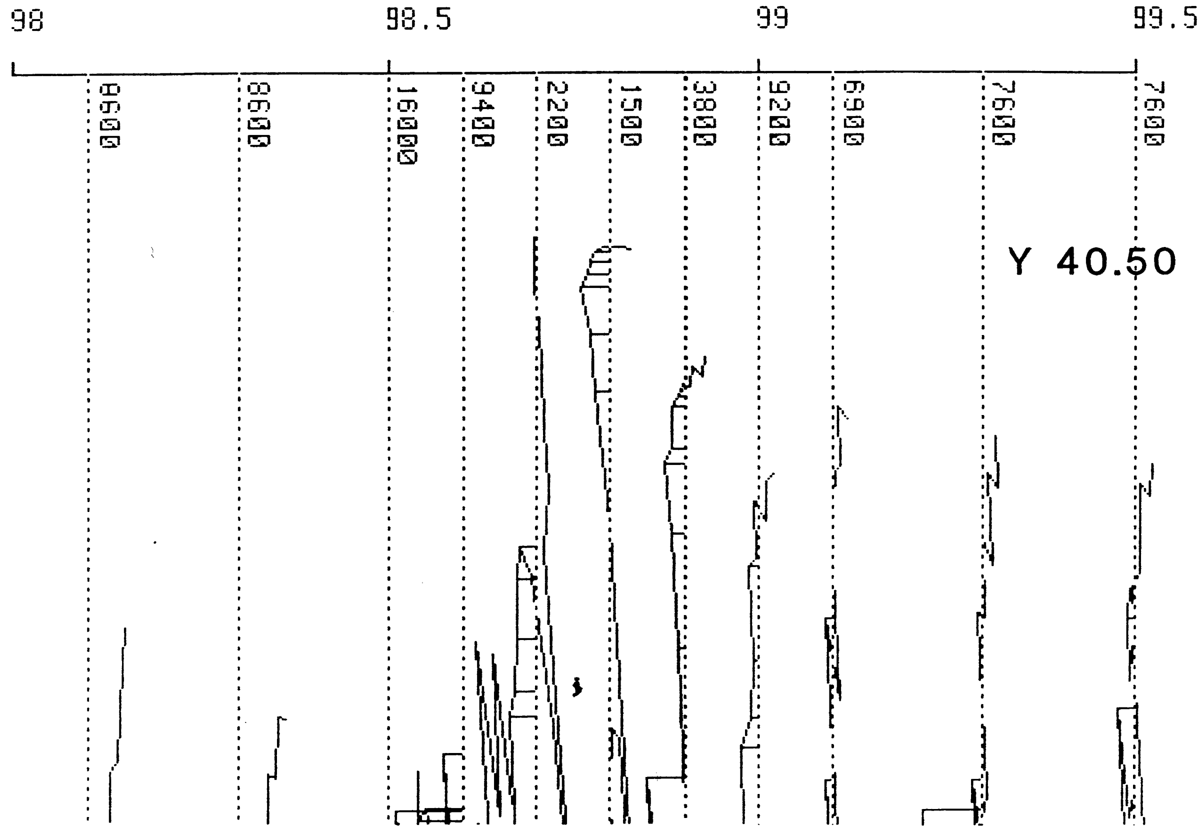

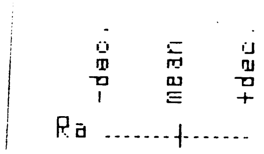

OUTOKUMPU OY Exploration	1:10 000	
		JL -85
LÖKKEN , Urvatnet		433
DIT-plots Y 40.00 Y 40.50	App. 11/9	

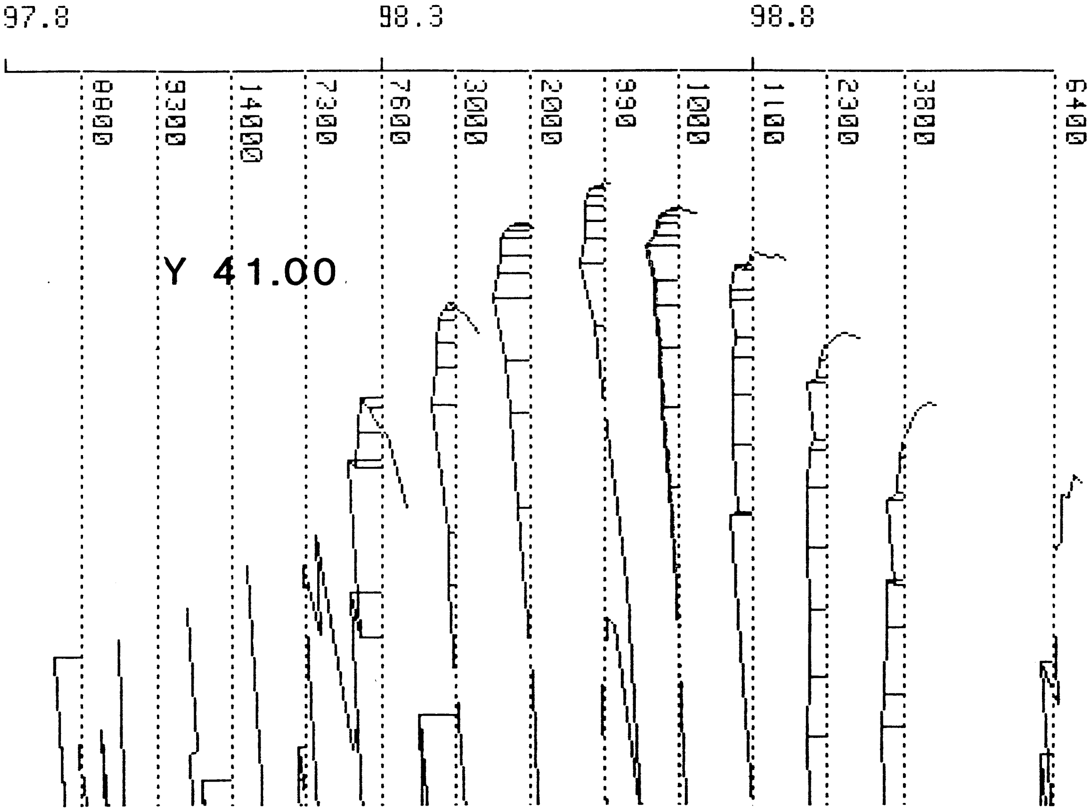

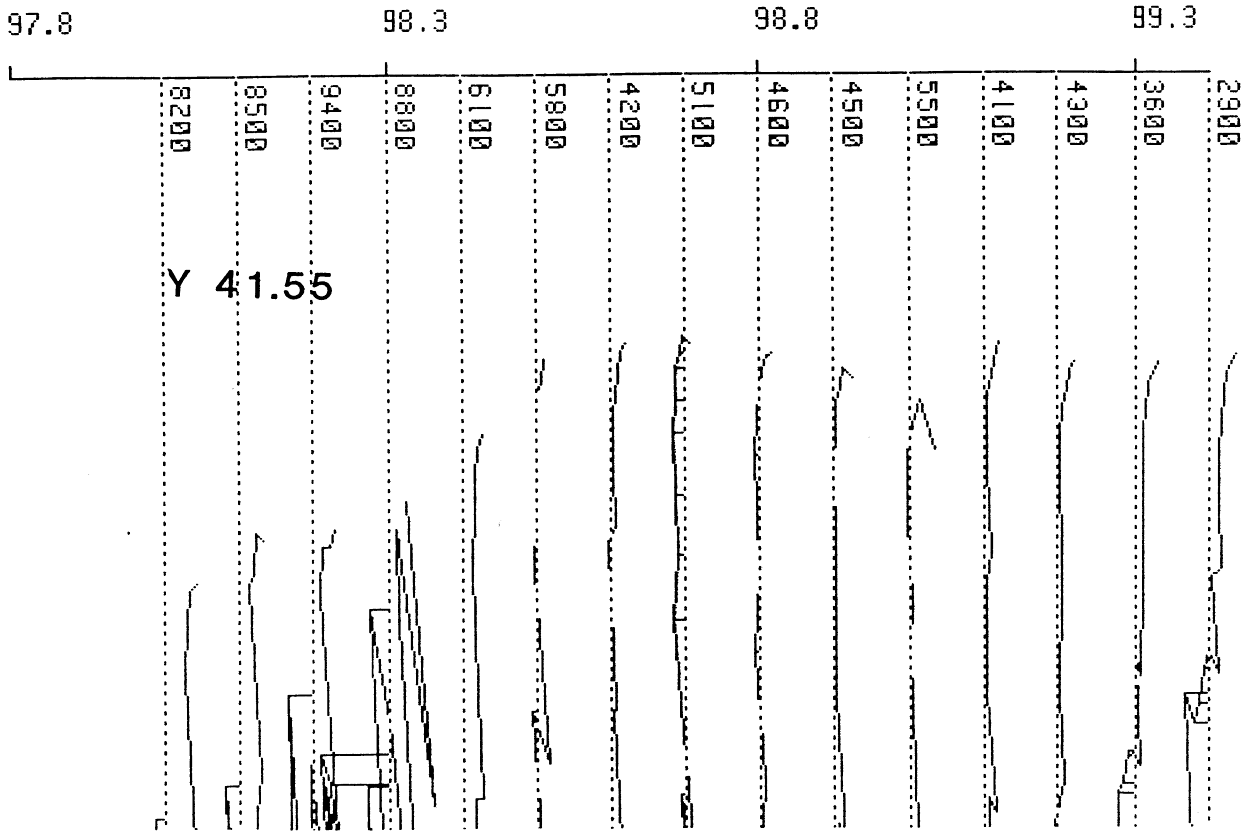

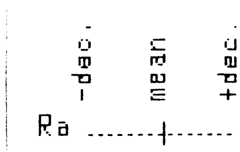

OUTOKUMPU OY Exploration	1:10000	
		JL -85
LÖKKEN , Urvatnet		433
DIT-plots Y 41.00 Y 41.55	App. 11/10	

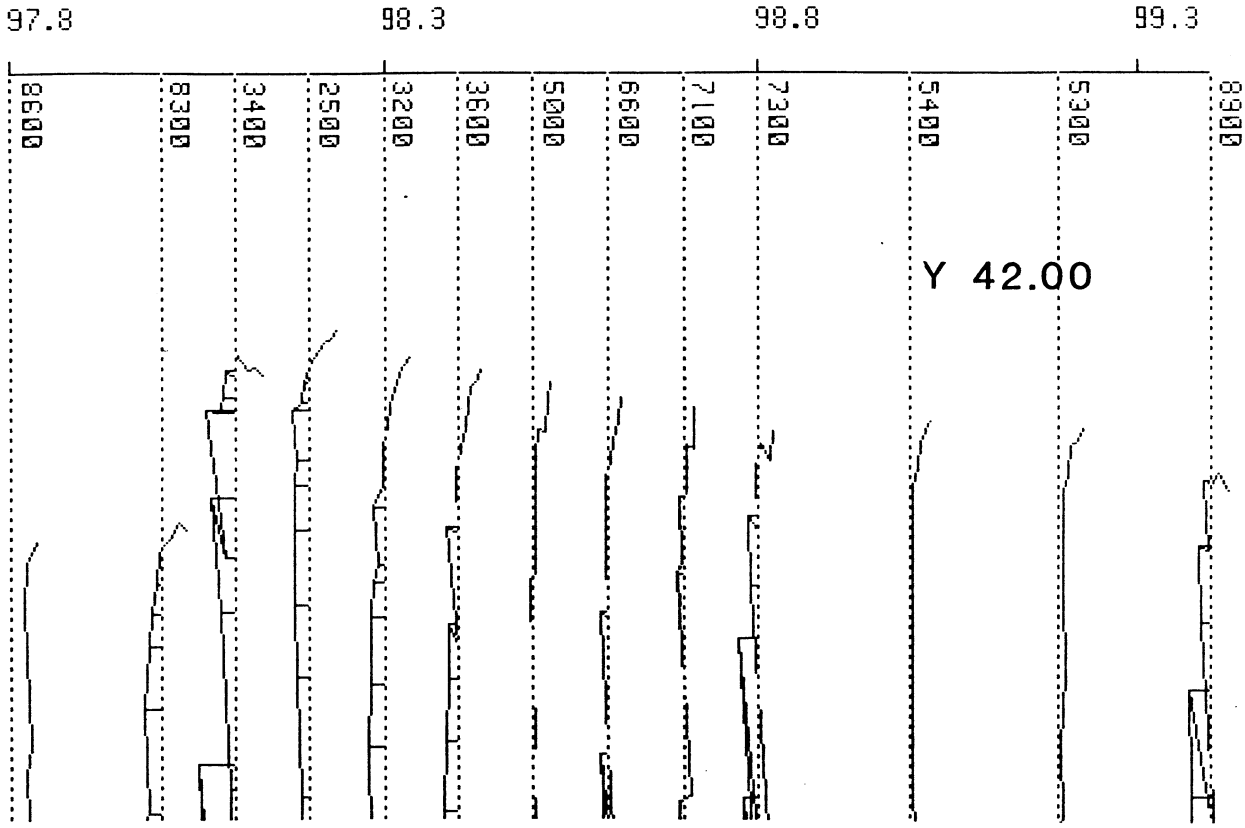

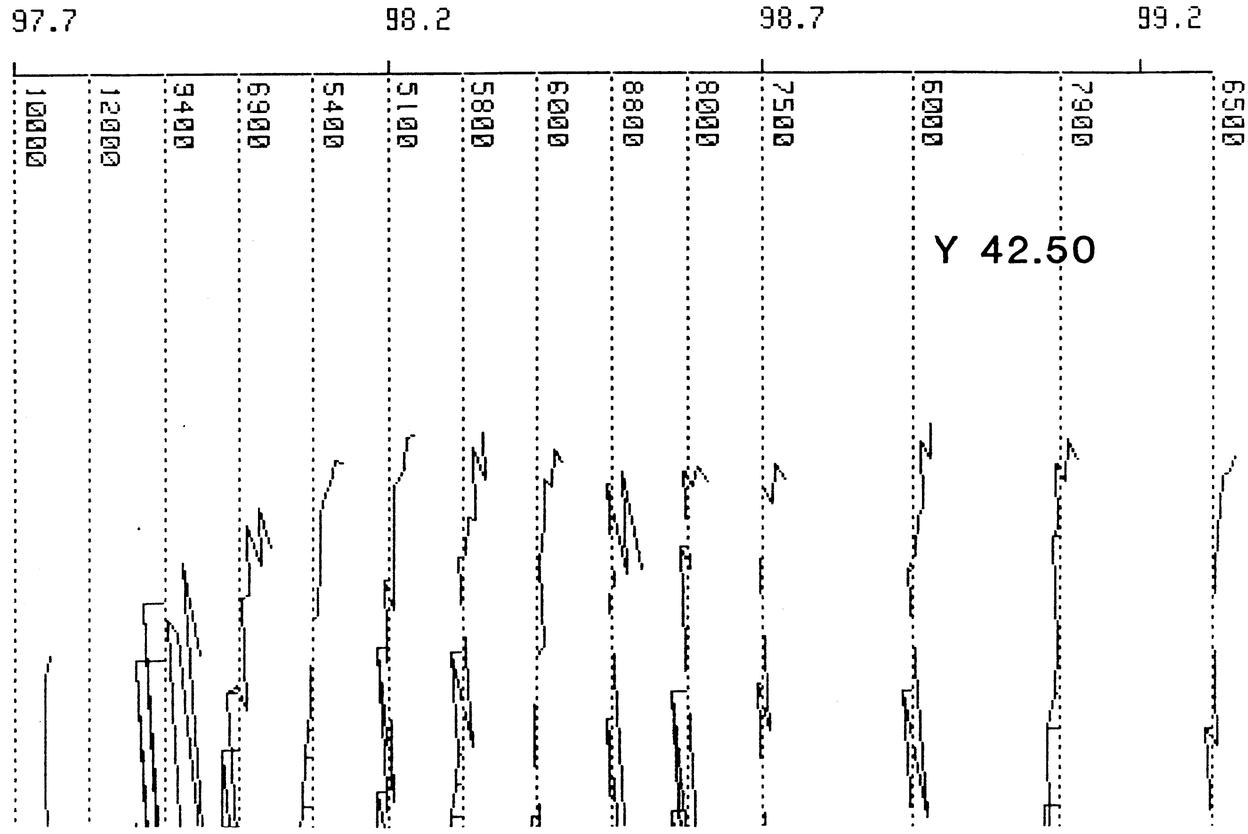

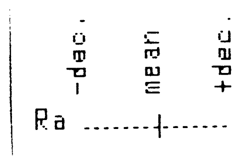

OUTOKUMPU OY Exploration	1:10 000	
		JL -85
LÖKKEN , Urvatnet		433
DIT-plots Y 42.00 Y 42.50	App. 11/11	

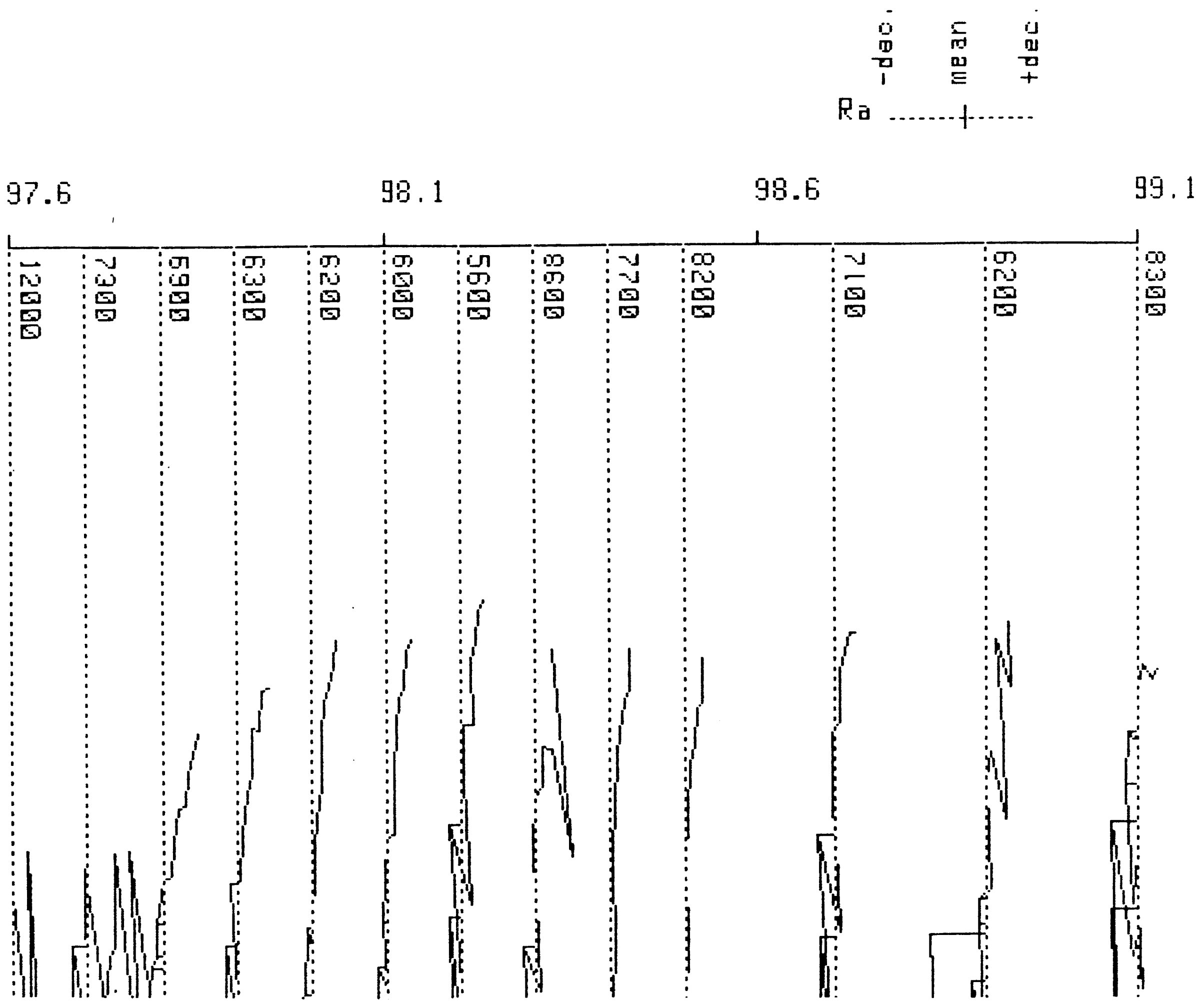

OUTOKUMPU OY Exploration	1:10000	
		JL -85
LÖKKEN , Urvatnet		433
DIT-plot Y 43.00	App. 11/12	

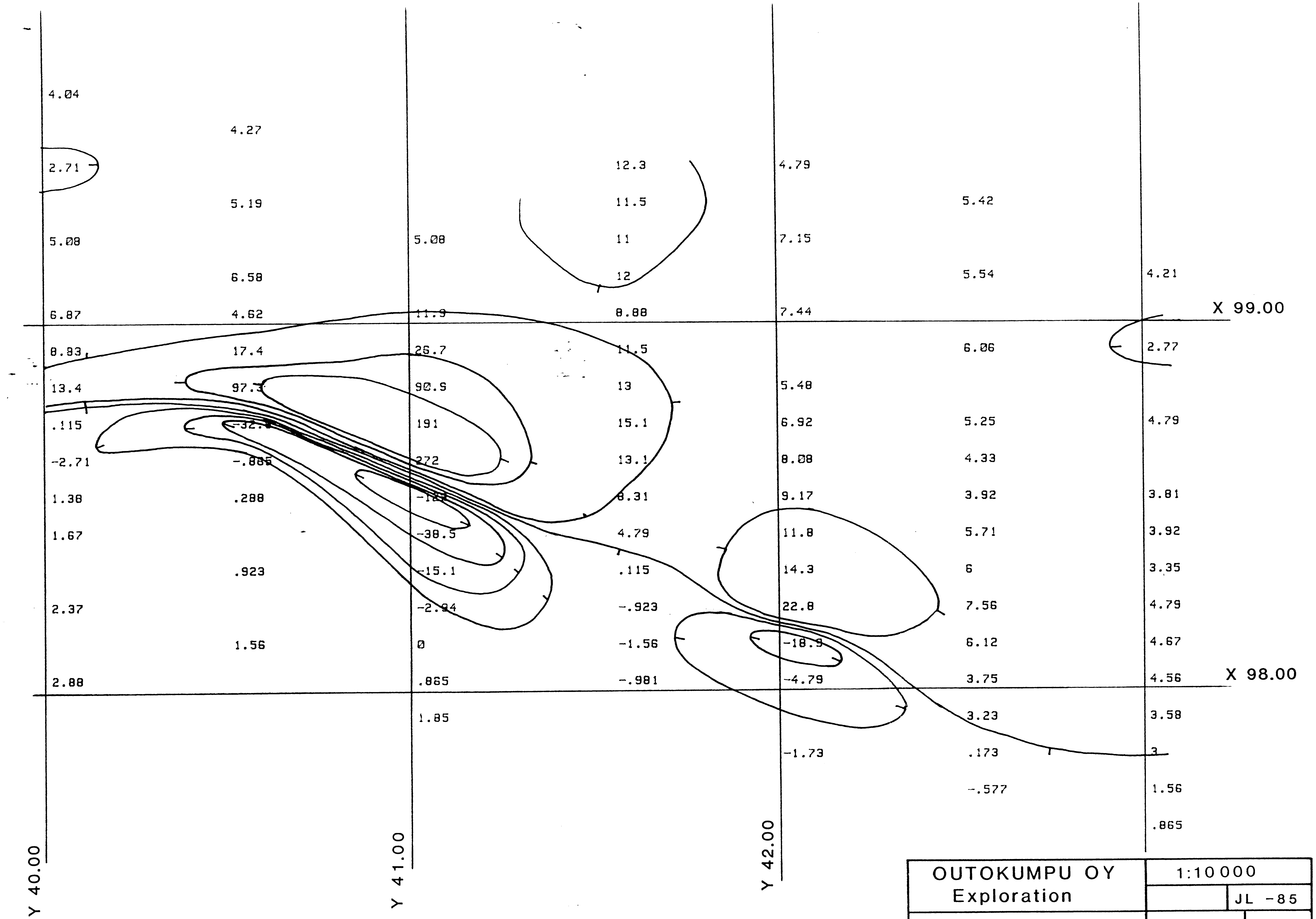

OUTOKUMPU OY Exploration	1:10 000	
		JL -85
LÖKKEN , Urvatnet		432
contoured map TDEM/Z-comp. channel no. 5 (.22ms)	App. 11/13	

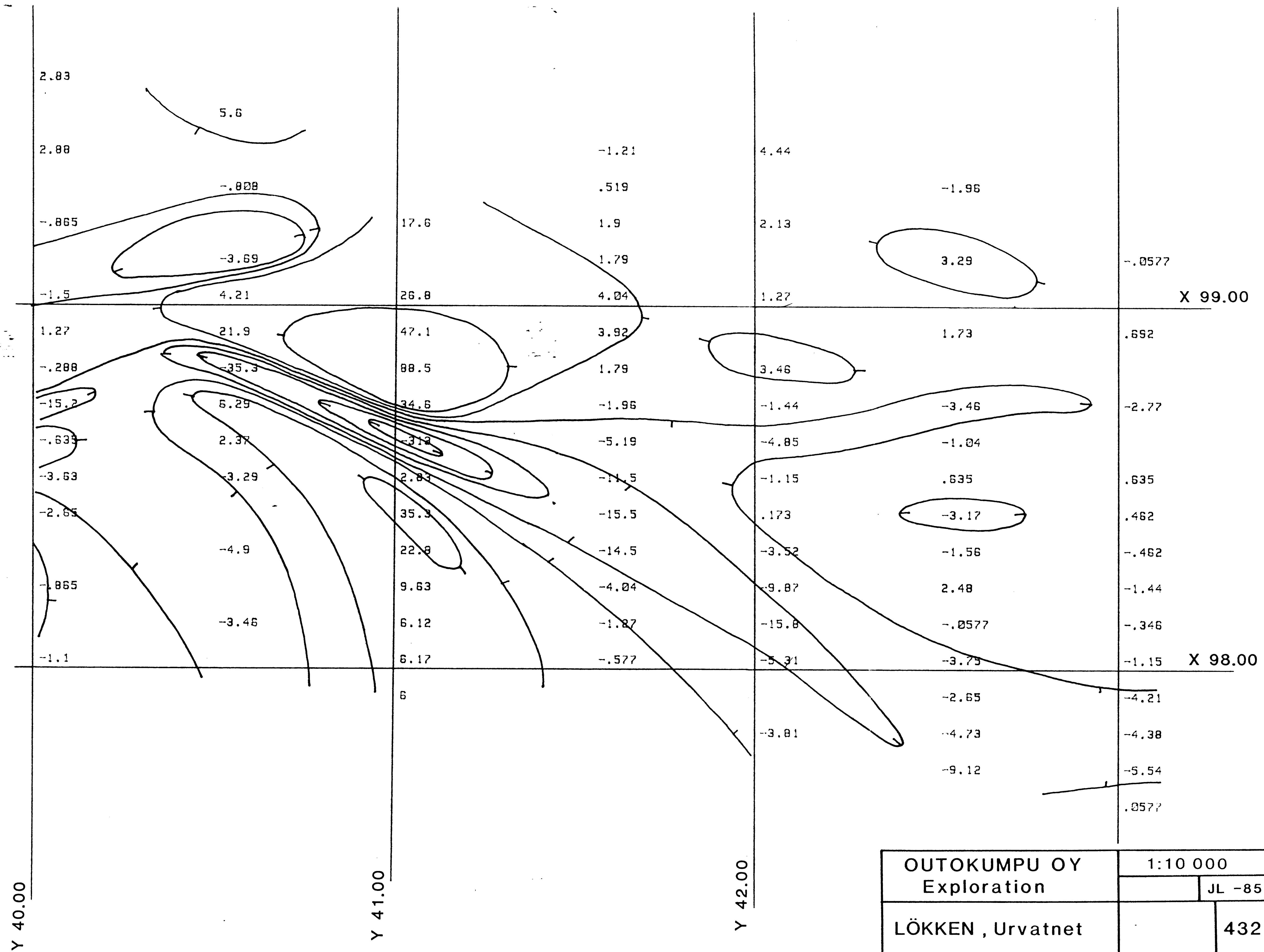

OUTOKUMPU OY Exploration	1:10 000	
		JL -85
LÖKKEN , Urvatnet		432
contoured map TDEM/X-comp. channel no. 5 (.22ms)	App. 11/14	

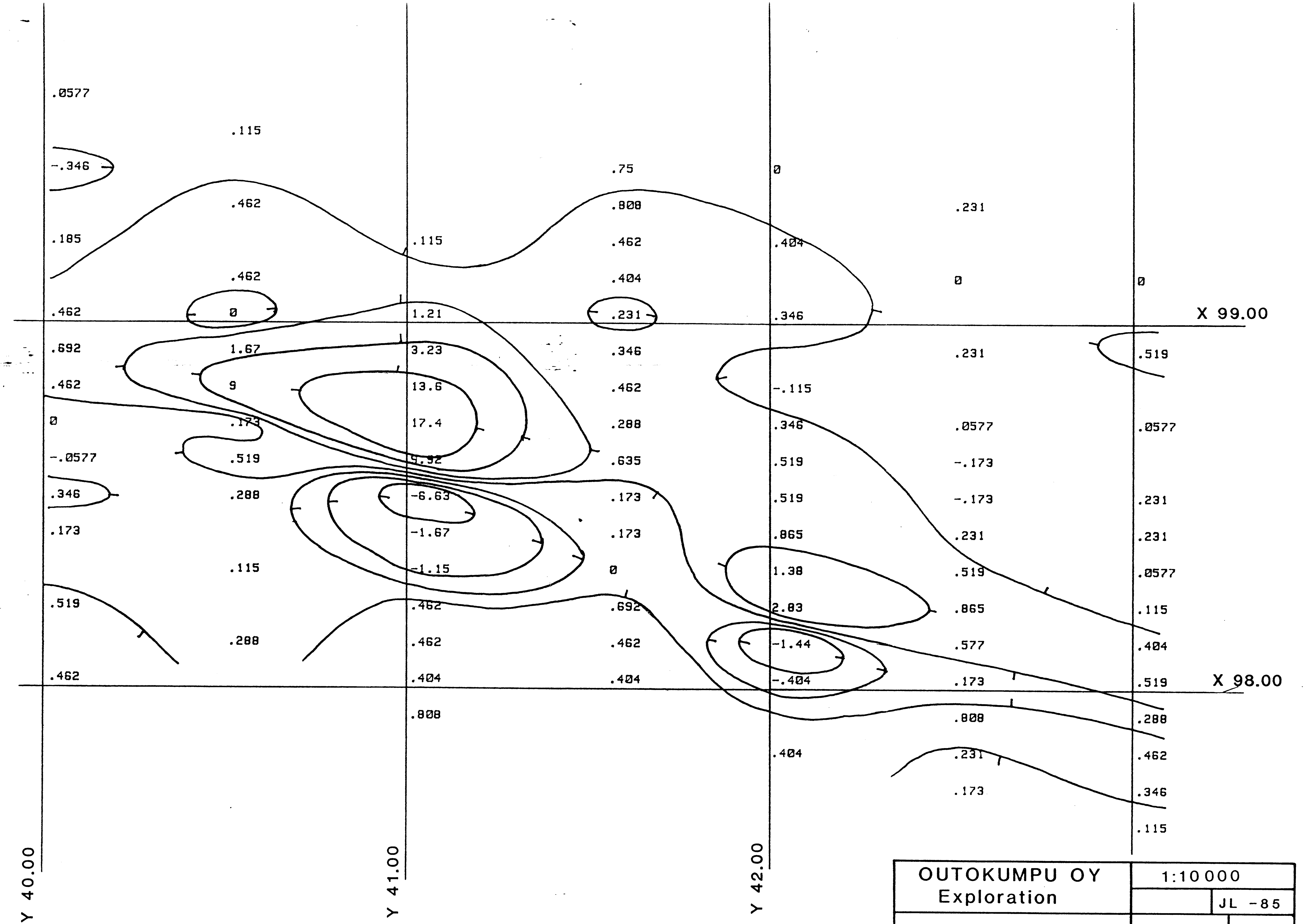

OUTOKUMPU OY Exploration	1:10000	
		JL -85
LÖKKEN , Urvatnet		432
contoured map TDEM/Z-comp. channel no. 10 (.71ms)	App. 11/15	

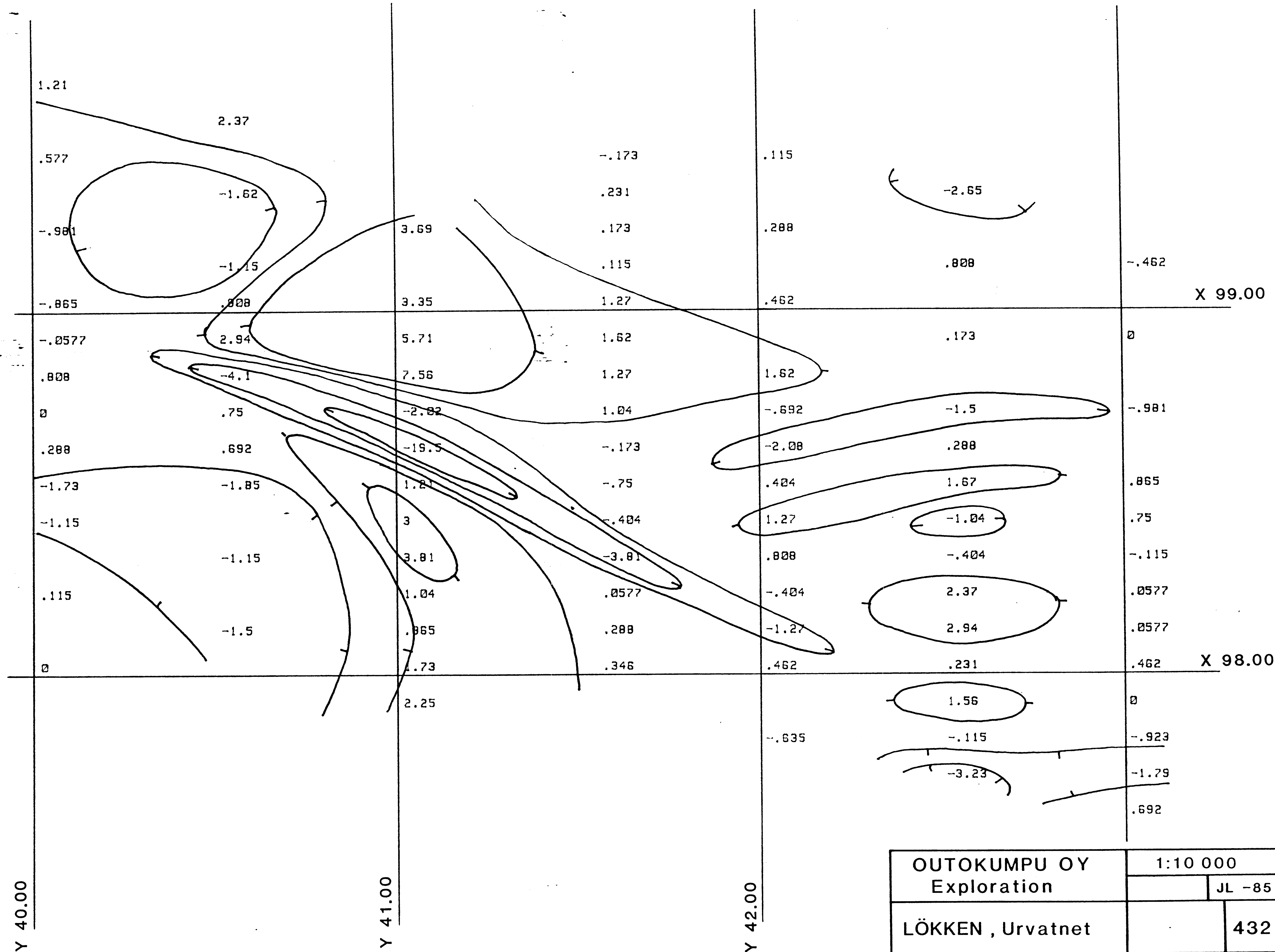

OUTOKUMPU OY Exploration	1:10 000	
		JL -85
LÖKKEN , Urvatnet		432
contoured map TDEM/X-comp. channel no. 10 (.71ms)	App. 11/16	

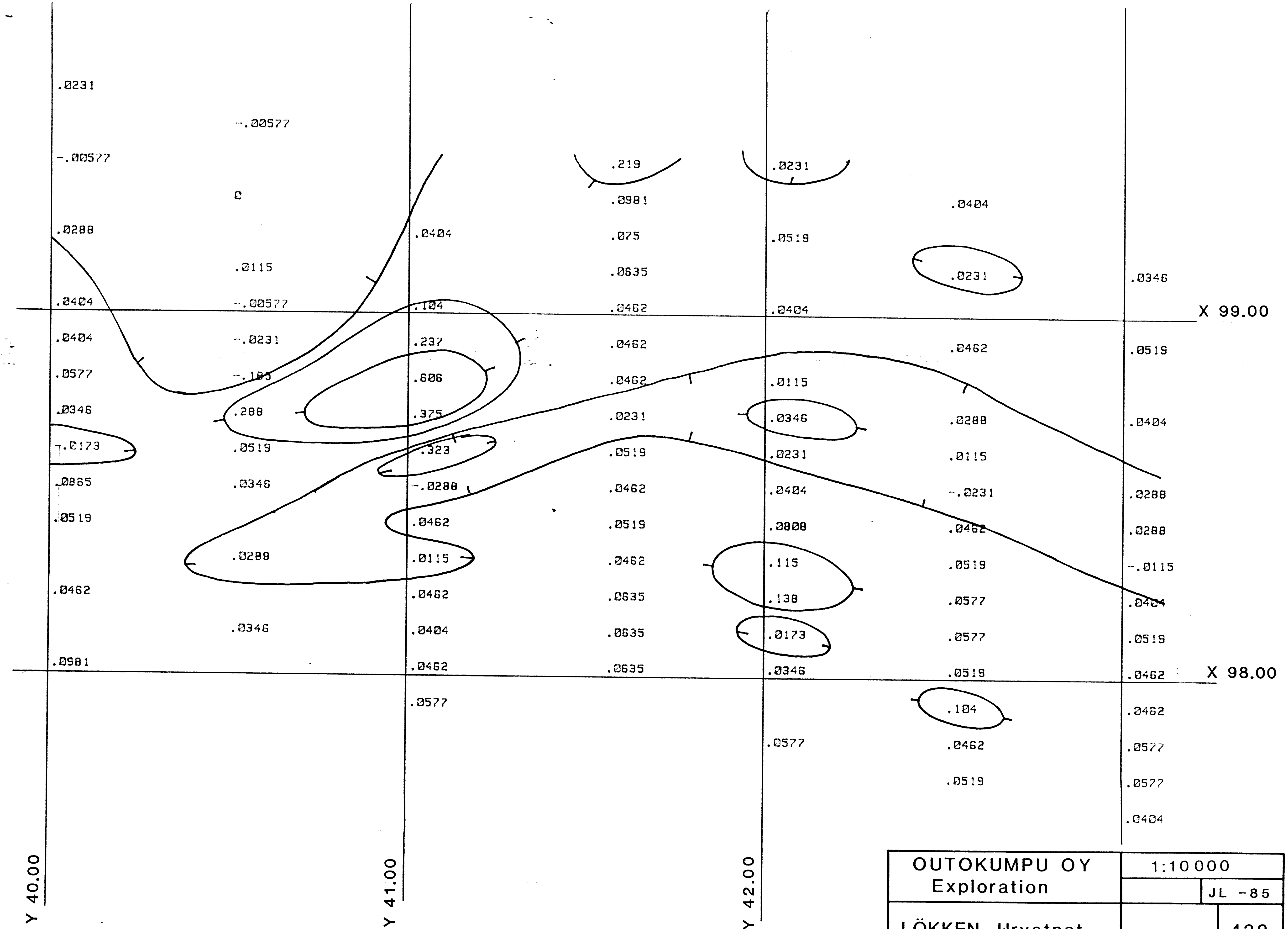

OUTOKUMPU OY Exploration	1:10000
	JL -85
LÖKKEN, Urvatnet	432
contoured map TDEM/Z-comp. channel no. 15 (2.22ms)	App. 11/17

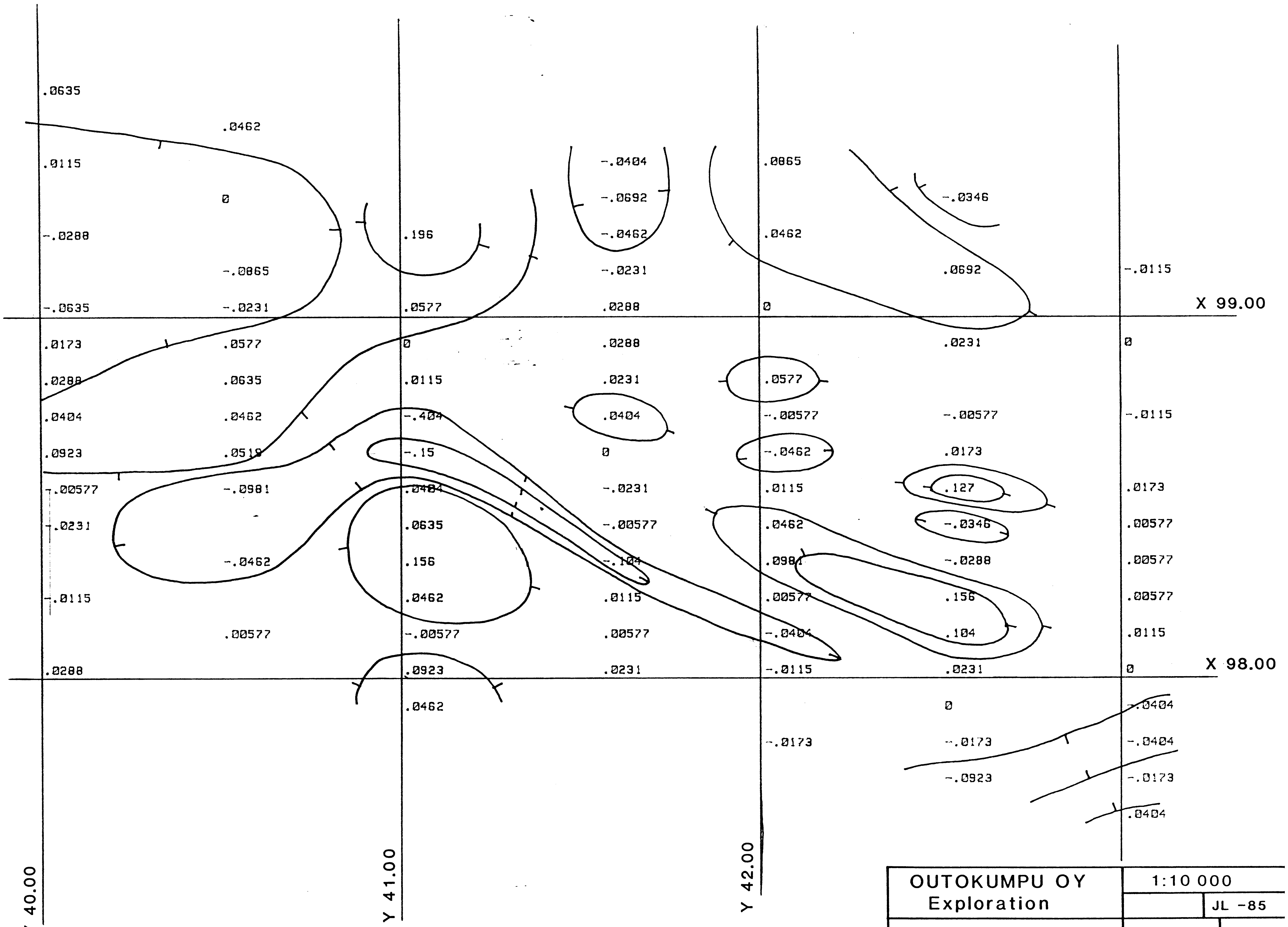

OUTOKUMPU OY Exploration	1:10 000	
		JL -85
LÖKKEN , Urvatnet		432
contoured map TDEM/X-comp. channel no. 15 (2.22ms)	App. 11/18	

12

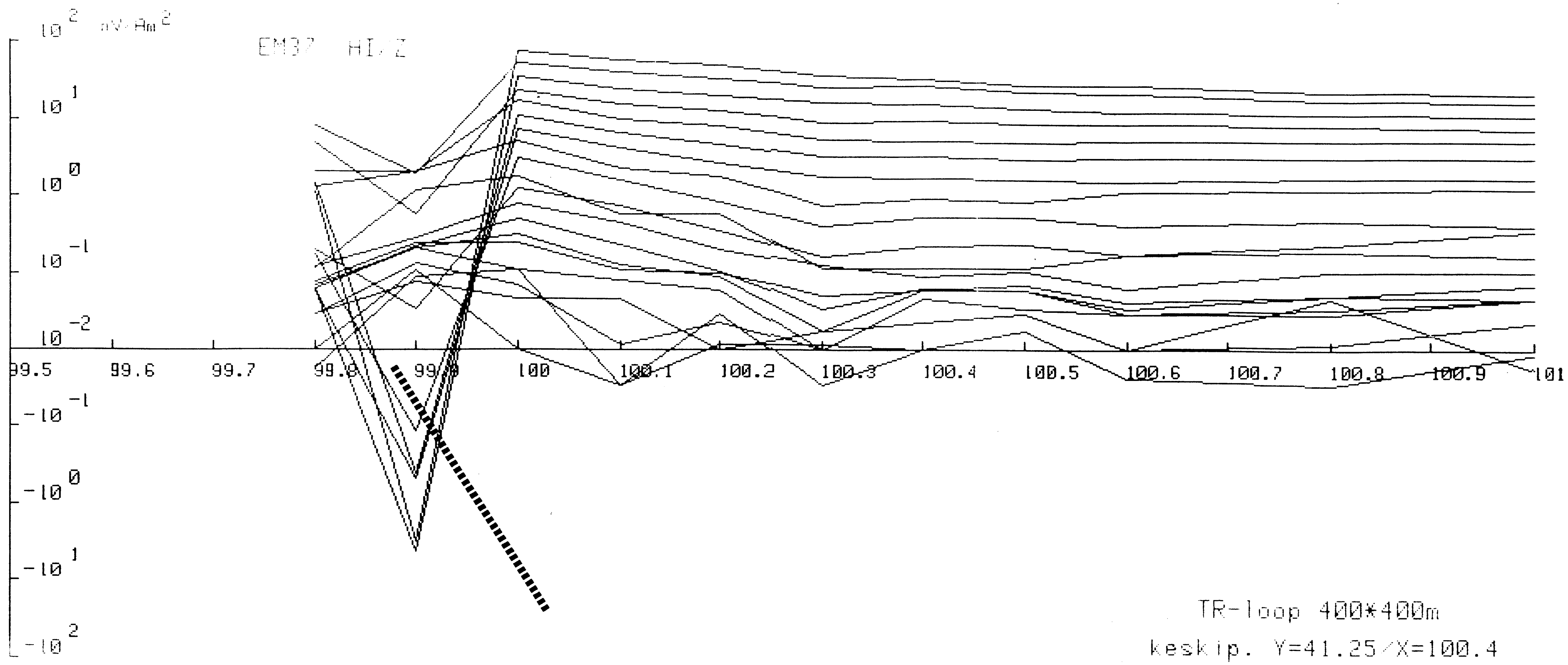

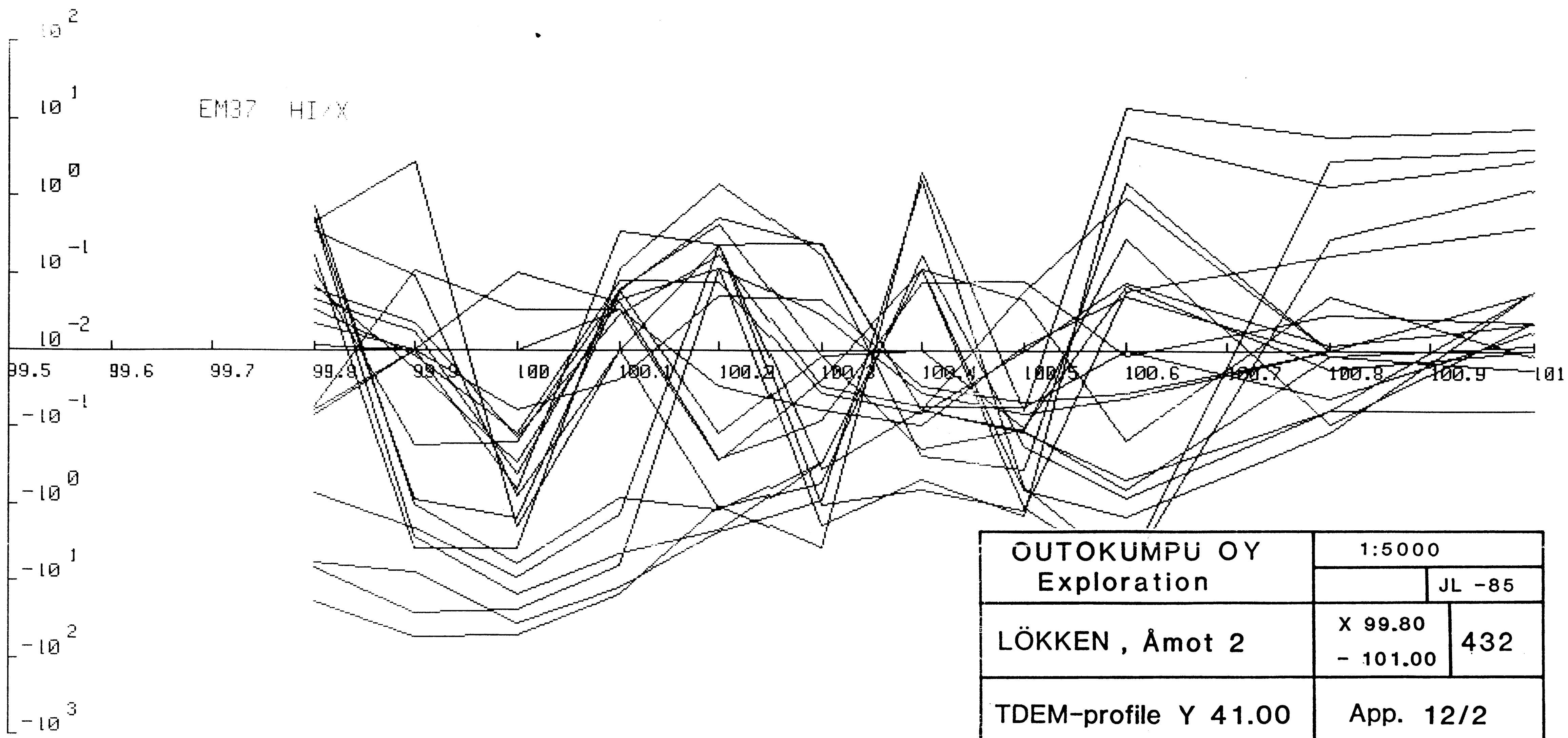

OUTOKUMPU OY Exploration	1:5000	JL -85
LÖKKEN , Åmot 2	X 99.80 - 101.00	432
TDEM-profile Y 41.00	App. 12/2	

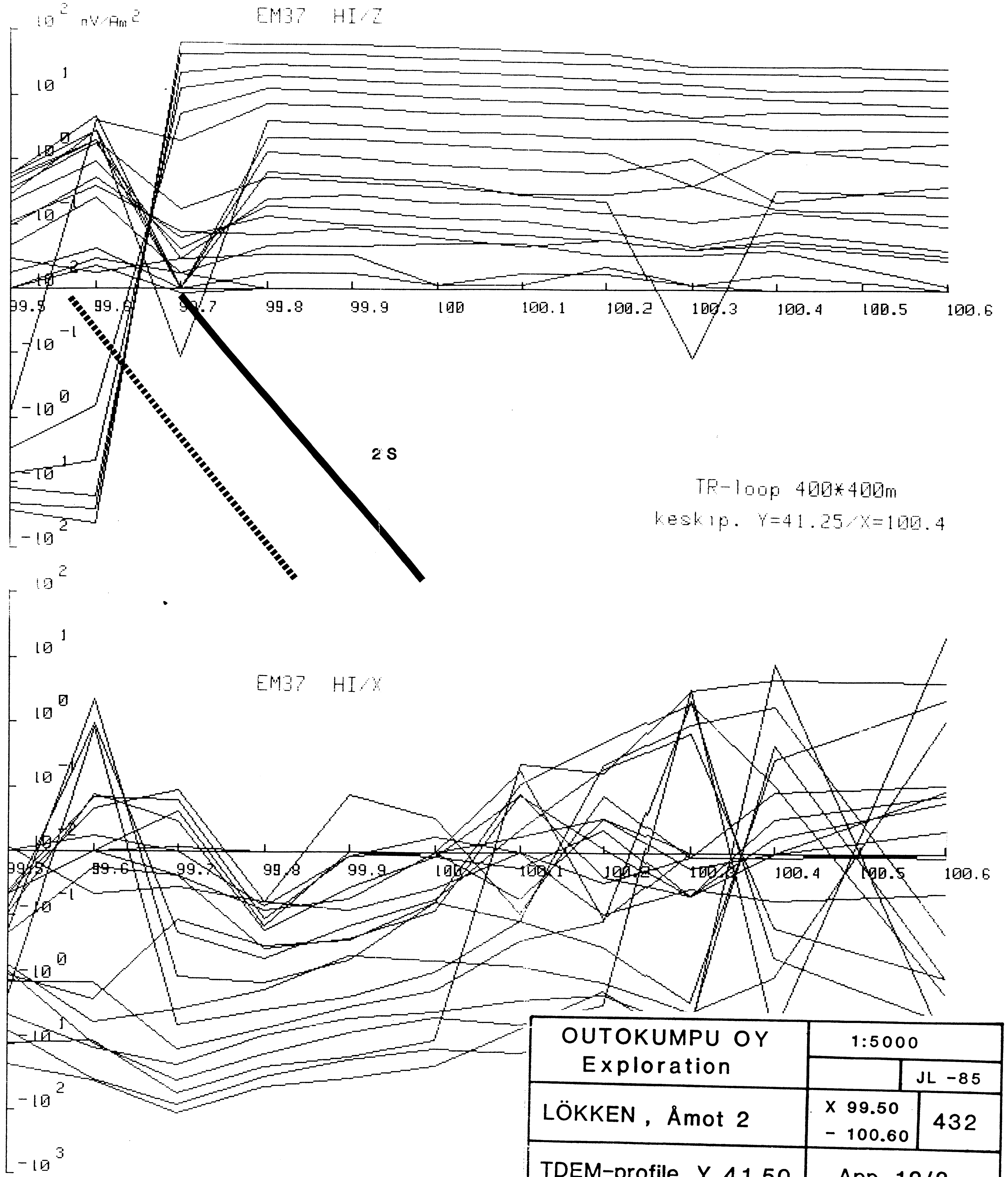

OUTOKUMPU OY Exploration	1:5000	
		JL -85
LÖKKEN , Åmot 2	X 99.50 - 100.60	432
TDEM-profile Y 41.50	App. 12/3	

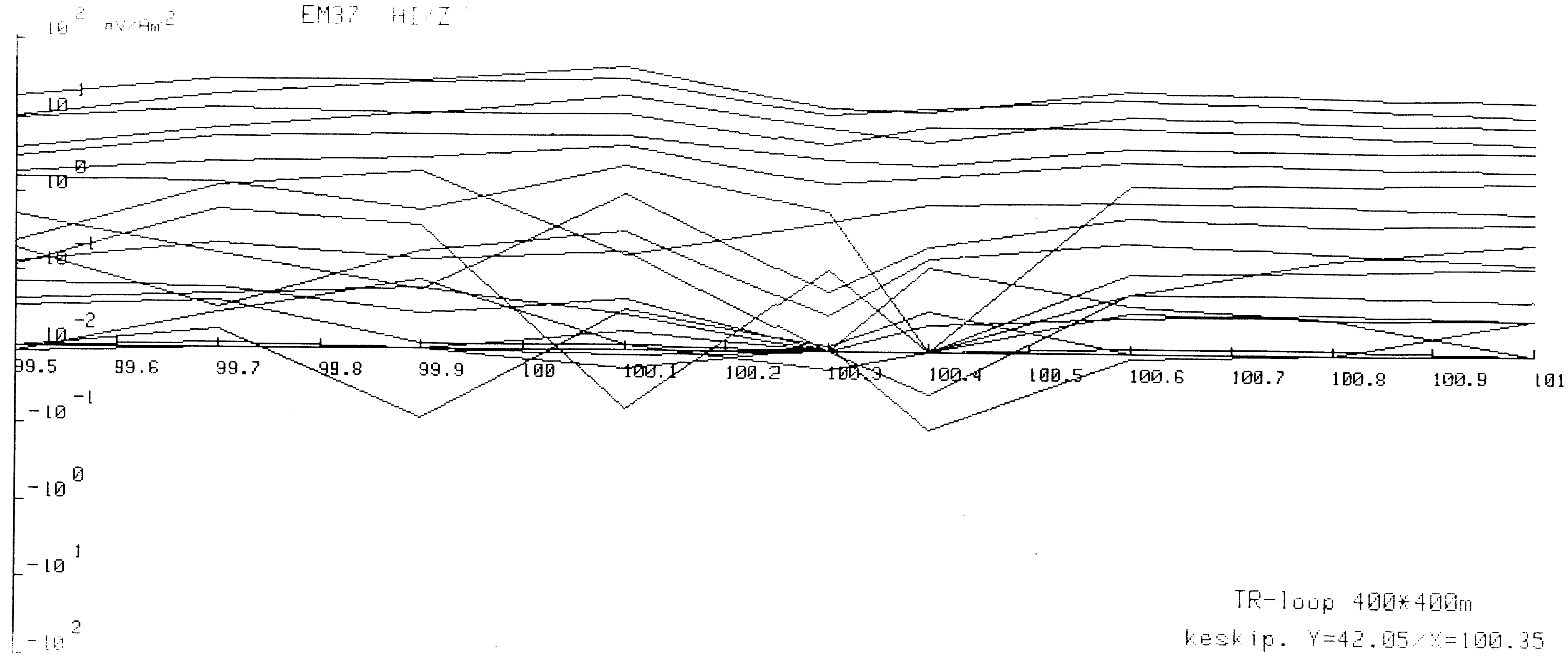

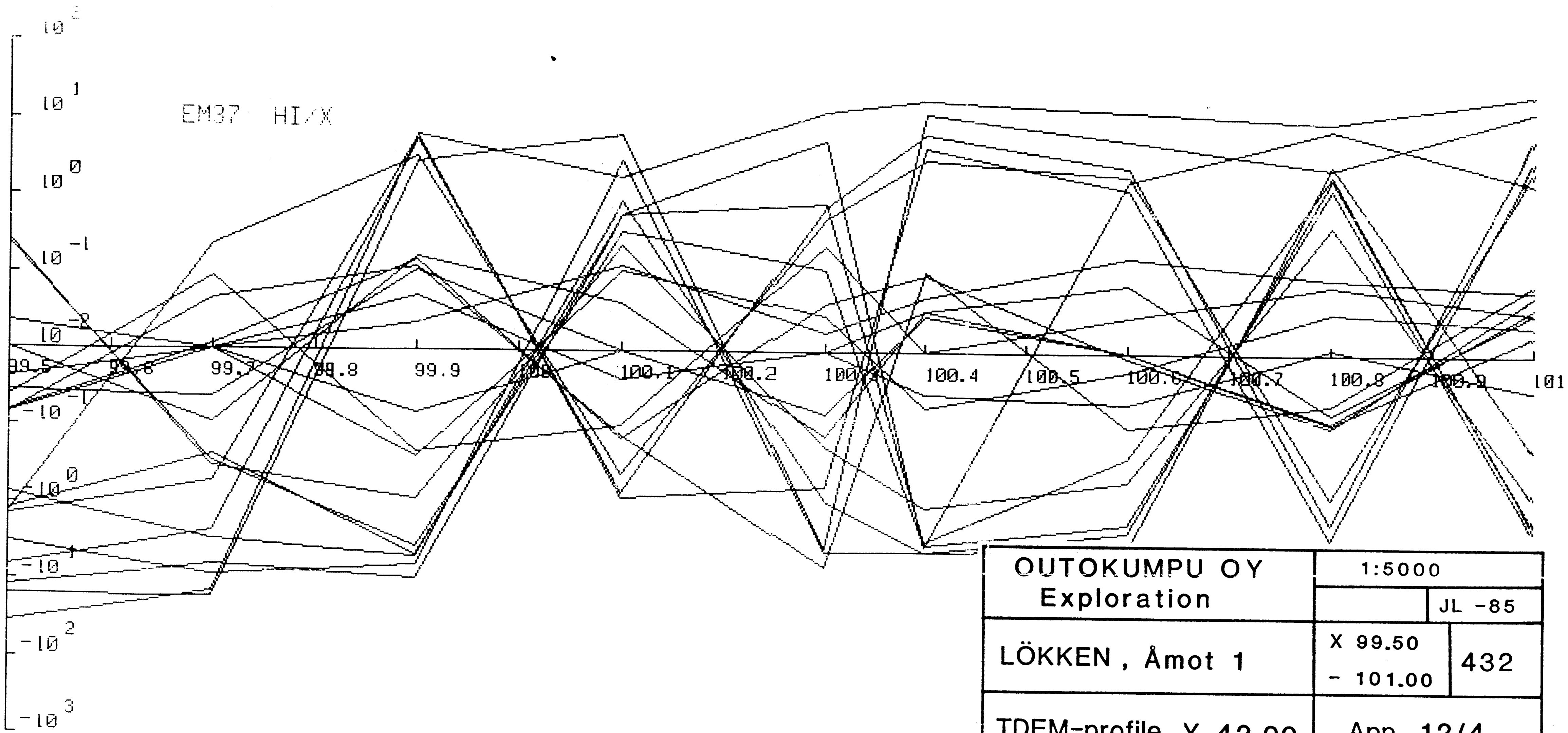

OUTOKUMPU OY Exploration	1:5000	
		JL -85
LÖKKEN , Åmot 1	X 99.50 - 101.00	432
TDEM-profile Y 42.00	App. 12/4	

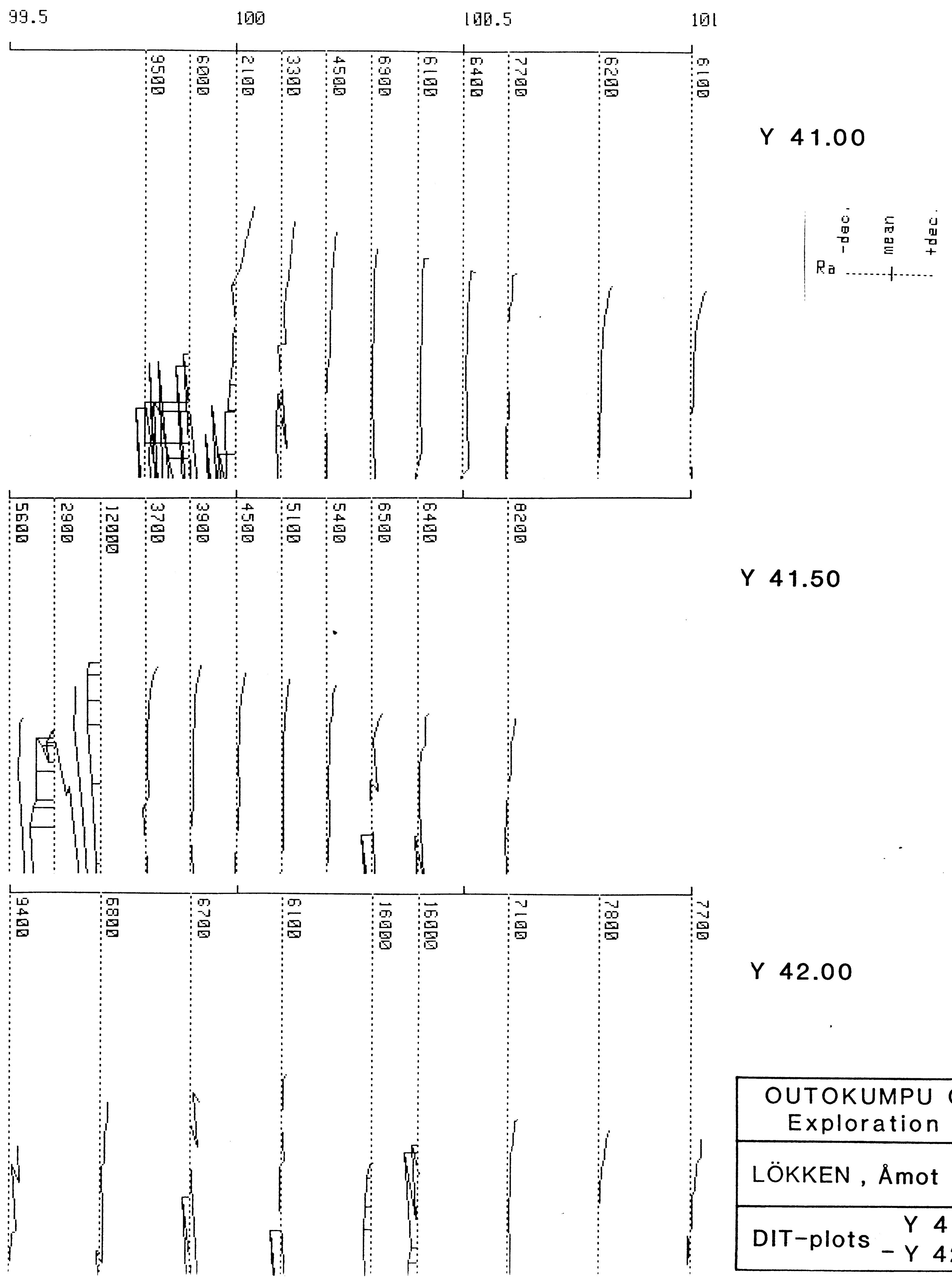

OUTOKUMPU OY Exploration	1:10 000	JL -85
LÖKKEN , Åmot		433
DIT-plots Y 41.00 – Y 42.00	App. 12/5	

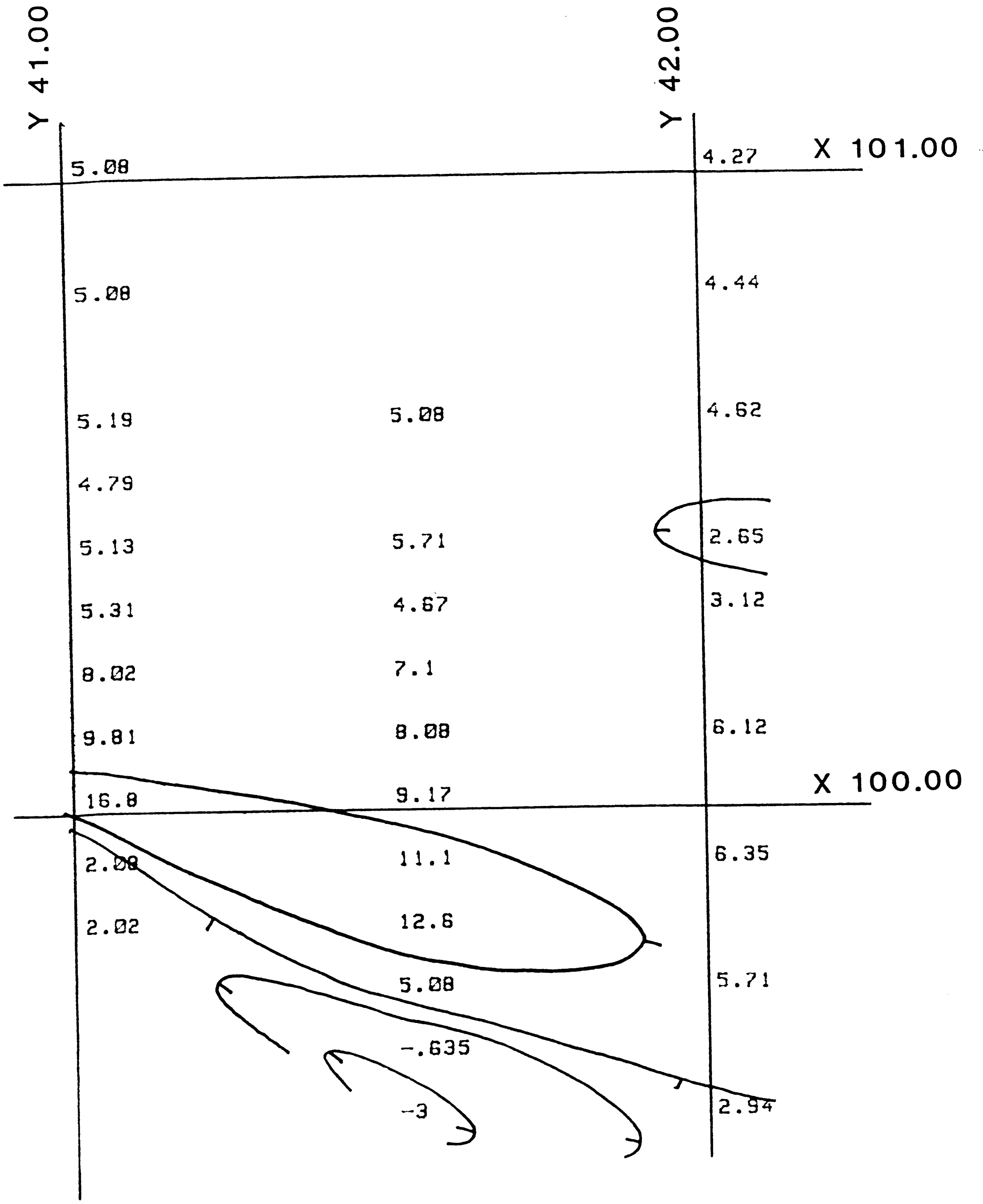

OUTOKUMPU OY Exploration	1:10 000	
		JL -85
LÖKKEN , Åmot		432
contoured map TDEM/Z-comp. channel no. 5 (.22ms)	App. 12/ 6	

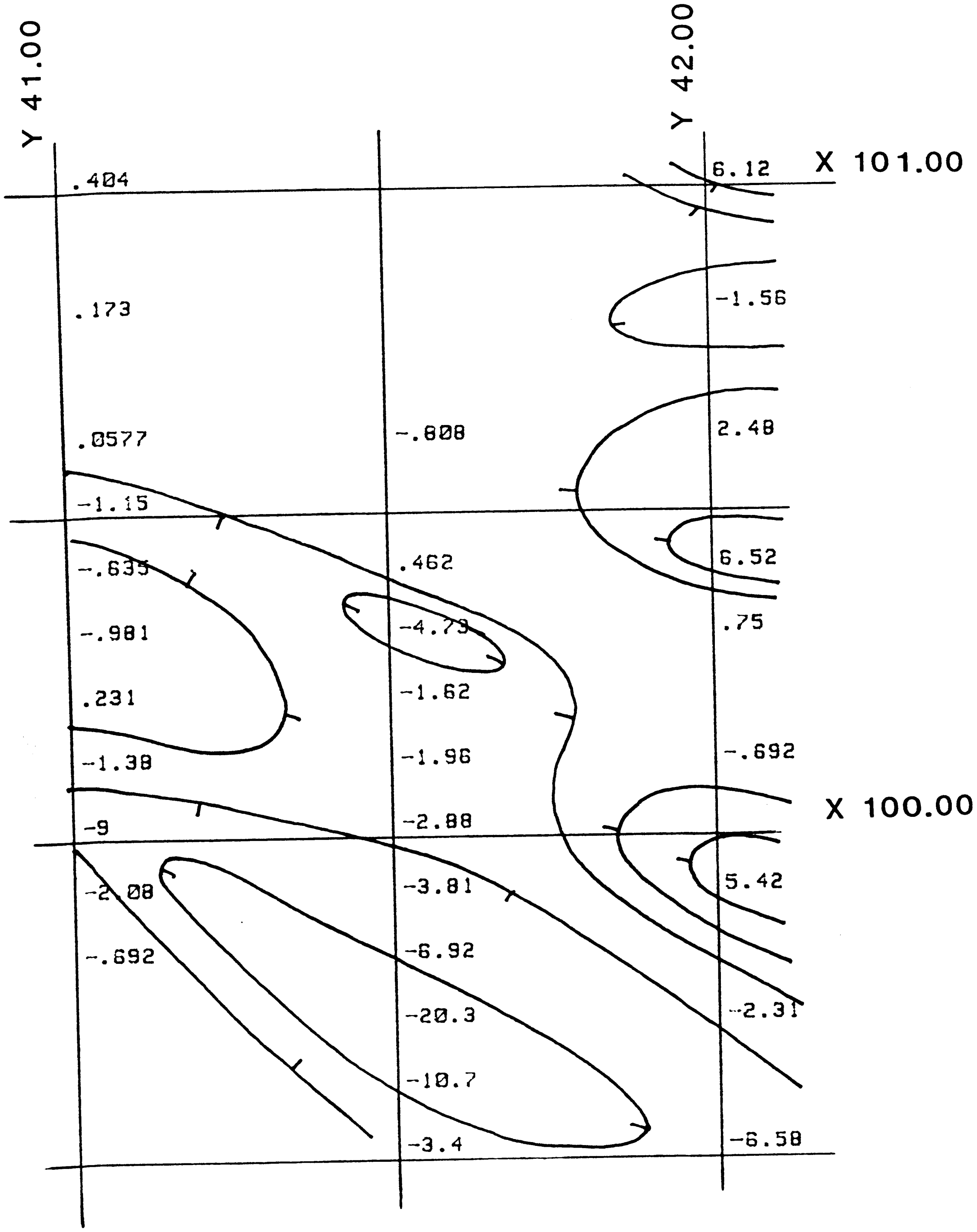

OUTOKUMPU OY Exploration	1:10 000	
		JL -85
LÖKKEN , Åmot		432
contoured map TDEM/X-comp. channel no. 5 (.22ms)	App. 12/ 7	

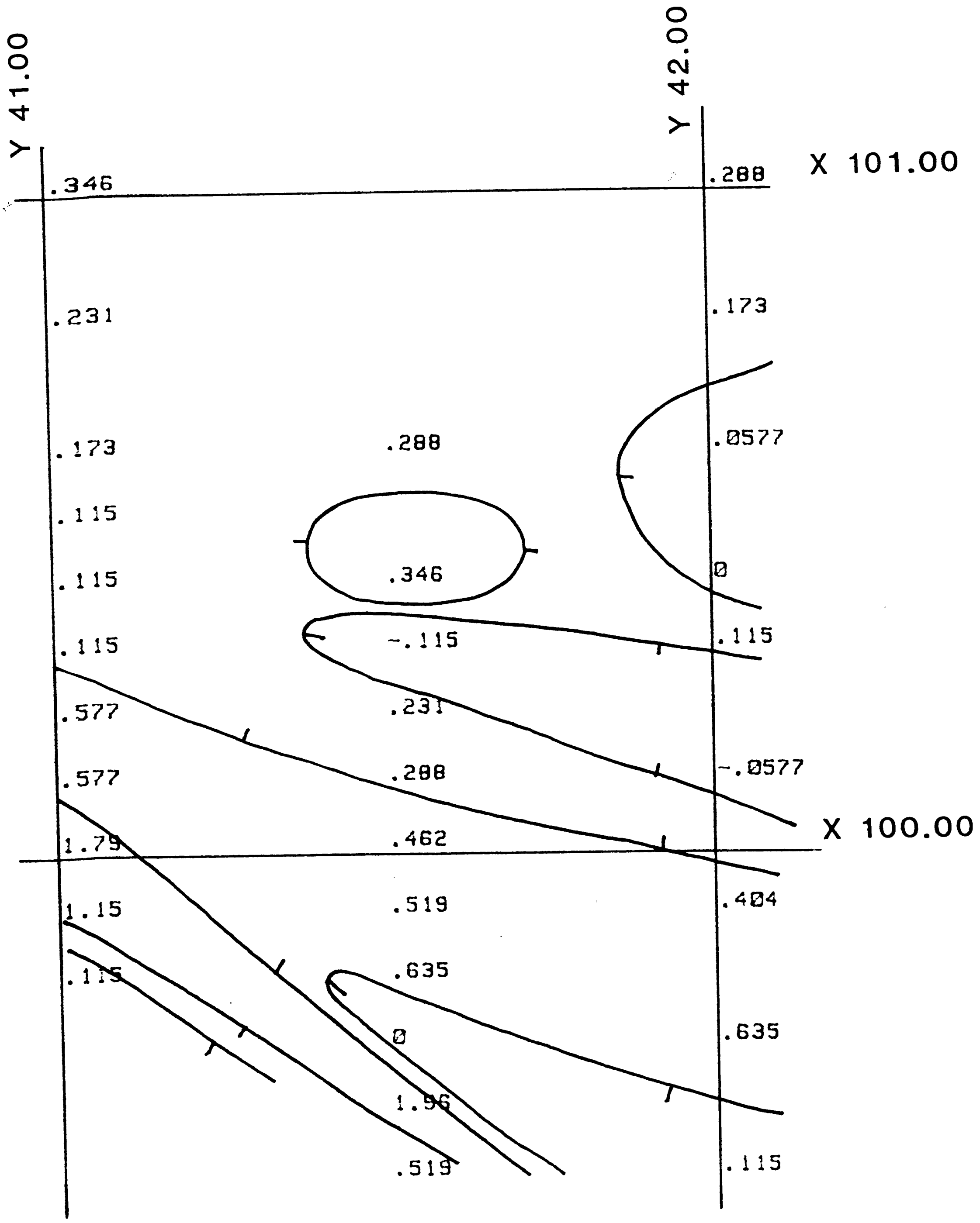

OUTOKUMPU OY Exploration	1:10 000	
		JL -85
LÖKKEN , Åmot		432
contoured map TDEM/Z-comp. channel no. 10 (.71ms)	App. 12/ 8	

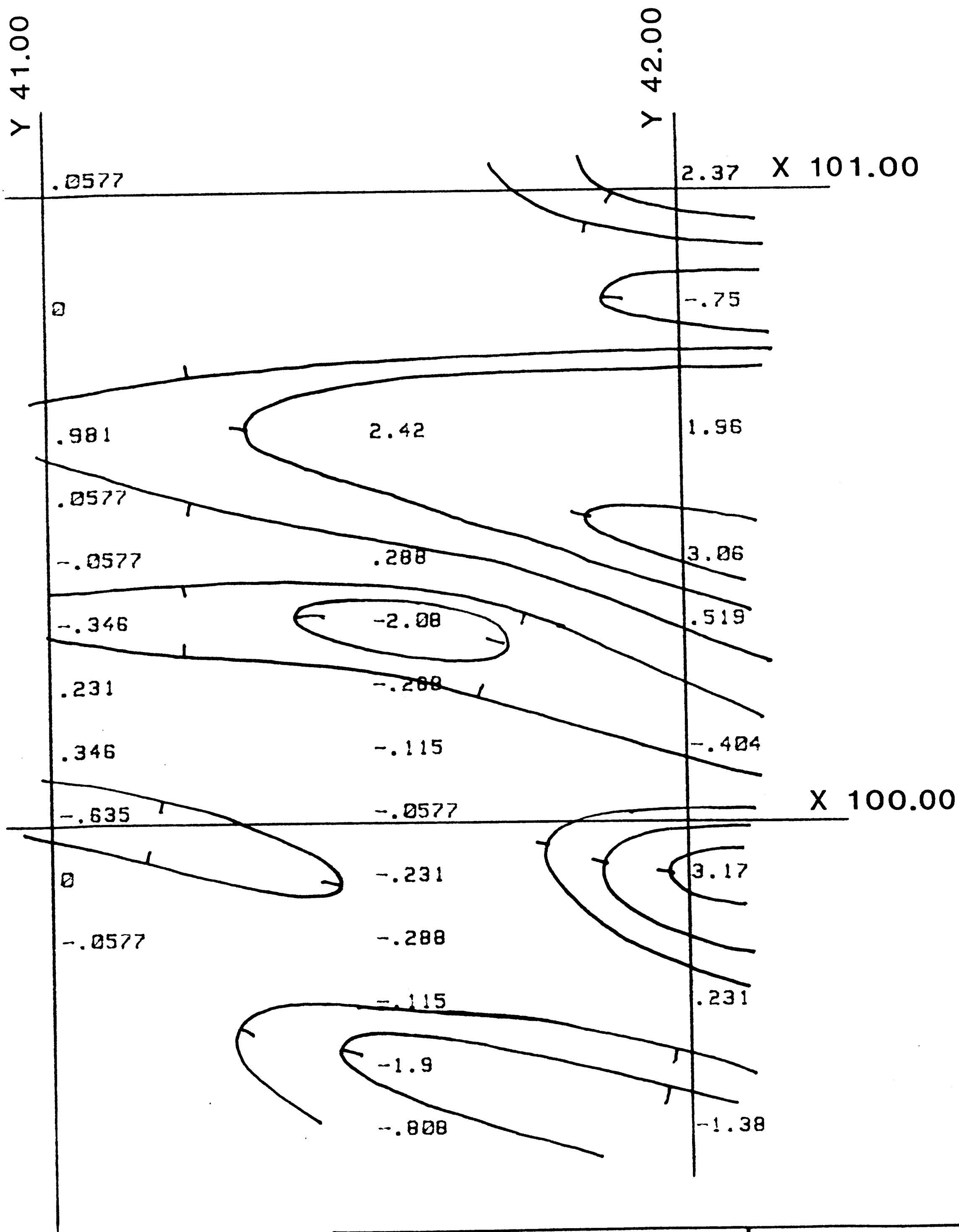

OUTOKUMPU OY Exploration	1:10 000	JL -85
LÖKKEN , Åmot		432
contoured map TDEM/X-comp. channel no. 10 (.71ms)	App. 12/ 9	

13

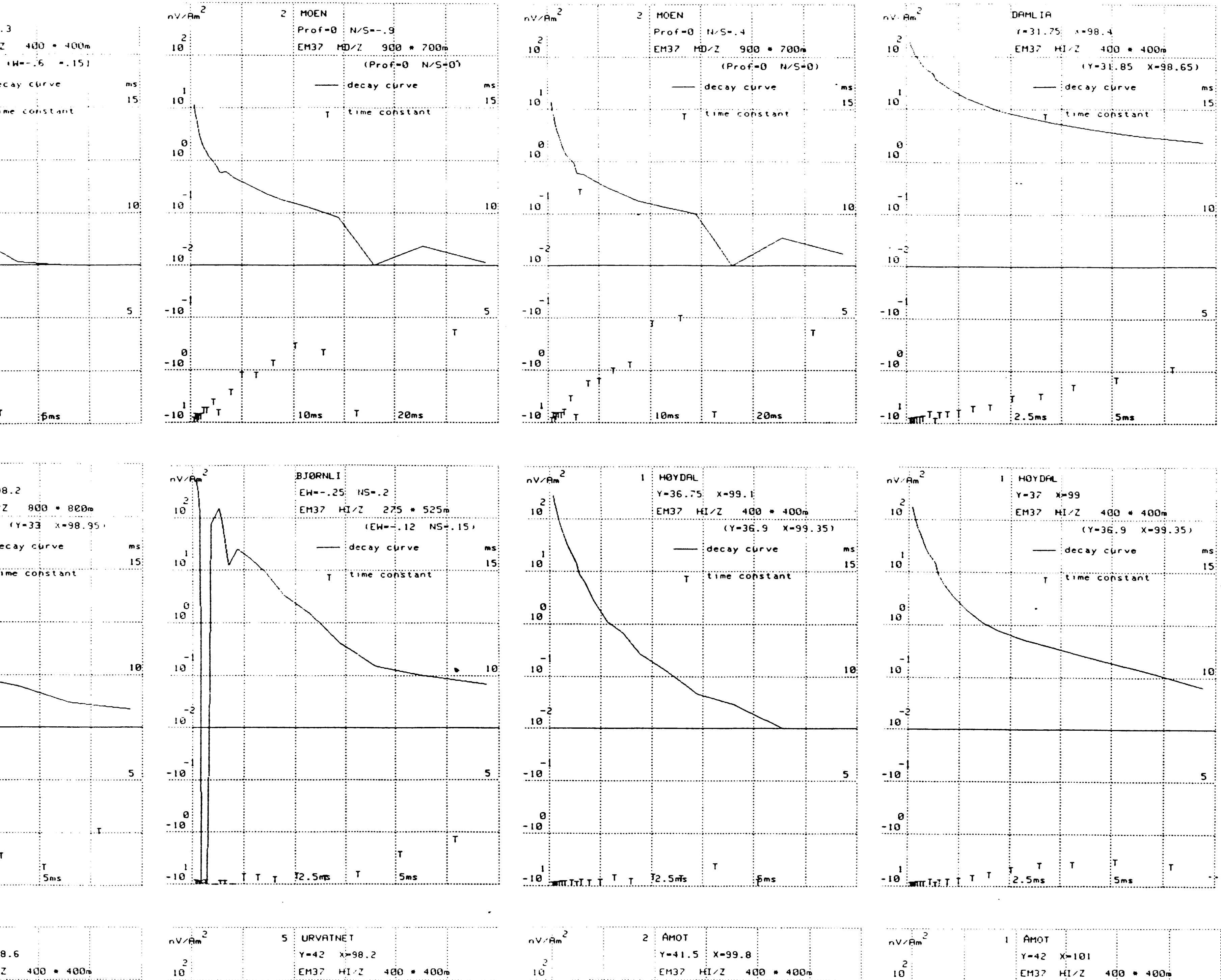
2 MOEN
Prof=0 N/S=-.9
EM37 MD/Z 900 * 700m
(Prof=0 N/S=0)
decay curve
time constant
2 MOEN
Prof=0 N/S=.4
EM37 MD/Z 900 * 700m
(Prof=0 N/S=0)
decay curve
time constant
DAMLIA
Y=31.75 X=98.4
EM37 HI/Z 400 * 400m
(Y=31.85 X=98.65)
decay curve
time constant
BJØRNLI
EW=-.25 NS=.2
EM37 HI/Z 275 * 525m
(EW=-.12 NS=.15)
decay curve
time constant
1 HØYDAL
Y=36.75 X=99.1
EM37 HI/Z 400 * 400m
(Y=36.9 X=99.35)
decay curve
time constant
1 HØYDAL
Y=37 X=99
EM37 HI/Z 400 * 400m
(Y=36.9 X=99.35)
decay curve
time constant
5 URVATNET
Y=42 X=98.2
EM37 HI/Z 400 * 400m
2 ÅMOT
Y=41.5 X=99.8
EM37 HI/Z 400 * 400m
1 ÅMOT
Y=42 X=101
EM37 HI/Z 400 * 400m
nV/Am²

JL -85

App. 13/1

/BJØRNLI/Line EW=-.25 Z and X-Comp.

415/432 1:10000 Date 18.03.1986 nV/Am^2

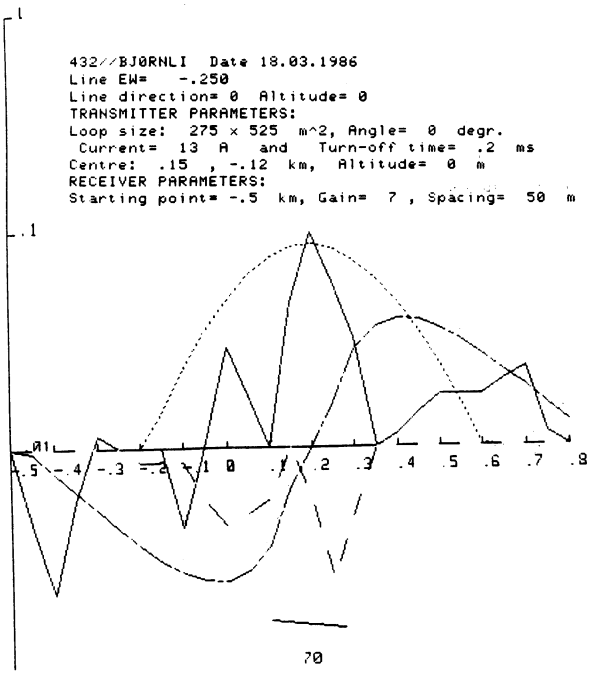

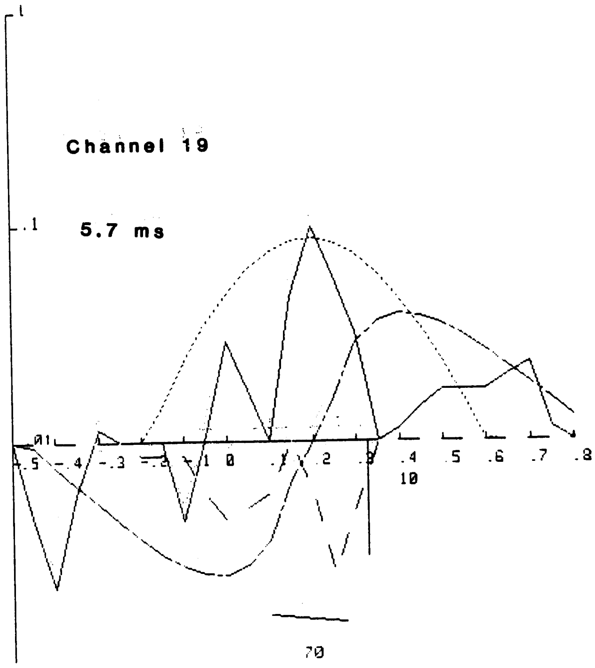

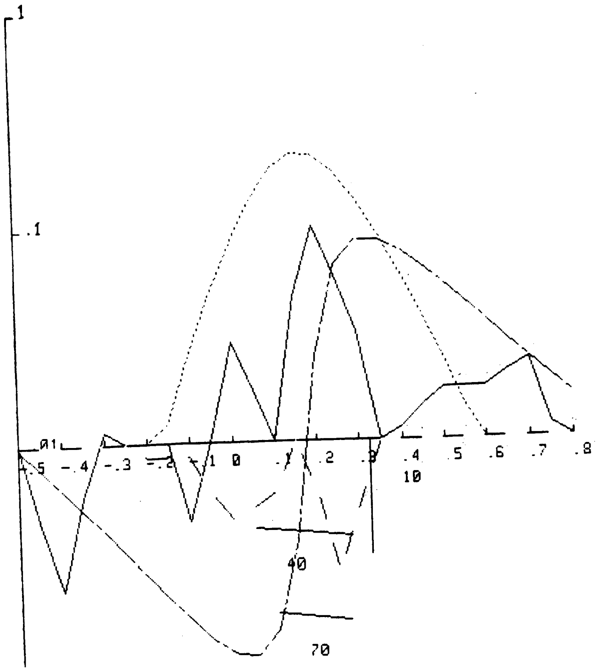

INTERPRETED PARAMETERS OF MODEL NO. 1

CONDUCTANCE= 70.000 S, LOCATION= 100.00 m
DEPTH=400.0, LENGTH= 600 and HEIGHT= 15 m
y-COORD. OF CENTRE= 0.0 m
DIP= 5.0 STRIKE= 0.0 (0 means perpendicular to line) and
PLUNGE= 0.0 degrees

INTERPRETED PARAMETERS OF MODEL NO. 2

CONDUCTANCE= 10.000 S, LOCATION= 325.00 m
DEPTH= 4.0, LENGTH= 500 and HEIGHT= 260 m
y-COORD. OF CENTRE= 0.0 m
DIP= 90.0 STRIKE= 0.0 (0 means perpendicular to line) and
PLUNGE= 0.0 degrees

INTERPRETED PARAMETERS OF MODEL NO. 3

CONDUCTANCE= 40.000 S, LOCATION= 50.00 m
DEPTH=200.0, LENGTH= 200 and HEIGHT= 20 m
y-COORD. OF CENTRE= 0.0 m
DIP= 5.0 STRIKE= 0.0 (0 means perpendicular to line) and
PLUNGE= 0.0 degrees

/MOEN/Line Prof=0 Z and X-Comp.

415/432 1:10000 Date 18.03.1986 nV/Am^2

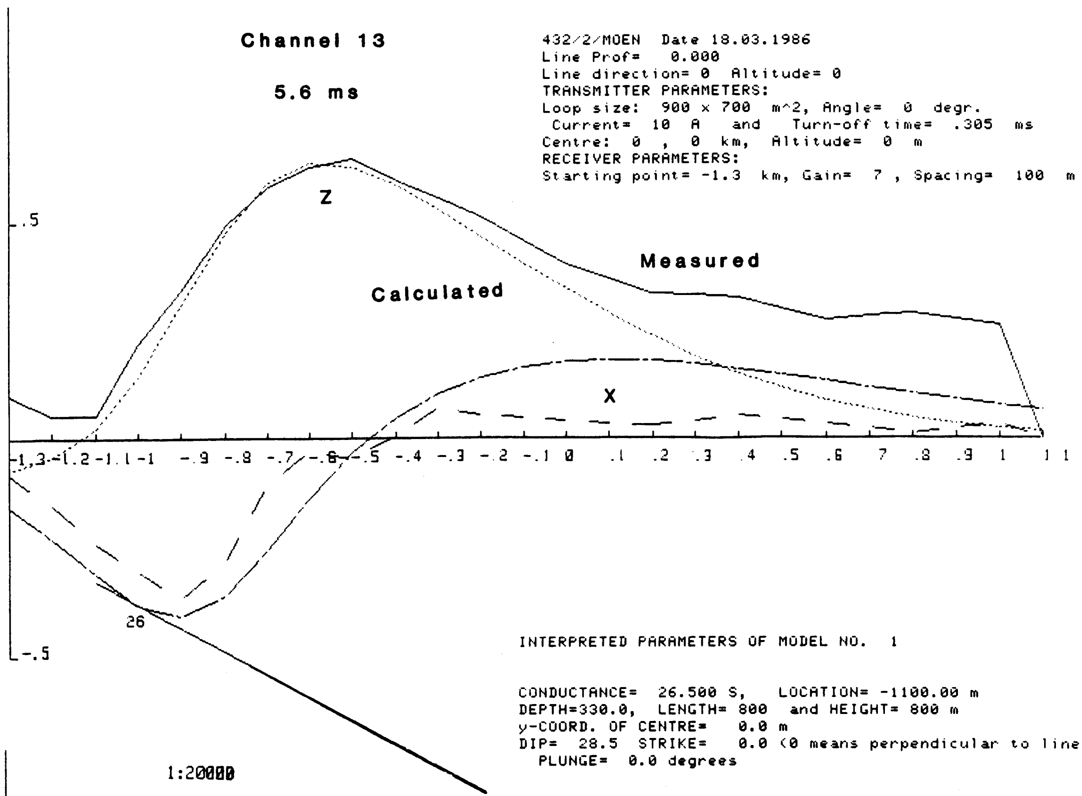

INTERPRETED PARAMETERS OF MODEL NO. 1

CONDUCTANCE= 26.500 S, LOCATION= -1100.00 m
DEPTH=330.0, LENGTH= 800 and HEIGHT= 800 m
y-COORD. OF CENTRE= 0.0 m
DIP= 28.5 STRIKE= 0.0 (0 means perpendicular to line) and
PLUNGE= 0.0 degrees

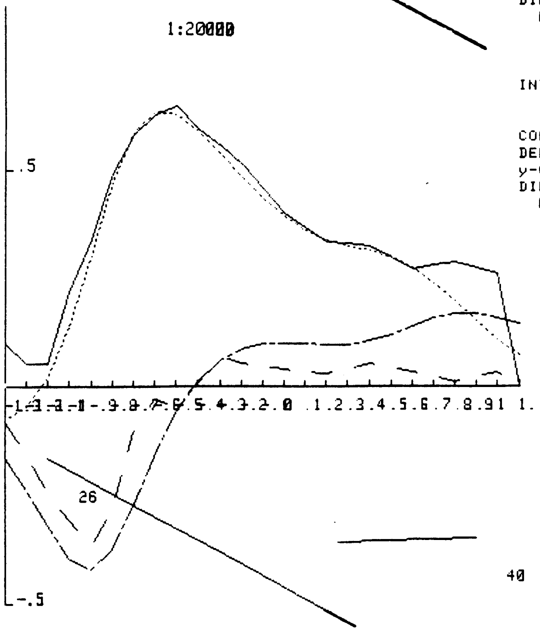

INTERPRETED PARAMETERS OF MODEL NO. 2

CONDUCTANCE= 40.000 S, LOCATION= 900.00 m
DEPTH=700.0, LENGTH= 800 and HEIGHT= 18 m
y-COORD. OF CENTRE= 0.0 m
DIP= 178.4 STRIKE= 0.0 (0 means perpendicular to line) and
PLUNGE= 0.0 degrees

HOGASEN/Line Y=32.5 Z and X-Comp.

#15/432 1:10000 Date 18.03.1986 nV/Am^2

432//HØGÅSEN Date 18.03.1986
Line Y= 32.500
Line direction= 0 Altitude= 0
TRANSMITTER PARAMETERS:
Loop size: 800 x 800 m^2, Angle= 0 degr.
Current= 10 A. and Turn-off time= .295 ms
Centre: 98.95 , 33 km, Altitude= 0 m
RECEIVER PARAMETERS:
Starting point= 98 km, Gain= 7 , Spacing= 100 m

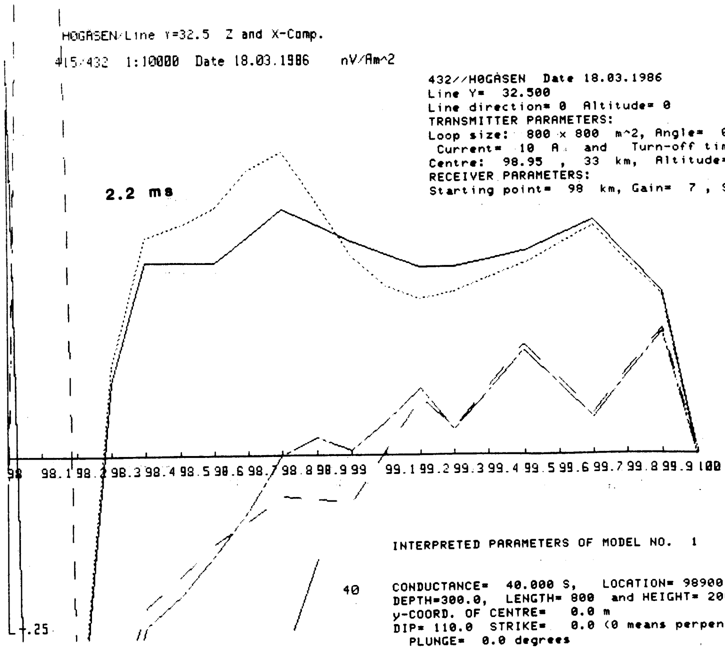

INTERPRETED PARAMETERS OF MODEL NO. 1

CONDUCTANCE= 40.000 S, LOCATION= 98900.00 m
DEPTH=300.0, LENGTH= 800 and HEIGHT= 200 m
y-COORD. OF CENTRE= 0.0 m
DIP= 110.0 STRIKE= 0.0 (0 means perpendicular to line) and
PLUNGE= 0.0 degrees

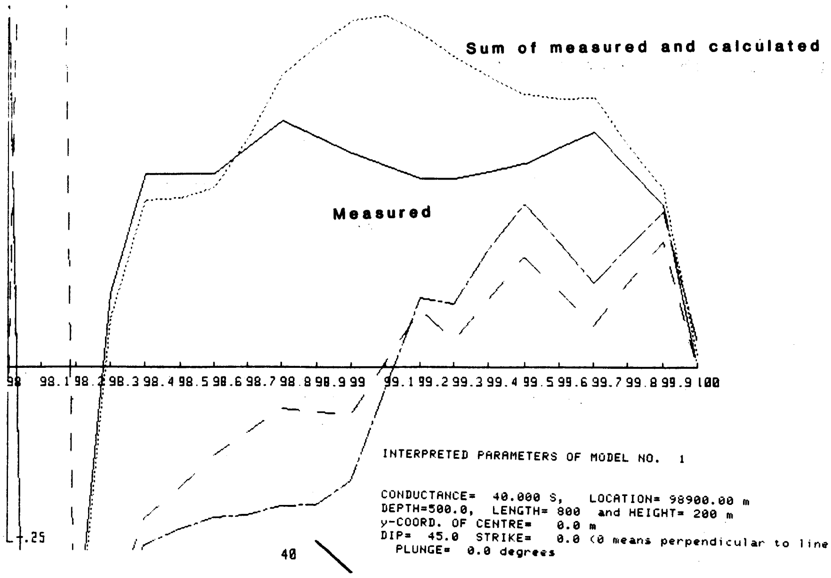

INTERPRETED PARAMETERS OF MODEL NO. 1

CONDUCTANCE= 40.000 S, LOCATION= 98900.00 m
DEPTH=500.0, LENGTH= 800 and HEIGHT= 200 m
y-COORD. OF CENTRE= 0.0 m
DIP= 45.0 STRIKE= 0.0 (0 means perpendicular to line) and
PLUNGE= 0.0 degrees

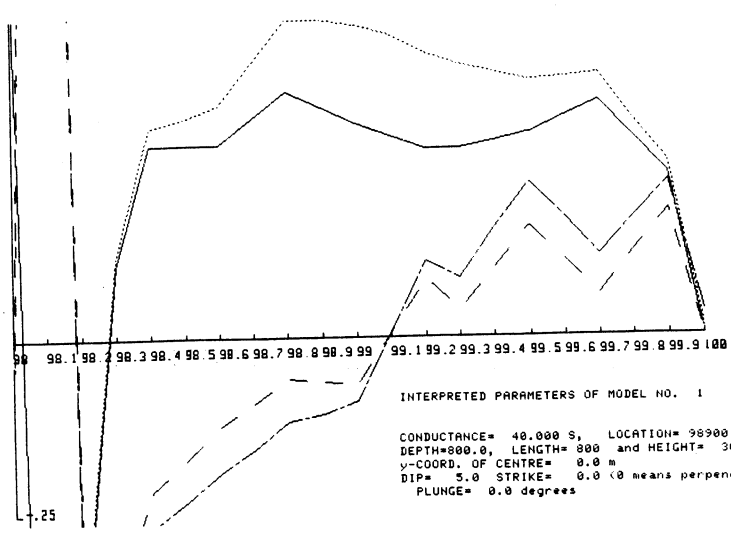

INTERPRETED PARAMETERS OF MODEL NO. 1

CONDUCTANCE= 40.000 S, LOCATION= 98900.00 m
DEPTH=800.0, LENGTH= 800 and HEIGHT= 30 m
y-COORD. OF CENTRE= 0.0 m
DIP= 5.0 STRIKE= 0.0 (0 means perpendicular to line) and
PLUNGE= 0.0 degrees

2/HØYDAL/Line Y=37.5 Z and X-Comp.
415/432 1:10000 Date 18.03.1986 nV/Am^2

432/2/HØYDAL Date 18.03.1986
Line Y= 37.500
Line direction= 0 Altitude= 0
TRANSMITTER PARAMETERS:
Loop size: 400 x 400 m^2, Angle= 0 degr.
Current= 13 A and Turn-off time= .2 ms
Centre: 99.25 , 37.4 km, Altitude= 0 m
RECEIVER PARAMETERS:
Starting point= 98.5 km, Gain= 7 , Spacing= 100 m

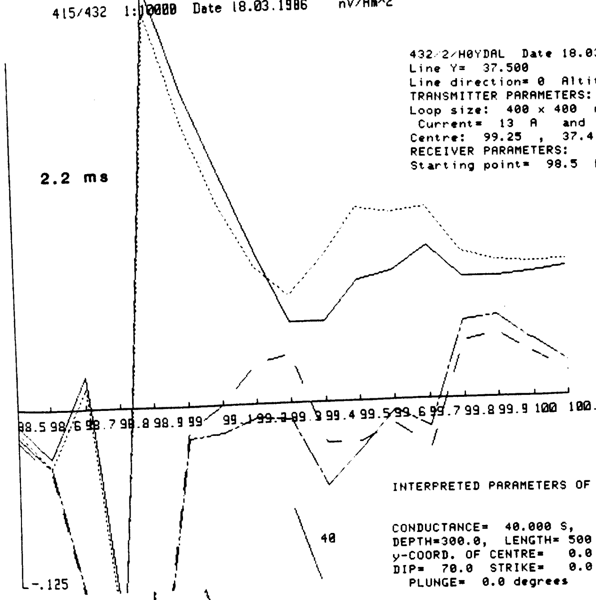

INTERPRETED PARAMETERS OF MODEL NO. 1

CONDUCTANCE= 40.000 S, LOCATION= 99300.00 m
DEPTH=300.0, LENGTH= 500 and HEIGHT= 200 m
y-COORD. OF CENTRE= 0.0 m
DIP= 70.0 STRIKE= 0.0 (0 means perpendicular to line) and
PLUNGE= 0.0 degrees

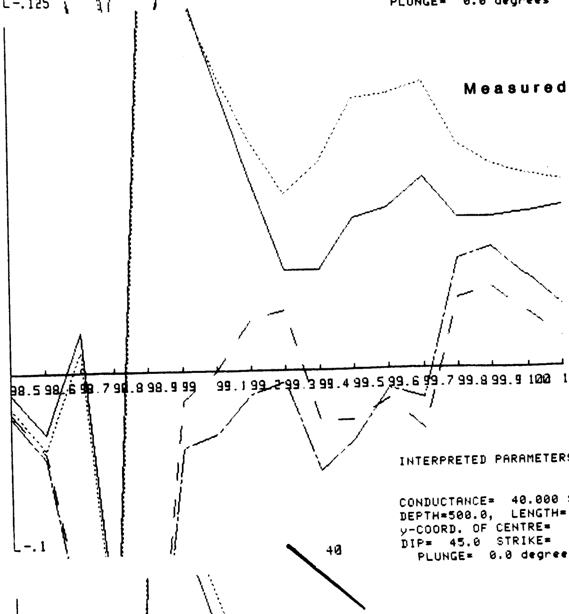

INTERPRETED PARAMETERS OF MODEL NO. 1

CONDUCTANCE= 40.000 S, LOCATION= 99300.00 m
DEPTH=500.0, LENGTH= 500 and HEIGHT= 200 m
y-COORD. OF CENTRE= 0.0 m
DIP= 45.0 STRIKE= 0.0 (0 means perpendicular to line) and
PLUNGE= 0.0 degrees

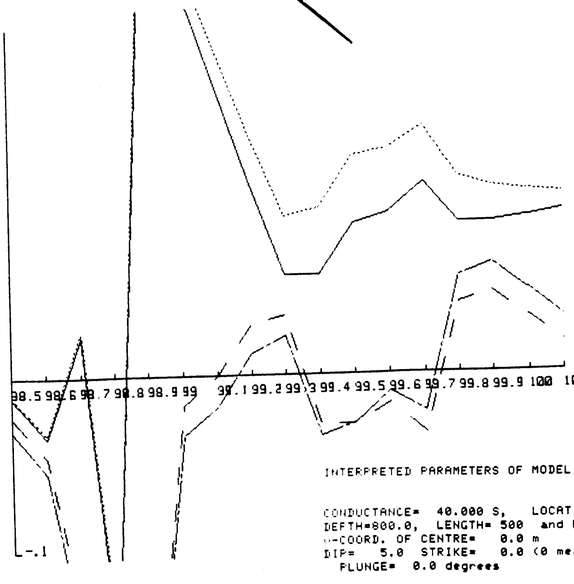

INTERPRETED PARAMETERS OF MODEL NO. 1

CONDUCTANCE= 40.000 S, LOCATION= 99300.00 m
DEPTH=800.0, LENGTH= 500 and HEIGHT= 30 m
y-COORD. OF CENTRE= 0.0 m
DIP= 5.0 STRIKE= 0.0 (0 means perpendicular to line) and
PLUNGE= 0.0 degrees

40

OUTOKUMPU OY Malminetsintä

Menet. GENIE

Laite 25m / 2 / 112

Pvm/Mitt. 31/10-85

Linja Y= 38.00

Karttal. ~~[illegible]~~

Pitäjä ~~[illegible]~~ Løkk

Tutk.k. Høydal

Y	X		1		2		3			Note
9099	890		[illegible]		[illegible]		[illegible]			
	888	↓	[illegible]		[illegible]		[illegible]			
	[illegible]		[illegible]		[illegible]					
	[illegible]		[illegible]		[illegible]		[illegible]			
			[illegible]		[illegible]					
			[illegible]							
			[illegible]							
	[illegible]									Rain
	[illegible]		[illegible]		[illegible]					
			[illegible]		[illegible]					
	[illegible]									
	[illegible]		1,2		[illegible]		[illegible]			
	[illegible]		2,0		3,1		[illegible]			
	[illegible]		1,6		3,3		[illegible]			
	[illegible]		-3,8		-[illegible]		-[illegible]			
	[illegible]		-[illegible]		-[illegible]		-[illegible]			
	[illegible]		[illegible]		2,[illegible]		[illegible]			1sec
	[illegible]		[illegible]		-[illegible]2		[illegible]			
	[illegible]		[illegible]		0,1		[illegible]			
	[illegible]		[illegible]		0,5		[illegible]			
			-[illegible]		[illegible]		[illegible]			
					[illegible]					

ME 101 300×50 2 80 Esa

OUTOKUMPU OY Malminetsintä

Menet. GENiE
Laite 25m/2/112
Pvm/Mitt. 4/11-85
Linja Y = 36.50
Karttal.
Pitäjä Løkken
Tutk.k. Høydal

Y	X	1	2	3	
36.50	9894	2,0	1,5	-0,3	
	896	1,0	0,5	0,5	
	898	0,5	0,3	-1,6	
	900	-0,7	-0,8	-6,0	Snow
	902	0,8	1,9	1,0	
	904	0,4	0,6	-0,7	
	906	2,8	5,0	1,7	
	908	2,9	0,2	-4,0	
	910	-14,9	-30,0	-46,0	S.S.
	912	4,2	3,8	4,9	
	914	1,3	2,8	3,7	
	916	3,6	1,9	1,1	
	918	2,2	1,4	1,5	
	920	2,0	0,7	1,7	
	922	0,4	0,7	1,9	
	924	0,7	1,3	2,6	
	926				
	9928				

OUTOKUMPU OY Malminetsintä

Menet. GENIE

Laite 25m/2/112

Pvm/Mitt. 7/11-85

Linja Y=36.75

Karttal.

Pitäjä Løken

Tutk.k. Høydal.

X	Y	1	2	3
9880		[illegible]	[illegible]	
[illegible]		[illegible]	1,6	[illegible]
[illegible]		-0,5	[illegible]	[illegible]
[illegible]		-1,8	[illegible]	[illegible]
[illegible]		[illegible]	[illegible]	-7,2
[illegible]		-5,8	[illegible]	[illegible]
[illegible]		-4,7	[illegible]	[illegible]
[illegible]		[illegible]	[illegible]	[illegible]
[illegible]		[illegible]	[illegible]	[illegible]
[illegible]		[illegible]	[illegible]	[illegible]
9100		[illegible]	[illegible]	0,8
[illegible]		[illegible]	[illegible]	[illegible]
[illegible]		[illegible]	[illegible]	[illegible]
[illegible]		[illegible]	[illegible]	[illegible]
[illegible]		[illegible]	2,3	[illegible]
[illegible]		[illegible]	[illegible]	[illegible]
912		[illegible]	[illegible]	[illegible]
[illegible]		[illegible]	[illegible]	[illegible]
916		1,2	[illegible]	[illegible]
918		[illegible]	[illegible]	[illegible]
920		[illegible]	[illegible]	[illegible]
922		[illegible]	[illegible]	[illegible]
924		1,8	[illegible]	[illegible]
926		-1,1	[illegible]	[illegible]
928		[illegible]	[illegible]	[illegible]

930

Very heavy raining/ Instrument wet

M 101 200×50 2 80 Esa

OUTOKUMPU OY Malminetsintä

Menet. GENIE

Laite 25 m / 2 / 112

Pvm/Mitt. 1/11-85

Linja [illegible]

Karttal.

Pitäjä [illegible]

Tutk.k. Höydal

	X	1	2	3	
9.	[illegible]	0,7	9,4	3,7	
	848	[illegible]	[illegible]	4,6	
	[illegible]	[illegible]	[illegible]	[illegible]	
	[illegible]	2,2	4,3	[illegible]	
	[illegible]	[illegible]	[illegible]	[illegible]	
	[illegible]	[illegible]	[illegible]	[illegible]	Snow/rain
	[illegible]	-0,7	[illegible]	[illegible]	
	[illegible]	0,4	[illegible]	[illegible]	
	[illegible]	[illegible]	[illegible]	[illegible]	
	[illegible]	2,1	[illegible]	[illegible]	
	[illegible]	[illegible]	1,4	2,7	
	[illegible]	[illegible]	2,2	0,6	
	[illegible]	[illegible]	-0,7	[illegible]	
	[illegible]	[illegible]	-0,5	[illegible]	
	[illegible]	2,0	[illegible]	[illegible]	
	870	1,3	[illegible]	[illegible]	
	868				

ME 101 300×50 2 80 Esa

OUTOKUMPU OY Malminetsintä

Menet. GENIE

Laite 25m/2/112

Pvm/Mitt. 1/11-85

Linja y = 37.25

Karttal.

Pitäjä Løkken

Tutk.k. Høydal

Y	X		1		2		3			[illegible]
	9860		0,6		1,0		-0,4			
	862		0,8		0,7		-1,1			
	864		0,3		0,2		-0,5			
	866		0,0		[illegible]		-1,0			
	868		0,5		0,1		-1,2			Snow/[illegible]
	870		-0,1		-0,4		-1,9			
	872		-2,4		-3,3		-9,5			
	874		0,2		-1,9		-3,9			
	876		[illegible]		-2,3		-11,6			
	878		0,1		-0,9		-4,1			
	8[illegible]		-1,2		-14,0		-21,3			
	8[illegible]		[illegible]		[illegible]		-4,0			
	884		0,6		0,0		-0,7			
	5[illegible]		0,9		2,4		4,6			
	888		2,8		1,2		1,1			
	890		0,6		0,7		0,4			
	9892									

ME 101 300×50 2 80 Esa

OUTOKUMPU OY Malminetsintä

Menet. GENIE

Laite 25m/2 /112

Pvm/Mitt. 1/11-85

Linja 37.50

Karttal.

Pitäjä Løkken.

Tutk.k. Høydal

Y	X		1		2		3			NOTC
	9900		0,3		0,5		1,5			
	898		0,7		1,3		0,8			
	896		0,5		0,4		-0,5			
	894		1,1		1,0		0,5			
	892		0,6		0,7		0,8			
	890		0,4		0,8		0,9			[illegible]
	888		0,6		0,8		0,6			
	886		0,3		0,5		0,0			
	884		-0,2		-0,4		-0,8			
	882		0,6		1,6		1,1			
	880		1,3		3,1		4,6			
	878		0,1		3,8		2,7			
	876		-0,3		-7,0		-18,6			
	874		-3,0		-7,9		-1,8			
	872		-0,5		-4,4		-11,6			
	870		2,0		2,8		4,8			
	868		1,4		1,2		2,6			
	866		2,0		1,7		2,4			
	864		0,1		0,3		1,5			
	862		0,3		0,4		0,7			
	860		0,[illegible]		0,6		1,2			
	858		0,7		0,7		1,2			
	856		0,6		0,6		0,3			
	854									

ME 101 300×50 2 80 Esa

OUTOKUMPU OY Malminetsintä

Menet. GENIE

Laite 25m/12/112

Pvm/Mitt. 21/10-85

Linja

Karttal.

Pitäjä ~~Holanda~~ Løkk

Tutk.k. Høydal.

	9										
											Rain
	898										

ME 101 300×50 2 80 Esa

OUTOKUMPU OY Malminetsintä

Menet. GENIE

Laite 25 m / 2 / 112,5 Hz

Pvm/Mitt. VH ja H / 29.-85

Linja Y = 32,25

Karttal. 15...

Pitäjä Løkken

Tutk.k. Dambia...

Y	X	1	2	3	Not
	9848	-0,5	0	-0,2	
	846	0,4	0,3	-0,9	
	844	-0,1	-0,2	-0,9	
	842	-0,7	-0,1	-0,8	
	840	-0,6	-0,4	-1,2	
	838	-1,7	-1,2	-2,0	Rain
	836	-0,7	-0,4	-1,2	
	834	0,4	0,8	-0,5	
	832	2,0	2,9	+3,4	
	830	1,0	3,0	4,2	
	828	-0,5	-5,0	-9,7	
	826	-0,3	+1,8	5,1	
	824	+0,8	0,9	-2,2	
	822	-0,5	-0,7	-4,2	
	820	-2,9	-7,9	-11,8	
	818	1,0	1,7	1,5	
	816	0,5	1,1	0,9	
	814	0,4	0,3	0,4	
	812	0,7	0,5	1,0	
	810				

MF 101 300×50 2.80 Esa

OUTOKUMPU OY Malminetsintä

Menet. GENIE

Laite 25m / 2 / 112 Hz

Pvm/Mitt. 30/10-85

Linja Y = 32,50

Karttal.

Pitäjä Løkken

Tutk.k. Danlia / Hogåsen

Y	X	1	2	3
	9830	2,5	1,9	0,6
	828	1,8	2,0	1,1
	826	1,0	1,0	0,4
	824	0,9	1,1	0,5
	822	1,5	0,9	0,6
	820	1,1	1,0	0,1
	818	1,0	1,0	-0,4
	816	2,4	3,6	5,2
	814	0,7	1,1	1,2
	812	-0,5	-4,8	-7,7
	810	2,1	3,6	2,0
	808	-0,2	-0,6	-1,3
	806	2,0	1,9	1,3
	804	1,1	1,1	0,8
	802	0,8	0,9	0,4
	800	1,1	1,2	1,0
	798	0,9	0,8	0,4
	796	1,4	1,3	0,7
	794	0,8	-0,6	1,3
	792	1,1	1,3	1,8
	790			

Rain

MF 101 300x50 2 80 Esa

OUTOKUMPU OY Malminetsintä

Menet. Genie
Laite 25 m/2 (112
Pvm/Mitt. 5/11-85

Linja [illegible]
Karttal.
Pitäjä Lohja
Tutk.k. Buulia/Högman

	X									
	97.90									
	[illegible]									
	[illegible]									
	79,5									
	79,8									
	800				1,3		1,0			Snow
	[illegible]	↓	1,4		1,2		0,9			
	[illegible]		[illegible]		[illegible]		1,7			
			[illegible]		[illegible]		[illegible]			
			1,7		[illegible]		[illegible]			
			1,5		[illegible]		[illegible]			
	1,2		[illegible]		[illegible]					
	[illegible]		[illegible]		[illegible]		2,5			
	816		[illegible]		[illegible]		[illegible]			
	[illegible]		[illegible]		-1,1		[illegible]			
	820		[illegible]		[illegible]		0,7			
	[illegible]		[illegible]		-0,1		[illegible]			
	824		1,4		[illegible]		[illegible]			
	[illegible]		0,8		[illegible]		[illegible]			
	[illegible]		-0,3		-0,4		[illegible]			
	~~830~~									
	[illegible]		[illegible]		[illegible]		[illegible]			
	[illegible]	↓	0,7		[illegible]		[illegible]			
	79[illegible]		[illegible]		[illegible]		[illegible]			
	[illegible]		[illegible]		[illegible]		[illegible]			
	[illegible]									

ME 101 300×50 2 80 Esa

OUTOKUMPU OY Malminetsintä

Menet. Genie

Laite 2 Sw/ 2 / 112

Pvm/Mitt. 5/11-85

Linja Y=31.[illegible]

Karttal.

Pitäjä Lohtaja

Tutk.k. Daulia/Högåsen

Y	X	1	2	3
9	822	0.4	0.1	0
	824	0.3	0.[illegible]	0.2
	826	0.2	0.3	-0.1
	828	0.2	0	-0.2
	830	0.5	0.3	0.5
	832	0.8	0.7	0.2
	834	1.[illegible]	1.5	[illegible]
	836	0.7	[illegible]	0
	838	[illegible]	0.8	[illegible]
	840	-0.9	[illegible]	-1.[illegible]
	842	[illegible]	0.7	0.[illegible]
	844	1.0	0.6	0.1
	846	0.4	[illegible]	5.2
	848	[illegible]	[illegible]	-0.8
	850	-0.3	0	-1.2
	852	0.8	[illegible]	-0.4
	854	1.0	1.5	[illegible]
	856	[illegible]	[illegible]	-0.3
	858	0.7	0.3	[illegible]
	860	0.3	0.5	[illegible]
	862	0	[illegible]	0.5
	864	[illegible]	0.3	-0.4
	866	[illegible]	0.2	0
	868	0.1	-0.2	-0.4
	[illegible]	0	[illegible]	[illegible]
	[illegible]	[illegible]	0.5	[illegible]

Snow

874

ME 101 300×[illegible] Esa

Forts.

OUTOKUMPU OY Malminetsintä

Menet. Genie

Laite

Pvm/Mitt. 5/11-85

Linja 31.50

Karttal.

Pitäjä

Tutk.k. Damlén/Hedgåsen

	X		1		2		[illegible]			
	9874		[illegible]		0.3		0.4			Snow
	[illegible]		1.2		1.4		[illegible]			
	[illegible]		1.2		[illegible]		[illegible]			
	[illegible]		0.1		[illegible]		-0.3			
	882									

ME 101 300×50 2 80 Esa

OUTOKUMPU OY Malminetsintä

Menet. Genie
Laite 25m / 2 / 112
Pvm/Mitt. 5/11-85

Linja Y = 31.25
Karttal.
Pitäjä [illegible]
Tutk.k. Daulia/Högåsen

Y	X	1	2	3	
9	878	0.8	0.6	0.1	
	876	0.6	0.3	0.2	
	874	0.2	0.1	-0.4	Snow
	[illegible]	[illegible]	[illegible]	0	
	[illegible]	[illegible]	[illegible]	0.4	
	[illegible]	0	[illegible]	[illegible]	
	[illegible]	0.3	0.3	0.1	
	[illegible]	[illegible]	-0.1	-0.1	
	[illegible]	0.3	0.2	[illegible]	
	[illegible]	[illegible]	0.3	[illegible]	
	858	1.1	1.2	0	
	856	1.4	1.1	-0.2	
	[illegible]	[illegible]	0	[illegible]	
	[illegible]	[illegible]	[illegible]	-0.1	
	[illegible]	[illegible]	[illegible]	[illegible]	
	[illegible]	[illegible]	[illegible]	0	
	[illegible]	[illegible]	0.5	[illegible]	
		[illegible]	0.3	0	
	842	[illegible]	0	-0.2	
	840	[illegible]	[illegible]	0.5	
	838	[illegible]	[illegible]	[illegible]	
	836	[illegible]	[illegible]	[illegible]	
	834	[illegible]	[illegible]	[illegible]	
	832	[illegible]	[illegible]	[illegible]	
	830	[illegible]	[illegible]	[illegible]	

ME 101 300×50 2 80 Esa

Farh

OUTOKUMPU OY Malminetsintä

Menet. Genie

Laite

Pvm/Mitt. 5/11-85

Linja 1

Karttal.

Pitäjä

Tutk.k. Daulia/Högåsen

		X	1		2		3			
9	28		-10.1		-20.1		-30			Snow
	926		-1.7		-2.6		-7.3			
	924		0.9		1.3		0.4			
	822									

ME 101 300×50 2 80 Esa